FATIGUE IN RUBBER VULCANISATES

by

GABRIEL AIGBIBHALU IHENYEN

A Thesis Submitted for the Degree of

DOCTOR OF PHILOSOPHY

of the University of Aston in Birmingham

December 1982

THE UNIVERSITY OF ASTON IN BIRMINGHAM

FATIGUE IN RUBBER VULCANISATES

GABRIEL AIGBIBHALU IHENYEN

Submitted for the Degree of PhD December 1982

SUMMARY

A study has been made of the effect of single extensions and continuou fatigue on the structures of various natural rubber networks. The change in network structure of a conventional vulcanisate on a single extension manifests itself as permanent set. The change in network structure has been assessed by the use of the chemical probes, propar 2-thiol/piperidine, hexane-thiol/piperidine and triphenyl phosphine, which determine the polysulphide and disulphide crosslink densities and main chain modification respectively. The permanent set induced on a single extension of a conventional sulphur vulcanisate has been shown to result from the destruction and reformation of polysulphide crosslinks. The magnitude of the effect was dependent upon the degree of extension and showed a maximum at extensions corresponding to the onset of stress-induced crystallisation. The incorporation of a reinforcing filler, HAF-carbon black, magnified the effect. Vulcanisates that possessed only mono and disulphide crosslinks did not show any significant permanent set.

The continuous changes in network structure during fatigue have also been determined, and the effects of carbon black and anti-oxidants on these changes and the fatigue life have been assessed. During fatigue the overall crosslink density increased slightly, which resulted from the destruction of polysulphide crosslinks and their replacement by principally disulphide crosslinks. Anti-oxidants reduced the rate of destruction of polysulphide crosslinks and increased the fatigue life of the rubber network.

The fatigue life of the network also depended upon the concentration of free chain ends. These chain ends were incorporated into the network by masticating rubber under nitrogen in the presence of bis(diisopropyl)thiophosphoryl disulphide, which improved the fatigue resistance by up to 9%.

KEY WORDS

Fatigue
Rubber networks
Single extension
Network defects
Antioxidants

DECLARATION

This work was carried out between April 1980 and June 1982 at the University of Aston in Birmingham. It has been done independently and has not been submitted for any other degree.

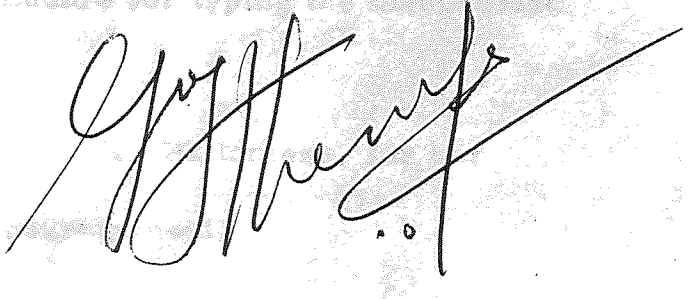

ACKNOWLEDGEMENTS

I would like to give my special thanks to Dr A J Amass and Mr J E Stuckey for providing unfailing help, guidance and supervision throughout the project.

I wish to acknowledge the assistance of the technicians of the Department of Chemistry in making this work possible. My thanks are also due to Mrs L Ludlow for typing the manuscript.

Finally, I would like to thank my wife, Philomena, for her understanding, support and encouragement.

LIST OF CONTENTS

LIST OF TABLES

LIST OF FIGURES continued

LIST OF FIGURES continued

CHAPTER ONE

THEORY

1.1 Natural Rubber

Natural rubber (NR) is commonly obtained from the latex of Hevea Brasiliensis. The coagulum obtained by treatment of the latex with an acid, followed by washing and drying, contains a high proportion of a hydrocarbon, mixed with proteins, resins and other constituents; a typical weight analysis[1] is: rubber hydrocarbon 94.2%; acetone extract 2.5%; protein 2.5%; ash 0.3%; moisture 0.5%.

Studies by Harries[2], Katz[3] and Pummerer[4] have demonstrated that the structure of NR is essentially cis-1,4-polyisoprenoid, with the monomer units in a "head to tail" formation as described by:

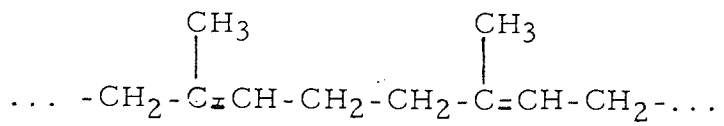

cis-1,4-polyisoprene

Natural rubber exhibits two phases, sol and gel. The differences are exhibited in degree of solubility in some organic solvents due to different amounts of highly branched and lightly crosslinked components interwound in the rubber. Natural rubber hydrocarbon is a polymer of very high molecular weight and, in common with others of its kind, the molecules are heterogeneous with

respect to molecular weight. Since raw NR is very tough and resilient, it is difficult to incorporate compounding ingredients without first reducing its viscosity by mechanical shear. The physical properties of NR may vary slightly due to the non rubber constituents present and to the degree of crystallinity.

Table 1.1 Some physical properties of natural rubber[1]

Density	0.92 Mgm^{-3}
Refractive index ($20^{o}K$)	1.52
Coefficient of cubical expansion	0.00062 K^{-1}
Cohesive energy density	0.000267 Jm^{-3}
Heat of combustion	44769874 JKg^{-1}
Thermal conductivity	1.339×10^{-9} $Jsec^{-1}m^{-3}K^{-1}$
Dielectric constant	2.37
Power factor (1,000 cycles)	0.15 - 0.2
Volume resistivity	10^{9} ohms m^{-3}

1.1.1 Mastication and Mechanochemical Reactions of Rubbers

The process of mastication, to increase the plasticity of rubber, was discovered by Hancock[5] in the 1820's, but it was Staudinger[6] who later attributed the increase in plasticity to the occurrence of a mechano-degradation process during mastication. The free radical nature of this process was realised by Pike and Watson[7], who suggested that rupture

occurred at the α-methylene groups in the cis-1, 4-polyisoprene molecule as follows:

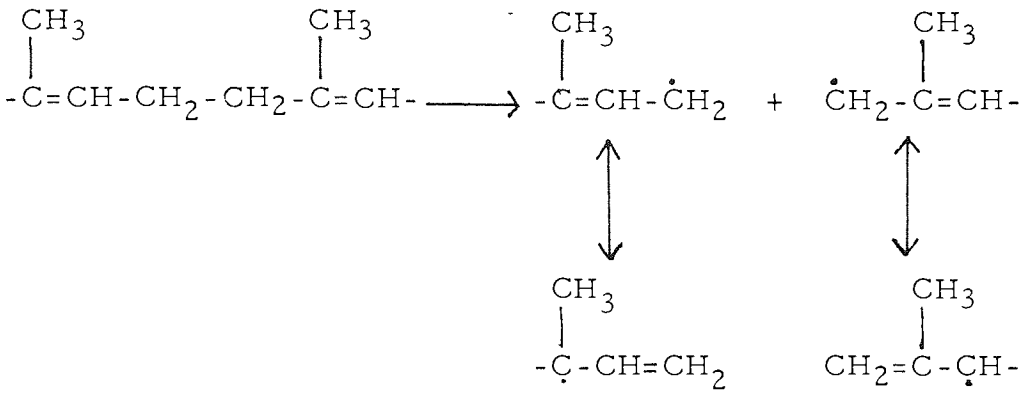

(1-1)

Pike and Watson[7] further showed that mastication at ambient temperatures in nitrogen produces no appreciable change in molecular weight. In oxygen, however, degradation is immediate and rapid. These workers confirmed the work of Busse[8], Cotton[9] and Kauzman and Eyring[10] who independently showed that the presence of oxygen is necessary for the efficient breakdown of rubber. The greatly reduced rate of degradation noted on masticating NR under nitrogen led them to believe that in nitrogen, the radicals formed by shear recombine whereas they react with oxygen. Pike and Watson reasoned that other free radical acceptors should be able to compete in a manner similar to oxygen to stabilize the free rubber radicals. Thiophenol was to react in this manner:

$$R^{\cdot} + H\text{-}S\text{-}Ph \longrightarrow RH + {\cdot}S\text{-}Ph \qquad (1\text{-}2)$$

where R· is the rubber hydrocarbon radical. The benzenesulphenyl

radical reacted subsequently with a second polymeric radical or dimerized.

There has been further positive analytical evidence[11] to support this view that free radical acceptor fragments become attached to rubber during mastication. Ayrey, Moore and Watson[11] have demonstrated such attachment for the fragments from 1-1′-dinaphthyl disulphide (DND), labelled with radioactive sulphur (^{35}S) and 1-1′-diphenyl-2-picryl hydrazyl (DPPH). The aromatic disulphide (DND), which acts as an efficient radical acceptor during the mastication of natural and poly(styrene-butadiene) rubbers[11], reacts with free radicals by homolytic cleavage of the S-S bonds:

$$R\cdot + Ar\text{-}S\text{-}S\text{-}Ar \longrightarrow R\text{-}S\text{-}Ar + Ar\text{-}S\cdot \qquad (1\text{-}3)$$

$$R\cdot + ArS\cdot \longrightarrow R\text{-}S\text{-}Ar \qquad (1\text{-}4)$$

$$ArS\cdot + ArS\cdot \longrightarrow Ar\text{-}S\text{-}S\text{-}Ar \qquad (1\text{-}5)$$

where Ar = 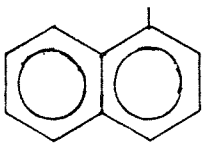

DPPH exists, even in the crystalline state, as a free radical which is stable to oxygen, and it has been used to provide a known number of free radicals to scavenge quantitatively the transient free radicals produced as intermediates in other complex reactions. The rate of combination of DPPH with NR during mastication has been found to be greatest during the early stages of mastication[11].

At this stage the rate of bond rupture would be expected to be a maximum because the rate of shear is also at its greatest.

Further evidence for the production of free radicals during mastication has been provided by Angier and Watson[12, 13, 14], who studied the production of interpolymers of natural rubber, styrene-butadiene and butadiene-acrylonitrile rubbers and polychloroprene during cold mastication[7] under nitrogen in an internal mixer. Evidence for inter-polymer formation was provided by differences in the gel content of the products after mastication compared with those of simple polymer mixtures. Slonminskii[15] has investigated SBR and BR blends and found that in the absence of oxygen, mechanochemical grafting produced materials whose property-composition relationships differed from those of simple milled mixtures.

It has been established [16, 17] by electron spin resonance spectroscopy (ESR) that mechanical loading of elastomers, such as stretching and fatigueing, causes chain scission and formation of mechano-radicals resulting in degradation. Formation of mechano-radicals and their reactivity have been reviewed by Sohma and Sakaguchi [18].

1.1.2 Accelerated Sulphur Vulcanisation

The discovery of vulcanisation with sulphur by Goodyear[19] and Hancock[20] makes it possible to use natural rubber as an engineering material. The further development[21] and use of activators has reduced considerably both the amount of sulphur required for vulcanisation and, more importantly, the vulcanisation time as shown in Table 1.2. During vulcanisation the long chains of the rubber molecule form an elastic three dimensional network. The rubber looses its tackiness and becomes insoluble and is slightly more resistant to the deterioration normally caused by heat and light ageing processes. The major effects of vulcanisation on a wide range of properties have been studied[22-25].

A detailed knowledge of the chemistry[26, 27, 28] and kinetics[29, 30] of vulcanisation and of the final vulcanisate structure[28, 31] has been provided by the reactions of simple organic model compounds. 2-methylpent-2-ene, is an example and has been reacted with elemental sulphur, accelerators and other curing agents.

Elemental sulphur (S_8) undergoes a series of reactions with accelerators and activators to yield an active sulphurating agent[26, 2 which then reacts with the rubber hydrocarbon to produce a rubber bound intermediate. The intermediate is the precursor to cross-link formation. Polysulphide crosslinks are formed initially either by reactions between two rubber bound intermediates or

Table 1.2 Development of vulcanisation of natural rubber[21]

Date		Formulation[a]	Cure time at 140°C[b]
1840	rubber	100	6 hr
	sulphur	8	
1850	rubber	100	4 hr
	sulphur	8	
	metal oxide	5	
1906	rubber	100	2 hr
	sulphur	6	
	ZnO	5	
	Acc TC	2	
1921	rubber	100	20 min
	ZnO	5	
	sulphur	3	
	MBT	1	
	stearic acid	1	
1920s	early heat-resistant systems (very scorchy, e.g. TMT)		15 min
1940s	delayed action systems		30 min
1950s	EV systems (low sulphur/ high accelerator ratio)		60 min
1969	Soluble EV systems		60 min
1970	Soluble zinc soaps		

(a) Formulation - these figures refer to parts by weight
(b) Cure time - it is usual to vulcanise at higher temperatures (especially the EV systems) to obtain economic cure r

by reaction of the intermediate with another rubber hydrocarbon molecule. The maturing reactions shown in fig 1.1 then take place to yield the final vulcanisate structure shown in fig 1.2. The probable course of the sulphur vulcanisation of natural rubber in the presence of accelerators and activators is summarised in fig 1.1.

The sulphur crosslinking systems produce crosslinks containing mono-, di- and polysulphide crosslinks (fig 1.2: a, b, c), the sulphur generally located at an allylic carbon atom. Sulphur may also be present as

(i) pendant accelerator fragments (d)

(ii) cyclic monosulphide (e), and

(iii) cyclic polysulphides (f)

The original rubber chain may be modified further at the cross-link sites by chain scission (g) and conjugated unsaturation (h, i). There is evidence for a cis/trans inversion in some cases and for a limited migration of the double bond along the chains. There is always other material associated but not combined with, the vulcanisate (j) known as extra-network material (ENM).

In a conventional sulphur vulcanisate of natural rubber, containing 2.5 parts by weight of sulphur and 0.5 parts of accelerator per

Fig 1.1 The probable course of sulphur vulcanisation of natural rubber in the presence of accelerators and activators[26]

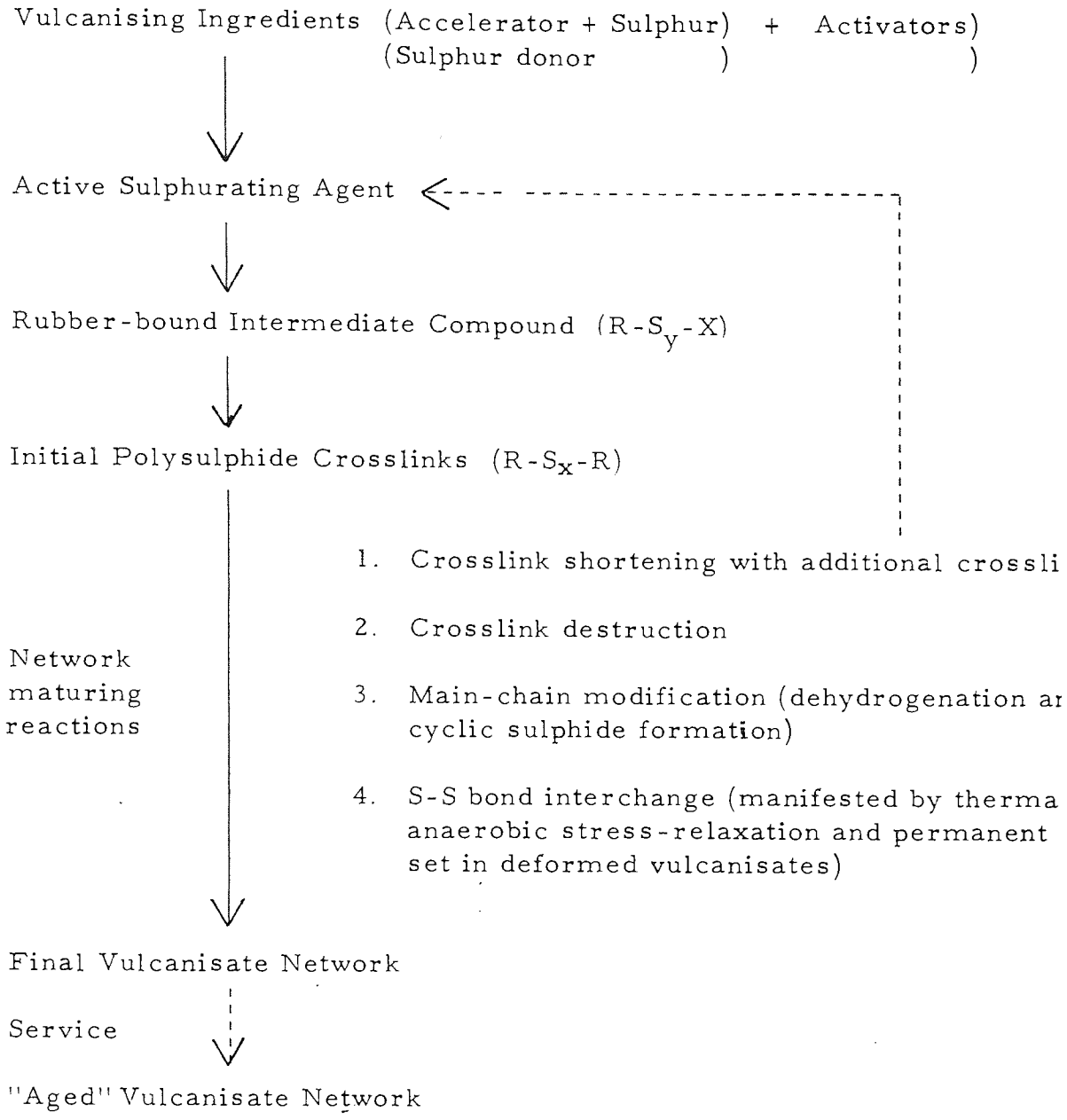

Fig 1.2 Typical chemical groupings present in a sulphur vulcanised natural rubber network

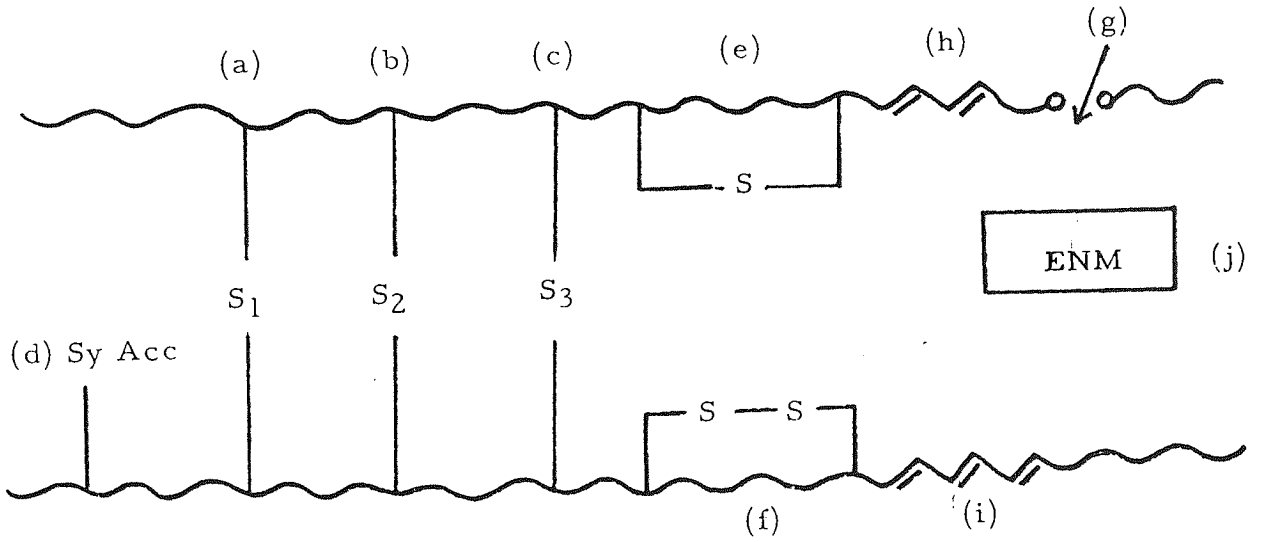

hundred parts of rubber, the crosslinks are mainly polysulphidic. By increasing the accelerator-to-sulphur ratio and retaining a relatively long cure time a vulcanisate is obtained which contains predominantly monosulphidic crosslinks. Such a system is called an efficiently vulcanised (EV) system. The term 'semi-EV' has been applied to vulcanisation systems with sulphur levels intermediate between those of the conventional and EV. Such semi-EV systems are used widely as a compromise of costs and/or performance[32]. EV and semi-EV systems have proved to be of particular value because of their high rates of cure[32, 33] and low reversion[34] in NR vulcanisates.

1.1.3 Non-Sulphur Vulcanisation Systems

The use of sulphur donors in place of elemental sulphur has been developed since the 1920's when it was found that the accelerators tetramethyl thiuram disulphide (TMTD) and tetraethyl thiuram disulphide (TETD) with zinc oxide gave vulcanisates with improved thermal and oxidative resistance. Scheele et al[35] and Moore[36] have demonstrated that during vulcanisation, the disulphide reacts with the zinc oxide to yield a tetraalkyl thiuram polysulphide which then reacts with the rubber molecule and further zinc oxide to produce a rubber-bound intermediate polysulphide. This then cross links to eventually yield monosulphidic crosslinks.

The use of organic peroxides as crosslinking agents for NR was first investigated in 1915 by Ostromislenskii[37], who used benzoyl peroxide. However, it is only since dicumyl peroxide was discovered[38,39] that this method of vulcanisation has been employed commercially. The crosslinks produced are carbon-carbon bonds, and the reversion resistance is consequently high. Peroxide vulcanisates show low compression set and creep, may be compounded for high transparency and do not exhibit the staining problems encountered with sulphur-cured rubbers. However, the vulcanisates have low tensile and hot tear strengths, slower rates of cure and absence of delayed action during cure. Chow and Knight[40] have recently developed a delayed action peroxide vulcanisation system involving the use of radical scavengers.

Diene rubbers may be crosslinked by exposure to high energy radiation and a free radical mechanism is believed to be involved[41]. Radiation cured vulcanisates appear weaker than those cured conventionally with sulphur and have not become of much industrial importance.

Recently[42, 43] a new crosslinking system has been developed using urethane crosslinks. The crosslinks are mainly of the urea type and their excellent stability provides good ageing and reversion resistance as well as good initial vulcanisate properties[43]. Improvements in scorch safety have been achieved by incorporation of mercaptosilanes during compounding

1.2 Vulcanisation of Synthetic Rubbers[45]

Compound development of synthetic rubbers based on diene has followed a similar pattern to that of natural rubber. Sulphur, organic accelerators and activators are used in curing systems for elastomers of the following types:

(i) styrene-butadiene rubber (SBR)

(ii) butadiene-acrylonitrile rubber (NBR)

(iii) butyl rubber (IIR)

(iv) polyisoprene rubber (IR)

(v) polybutadiene rubber (BR), and

(vi) ethylene-propylene-diene modified rubber (EPDM)

in the same way as they are in NR. Sulphur levels have been established for the various rubbers. Accelerator types and quantities required for vulcanisation at acceptable rates have also been studied extensively.

In other synthetic rubbers, vulcanisation is accomplished by different means. Organic peroxides have been found to be effective in some cases, notably silicones, fluorocarbons and ethylene propylene copolymers. Zinc oxide-magnesia combinations provide the main curing activity in neoprene, with sulphur and organic accelerators supplementing the

metallic oxides in some types. Polysulphide elastomers require zinc oxide and organic accelerators for vulcanisation. Acrylic elastomers vulcanise in the presence of alkalis and certain organic accelerators.

1.3 Network Structure Analysis

1.3.1 Introduction

One of the general aims of this project is to assess the effect of fatigue and single extensions on the crosslink structure of natural rubber vulcanisates. In order to achieve this aim, a knowledge of the following parameters is required:

(a) the original crosslink density of the vulcanisates investigated,
(b) the nature of the crosslink network formed during vulcanisation,
(c) the changes in crosslink density and crosslink structure during both fatigue tests and single extensions of vulcanisates.

1.3.2 Measurement of Crosslink Density

1.3.2.1 Introduction

An understanding of the elastomeric nature of rubber was made possible by the development of the theory of elasticity, which has been utilised in later years to calculate the degree of crosslinking.

Major developments by Staudinger[46] and Mayer et al[47] showed that rubber molecules were of a long polymeric nature and assumed irregular and statistically random configurations under thermal motion. On deformation they tend to elongate and elongation causes a decrease in the entropy of the system. The application of these ideas to a crosslink network[48-51] led to the statistical theory of rubber elasticity.

The most fundamental characteristic of a rubber network is the average molecular weight between crosslinks ($\overline{M}_c$) which is related to the crosslink density. Three principal approaches to the determination of $\overline{M}_c$, and hence crosslink density, have been used.

(a) A modulus-related constant (C_1), related to $\overline{M}_c$, may be computed from dry extension stress/strain measurements.

(b) The elastic parameter C_1 may be determined from the compression modulus of swollen vulcanisates.

(c) Equilibrium swelling data may be related to $\overline{M}_c$ by use of the Flory-Rehner equation[50, 51].

The determination of $\overline{M}_c$ by these techniques gives the physically manifested degree of crosslinking, which may then be related to the chemical degree of crosslinking by using the Moore, Mullins

and Watson equation[52, 53]. The use of this equation is discussed in detail in a later section. This procedure is justified by the fact that the determination of crosslink density by a chemical method is virtually impossible with an accelerated sulphur-cured vulcanisate because of the complexity of the system and the formidable obstacles to analysis.

1.3.2.2 Dry Extension

For an ideal network, the statistical theory of rubber elasticity[54-56] states that the force (F) required to sustain a perfectly elastic network in a small extension, is given by:

$$F = fA_oNkT(\lambda - \lambda^{-2}) = 2C_1A_o(\lambda - \lambda^{-2}) \qquad (1\text{-}6)$$

where: λ is the extension ratio (l/l_o)

A_o is the unstrained cross-sectional area

N, the number of network chains per unit volume

T, the absolute temperature

k, Boltzman's constant

C_1 is a convenient elastic constant for a given temperature, and f is a 'front factor'[57, 58, 59] usually taken to be almost unity (but which may be related to the conformational aspects of network chains)[60].

Significant deviations from the predictions of the statistical theory occur at low and moderate extensions. Under conditions of moderate extensions the network approaches a limiting extension where the use of a Gaussian distribution of network chain displacement lengths no longer applies. The error may be reduced by removing the restriction that the displacement length is many times smaller than the contour length of the molecule i. e. the distance between junction points of the molecule is small compared to the length of the molecule as a whole.

This extended theory now provides a description of elastomeric behaviour in the region of moderate or large extensions in contrast to the statistical theory. Equations have been derived by Rivlin and Saunders[52], Mooney[53], and Gent and Thomas[61] for vulcanised rubber. The stress-strain behaviour of dry networks up to moderate strains complies with the Mooney-Rivlin expression[52, 53]

$$F = 2A_o(C_1 + C_2 \lambda^{-1})(\lambda - \lambda^{-2}) \qquad (1-7)$$

where: C_1 and C_2 are constants having units of force per unit area.

C_1 is identifiable with that prediced by statistical theory[62, 63]

If the front factor, f, is assumed to be unity, then

$$C_1 = \tfrac{1}{2}NkT \qquad (1-8)$$

$$\text{or} \quad C_1 = \tfrac{1}{2}\rho RT(\overline{M}_c)^{-1} \qquad (1-9)$$

where: ρ is the density of the rubber

$\overline{M}_c$ is the number average molecular weight of the chain segments of the rubber between adjacent crosslinks, and

R is the universal gas constant.

Hence the crosslink density is $\frac{1}{2}\overline{M}_c$.

Ideally, according to equation (1-7) a graph of $F/(\lambda - \lambda^{-2})$ against $1/\lambda$ should be a straight line of slope $2A_oC_2$. A limitation of equation (1-7) occurs at high extensions, where values of $F/(\lambda - \lambda^{-2})$ are higher than predicted. This was initially associated with strain induced crystallisation[64, 65] but later work indicates the deviation to result from the finite extensibility of the network chain segments[66-71]. Taking data obtained at a variety of extensions and using the graphical procedure outlined above, both constants C_1 and C_2 may be obtained, and the degree of crosslinking may then be calculated using equation (1-9).

Gumbrell et al[63] have shown experimentally that whilst C_1 appears dependent on the density of crosslinks, the value of C_2 does not. C_2 does not appear either to be greatly affected by the type of rubber in the swollen and unswollen state and tends to zero if the rubber is highly swollen. Boyer and Miller[72] have however been able to demonstrate some variation from rubber to rubber which appears to be related to interchain distance. C_2 appears to have the most significance in tensile tests.

1.3 2.3 Swollen Compression

Measurements on swollen rubbers in extension and compression have indicated that at low or moderate extensions the departures from the predicted behaviour are less than in dry rubbers, whilst in highly swollen samples, the volume fraction of rubber in the swollen network $V_r < 0.2$, the deviations can be ignored[63].

The stress-strain behaviour of swollen rubbers is described over a limited range of strain by the modified equation of Mooney, Rivlin and Saunders[52, 53]:

$$F = 2A_o V_r^{-\frac{1}{3}} (C_1 + \lambda^{-1} C_2) (\lambda - \lambda^{-2}) \qquad (1\text{-}10)$$

For high degrees of swelling, C_2 becomes zero[63] and the dependence of stress on strain agrees with statistical theory[73], thus reducing equation (1-10) to the Gaussian expression[54]:

$$F = 2A_o V_r^{-\frac{1}{3}} C_1 (\lambda - \lambda^{-2}) \qquad (1\text{-}11)$$

Rearrangement of this equation gives an expression for C_1, i.e.

$$C_1 = \frac{F V_r^{\frac{1}{3}}}{2A_o (\lambda - \lambda^{-2})} \qquad (1\text{-}12)$$

When the strain induced by a compression stress is measured,

F is the compressive force,

A_o the unswollen cross-sectional area,

V_r the equilibrium volume fraction of rubber in the swollen sample, and

λ the actual compression ratio of the sample.

When considering the deformation of a swollen rubber in compression using the approximations introduced by Cluff, Gladding and Pariser[74] and extended by others[75-79], equation (1-12) may be rewritten as [74-76]:

$$C_1 = \frac{F}{\Delta h} \cdot \frac{h_o}{6A_o} \qquad (1\text{-}13)$$

where: F is the load producing a deformation Δh on the equilibrium swollen sample, and

h_o and A_o are the unswollen height and cross-sectional area of the sample respectively.

C_1 may be determined from the slope of the plot of the compressive load F against the experimental deflection Δh, h_o and A_o having been determined by mensuration.

Using a more refined approximation, Khadin and Smith[78] arrived

at the following expression:

$$C_1 = \frac{F}{\Delta h} \cdot \frac{h_o}{6A_o} \left[\frac{1}{1 + V_r^{\frac{1}{3}} \Delta h \, h_o^{-1}} \right] \qquad (1\text{-}14)$$

Kay, Moore and Thomas[77] derived an exact equation involving no approximations from which it is possible to calculate C_1 from a single compression measurement:

$$C_1 = \frac{F h_o h_d^2}{2A_o (h_d^3 - h_s^3)} \qquad (1\text{-}15)$$

where: h_s and h_d are the heights of the swollen undeformed sample and of the swollen deformed sample, respectively.

Melley and Stuckey[79], using no mathematical approximations, have rewritten equation (1-15) in terms of more meaningful parameters:

$$C_1 = \frac{F V_r^{\frac{1}{3}}}{2A_o} \left[\frac{3h_s \Delta h^2 - 3h_s^2 \Delta h - \Delta h^3}{h_s^3 - 2h_s^2 \Delta h + h_s \Delta h^2} \right] \qquad (1\text{-}16)$$

Although (1-15) and (1-16) are much more accurate forms of the expression for C_1, the difficulties normally experienced with the measurement of the swollen compressed and uncompressed heights of a sample, usually means that (1-13) is used in practice.

1.3.2.4 Equilibrium Volume Swelling

Cross-linked rubbers swell to equilibrium when immersed in liquids of low molecular weight. For natural rubber gum vulcanisates, the volume fraction of rubber in the swollen gel (V_r) can be related to the number average molecular weight ($\overline{M}_c$) of the rubber network chains between cross-links by the fundamental equation proposed by Flory and Rehner[50, 51]:

$$-\left[\ln(1 - V_r) + V_r + \chi V_r^2\right] = \rho V_o (\overline{M}_c)^{-1} V_r^{\frac{1}{3}} \qquad (1\text{-}17)$$

and which was later modified to[80]:

$$-\left[\ln(1 - V_r) + V_r + \chi V_r^2\right] = \rho V_o (\overline{M}_c)^{-1} (V_r^{\frac{1}{3}} - V_r/2) \qquad (1\text{-}18)$$

where: V_o is the molar volume of the swelling liquid,

χ is an interaction constant characteristic both of the rubber and of the swelling liquid, and

ρ is the density of the rubber.

The use of equation (1-18) requires a precise knowledge of the interaction constant (χ), which must first be determined by substituting in (1-18) the value obtained for $\overline{M}_c$ by an independent method (such as swollen compression or stress-strain measurements) together with the corresponding values of V_r. For vulcanisates using simple crosslinking systems, such as tertiary peroxides,

χ appears to be independent of $\overline{M}_c$ [81, 82, 83]. However, with sulphur cured vulcanisates, χ is affected by the type, level and time of cure; this is caused by the alteration in the chemical constitution of the network chains [84, 85, 86], the lengths of the sulphur crosslinks and the extent of crosslinking during vulcanisation.

χ also changes significantly after treatment of a vulcanisate network with chemical probe reagents [86, 87]. Erroneous values of crosslink concentration may therefore be obtained if the unamended values of χ are used. Porter [88] has indicated the magnitude of errors, which in some cases can be large, that could be obtained in $\overline{M}_c$ determinations if the value of χ is not known with high precision.

Assuming that χ is known precisely, equation (1-19) derived from (1-18) and (1-9) enables the translation to be made of V_r values to values of C_1 and then to the degree of chemical crosslinking via the Mullins treatment [62, 81].

$$- \left[\ln (1 - V_r) + V_r + \chi V_r^2 \right] = \frac{2C_1 V_o \left(V_r^{\frac{1}{3}} - \frac{1}{2} V_r \right)}{RT} \qquad (1\text{-}19)$$

Bristow and Porter [89] have rewritten (1-19) by taking into account the volume fraction of fillers (V_f). Their expression (1-20) yields a value $C_{1(RH)}$ which is the value of C_1 of the

rubber hydrocarbon component of the vulcanisate:

$$-\left[\ln(1 - V_r) + V_r + \chi V_r^2\right] = \left[\frac{2V_o C_{1(RH)}}{RT}\right]\left[\frac{V_{(RH)} V_r^{\frac{1}{3}}}{V_{(RN)}^{\frac{1}{3}}(1 - V_f)^{\frac{2}{3}}}\right] \quad (1-2$$

where: $V_{(RH)}$ is the volume fraction of rubber hydrocarbon componant of the network, and

$V_{(RN)}$ is the volume fraction of the rubber network

1.3.2.5. Calculation of Crosslink Density

The contribution of the term involving C_1 to the force extending the rubber has been identified with that predicted by statistical theory[62, 73, 81]. It was shown that:

$$C_1 = \tfrac{1}{2}NkT = \tfrac{1}{2}\rho RT\overline{M}_{c(phys)}^{-1} \quad (1-2$$

The physical degree of crosslinking equates to

$$\left[2\overline{M}_{c(phys)}\right]^{-1} = \frac{C_1}{\rho RT} \quad (1-2$$

$$\text{or} \quad \overline{M}_{c(phys)} = \frac{\rho RT}{2C_1} \quad (1-2$$

Since the values of C_1 change with conditions and with any pre-treatment, it is necessary to standardise its determination.

Where C_1 is not measured at 25°C, the C_1 value obtained is corrected to 25°C by means of the expression:

$$C_{1(RV)} = C_1 \text{ (measured at } t^{o}C) \times \frac{298}{(273 + t)} \qquad (1\text{-}24)$$

where: $C_{1(RV)}$ is the C_1 term for the rubber vulcanisate at 25°C.

$C_{1(ERV)}$ (extracted rubber vulcanisate) may be corrected to allow for the stiffening effect of non-reinforcing fillers e.g. zinc oxide, by using the expression[90]:

$$C_{1(ERM)} = C_{1(ERV)} (1 + 2.5V_f + 14.1V_f^2)^{-1} \qquad (1\text{-}25)$$

where: V_f is the total volume fraction of fillers in the vulcanisate.

The derived $C_{1(ERM)}$ is for the supercoiled rubber network from which all rubber-soluble extra network materials have been extracted, and from which solid particles such as zinc oxide and zinc sulphide have been removed.

1.3.2.6. Relationship Between Physical and Chemical Degrees of Crosslinking

The determination of C_1 and $\overline{M}_c$ by the physical techniques already described gives the physically manifested degrees of crosslinking. Such values take no account of the contributions due to chain entanglements and chain ends. This problem is overcome by the use of the expression (1-26) derived by Moore, Mullins and Watson[62, 81, 93] which relates C_1 to $\overline{M}_{c(chem)}$ the molecular weight between chemical crosslinks.

$$C_1 = \left[\frac{\rho RT}{2\overline{M}_{c(chem)}} + 0.78 \times 10^6\right] \left[1 - 2.3\overline{M}_{c(chem)}\overline{M}_n^{-1}\right] \text{ dynes cm}^{-}$$

(a) (b) (1-26

where: (a) represents the maximum entanglement contribution, and

(b) is a correction for the effect of chain ends

1.3.3 Measurement of Crosslink Density in Filled Vulcanisates

1.3.3.1 Introduction

So far, the treatment of the use of stress-strain data and swelling measurements for the determination of crosslink concentrations in gum vulcanisates is not valid without modifications for filled systems. In such systems, because of the presence of the filler, the deformation of the rubber component can no longer be related

to the deformation of the test piece as a whole and the theory of rubber elasticity can no longer be applied to the conditions of equilibrium volume swelling or stress-strain measurements.

A further complication arises with stress-strain measurements since the stress-strain behaviour of filler loaded vulcanisates does not follow even at low extensions, the Mooney Rivlin equation[91]. Mullins[91, 92] has shown that the stiffness of filler loaded vulcanisates decreases as a result of extension; the so called stress-softening effect. Accordingly the values of C_1 obtained during the initial extension in stress-strain measurements may be significantly different from those obtained on subsequent extensions. This makes it difficult, if not impossible, to determine accurate values of C_1 from stress-strain measurements for filled vulcanisates.

1.3.3.2 Stress-Strain Measurements

Many attempts have been made to establish a quantitative physical basis for interpreting the stress-strain behaviour of filled vulcanisates. Such attempts[94-99] have led to the derivation of expressions relating elastic modulus E of the filled vulcanisate to the modulus E_o of the matrix (rubber component of the vulcanisate).

Smallwood[96] showed that for spherical filler particles at low concentrations:

$$E = E_o (1 + 2.5c) \qquad (1\text{-}27)$$

where: c is the volume concentration of filler

Guth and Gold[90] added an extra term to equation (1-27) to take into account the interaction between pairs of filler particles and proposed the expression:

$$E = E_o (1 + 2.5c + 14.1c^2) \qquad (1\text{-}28)$$

Guth[97, 98] has further suggested that the departures observed with the more reinforcing carbon blacks were due to their tendency to agglomerate into chain-like clusters. For such materials he proposed (1-29):

$$E = E_o (1 + 0.67fc + 1.62f^2c^2) \qquad (1\text{-}29)$$

where: f is a structure factor describing the asymmetric nature of the aggregated cluster and usually expressed in terms of the ratio of the length to width of the agglomerate.

Mullins and Tobin[99] applied (1-28) and (1-29) to filled vulcanisates containing M. T. black and H. A. F. black respectively. They considered that the ratio of the actual strain in the rubber matrix

to the measured overall strain could be given by a strain amplification factor, X, i.e.

$$X = \frac{E}{E_o} \qquad (1\text{-}30)$$

They believed that during deformation, the matrix is prevented from deforming uniformly by adhesion of the rubber to the surfaces of the particles and thus the overall apparent strain is less than the strain occurring locally in the rubber matrix. By using the above expressions Mullins and Tobin were able to show that vulcanisates containing volume concentrations of filler up to 8% fitted the Mooney-Rivlin equation and their C_1 and C_2 values were similar to those of the unfilled rubber.

Their results were thus consistent with the concept that the elastic properties of the rubber matrix are unmodified by filler and its effective deformation is equivalent to (X) times the measured overall deformation. Although they found that significant departures occurred at higher concentrations of filler, these were still relatively small and to a first approximation, in agreement with the concept of the use of a strain amplification factor. None of the above treatments, however, offers an unequivocal method for determining the degree of crosslinking in the rubber matrix of intermediately loaded vulcanisates.

1.3.3.3 Equilibrium Volume Swelling Measurements

Fillers have much less drastic effects on the swelling properties than on the stress-strain properties of rubber vulcanisates. Swelling measurements, therefore, seem more appropriate for measuring crosslink concentrations in filled systems via the Flory-Rehner treatment[50, 51].

Bueche[100], Kraus[101] and Porter[102] have observed that in filled vulcanisates the apparent values of concentration of chemical crosslinks were in general much larger than the corresponding values in gum vulcanisates. Porter[102] has attributed this apparent increase to one or more of the following reasons:

"(i) the filler may cause an increase in crosslinking efficiency of the vulcanising agents thus leading to additional polymer to polymer crosslinks,

(ii) the presence of the filler may enhance (by some unspecified mechanism) the degree to which existing polymer to polymer crosslinks or physical chain entanglements (or both) restrict swelling of the rubber,

(iii) the filler may restrict the swelling of the rubber because of adhesion of the rubber to the filler surface either by physical adsorption or through the formation of rubber to filler bonds, and,

(iv) the filler may alter the affinity of the swelling agent for the rubber as reflected in the magnitude of the parameter χ."

The apparent concentration of crosslinks at optimum crosslinking has been shown[103, 104, 105] to be directly proportional to the actual concentration of crosslinks in the corresponding gum vulcanisates, and may be represented as:

$$\text{CLD chem (filled)} = K_{chem} \times \text{CLD}_{chem(gum)} \qquad (1\text{-}31)$$

or

$$\text{CLD phys (filled)} = K_{phys} \times \text{CLD}_{phys(gum)} \qquad (1\text{-}32)$$

where: K_{chem} and K_{phys} are constants which are thought to be independent of the vulcanising system employed provided the filler does not undergo any chemical reaction during vulcanisation.

Kraus[106] has developed a theory to account for the restricted swelling in solvents of crosslinked elastomers containing reinforcing fillers. Assuming swelling to be completely restricted at the filler-rubber interphase due to adhesion, he proposed the following relation:

$$\frac{V_{rg}}{V_{rf}} = 1 - \left[3c \left(1 - V_{rg}^{\frac{1}{3}}\right) + V_{rg} - 1 \right] \left[\frac{\varphi}{(1 - \varphi)} \right] \qquad (1\text{-}33)$$

where: V_{rg} is the volume fraction of rubber in the swollen gum phase,

V_{rf} is the volume fraction of rubber in the swollen filled phase,

φ is the volume concentration of filler, and

c is a constant characteristic of the filler.

Other available evidence[102, 107] seems to suggest that (1-33) is not generally applicable.

Lorenz and Parks[105] have shown that the restriction of swelling by fillers is dependent on the concentration of filler. They expressed their results in the following emperical relation:

$$\frac{Q_f}{Q_g} = ae^{-z} + b \qquad (1\text{-}34)$$

where: Q_g and Q_f are weights of imbibed swelling agent per unit weight of rubber in gum and filled vulcanisates respectively, and a and b are constants characteristic of the filler.

z is the weight of filler per unit weight of rubber.

Equation (1-34) is equivalent to[102]:

$$\frac{V_{rg}(1 - V_{rf})}{V_{rf}(1 - V_{rg})} = ae^{-z} + b \qquad (1\text{-}35)$$

The theories proposed by Kraus[106] and by Lorenz and Parks[105] are based on the assumption that the presence of the filler has no effect on the concentration of crosslinks. Porter[102] has however shown that these theories are not generally applicable. He found that H.A.F. black causes an increase of up to 25% in the yield of polymer to polymer crosslinks in conventional accelerated sulphur systems. His results fit the form of equation (1-34) but not (1-35). Based on his data Porter proposed the following relation:

$$\frac{CLD_{chem(app)}}{CLD_{chem(act)}} = 1 + K_{chem}\,\varphi \qquad (1\text{-}36)$$

where: $CLD_{chem(app)}$ and $CLD_{chem(act)}$ are the apparent and actual concentrations of chemical crosslinks in the rubber matrix of the black loaded vulcanisate.

Similarly,

$$\frac{CLD_{phys(app)}}{CLD_{phys(act)}} = 1 + K_{phys}\,\varphi \qquad (1\text{-}37)$$

where: $CLD_{phys(app)}$ and $CLD_{phys(act)}$ are the apparent and actual concentrations of physical crosslinks.

K_{chem} and K_{phys} are constants characterising the filler.

For HAF black it was found that $K_{chem} = 3.63$ and $K_{phys} = 2.6$

Russel[108] has proposed an expression based on Porter's data for obtaining the actual chemical crosslink density in filled vulcanisates:

$$\frac{V_{rg}}{V_{rf}} = 0.56e^{-z} + 0.44 \qquad (1\text{-}38)$$

Russel and Porter's expressions are essentially the same since the former used the latter's swelling data in deriving his expression. It seems reasonable to assume therefore that equation (1-36) should be used in measurements of chemical crosslink concentrations in filled vulcanisates.

1.3.4 Chemical Probes

1.3.4.1 Introduction

Chemical probes have been used in many cases to assess the chemical structure of a vulcanised rubber network. A chemical probe is a reagent that will attack and either destroy or alter selectively specific crosslinks in a rubber vulcanisate but which ideally will not affect the rest of the vulcanisate. For a reagent to qualify as a chemical probe, it must be capable of being introduced homogeneously into the vulcanisate network and should also be easily extracted after completion of the expected chemical reaction.

The following examples of probes will be discussed in detail:

(i) Propan-2-thiol

(ii) Hexan-thiol, and

(iii) Triphenylphosphine.

1.3.4 2 Thiol-Amine Probes

Both propan-2-thiol and hexan-thiol piperidine complexes exhibit ideal probe properties because they are easily transported into and out of a swollen rubber network. Propan-2-thiol cleaves polysulphide crosslinks and hexan-thiol cleaves di- and poly-sulphide crosslinks, both reactants being quantitative in their

reactions. In a typical network, treatment with propan-2-thiol or hexanthiol leaves respectively only the di and monosulphide or monosulphide crosslinks originally present in the network.

The application of thiol-sulphide reactions to rubber analysis was developed by Moore, Saville and Trego[109] and Trego[110]. It was found that a solution of propan-2-thiol (0.4M) and piperidine (0.4M) in n-heptane when swollen into a rubber network cleaved the polysulphidic crosslinks when reacted for two hours at 20°C but was unreactive towards disulphidic, monosulphidic and carbon-carbon crosslinks.

Evans and Saville[111] indicated that the above mixture cleaves di-(2-alkenyl) polysulphide by the formation of an ion-pair possessing enhanced nucleophilic properties so that although organic trisulphides are cleaved, the reaction with organic disulphides is many times slower. Similar evidence is given by Campbell and Saville[112] who studied reactions of propan-2-thiol and piperidine in n-heptane with organic di-(2-alkenyl) di-, tri- and tetrasulphides. The rates of reaction of dialkenyl, tri- and polysulphides were found to be 1,000 times greater than with dialkenyl-disulphides so that after treatment for two hours at 25°C decomposition of the trisulphides had taken place whilst the disulphides were virtually unaffected.

An increase in the nucleophilic character of the reagent is found to increase the rate of cleavage of poly- and disulphide. The reaction with disulphides is sufficiently fast to be useful for distinguishing between disulphides and monosulphides. The monosulphides are not cleaved because the carbon-sulphur bond has a high resistance to nucleophilic displacement.

By using a primary alkane thiol, such as hexan-thiol, at increased concentrations with piperidine, di-(2-alkenyl)disulphides react to equilibrium in a few hours at 25°C,[112] after which time a low concentration of unreacted disulphide is present[112, 113]. The equilibrium is important[114] but it has been shown that when the thiol concentration is in ten-fold excess over the reactant disulphide concentration in a rubber network, virtually no unreacted disulphide remains[113].

Although the absolute rates of sulphide cleavage in a vulcanisate are unlikely to remain the same as for the model systems, the relative rates of cleavage are believed to be similar[112, 113]. A postulated mechanism for the reaction is shown in Fig 1.3. By obtaining crosslink density measurements before and after application of a chemical probe an estimation of the concentration of mono-, di- and polysulphidic crosslinks present in a sulphur vulcanised rubber may be obtained.

Fig 1.3 Reaction mechanism for thiol/amine probes

Propan-2-thiol (PrSH)

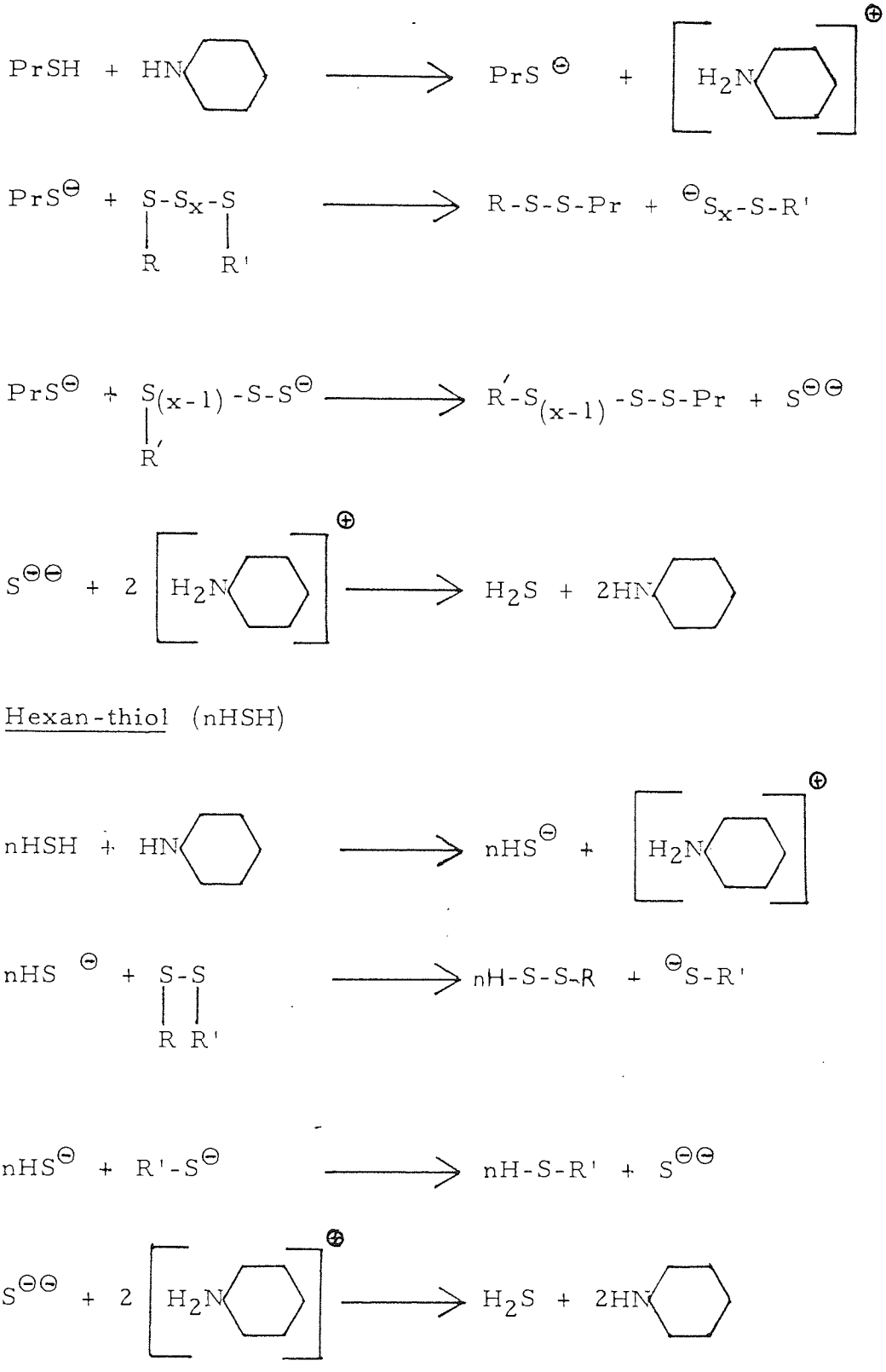

Hexan-thiol (nHSH)

1.3.4.3. Triphenylphosphine Probe

Triphenylphosphine was first used for structural resolution by Moore and Trego[115] using an unaccelerated sulphur vulcanisate. Reaction of the reagent with simple mono-, di- and polysulphides showed that monosulphides are unreactive, the mode of reaction with di- and polysulphides depends upon the nature of R and R' in $R\text{-}S_x\text{-}R'$[116, 117]. When R and R' are both alkyl then triphenylphosphine reacts with the polysulphide to yield the disulphide but if R and R' are both alkenyl then the monosulphide is produced. Unlike the action of thiol-amine complexes triphenylphosphine does not change the crosslink density of a network but only changes the nature of the crosslink. The mechanism of reaction is thought to be as shown in Fig 1.4.

It has been shown[118, 119] that if an accelerated sulphur vulcanisate is composed mainly of alkenyl, alkenyl sulphur crosslinks, the action of dry triphenylphosphine is to desulphurate a polysulphide network into a monosulphidic one, without change in crosslink density. Cleavage of disulphide will occur, however, if triphenylphosphine is moist[120, 121].

By determination of the total sulphur before and after treatment with triphenylphosphine and with a knowledge of the chemical cross-link density, information about main chain modifications in a vulcanisate may be obtained.

Fig 1.4 Mechanism of reaction of triphenylphosphine

For dialkylpolysulphides

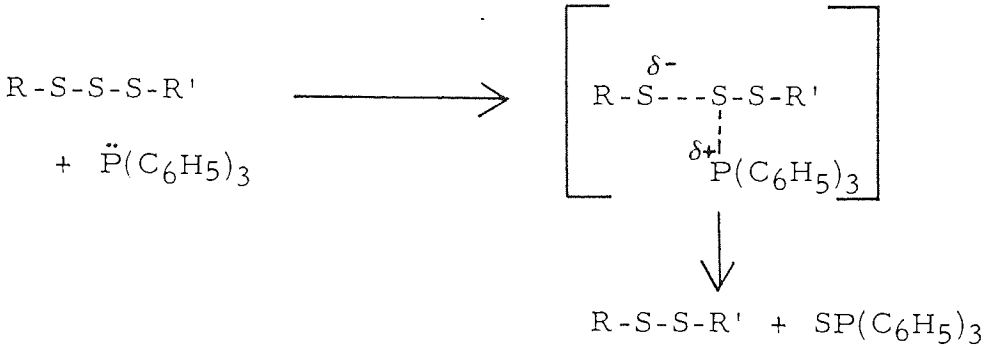

For dialkenyl disulphides, the mechanism is thought to be SN_i in character with an allylic rearrangement.

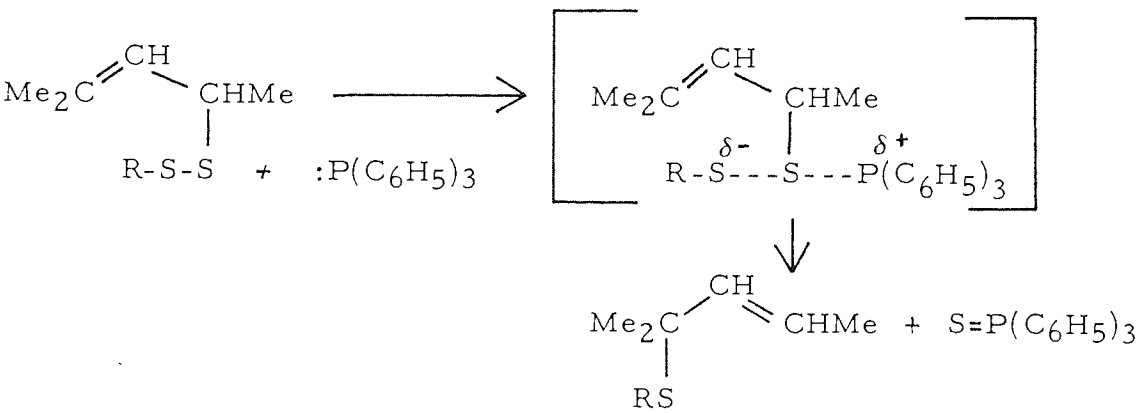

Mechanism of reaction for moist triphenylphosphine

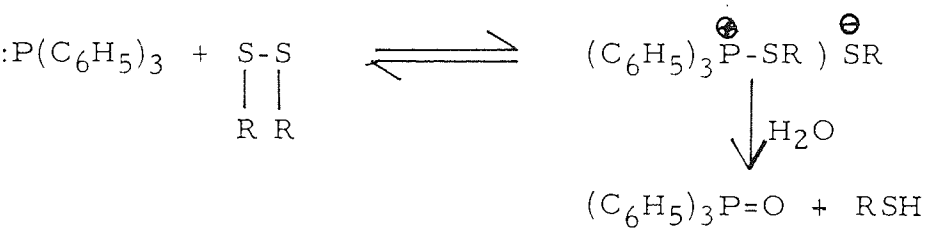

1.3.4.4 The Efficiency Parameter (E)

The molecular complexity of sulphur vulcanised rubber networks can be expressed by the relationship between network bound sulphur and crosslink density. Moore and Trego[122] introduced the use of an efficiency parameter (E) which is given by:

$$E = \frac{\text{No of gram atoms of combined sulphur/gram network}}{\text{No of gram molecules of chemical crosslinks/gram network}} \quad (1\text{-}39)$$

$$= \frac{\left[S_c\right]}{\left[2\overline{M}_{c(chem)}\right]^{-1}} \quad (1\text{-}40)$$

where: $\left[S_c\right]$ is the network combined sulphur, i.e. crosslinks and main chain modifications, and

$2\overline{M}_{c(chem)}^{-1}$ the chemical crosslink density.

E in fact gives a measure of the average number of sulphur atoms contained in a crosslink, bearing in mind that account has not been taken of any main chain modification of the network at this stage.

To determine the amount of combined sulphur, the concentration of sulphur in the network combined as zinc sulphide ($S^{=}$) is subtracted from the total concentration of sulphur (S_T) in an extracted vulcanisate:

$$\left[S_c\right] = \frac{S_T - S^{=}}{3200} \quad \text{gram atoms} \quad (1\text{-}41)$$

where: S_T and $S^=$ are expressed in per cent concentration.

Values of E becomes of further significance when compared with a second parameter E', the efficiency of vulcanisation after treatment with triphenylphosphine when all crosslinks have been converted to monosulphide. E' is determined by measuring the concentration of total sulphur in the extracted vulcanisate after treatment with triphenylphosphine, the degree of chemical cross-linking and zinc sulphide concentration remaining the same. If all the sulphur at this stage is present as monosulphide crosslinks E' = 1. Accordingly value E' - 1 represents the number of sulphur atoms per crosslink combined in the network and not involved in chemical crosslinks.

If it is assumed that polysulphidic 'removable' sulphur is found only in crosslinks then the average number of sulphur atoms in a crosslink may be represented as E - (E' - 1). However, there is a possibility that sulphur may be removed from other sources apart from crosslinks[123] e.g. pendant accelerator groups.

Another parameter used to obtain information regarding a vulcanisate is the concentration of zinc sulphide formed per chemical crosslink generated during vulcanisation, the F-value. F is defined as the number of gram ions per gram mole of chemical crosslink present per gram of rubber hydrocarbon in the network[123]:

$$F = \frac{\left[S^{=}\right]}{\left[2\bar{M}_{c(chem)}\right]^{-1}} \qquad (1\text{-}42)$$

Low yields of zinc sulphide per crosslink formed are associated with efficient use of sulphur while high yields reveal inefficient use of sulphur as a crosslinking agent.

1.4 Fatigue of Vulcanised Rubbers

1.4.1 Introduction

Rubber is used in a vast number of articles which subsequently find service under very stringent and demanding conditions and these may cause it to fail. Of the many possible observed modes of failure of vulcanised rubbers, one particular process, fatigue, is of great importance.

Fatigue could be defined as any deterioration in the properties of a material caused by prolonged action of a stress or strain. This general definition would however include creep and stress relaxation. The term 'fatigue' is usually reserved only for the gradual weakening and eventual fracture of a material brought about by repeated cyclic deformations at strains lower than the breaking strain.

The rubber literature abounds with studies on the fatigue of vulcanised rubbers. These can be broadly classified into attempts

to explain fatigue as a physical phenomenon (mechanical fatigue), in which the response to a continuous external stimulus in the stretched rubber is considered or as a chemical phenomenon (chemical fatigue) in which the effects of atmosphere, radiation, temperature etc., on the scission of crosslinks or main chains are considered.

1.4.2 Initiators of Fatigue Failure

The presence of inhomogeneities and naturally occuring flaws or cuts are two of the chief initiators of fatigue failures in rubber vulcanisates.

Hess and Burgess[124] and Smith and Black[125] have reported that during fatigue reagglomeration of materials, normally dispersed in rubber occurred to form areas of heterogeneity. These areas of inhomogeneities serve as loci of fatigue failure by forming highly localised stress concentrations[126, 127]. During fatigue, cracks will form and grow when the ultimate elongation is exceeded locally in such an area of the stress concentration.

Angioletti[126] discussed the effects of inhomogeneities on cracking, by introducing small discs of metal into vulcanised rubber and following the effects on cracking by photoelasticity. He showed that a more severe stress concentration is formed when

no bonding occurs between the discs and rubber. Such findings were suggested to apply to inhomogeneities of all kinds. Flaws or cuts are effectively similar to inhomogeneities. They are formed by accidental damage during processing or in service. Flaws are also formed from voids in the vulcanisate caused by air entrapped during vulcanisation.

The different initiators of fatigue discussed above are usually superimposed and the relative parts played by each of them in determining the formation of cracks are not easily defined which makes any analysis of their separate contributions very difficult.

1.4.3 Fracture Mechanics

The basic processes of cut growth under static and dynamic conditions have been extensively studied[127-140] in the laboratories of the Malaysian Rubber Producers Research Association (MRPRA). It was shown that a cut would grow only if the energy required to form two new surfaces at its tip was less than the energy available at the tip of the crack owing to the applied stress[127, 128].

The energy available per unit area of growth is termed the tearing energy, T, and is defined by[129]:

$$T = -\frac{\delta U}{\delta A} \qquad (1\text{-}43)$$

where U is the total elastic strain energy stored in the sample, and A is the underformed area of one fracture surface of the crack.

When expressed in terms of T, the cut growth behaviour of rubbers is shown to be independent of the shape of the test piece used, and is a basic characteristic of the vulcanisate[127-130].

The magnitude of the tearing energy may be calculated from readily measurable parameters for various simple forms of test piece[129, 130, 131]. A test piece strip containing an edge cut of length c, which is under tension, has a tearing energy given by the expression[129]:

$$T = 2KWc \qquad (1\text{-}44)$$

where: W is the strain energy per unit volume in the region of the test piece removed from the cut, and

K is a slowly varying function of the extension ratio[132].

For repeated cycling through zero strain, the crack growth per cycle may be expressed by:

$$\frac{dc}{dn} = f(T) \qquad (1\text{-}45)$$

where: c is the crack length in the unstrained state,

n is the number of cycles, and

T is the maximum tearing energy attained during the cycle.

The number of cycles (n) required for a crack to grow from a length c_1 to c_2 would then by given by:

$$n = \int_{c_1}^{c_2} \frac{dc}{f(T)} \qquad (1\text{-}46)$$

which can be evaluated provided that the relation between T and c, which depends on the sample shape[128-130] and type of deformation, is known.

For a natural rubber gum vulcanisate under dynamic deformation, the rate of cut growth is proportional to the square of the tearing energy[134]:

$$\frac{dc}{dn} = \frac{T^2}{G} \qquad (1\text{-}47)$$

where G is a cut-growth constant.

Combining equations (1-44) and (1-47) and integrating

$$n = \frac{G}{(2KW)^2} \left[\frac{1}{c_o} - \frac{1}{c} \right] \qquad (1\text{-}48)$$

where n is the number of cycles causing the cut to grow from length c_o to c.

When n is large compared to c_o, equation (1-48) becomes:

$$N = \frac{G}{(2KW)^2} \cdot \frac{1}{c_o} \qquad (1\text{-}49)$$

where N is the number of cycles to failure or the fatigue life.

The predictions of equation (1-49) have been verified[127, 128] by experiments on test pieces containing edge cuts of various lengths. When fatigued to failure without any cut, c_o becomes the effective initial flaw size. The flaw size required to give the best quantitative correlation is 2.5×10^{-3} cm for natural rubber[127, 134] and about 5×10^{-3} cm for SBR[128]. Such flaws have been observed in rubber[135, 136, 137] due to moulding or die stamping imperfections, particulate impurities or other sources of inhomogeneity.

Lake and Lindley[135, 138, 139] have shown that there is a minimum tearing energy, T_o, at which mechano-oxidative cut growth can occur. At tearing energies less than T_o, cut growth is attributable solely to chemical attack by ozone and is normally very much slower than mechano-oxidative cut growth. At tearing energies above T_o, there is a rapid increase in the cut growth until catastrophic failure occurs at T_c. When T_o is exceeded, the cut growth behaviour appears to be controlled by the mechanical hysteresis of the rubber at high strains. T_o is of the order of 5×10^{-7} Joules/m^2 for a range of elastomers[139] including NR and SBR, which have widely

different strength properties, under relaxing conditions. The similarity of T_o values for different elastomers prompted an attempted explanation of the occurrence of T_o in relation to the carbon-carbon bond strength of the elastomers[140] and fairly good agreement with experimental results has been obtained.

It is found that there is a critical strain (Σ_o) in fatigue tests corresponding to T_o below which the number of cycles to failure increases rapidly. The fatigue limit for natural rubber in simple extension is approximately 75% extension if during the cycle the sample is allowed to relax completely. This critical strain constitutes a mechanical fatigue limit for a rubber, which is analogous to the fatigue limit found in metals[138, 139].

1.5 Factors Affecting Crack Growth and Fatigue

1.5.1 Effect of Strain and Strain Cycle

Studies have shown that a range of rubber vulcanisates show similar fatigue behaviour if during the cycling test the minimum strain experienced by the sample is zero. A distinct difference occurs in the behaviour of crystallising and non-crystallising rubbers when the minimum strain in a test is not zero.

The early work of Busse[141] and Cadwell et al[142] on the effects of strain cycle on fatigue life, is widely quoted in the literature. Busse's results showed that even though energy input decreases slightly as minimum strain energy increases, the effect on fatigue life was mostly the effect of the minimum strain imposed on the samples Busse's results on an NR compound are tabulated in Table 1.3. Cadwell and co-workers[142] have substantiated the results obtained by Busse and have extended their investigations to both shear and compression as well as extension by the use of specimens bonded to metal so that the required strain cycles could be obtained. Dillon[143] has given a qualitative analysis to the observations of Cadwell and co-workers and explains the phenomenon, quoting Busse, that a minimum life near zero strain is associated with 'anisotropy' effects connected with 'semi-racking' in gum natural rubber compounds and a 'mechanically fibrous structure' for black loaded vulcanisates.

Table 1.3 Effect of strain cycle[141]

Strain cycle	Fatigue Life, min
5 - 60% extension	10
10 - 60% extension	25
15 - 60% extension	90
17 - 60% extension	150+
20 - 60% extension	∞

Derham, Lake and Thomas[144] and other authors[135, 145] have shown that crystallising rubbers such as NR and polychloroprene, show a marked improvement in the fatigue life if the specimen is not allowed to relax completely during cycling. It is shown[144] that by increasing the minimum strain during a cycle from zero to 50% a hundred fold improvement in fatigue life is obtained. The effect is considerably smaller in non-crystallising SBR[146].

This effect is widely attributed[140, 144, 147] to strain induced crystallisation at the tip of the crack growth. This can be understood from the mechanism for the effect of hysteresis, since if the minimum strain is sufficiently high, the crystalline structure at the crack tip will be partially retained and will impede the advance of the stress concentration on the next loading cycle. Other authors[148, 149, 150] are in general agreement with this conclusion, whether their work is concerned with tear or observation of cut growth tests. Amorphous rubbers display hysteresis resulting from viscoelastic behaviour[151-153] and, although this is generally of a lower order than that arising from crystallisation, the extent of the hysteresis again markedly influences resistances to crack growth and fatigue.

1.5.2 Effect of Energy Input

An increase in the energy input in a deformation cycle generally results in a decrease in the fatigue life. This is believed to be

due to several factors[142, 154, 155]. Since more work is done on the rubber, the internal temperature generated will increase, which will tend to reduce the ultimate physical properties of the rubber. The strain level in the rubber will also increase and approach locally, the ultimate elongation. The higher strain level may also render the rubber more susceptible to chemical attack.

Greensmith, Mullins and Thomas[155] have compared the effect of strain energy on fatigue life of gum and filled vulcanisates of NR and SBR and found a greater reduction in fatigue life of SBR vulcanisates compared with NR at the same energy input. This effect has also been explained in terms of stress induced crystallisation.

1.5.3 Effect of Frequency of Cycling

The effects of frequency[128] on the cyclic crack growth of SBR can be large at low frequencies (less than 1 c.p.m) where time dependent cut growth predominates. At higher frequencies there is an appreciable cyclic component in the growth and the behaviour is similar to that of natural rubber, for which the cut growth rate decreases by a factor of 2 to 3 over the range 1 to 1,000 cycles per minute. As will be discussed in a later section the latter variation appears to be associated mainly with the oxidative contribution to the growth.

1.5.4 Effect of Atmosphere on Fatigue

The atmosphere surrounding a vulcanisate specimen subjected to repeated deformations can affect its fatigue behaviour in several ways. The most important of these is an alteration of the physical properties of the specimen at or near its surface, whether this surface be the original surface or the new surface generated by a growing flaw. The two primary atmospheric agencies that can influence cyclic crack growth are oxygen and ozone. Table 1.4 shows the effect of atmosphere on fatigue life of EPC black-filled NR vulcanisate tested at room temperature with a frequency of 200 c.p.m.

Table 1.4 Effect of atmosphere[154]

Atmosphere	Cycles to failure
Nitrogen	8.5×10^6, no sign of failure
Air, ozone free	3.5×10^6
Air	2.2×10^6
Oxygen	2.5×10^6
Ozone, 10 p.p.h.m.	1.6×10^6

1.5.4.1 Oxygen

For a long time atmospheric oxygen has been known to play a central role in the fatigue failure of rubbers[156-163]. This

process is distinct from oxidative ageing in that it can and normally does occur in the absence of detectable changes in bulk properties such as modulus; it is thus a localised effect which is restricted to the vicinity of a crack[146, 149, 158]. Slonimskii et al[164] have however found that fatigued rubbers have different physical properties (e.g. resilience) in the direction of stress to those found at right angles to it. From these observations the authors have concluded that not only does stress mechanically activate the oxidative process, but that this must occur by scission of the polymer network structure to give rise to alkyl free radicals. The subsequent reactions of these radicals, besides accelerating autoxidation processes, lead to the restructure of the rubber network.

The effect of oxygen on crack growth differs from that of ozone in that it commences only at tearing energies close to those required to initiate mechanical rupture[139, 146, 165]. The crack growth limit (T_o) is reduced by oxygen by about 2.5 fold at atmospheric pressure for unprotected vulcanisates of NR and SBR, and appears to decrease further with increasing oxygen pressure[166, 167, 168]. The significant role that oxygen can play in fatigue was illustrated by Gent[149] who found that the fatigue life of NR vulcanisate which contains no protective agent is greater in vacuo or nitrogen than in air by a factor that increased from about 5 for a maximum tensile strain of 300% to 12 for a maximum strain of 150%. Similar

behaviour [169, 170] has been observed for SBR. Neal and Northam[156] have presented evidence to suggest that flex-cracking is primarily an oxidative degradation process.

The detailed mechanism of the effect of oxygen on fatigue is quite complex[171-174] and remains obscure. However, it has been suggested [146] that the very high mechanical energy in the rubber at the tip of a crack acts similarly to high thermal energy and accelerates the rate of oxidative bond scission. Gent[149] envisaged two possible roles for the action of oxygen in cut growth and fatigue:

(a) the free radicals produced by the primary mechanical rupture may be stabilised by reaction with oxygen thus preventing recombination, and

(b) to promote oxidative deterioration in the vicinity of the crack tip. The free radicals formed by the mechanical rupture may react with oxygen to form eventually hydroperoxides or peroxy radicals which may then initiate further deterioration.

From examination of the effects of antioxidants and radical acceptors he concluded that (b) was the more probable mode of action. Further evidence supporting this conclusion has been obtained from experiments on butyl rubber. Slonimskii and co-workers[164, 175] believe that the nature of the free radical produced during mechanical scission of the rubber chain has a profound influence upon the

subsequent processes which probably involve molecular oxygen.

1.5.4.2 Ozone

The deteriorating effects of ozone in the atmosphere are reported to have been known to Morse[176] in 1868 while Thomson[177] in 1885 noted that ozonised air had little action on unstretched rubber but acted very rapidly on rubber in the stretched condition. The role of ozone in crack initiation has since been definitely established by a succession of investigators[178-181]. The phenomenological features of ozone cracking and methods of protection that may be adopted have been described in a number of excellent reviews[182-188].

The attack of ozone on rubber differs from that of oxygen in that it has a very low energy requirement and hence ozone cracking can occur at much lower stresses than required to produce mechano-oxidative growth. Studies[189-191] of single crack growth by ozone under constant loading have shown that for a number of rubbers including NR and SBR, the time dependent rate of crack growth is essentially proportional to the ozone concentration and is substantially independent of tearing energy at temperatures well above the glass transition temperature(Tg)[189, 192, 193]. At temperatures fairly close to the Tg, the rate of crack growth is much reduced and varies with temperature in a manner that parallels closely the variation of the viscoelastic behaviour.

Crack growth by ozone does not occur unless the tearing energy reaches a small but finite value (Tz)[189, 194]. Above this, the growth is time dependent and has a rate which is essentially independent of the strain in the rubber, and crack size. Under constant loading the critical energy (Tz) is of the order of a few hundred Joules/M^2 for vulcanisates of most rubbers in the absence of added protective agents[186]. However, for repeated loading Tz is much lower, suggesting that it probably represents the strength of the ozone-degraded material rather than simply a surface energy requirement.

The rate of crack growth is most rapid immediately above a critical strain (Σz) required for cracking to occur and progressively decreases at higher strains. The critical strain corresponds to the strain at which the stress at the largest naturally occurring flaws is sufficient to rupture ozone degraded rubber. The concept of a critical strain in ozone cracking has been substantiated for a number of different vulcanisates and Braden and Gent[189] have suggested that the ultimately important quantity is the critical stored elastic energy (equivalent to Tz) which appears to be essentially similar for different rubbers.

In contrast to the critical stored elastic energy which is sensibly constant, the rate of cut growth and fatigue is markedly dependent upon the nature of the rubber. The well-known resistance of butyl rubber to ozone attack[195] is in fact due to the greater

internal viscosity of this polymer, since plasticisation markedly reduces the ozone resistance[189]. The argument which emerges from the work of Braden and Gent[189] is that the ability of a cut to grow depends upon the ability of the broken polymer chain ends to separate which depends on the internal viscosity of the polymer. It follows that, although ozone attack does take place at the ethylenic double bonds in butyl or butadiene-acrylonitrile rubbers at room temperature, the degree of recombination of the scission products is closer to that of the unstressed polymer than in the case of NR or SBR. The effect of plasticisation is to reduce the rate of recombination and butyl rubber approaches NR in its properties.

The effect of ozone concentration on fatigue life, for fairly rapid continuous cycling, can be calculated by assuming that cracks will grow at the single crack rate when the rubber is stretched and that the ozone contribution is essentially additive to the mechano-oxidative growth. The mechanics of multiple cracking in surfaces under constant load is more complex than in single crack growth and appears under many circumstances to be governed by a boundary layer diffusion control mechanism.

1.5.4.3 Antioxidants and Antifatigue Agents

It is well known that antifatigue agents are effective antioxidants, however, the converse is not necessarily true. Kuzminsky[196]

illustrates the concept that the efficiency of an antifatigue agent is directly related to the antioxidant inhibition period in unstressed rubber and concludes that only the most powerful antioxidants may serve as antifatigue agents.

A useful contribution to the understanding of the mechanism of antifatigue agents has been made by Begunovskaya et al[197]. These authors have compared the action of a typical antioxidant, phenyl-β-naphthylamine (PBN), with 2, 4-diaminodiphenylamine an antioxidant which is less efficient than PBN as a thermal antioxidant but is more effective as a fatigue preventive. In fact there was evidence that during the initial stages of milling, structuring of the rubber occurred with 2, 4-diaminodiphenylamine which led to an increase in bulk viscosity. This gives strong support for the view that during ageing anti-fatigue agents may be actually involved in crosslinking reactions. There is also evidence [197] that, in the vulcanisate, similar structuring may occur which is activated by oxygen.

Extensive comparison of antioxidants and antifatigue agents and their detailed mechanism of action is provided by Scott in a number of reviews and monograms[159, 196, 198].

1.5.4.4 Antiozonants

Protection against ozone attack can be obtained by incorporation in the rubber, normally prior to vulcanisation, of chemicals known as antiozonants. The most efficient of these can modify the single crack growth behaviour in two ways:

(a) by effectively increasing the energy required to initiate growth, and,

(b) by reducing the rate of growth.

The results of numerous investigations into the reaction of polymers with ozone and the effects of antiozonants have been summarised by Razumovsky and Zaikov[199]. The authors suggested the following scheme of chemical transformations to take account of the transition from the initial attack on the double bond to the cracking of rubber:

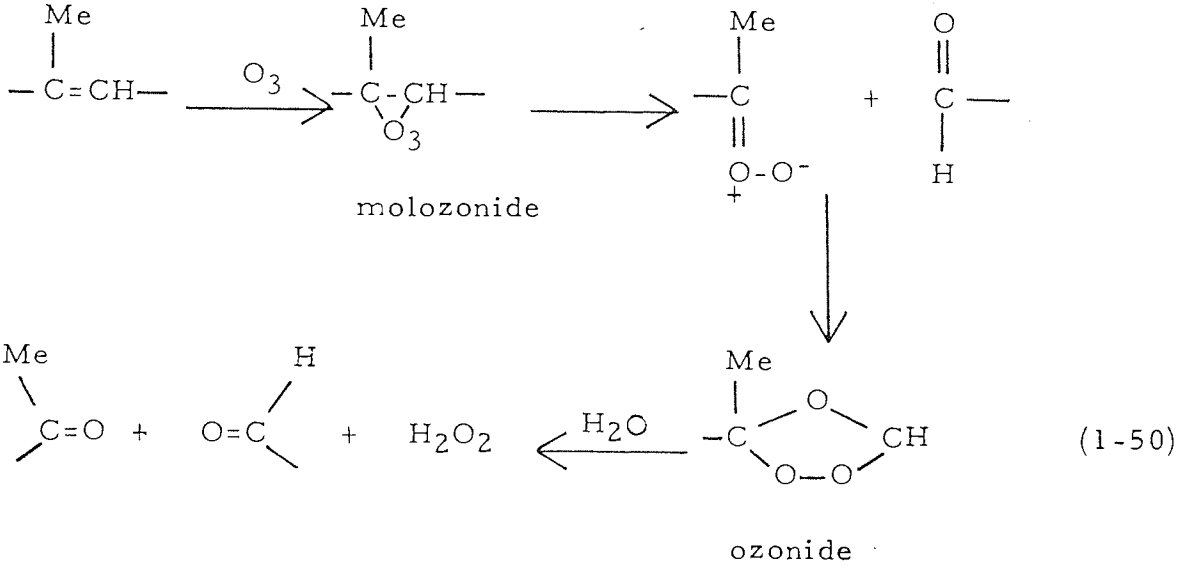

(1-50)

Typically, certain substituted p-phenylene diamines and in particular branched alkylaryl-p-phenylene diamines are effective as antiozonants even in dynamic applications[200-203]. They decrease the rate of crack propogation and increase the tearing energy (T_o) of rubbers.[139, 186] Of the many theories[204-206] which have been proposed for the action of antiozonants, a diversionary theory proposed by Loan et al[185] has received popular support. In this mechanism, the antiozonant is believed to react with the initial reaction products of ozone and rubber thus preventing the formation of high modulus and brittle ozonides which cause the rubber to crack.

The incorporation of sparingly soluble hydrocarbon waxes has been found to give some protection to rubbers against ozone attack. Their activity is believed to be due to the formation of a physical barrier on the surface of the rubber which is not attacked by ozone.[207] The combination of waxes and diamine antiozonants appears to have a synergistic effect on rubbers[159]. Depletion of antiozonants may occur by oxidation[209-211] or more commonly as a result of leaching by water[211, 212] or chemical solutions[213]. It is important, therefore, that antiozonants be tested for specific applications.

1.5.5 Effect of Temperature

The effect of temperature on the fatigue of rubbers is complicated by simultaneous rapid chemical changes of an irreversible nature.

A further complicating factor is the degrees to which the elevated temperature affects the modulus and ultimate elongation of the rubber. Natural rubber compounds, when highly loaded, tend to obey essentially the kinetic theory prediction that the modulus is proportional to the absolute temperature and a maximum in the ultimate elongation is obtained at about 212°C. For SBR and most other rubbers, however, ultimate elongation decreases linearly with temperature and the modulus decreases in many cases as temperature increases. The fatigue life of a highly loaded NR compound would be adversely affected by the increase in modulus with temperature but aided by the increase in elongation. The reverse in both cases would apply to an SBR vulcanisate.

Clapson and Dove[214] have made measurements of fatigue life at temperatures between room and 100°C and have observed that in an inert atmosphere, the fatigue limit increases with temperature while the higher strain growth rate increases. The magnitude of these variations were found to depend on the composition of the vulcanisate and in particular on the polymer. The effect of temperature on SBR was much more marked than on NR. They also observed that the effect of temperature could be considerably modified by the presence of oxygen.

There has been some disagreement on the subject of the overall effect of temperature on fatigue life. Buist and Williams[158], in their early review article on cracking, point out that there is

some ambiguity as to the effect of temperature on natural rubber, but with SBR there is positive evidence that a decrease in life occurs as the temperature increases. Greensmith, Mullins and Thomas[155] agree with these conclusions regarding SBR and also show that NR exhibits the same effect but to a lesser degree. Crack growth tests[154] of black loaded vulcanisates of NR, SBR and CR have shown essentially the same dependence of crack growth on temperature as the fatigue data of Greensmith, Mullins and Thomas. A comprehensive review of high temperature stability of rubber vulcanisates (excluding urethane crosslinked networks) is provided by Stuckey[215].

1.6 Effect of Compounding and Network Structure on Fatigue

The fatigue performance of rubbers depend as much on structure and composition as on the presence of protective agents described in the preceding section.

1.6.1 Effect of Elastomer

The most important variable affecting the fatigue life is the nature of the rubber used in compounding. Generally, natural rubber and butyl rubber show longer fatigue life compared with other unsaturated elastomers such as SBR, neoprene and nitrile rubber. Table 1.5 shows the fatigue life of tread-type vulcanisates, tested

Table 1.5 Effect of elastomer[154]

Elastomer	Fatigue life x 10^5
NR	4.0
SBR (hot)	0.6
CR (Neoprene GN)	0.3
IIR (butyl)	4.0
NBR (Hycar 1001)	2.0

using a strain cycle of 0 to 100% extension, at ambient temperature, and at 475 cycles per minute. The order of fatigue life may, however change with different strain cycles. This may be related to the ability of the rubber to redistribute strains during the strain cycle either due to the ability to crystallise or resistance of the rubber to the effects of ozone and oxygen. It has been shown for example that EPDM appears to have a large ratio of time for crack initiation to that for crack growth than any other elastomer, because of its ozone resistance.

A mixture of different rubbers is sometimes found to have better fatigue life than those of the individual rubbers. The increased fatigue life of binary compounds is usually accounted for by the presence of transitional layers which promote the distribution of stresses more evenly. Shershnev et al[216] have analysed the dynamic properties of rubbers produced from binary compounds,

and found that the density of the three-dimensional network is increased significantly over the additive value. In addition to increased fatigue life, they found that the dynamic modulus increased, the internal friction modulus decreased and the hysteresis losses decreased as the heat generated by dynamic strain decreased.

1.6.2 Effect of Fillers

Fillers are generally classified into two groups (i) reinforcing and (ii) non-reinforcing. The effect of fillers on the modulus of a rubber has been given a comprehensive theoretical treatment by Mullins[217]. The reduction in fatigue limit caused by fillers is due mainly to the increased modulus of the rubber. The tearing energy, however, remains similar to that of the gum base for a wide range of fillers[139]. The critical stress (S_o) corresponding to (Σ_o) is increased by the addition of fillers, the effect being most marked for reinforcing fillers. Although reinforcing fillers such as HAF-black generally reduce considerably the rate of cut growth at tearing energies above T_o[218, 219], they also increase the naturally occurring flaw size[126, 139] so that a non-reinforcing filler (e.g. lamp black) may give superior fatigue properties[139, 230].

The work of Mullins[217] has shown that usually fillers with a small particle size have little effect on fatigue life when

comparisons are made on equal energy input basis. However, the effect of fillers can be influenced not only by particle size but by adhesion or compatibility between the rubber and filler[126, 139]. It would appear that good fatigue properties in a filled vulcanisate are better obtained by using a stiff gum base with minimum filler, rather than a soft gum base with a larger amount of filler.

1.6.3 Effect of Curing Systems and Crosslink Type

The fatigue strength of a rubber is markedly dependent on the nature of the network structure and hence upon the curing system used. It is generally agreed[231-233] that conventionally cured vulcanisates i.e. high sulphur:accelerator ratio, show superior fatigue properties to vulcanisates obtained with EV systems (low sulphur:accelerator ratio) or non-elemental sulphur or peroxide curing systems. Fatigue behaviour may, therefore, be improved by the use of a polysulphidic rather than monosulphidic or carbon-carbon cross-linked network[24, 234, 235]. The superior fatigue resistance of a polysulphidic network has been ascribed[236-238] to the slippage or exchange of polysulphide linkages under stress, thus serving to relieve the stress concentration.

McCall[239] has shown that the superiority of the polysulphidic network is limited to the initial fatigue resistance. He demonstrated that on ageing, a monosulphide network, with poor

initial fatigue resistance, may become a superior aged vulcanisate with excellent retention of fatigue properties. EV and semi-EV systems have therefore found use in applications where retention of fatigue resistance on ageing is critical.

Bristow and Tiller[240] suggested that the degree of main chain modification associated with a polysulphidic network has a significant effect on fatigue. They found that appreciable modification is conducive to good fatigue resistance and that even a monosulphidic network with extensive modification exhibits good unaged fatigue resistance. However, increasing the degree of modification reduces fatigue resistance on ageing[239]. Lal[241] has suggested that polysulphidic crosslinks are not essential for good fatigue resistance. He believes that the properties of this network can be attributed to other factors, including the distribution of network chains. Southern[242] provides an excellent review of the effect of crosslink type on the performance of rubber.

1.6.4 Effect of Cure Time and State of Cure

Increasing the degree of crosslinking decreases the fatigue resistance of rubbers; presumably the capacity of the segments of the rubber molecules to re-orientate is reduced by the resulting increase in modulus and hence increased molecular stresses.

A state of overcure in a conventional vulcanisate, which leads to a significant decrease in the density of polysulphidic crosslinks and the generation of more mono- and disulphide crosslinks, causes a reduction in the fatigue properties. Undercure produces a vulcanisate of low elasticity due to the insufficient formation of crosslinks, thus resulting in poor fatigue life. It has also been shown[243] that an excess of unreacted curatives in an undercured vulcanisate leads to poor ageing properties. Extensive studies on the effect of cure time on fatigue properties have been carried out by Lloyd[243].

1.7 Effect of Fatigue on Network Structure

Maturation reactions are known to occur within a rubber vulcanisate both during vulcanisation and in service[26, 27, 28]. However, some uncertainty exists as to the effects of fatigue on the maturation process. Cunneen and Russel[108, 241] have reported similar changes occurring in the chemical structures of tyre tread vulcanisates. Near the breaker edge, they found on ageing a marked decrease in the concentration of polysulphide crosslinks, an increase in the concentration of monosulphide crosslinks and an increase in the amount of sulphur bound to the rubber network as main chain modifications. They attributed their findings to thermal anaerobic reactions induced by heat build-up. The reduction in fatigue resistance through formation of monosulphide crosslinks was concluded to be the cause of tread lift and blow out.

Gregory[245] Rigby[246] and Stuckey[247] have shown that the deterioration of properties associated with maturation reactions outlined above can occur by fatigue alone, without the influence of heat.

Howard and Wilder[248] observed an increase in crosslink density in tyre treads during service. They showed that the extent of increase in crosslinking was dependent on the curative system used and the nature of the base polymer.

Dogadkin, Tarasova and Goldberg[233], found a slight increase in the concentration of polysulphide crosslinks with solvent extracted SBR vulcanisates flexed at ambient temperatures. A similar increase in polysulphide crosslink density was reported by Cox and Parks[24]. They used black filled accelerated sulphur natural rubber stocks and showed that whilst there was no overall change in crosslink density, a redistribution of crosslinks occurred resulting in a decrease in polysulphide sulphur with an increase in polysulphide concentration. There must therefore have occurred a maturation process that led to a decrease in the average length of the polysulphide crosslink.

Podkolzina, Petrova and Federova[249] have found that the structural changes in networks of vulcanised cis-1, 4-polyisoprene during heat ageing and in fatigue at elevated temperatures were analogous.

However, in fatigue they observed a sharp increase in the degree of main chain modification by cyclic sulphur and in fragments of combined accelerator.

Ohto, Ueda and Murakami[250] have studied the influence of mechanical and chemical factors on stress change and fatigue life in natural rubber gum vulcanisates, under repeated large extensions in air. They found that fatigue life and stress change were influenced by chemical crosslink structure and degree of extension.

Recently, Nando and De[251] have studied changes in network structure in both gum and black-filled NR vulcanisates after subjecting them to different physical tests. They found an increase in the concentration of polysulphide crosslinks in gum vulcanisates after fatigue tests. Polysulphide crosslinks were however found to decrease only in filled vulcanisates.

As may be observed from the foregoing, there is far from complete agreement on the precise effects of fatigue on network structure of vulcanised rubbers. More work would seem to be needed to elucidate the structural changes taking place during fatigue. It is one of the aims of this project to do this.

1.8 Chain Ends as Network Defects in Rubbers

When a vulcanised rubber is stretched only those chain sections between crosslinks are orientated by the external stress and contribute to the retractive force. A terminal chain section (chain end) relaxes despite the stress and does not contribute to the elastic resistance. Flory[252, 253] has suggested that to allow for such elastically ineffective chain ends in a direct determination of the retractive force, it is necessary to deduct from the total number of crosslinks introduced into the system, the number required to produce an infinite network from the elastomer molecules in the sample.

Mullins and Thomas[254] supported the above conclusion and have given a mathematical treatment of the subject, providing a relation which should be valid for all ratios of crosslinks to chain ends. Moore, Mullins and Watson[81, 92] have also developed an equation for the determination of molecular weight between chemical crosslinks in a vulcanisate, taking into account contributions made by free chain ends and molecular entanglements. These equations have been discussed in great detail in Section 1.3.2.6.

Helfand and Tonelli[255] demonstrated the practical consequence of chain end defects with randomly crosslinked cis polyisoprene. They showed that in a sample with a crosslink density of one

crosslink per 100 monomer units, elastically ineffective free chain ends account for 26.3% of the rubber used; with a crosslink density of one per 133 monomer units the ineffective concentration of polymer rose to 35.1%.

Oberth[256] has demonstrated experimentally using polyurethane model networks, that free chain ends are wasted material, as theory predicts, and function in a manner similar to added plasticizer of the same structure. He showed that as in plasticized elastomers, the tensile strength and elastic modulus are reduced approximately by a factor $(1 - V_{E,P})^2$, where $V_{E,P}$ is the volume fraction of free chain ends, plasticizer, or both. The equilibrium volume swelling ratio, (V_o/V), of rubbers having either terminal chains or an equivalent volume fraction of plasticizer were found to be identical provided that they did not differ in crosslink density. However, the volume fraction of 'network rubber' in the equilibrium swollen specimen was different owing to the non-extractability of terminal chains. On this basis, the author proposed a method which allows experimental determination of the volume fraction of loose ends.

Using α, ω-carboxyl terminated polybutadiene and a quantitative polyaziridine chain extension and crosslinking system, Kraus and Moczvgember[257] formed a substantially 'perfect' network and reconfirmed the validity of the equations of Scanlan[258] and others [253, 254, 259] and the elastic ineffectiveness of free chain ends and chain entanglements. The authors presented evidence

to suggest that the apparent deviation of elastomeric vulcanisates from the kinetic theory of rubber elasticity (resulting in the appearance of the Mooney-Rivlin C_2 term in the stress strain relation) arises from a slow relaxation process involving entanglement crosslinks.

Scanlan[258] has given a mathematical treatment of the relationship between the elastic modulus of a rubber vulcanisate and the molecular weight of the primary molecules. In this treatment full allowance is made for elastically ineffective material which exists either as sol or as loose ends in the network. The cases of linear primary molecules with either a random distribution or with uniform lengths are considered, and the results are compared with those of earlier theoretical treatments[253, 254].

Edwards[260] prepared α, ω-dibromopolybutadiene with the purpose of providing end free networks with superior mechanical properties. Hoffman and Gobran[261] made a network free of chain ends and developed better elastic properties by chain extending and cross-linking α, ω-dicarboxyl-polybutadiene.

A further effect of chain ends was probed by Fellers and Rahbar-Semanani[262]. They present evidence to support the idea that β-transition of polystyrene arises from chain end motions. These authors synthesized polystyrenes having both modified and unmodified end group structures and subjected them to dynamic

mechanical testing below their glass transition temperature. The modified structures were shown to influence the β-transition of polystyrene.

Baker and Greensmith[263], have studied the effects of viscosity (and hence molecular weight and chain ends) of compounded rubber on the properties of gum and tread vulcanisates. They showed that the dynamic property of resilience is the most sensitive to the effects of compound viscosity. They established a relationship between resilience and heat build-up as measured in the Goodrich flexometer, and concluded that the trends in these properties are associated with differences in compound viscosity.

1.9 Purpose of the Present Project

A review of most of the available literature on fatigue clearly shows that there is far from complete agreement on the precise effect of fatigue on network structure. However, there seems to be more agreement on the contribution of polysulphidic networks to improved fatigue properties. It is therefore one of the aims of the present study to elucidate the network structurisation process during fatigue of conventionally cured gum and filled natural rubber vulcanisates.

Stress relaxation studies[264-268] of rubber vulcanisates held at constant extension have shown that cleavage and crosslinking reactions occur within the vulcanisate. Andrews, Tobolsky and Hanson[268] proposed a 'two network' theory to describe quantitatively the permanent set taking place in vulcanised rubbers held at constant extension at elevated temperatures. Permanent set was considered to be the result of crosslink cleavage through chain scission and subsequent reformation of relaxed polymer chains. A dual molecular network in which the network chains are of two types: chains which are at equilibrium in the unstretched length and chains which are at equilibrium when the sample is at its stretched length results. Other workers[269-272] have given extensive experimental and theoretical interpretation to the two network model and its validity. However, there seems to be no available report on the distribution of chemical cross-

links after a single extension. It is not known for example, what type of crosslinks make up the secondary network in a conventionally cured rubber vulcanisate subjected to a single extension at ambient temperatures. If is one of the objectives of this project to carry out such investigations.

The comprehensive literature review of section 1.8 illustrates the fact that chain ends in rubber vulcanisates are not elastically effective and represent a wastage of the polymer's contribution to the overall strength of the network. These free chain ends may act as points of weakness during a fatiguing process and their concentration may affect the fatigue life of a vulcanisate. The presence of intentional flaws (e.g. cut initiated fatigue) or the presence of fillers may mask this effect.

Studies on model compounds such as 2-methylpentene-2 and 2, 6-dimethyloctadiene-2, 6 have shown the existence of pendant accelerator (or sulphur donor) groups which are believed to be the precursor to crosslinks. If during mastication of natural rubber, radical acceptors are added which would produce similar types of pendant groups, these would form at the ends of chains broken by the shear action and they should be capable of producing crosslinks during subsequent vulcanisation reaction. In the course of this study, it is proposed to assess the efficiency of such reactions first under ideal conditions with purified natural rubber and then conduct the 'mastication' under an atmosphere of

nitrogen to reduce the competition from indigenous free radicals and oxygen respectively.

CHAPTER TWO

GENERAL EXPERIMENTAL TECHNIQUES

2.1 Materials

Table 2.1 shows a list of the major materials that were used in this project together with the source and any other relevant information. Swelling solvents were of analytical grade. The molar volumes of swelling solvents (Vo), the universal gas constant (R) and the densities of raw natural rubber and solvents used for network structure analysis are quoted from the literature without qualification.

2.1.1 Preparation of bis(diisopropyl) thiophosphoryl disulphide(DIPDIS)

DIPDIS was prepared by oxidation of sodium diisopropyl-dithiophosphate (NaDIDIT) supplied by Albright and Wilson Ltd. The procedure adopted using sodium hypochlorite was that described by Mikeska[273] and modified by Pimblott[274].

100 g sodium diisopropyl dithiophosphate was dissolved in 200 ml of distilled water and cooled to 10°C. Sodium hypochlorite solution

Table 2.1 Major materials and their source

Material	Source	Information
Natural rubber (NR)	Dunlop Ltd	SMR 10
Sulphur (S_8)	Anchor Chemicals	Used as supplied
Zinc oxide (ZnO)	Amalgamated Oxides	" "
Stearic acid (SA)	Anchor Chemicals	" "
HAF-black	Sevalco Ltd	" "
N-cyclohexyl benzthiazole-2-sulphenamide (CBS)	Monsanto Chemicals	" "
N-isopropyl-N'-phenyl-p-phenylene diamine (IPPD)	I. C. I. Ltd	" "
4, 4'-Butylidene bis(2-t-butyl-5-methyl-phenol (SWP)	Monsanto Chemicals	" "
Tetramethyl thiuran disulphide (TMTD)	Monsanto Chemicals	" "
Dicumyl peroxide (DICUP)	Hercules Chemicals	" "
Di-morpholino-disulphide (DMDS)		" "
Triphenylphosphine (TPP)	Aldrich Chemicals	Recrystallised from Toluene
Propan-2-thiol (P-2-T)	Fisons Chemicals	Used as supplied

Table 2.1 continued

Material	Source	Information
Hexane-thiol (HT)	Fisons Chemicals	Used as supplied
Piperidine	Fisons Chemicals	Distilled and dried with sodium
Natural rubber latex (60% DRC)	Vulnax International	Diluted as required
Sodium oleyl p-anisidine sulphonate (vulcastab LS)	Vulnax International	Used as supplied
Sodium naphthalene sulphonate/formaldehyde (vulcastab LRN)	Vulnax International	" "
Zinc diethyl dithiocarbamate (vulcafor ZDEC)	Vulnax International	" "

(12% available chlorine) was added until a slight excess was present. The pale yellow precipitate which formed, was extracted with ether and separated from the residue. The residue was then evaporated in a rotary evaporator and recrystallised from diethyl ether.

Yield = 54 g (60%)

M. Pt = 91°C (90 - 91°C)[274]

Reaction:

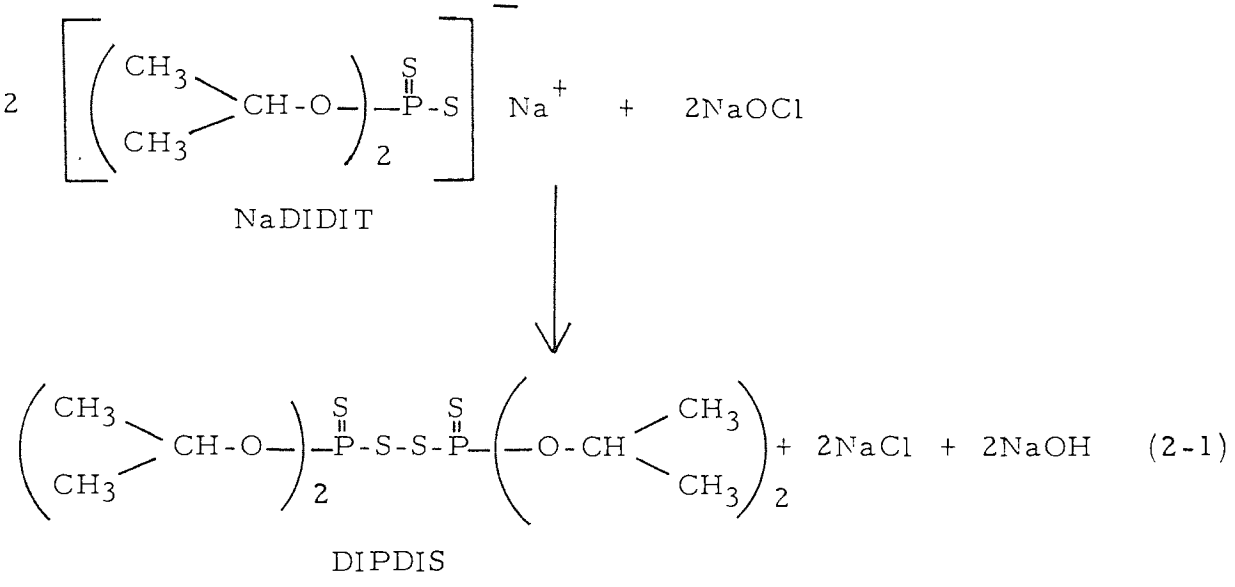

(2-1)

Analysis: Carbon found, 33.22%, 33.44%, 33.08% (calculated, 33.73%); hydrogen found, 6.65%, 6.55%, 6.68% (calculated 6.28%).

The IR spectrum was recorded using a Perkin-Elmer 457 grating spectrophotometer. The sample was contained in a KBr cell and showed the following peaks: Maxima (cm^{-1})

at 2990m, 2920w (C-H stretching), isoproply group; 1450m, doublet 1380-1370s (C-H bending), $C(CH_3)_2$ group; 1180m, 1145m, 1100m, 1020-970s (P-O-C stretching, mainly O-C); 890m, 800s (P-O-C stretching, mainly P-O); doublet 750-650s (-O-P, S P- S); 560-530w (S_2).

where s=strong, m=medium, w=weak

2.2 Compounding of Solid Rubber

2.2.1 Compounding Formulations

Compounding formulations for all the NR vulcanisates used are shown in Table 2.2.

2.2 2 Extraction Procedure

The raw rubber was extracted, when necessary, with acetone under nitrogen for 48 hours to remove indigenous materials. The vulcanisates were also extracted for the same period, when there was need to remove as much extra network material as possible which might otherwise interfere with network structure analysis. All extractions were carried out using a sohxlet apparatus; the extracted raw rubber and vulcanisate were deswollen in vacuo to a constant weight and stored at -20°C until required.

Table 2.2 Compound formulations

Compounding Ingredients (a)	A	B	C	D	E	F	G	H	I	J
NR	100	100	100	100	100	100	100	100	100	100
Sulphur	2.5	2.5			2.5	2.5	2.5	2.5	0.5	0.5
ZnO	5	5	5		5	5	5	5	5	5
SA	2	2	2		2	2	2	2	2	2
CBS	0.6	0.6			0.6	0.6	0.6	0.6		
TMTD			3							
DICUP				1.5						
IPPD					2		2			
SWP						2		2		
DMDS									1.63	1.63
DIPDIS									3	
HAF-Black		40					40	40		

(a) Parts by weight

2.2.3 Preparation of Gum Compounds

Gum compounds were prepared by three mixing procedures:

2.2.3.1 Open Milling

Gum formulations were prepared with a 12" laboratory two-roll mill with friction ratio of 1:1 and 1.25:1, capable of water cooling and steam heating. The compounding ingredients were mixed on the mill in a manner that best suited the particular study being carried out. In a typical milling cycle, the raw rubber was first passed several times through a tight nip before being allowed to band on to the rolls. Zinc oxide and stearic acid were added followed by the addition of the accelerator. Sulphur was always the last ingredient to be added before milling the compound to a required plasticity or for a specified time, to prevent premature vulcanisation.

2.2.3.2 The Vertical Masticator

The Baker-Perkins Vertical Masticator (Fig 2.1) was developed from a small unirotor mixer designed by Watson and Wilson[275]. It consists of a vertical rotor (A) which can turn at variable speeds inside a fixed mixing chamber (B). The rotor and stator are clamped together by means of a collar which is closed by a nut and bolt (C). An O-ring of silicone rubber hermetically seals the

chamber. A variety of designs of the mixing faces on the rotor and stator are available. A 'plough shaped' rotor was used for the present work. The distance between the mixing faces is controlled by a capstan operated screw (D) with left and right hand screw threads so that the shell casing around the rotor can be raised or lowered depending on the direction of the rotation of the capstan. The rotor is powered by an electric motor (E) which is connected to the shaft through a worm-gear (F) and a variable drive V-belt pulley (G); the latter is used to control the shaft speed. The temperature of the masticated compound is recorded by means of a thermocouple.located within about two millimeters of the hardened steel face of the mixer. Some measure of temperature control is achieved by raising a bath of thermostated liquid so that the head of the mixer (H) is completely immersed. In this work, where the lowest practical temperature was required (to achieve maximum mechanochemical efficiency from shear action[7]) a mixture of ice and water was used in the bath.

Either air or nitrogen were circulated through the mixing chamber and in the case of the latter, traces of air were removed by de-gassing the chamber at a reduced pressure for a few minutes and then flooding it with white spot nitrogen. This degassing was repeated three times. During mixing a positive gas pressure of 10 - 15 mm of mercury was maintained.

Fig 2.1 The Baker-Perkins
Vertical Masticator

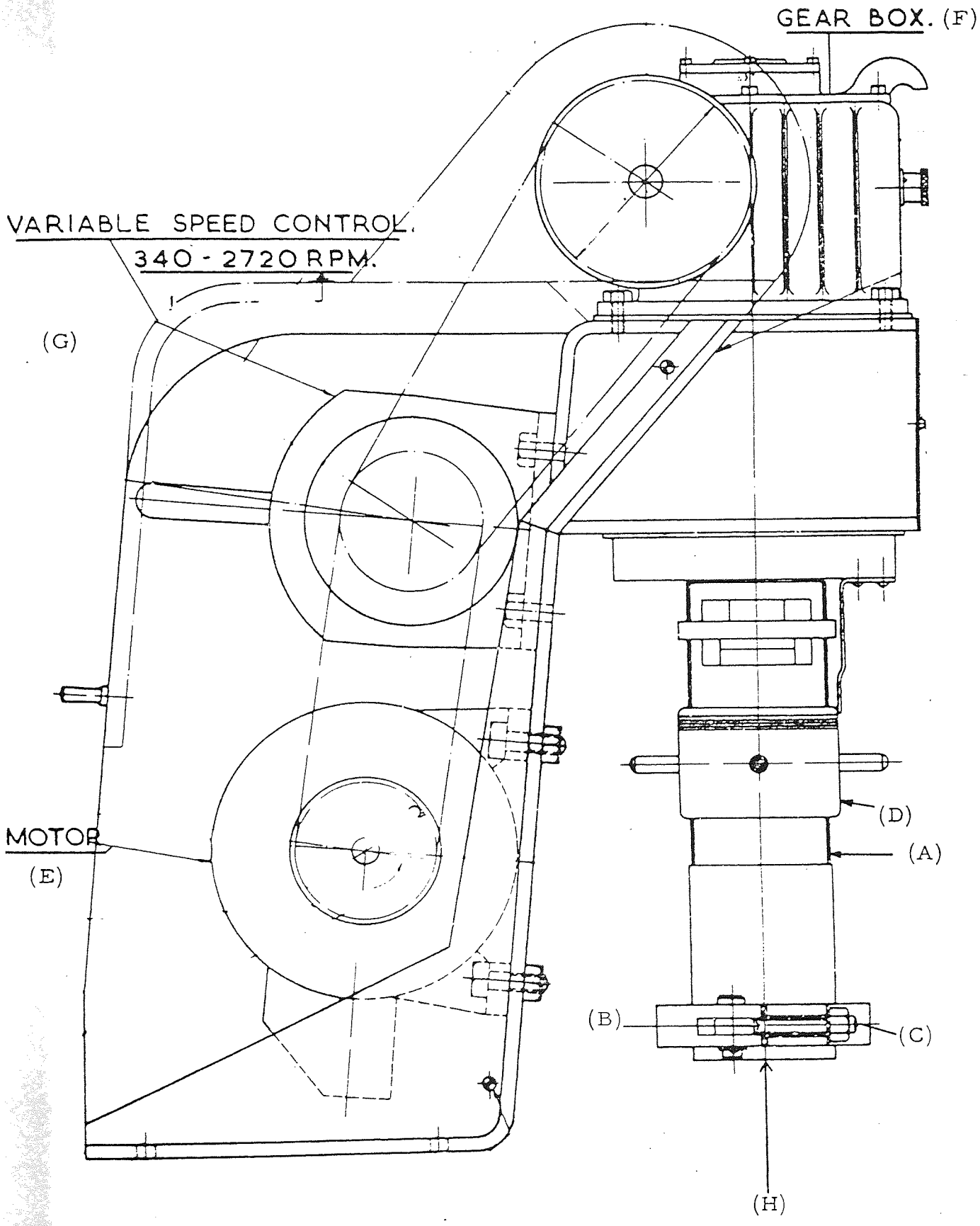

The shear rate exerted on the polymer in the mixing chamber is a function of the distance between the mixing faces, the relative speed of movement of the faces and their surface areas, and the viscosity of the polymer. In this work the shear rate was kept constant by using the same mixing chamber, a constant quantity of rubber (10g); the faces were pulled tightly together by the capstan and the amount of rubber between them controlled their distance apart. The speed of rotation used was 40 r.p.m. as this was the maximum speed that could be used without a significant rise in temperature above 25°C. The time of mastication was dependent upon the extent of degradation required and was determined by the time necessary to reach the desired molecular weight.

2.2.3.3 The RAPRA Torque Rheometer[221-223]

The RAPRA torque rheometer is essentially a small mixing chamber with mixing screws contra-rotating at different speeds. High and low shear rotor speeds are available, and the high rotor speeds corresponding to 60 r.p.m. was used in all mixing. The chamber may be operated either open to the atmosphere or closed by a pneumatic ram. When mixing was done in a closed chamber, the chamber was first flushed with nitrogen and a nitrogen atmosphere was maintained above the closed chamber during mixing. This was to ensure total exclusion of oxygen. The rheometer has a

capacity of 39.0 ml but in the present work 30.0 g of NR was used for effective mixing and the mixing temperature was about 50°C. After mixing, the compound was discharged into cold water to prevent any oxidation of the rubber on exposure to the atmosphere.

2.2.4 Preparation of Black Compounds

2.2.4.1 The Banbury Mixer

The Banbury mixer consists of three major features (i) the feed module, (ii) the mixing module and (iii) the drive module. The feed module incorporates the feed hopper section, through which the materials to be mixed are introduced, together with the weight cylinder and floating weight to force these materials into the mixing chamber. The mixing module includes the enclosed mixing chamber, rotors and the drop-door assembly for discharging the batch. The rotors are contra-rotating with shearing edges to keep the material in constant circulation. Mixing is accomplished between the rotors by four different actions: milling, kneading, longitudinal cut-back and lateral overlaying. These four actions, together with correct temperature control of the mixing chamber, result in high quality compounds with relatively short mixing cycle times.

HAF-black filled compounds were prepared with a laboratory size,

one litre capacity, type B Banbury mixer (Farrell-Bridge) capable of water cooling and steam heating The rotor speed was set at 3 (dial reading) for all mixing. A sulphur-less compounding was carried out in the mixer and sulphur was added to the master batch on an open mill. The mixing cycle used depended on the particular experiment to be carried out. A typical mixing cycle was as follows:

0 minutes, added rubber

2 minutes, added all ingredients except sulphur and black

3 minutes, added one half of black

4 minutes, added remainder of black

6 minutes, dump master batch.

Sulphur added on mill until good dispersion is obtained.

2.3 Vulcanisation of Compounds

2.3.1 The Monsanto Rheometer[276]

The Monsanto Oscillating Disc Rheometer (Model 100) was used to determine the cure characteristics of a compounded stock before curing sheets of the compound. The rheometer measures the changes in shear modulus that occur during vulcanisation of a rubber. An oscillating biconical disc is surrounded with the rubber compound under pressure at the vulcanisation temperature. The sample and

cavity are electrically heated and maintained to within $\pm 0.5^{o}C$ of the set temperature. The disc is oscillated through a 1^{o}, 3^{o} or 5^{o} arc by an eccentrically driven motor. During the vulcanisation the resistance offered to the constant amplitude oscillation of the disc is measured by strain guages and the torque required to maintain oscillation of the disc is plotted on an X-T plotter.

A typical rheograph is shown in Fig 2.2. The data obtained may then be used in the mathematical treatment of Coran[277, 278] to calculate (i) the induction period (t_i),

(ii) the cure rate constant (k)

(iii) maximum torque developed during vulcanisation (R_{max})

and (iv) cure time to optimum torque (t_{90})

The Monsanto rheometer could also be used to establish that uniform dispersion of compounding ingredients had been achieved when preparing the formulation. The rheographs obtained from pieces of stock taken from different parts of the sheet from the mill were compared. When good dispersion was obtained, identical curves were produced.

2.3.2 Press Curing

Curing of all rubber stocks to give the required test sheets was

Fig 2.2 Rheometer curve showing cure characteristics

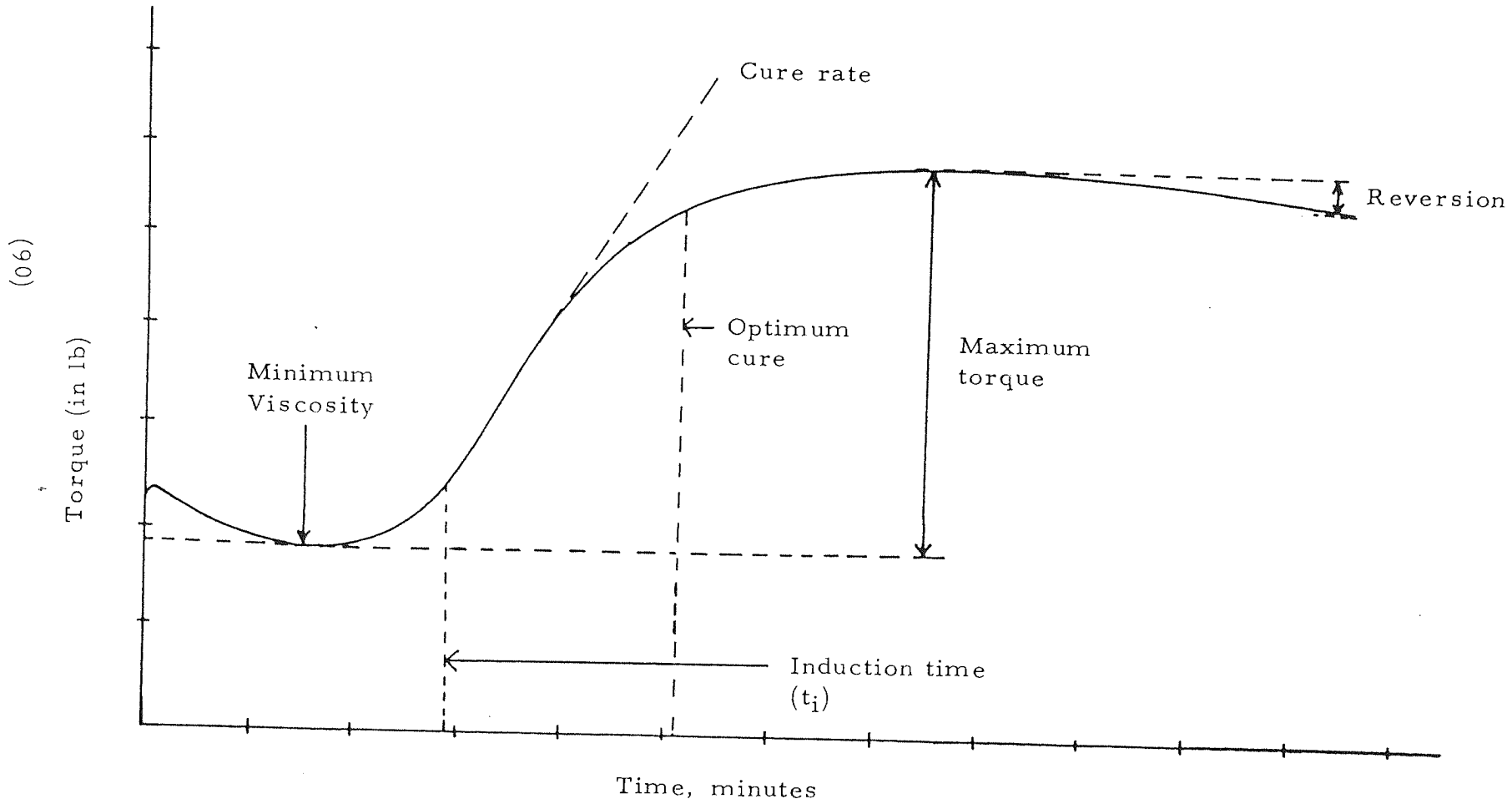

carried out in a mould placed between the heated platens of a press. A known weight of the compound was placed in the appropriate mould and cured at a set temperature. To ease the removal of the moulded sheets from the mould after curing, the mould was first lubricated with a 'mould release agent' before the curing process. The optimum cure times were determined from the Monsanto rheograph at the required temperature. The vulcanisation time was then varied according to the compound, and also the state of cure required. The curing of most compounds was done in a steam heated double daylight press equipped with a thermocouple and maintaining 50 tons on an eight inch ram. In some cases a Bradley and Turton hydraulic press with electrically heated platens was used.

2.4 Preparation of Vulcanisates from NR Latex

2.4.1 Introduction

The preparation of vulcanisates from latex involves:

(i) the mixing of compounding ingredients with the latex,

(ii) the coagulation of the fluid latex compound followed by removal of the water, and

(iii) the vulcanisation of the rubber compound.

As with the solid natural rubber, sulphur is used as the primary vulcanising agent with zinc oxide as activator, in the presence of one or more accelerator. An ultra-fast accelerator is usually employed since there is no danger of scorching as in solid rubber mixes.

2.4.2 Preparation of Aqueous Dispersions of Compounding Ingredients

To ensure uniform mixing of compounding ingredients and to avoid subsequent settling out, all water insoluble compounding ingredients were added to the latex as aqueous dispersions in which the size of the individual particles was of the same order as that of the rubber particles in the latex. The formulations used for the preparation of aqueous dispersions of sulphur, zinc oxide and accelerator (ZDEC) are shown in Table 2.3.

An aqueous dispersion of a compounding ingredient was prepared by placing in a ball mill, the solid ingredient, a dispersing agent and water as in the formulation (Table 2.3). The function of the dispersing agent was to wet the water-insoluble compounding ingredient, to prevent or reduce frothing and re-aggregation of the particles. The ball mill was sealed securely and placed on a pair of horizontal rubber-covered shafts which were mounted parallel to each other and so spaced that the container rode between them. The rate of

Table 2.3 Formulations for aqueous dispersions of sulphur, zinc oxide and accelerator

(a) 50% Sulphur dispersion

Ingredient	Parts by weight
Sulphur	50
Vulcastab LRN(*)	2
Water	48
(Ball-mill for 48 hours)	

(b) 50% Zinc Oxide dispersion

Ingredient	Parts by weight
Zinc oxide	50
Vulcastab LRN	1
Water	49
(Ball-mill for 24 hours)	

Table 2.3 continued

(c) 50% Accelerator dispersion

Ingredient	Parts by weight
Vulcafor ZDEC	50
Vulcastab LRN	1
Water	49
(Ball mill for 24 hours)	

(*) a dispersing agent: a condensation product of the sodium salt of napthalene sulphonic acid with formaldehyde

Table 2.4 Latex formulation

Compounding Ingredients	Parts by weight	
	Wet	Dry
60% NR latex	167	100
10% Vulcastab LS[(a)]	5	1
50% Sulphur dispersion	3	1.5
50% Zinc oxide dispersion	3	1.5
50% Vulcafor ZDEC	2	1
(Cure: 30 minutes at 100°C in air)		

(a) an anionic stabiliser: Sodium oleyl p-anisidine sulphonate

grinding by the mill is related to the diameter of the container. If the mill rotates too rapidly, centrifugal force will cause the charge to adhere to the container wall and no grinding results.

After the mill was allowed to run for the appropriate time, the contents were discharged by covering the outlet with a piece of metal gauze to retain the grinding charge in the container. Dispersions prepared individually were not mixed together prior to addition to the latex because even though no obvious flocculation may be apparent, the particles may aggregate and the quality of the mix could be impaired.

2.4.3 Mixing and Maturation

The mixing of the aqueous compounding ingredients with latex was done in a 500 ml beaker. The formulation used is shown in Table 2.4, tabulated in the order of incorporation of ingredients. The order in which the ingredients are added to latex, is very important in maintaining mix stability. During the addition of the compounding ingredients the mix was stirred slowly but thoroughly. As natural rubber latex is readily co-agulated by friction, contact between the glass rod stirrer and the beaker was avoided.

When mixing was complete, the mix was allowed to mature for a few hours at room temperature to ensure adequate dispersion of the compounding ingredients and to allow any entrapped air bubbles in the mix to rise to the surface.

2.4.4 Casting and Curing

A casting was prepared by pouring a known volume of the mix into an appropriate mould. A vulcanisate sheet for fatigue test was cast with a mould made of perspex with a groove along each length so that the sheet produced had beaded sides. The volume of mix necessary to give a desired sheet thickness was determined in a separate experiment in which the contraction of the cast on vulcanisation was taken into account. The vulcanisation of a cast sheet was carried out in an air oven at $100^{o}C$.

2.5 Physical Tests on Unvulcanised Rubber

2.5.1 Wallace Rapid Plastimeter

Plasticity can be defined as 'ease of deformation' so that a highly plastic rubber is one that deforms or flows easily. Viscosity is the resistance to plastic deformation or flow and hence the inverse of plasticity. The plasticity of a rubber stock is important because

it gives a measure of the processability of the rubber. It also gives a measure of the initial molecular weight of the raw rubber which has an influence on the physical properties of the vulcanisate produced[263].

In the present investigations, the plasticity of a rubber was measured by the Wallace Rapid Plastimeter (H. W. Wallace Ltd) which is a compression type plastimeter. The principle of a compression plastimeter is very simple; the test piece is compressed between parallel plates under a constant force and the compressed thickness measured. The complete test with the Wallace Rapid Plastimeter is divided into two periods. During the first period which lasts for 10 seconds, the test piece is compressed to exactly 1 mm in thickness and at the same time is heated to 100°C; this is known as the preheating and preforming period. During the second period which lasts for exactly 15 seconds, the test piece is subjected to a 10 kg load, so causing it to flow and be reduced in thickness. The final thickness of the test piece expressed in units of 0.01 mm is the plasticity number The greater the plasticity of the rubber, the lower the plasticity number.

2.5.2 Determination of $\overline{M}n$ from Intrinsic Viscosity Measurements

The initial number average molecular weight of rubber was determined

as soon as possible after compounding by measuring the intrinsic viscosity $[\eta]$ of solution of the rubber. Before measuring $[\eta]$, the solutions were filtered to remove spurious particles. The flow times for solvent and solutions in an Ubbelohde suspended level dilution viscometer (Fig 2.3) were then recorded.

2.5.2.1 Clarification Procedure

Solutions (0.2 - 0.5%w/v) of both gum and black compounds were centrifuged in a high speed centrifuge before filtering. The solutions were filtered in turn through grade 2, 3 and 4 glass filters under 5-7 p.s.i. nitrogen pressure. Rubber solutions will not normally pass through a grade 4 filter unless they have been previously filtered through coarser filters. In several cases, and in particular solutions from black compounds, extreme difficulty was experienced, and the filters frequently blocked. The concentrations of rubber in the solutions were determined after filtration by evaporating aliquouts and heating in vacuo to constant weight.

2.5.2.2 Measurement of Flow Times

Viscosity flow times were determined in the Ubbelohde viscometer (Fig 2.3). 5 ml of solution was pipetted into bulb D through A. The solution was then pumped into E by applying a pressure down A with

Fig 2.3 Ubbelohde Viscometer

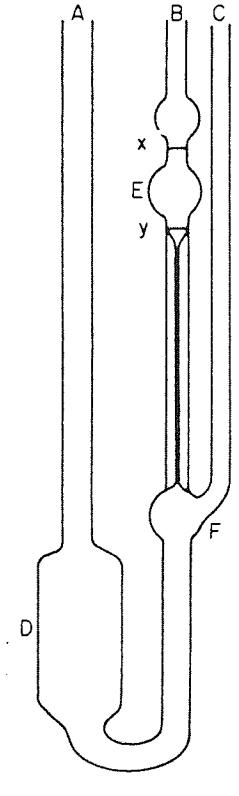

C closed off; the pressure was released and C opened to allow the excess solution to drain back into D. The flow time was the time taken for the solution meniscus to pass between the two marks in bulb E. Flow times were determined in triplicate (agreeing to within $\pm$ 0.2 sec) for four different concentrations (c) of solution. The concentrations were changed in situ by diluting with a known volume of pure filtered solvent. All measurements of flow times were carried out with the viscometer immersed in a thermostatically controlled water bath at 25°C. The flow time of the solvent was determined separately in the same viscometer.

2.5.2.3 Calculation of $\overline{Mn}$

The number average molecular weight of the rubber was determined from the flow time using the modified Mark-Houwink relation[279]:

$$[\eta] = KM^{\alpha} \qquad (2\text{-}2)$$

where $[\eta]$ was obtained from the dependence of $\frac{1}{c}\left(\frac{t - t_o}{t_o}\right)$ against c. Because so many samples were used, the results were evaluated using a computer program (see appendix 1.2). The values of K and α are 7.11×10^{-7} m^3kg^{-1} and 1.25 respectively.

2.5.3 Gel Permeation Chromatography (GPC)

Gel permeation chromatography is a method for the separation of polymer molecules according to their size. GPC was used to observe molecular weight changes ($\overline{M}n$, $\overline{M}w$, $\overline{M}v$ and $\overline{M}z$), as well as shifts in molecular weight distribution occurring during the mastication of natural rubber with DIPDIS.

GPC was kindly carried out by the Polymer Supply and Characterisation Centre of Rubber and Plastics Research Association (RAPRA), using Waters Associates Model 6000 gel permeation chromatograph equipped with styragel columns connected in series. The operating variables were as follows:

(i) Four columns with exclusion limits of 1×10^6 Å, 1×10^5 Å, 1×10^4 Å and 1×10^3 Å.

(ii) Flow rate of the mobile phase was 1 ml min^{-1}.

(iii) The solvent used was tetrahydrofuran stabilized with 2, 6-di-tert-butyl-p-cresol.

(iv) Concentration of test solution was 0.2%w/v.

(v) The instrument was operated at ambient temperature ($\pm$ 1°C).

(vi) The calibration for natural rubber was derived from polystyrene.. Mark-Houwink constants were used for conversion

Fig 2.4 A typical G. P. C. chromatogram

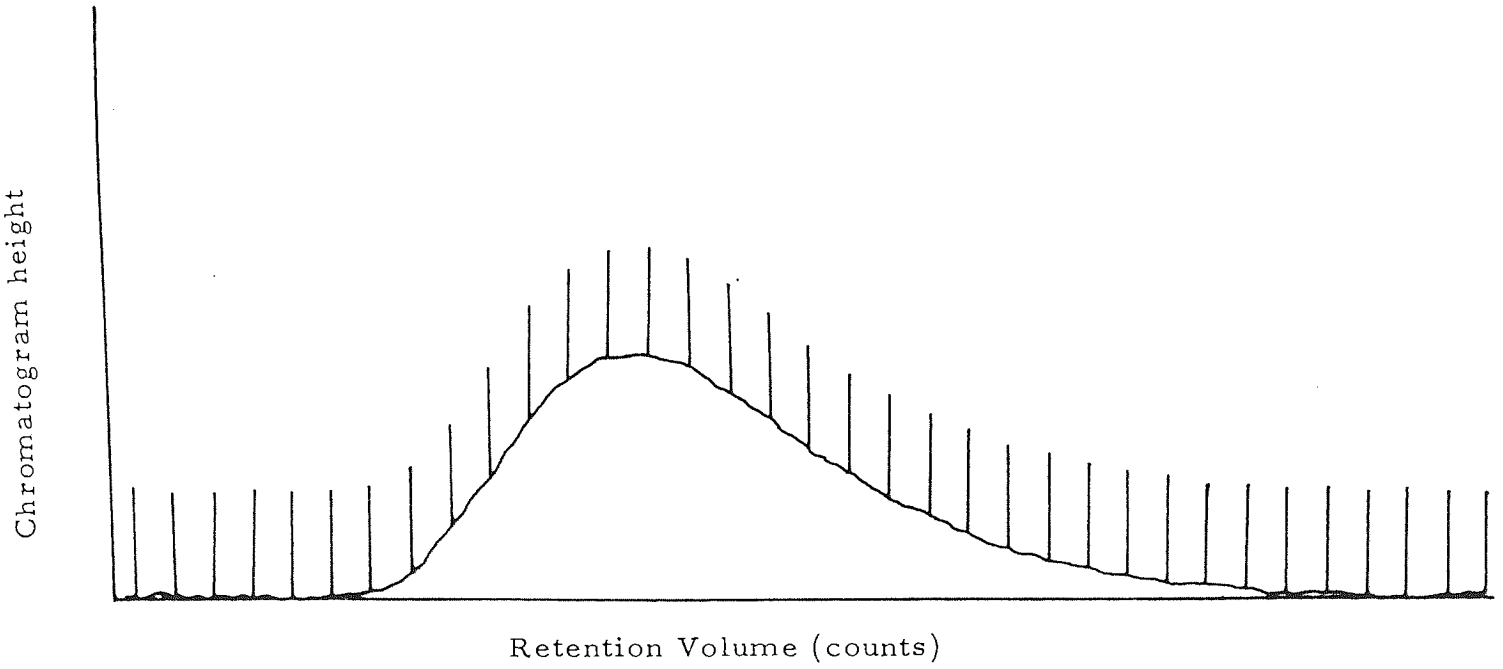

Fig 2.5 Fatigue to Failure Tester

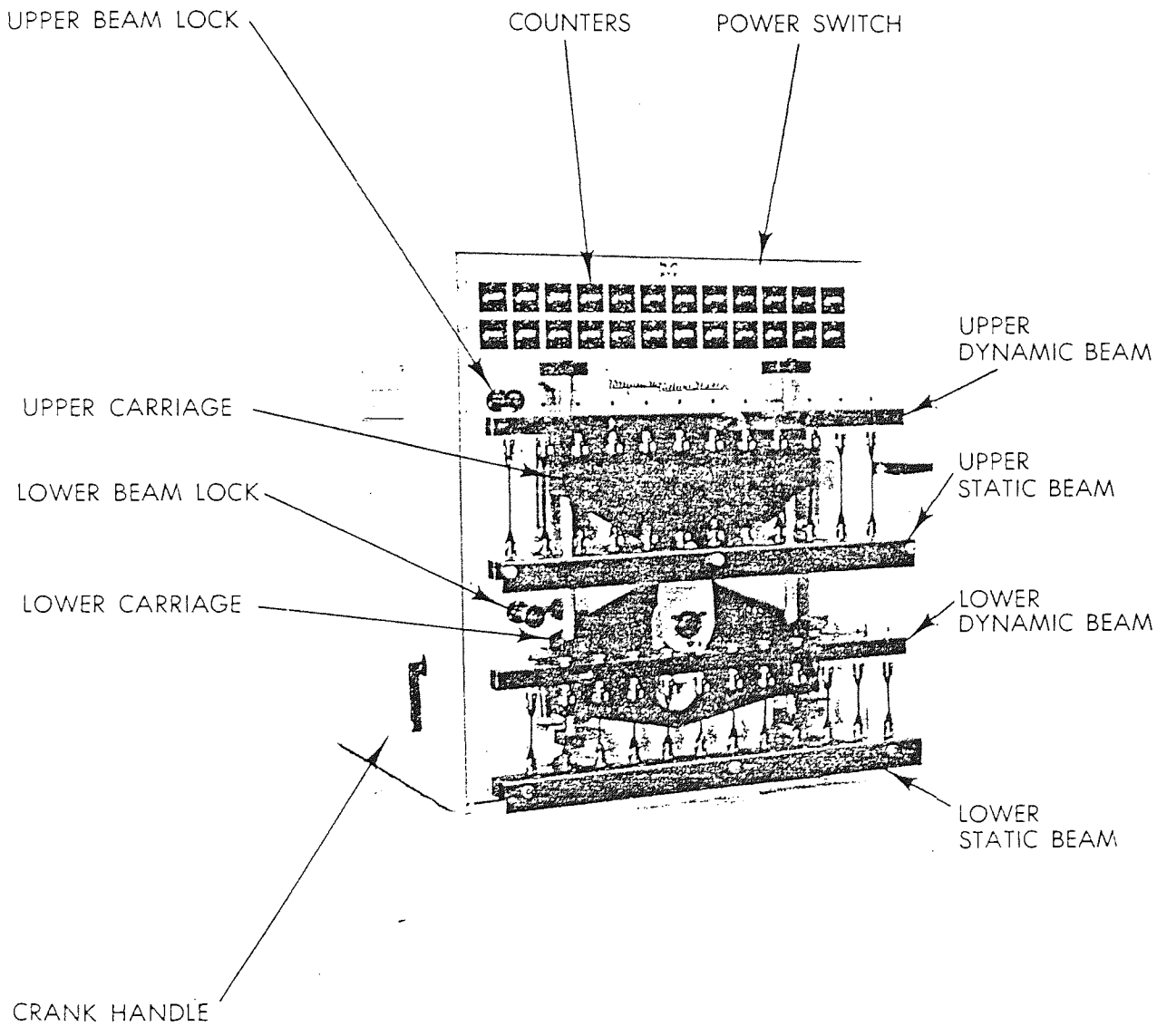

via the universal calibration curve:

Polystyrene, $K = 1.2 \times 10^{-4}\ m^3kg^{-1}$ = 0.71

Natural rubber, $K = 1.09 \times 10^{-4}\ m^3kg^{-1}$ = 0.79

(vii) The calibration was corrected for peak broadening effects and for variation of refractive index with molecular weight.

A digital computer was used to convert the information obtained from the chromatogram into a molecular weight distribution curve data, with the calculation of all the molecular weight averages ($\overline{Mn}$, $\overline{Mw}$, $\overline{Mv}$ and $\overline{Mz}$) and the dispersity ratios. A typical chromatogram is shown in Fig 2.4.

2.6 Physical Tests on Vulcanised Rubber

2.6.1 The Monsanto Fatigue to Failure Tester[280]

The Monsanto fatigue to failure tester (MFFT) (shown in Fig 2.5), was used to fatigue vulcanisate samples. This equipment was originally developed by the Natural Rubber Producers Research Association (NRPRA) to overcome the poor reproducibility associated with the De Mattia Flex Tester. The MFFT can examine simultaneously two banks of twelve samples at two different extensions. The dumbbell shaped samples with moulded beading edges are gripped by

sample clamps attached to beams which ride on cams connected to a 100 r.p.m. motor drive: the required extension is obtained by selecting an appropriate cam. The extension set which develops in samples after a number of cyclic deformations is taken up by adjustable supports after approximately 1000 cycles. This ensures that the preselected strain is maintained throughout the test.

The number of cycles to failure is recorded automatically for each sample by individual fatigue life counters. The lower sample clamps rise approximately 4 mm when a vertical stress is applied to the sample and in so doing operate microswitches which trigger individual impulse counters. A second pair of adjustable cams are attached to a 100:1 reduction gear which actuates the circuit controlling the fatigue life counters and registers one cycle for every 100 cycles of the main drive. Insignificant digits are, therefore, not registered. Failure of the sample automatically stops the appropriate counter.

2.6.1.1 Sample Preparation

Vulcanisates for fatigue tests were moulded as rectangular sheets ($23 \times 7.6 \times 0.18$ cm^3) with a beaded edge: 60 gm of compound was used for moulding each sheet. Sheets were stored for one day in an unstrained state prior to testing and not in contact with other

rubbers. Dumb-bell shaped test pieces were then cut from the sheet at right angles to the grain direction using a B. S. type 'E' cutter. The die cutting edge was always kept evenly sharp and free from any grease or oil as any flaw at the sample edge, caused by faulty cutting, could cause premature failure. The fatigue mould used was designed to give marks at regular intervals along the beaded edge of the cured sheet so that the die can be correctly aligned before cutting. All samples were examined for moulding or cutting imperfections before being tested.

2.6.1.2 Operation of the Monsanto Fatigue to Failure Tester

To ensure fatigue samples were loaded in an unstrained state, the long axis of the chosen cams were aligned manually, using the crank handle to operate the main drive, with a horizontal line engraved on the equipment (both main beams are then resting on their stops and the distance between each set of top and bottom beams is identical). The gap between the top and bottom sample holders was then adjusted to 6 cm by inserting a 6 cm long calibration rod between them and adjusting the thumb nut until a snug fit was attained. Having thus ensured identical starting conditions, each dumb-bell sample was loaded into the sample clamps and locked in place with a spring clip. The counters were set to zero and the equipment switched on. After 1,000 cycles, the equipment was stopped and the drive cams reset

to zero extension as already described and the set which had developed was taken up by means of the adjustable thumb nuts to maintain the original strain. The fatigue tester was then restarted and the samples fatigued to failure or to the desired number of cycles.

2.6.1.3. Expression of Fatigue Results

A minimum of six similar test pieces were fatigued and the fatigue life calculated by using a weighted average known as the J.I.S. average[281]:

$$\text{J.I.S. average} = 0.5A + 0.3B + 0.1(C + D) \qquad (2\text{-}3)$$

where A, B, C, D are the fatigue lives of the samples showing maximum resistance and where $A > B > C > D$. The samples with maximum fatigue resistance were selected because premature failure in the test pieces may be due to flaws and surface imperfections caused by the moulding or cutting processes. The results would not reflect the true value of fatigue life if such imperfect samples were considered.

2.6.1.4. Strain Energy Measurement

The fatigue life of samples, which differed widely in modulus, could

be compared at the same energy input per cycle (strain energy). Strain energy values at the maximum extension ratio used in carrying out the fatigue test, were obtained from the stress-strain curve of a sample which had been cycled either manually or by machine for more than 30 cycles. To obtain the stress-strain curve the width and thickness of the linear region of the dumb-bell sample were first measured with a thickness guage. Horizontal lines were then drawn on the sample in the linear region, when fully extended and the distance between marks was noted when relaxed. The extension ratio of the sample at successive loadings was determined from the extended length of the marked central region obtained by using a travelling microscope. The strain energy at a particular extension was obtained by determination of the area underneath the stress-strain curve up to that extension.

2.6.2 The Hounsfield Vertical Tensometer

The Hounsfield Vertical Tensometer (Fig 2.6) was used to subject vulcanisate samples to single extensions. It is a simple pendulum type machine with five load ranges from 0-20 lb up to 0-320 lb and a variable crosshead speed from 2" to 20" per minute. The load can be recorded on the graph (A) at any time during a test by the use of a manual trigger associated with the elongation scale. A fully automatic recording Extensometer (not shown in figure) is

Fig 2.6 The Vertical Hounsfield Tensometer

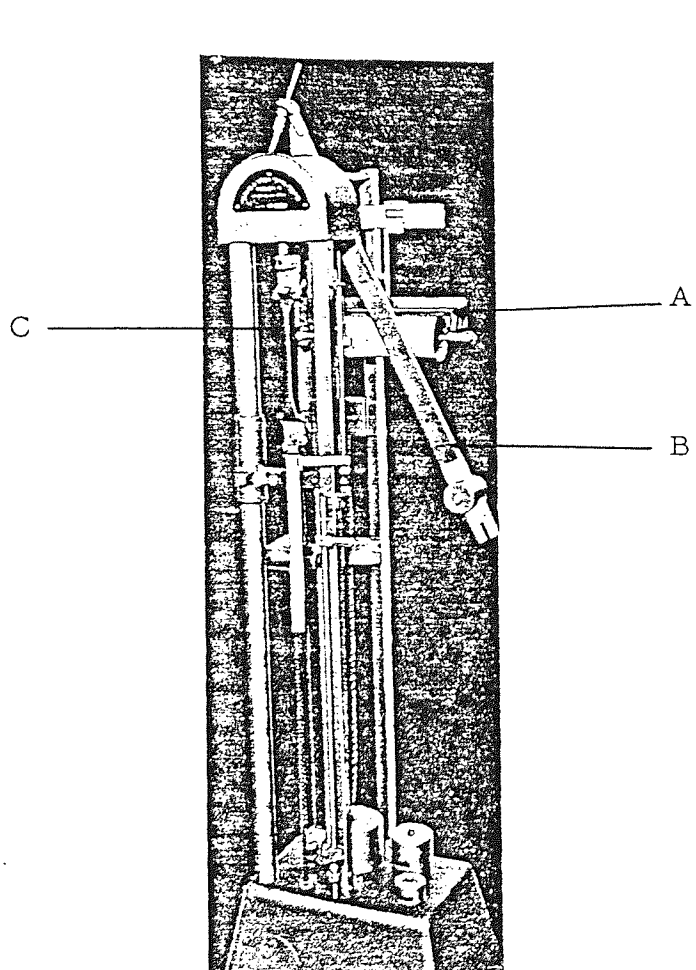

fitted to the machine and measures the elongation by means of freely moving grips attached to the dumb-bell test piece. An electronic control unit, which incorporates the variable speed drive unit and provides automatic starting and stopping of the motor, mounts on a frame fixed to the machine (not shown in figure).

Test pieces similar to those used in fatigue were moulded and cut as described in Section 2.6.1.1. These were particularly suited because the beaded edges ensured that the test pieces did not slip from the grips of the machine. Two bench marks were made at the central portion of each labelled sample and the distance between these marks was measured accurately with a vernier microscope. The appropriate bob weight was attached to the pendulum (B) of the tensometer and the dumb-bell sample (C) was located in the top grip. The two extensometer grips were clamped on the guage length of the sample, making sure that the extensometer sliders were touching. This automatically gives a one inch guage length. The lower grip was then attached to the test piece. The test piece was rapidly extended to the required extension and was left at this extension for the required time. The stress was removed and the sample allowed to recover for a specified time. At the end of the recovery period the distance between the bench marks in the central region was again measured accurately and the set in this region produced by the extension was determined.

2.6.3 Resilience Tester (The Wallace Dunlop Tripsometer)

A proportion of the energy required to deform a rubber is dissipated as heat during recovery from this deformation and thus is not available as elastic energy. The Wallace Dunlop Tripsometer measures the rebound resilience which is the percentage of the energy returned during an impact.

The Tripsometer shown in Fig 2.7 consists of a pendulum (A) which is in the form of a solid steel disc and has a striking ball (B) attached to its periphery. The ball and its mounting bracket add an unbalanced mass of 60 g to the disc. A semi-circular scale (C) graduated in degrees from 0 to 180 is attached to the main casting, and has its centre coinciding exactly with the centre of the pendulum. A pointer (D), containing a Vernier scale, is attached to the pendulum and passes round the periphery of the scale as the pendulum swings or oscilates. The scale and pointer indicate the angular displacement of the pendulum. An electrically operated Pendulum Release Mechanism (G) holds the pendulum in the position of initial displacement until the instant of release. A specimen holder (K) which contains an electrically heated element and an adjustable thermostat is provided so that the specimen can be maintained at the desired temperature.

Fig 2.7 The Wallace-Dunlop Tripsometer

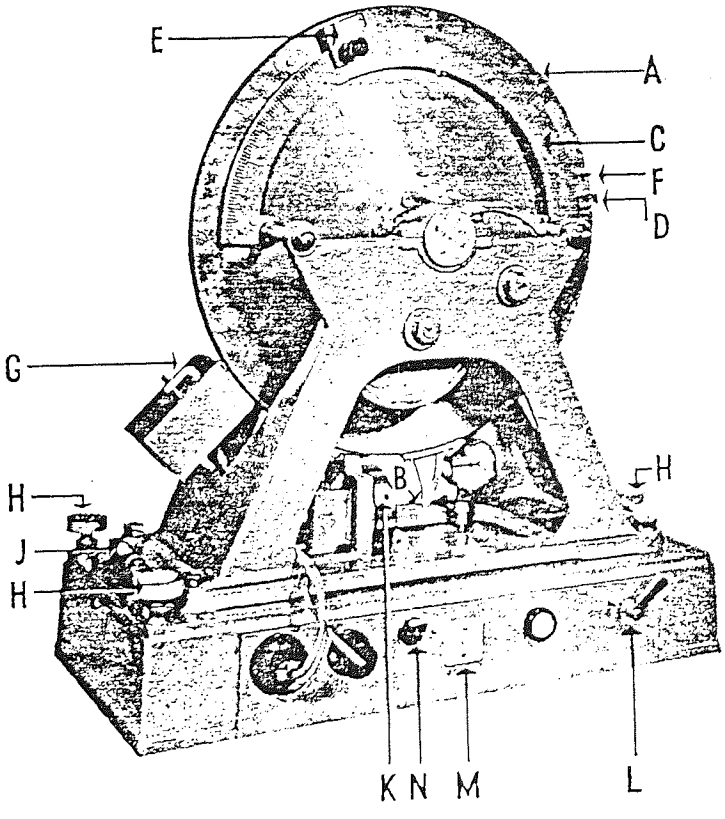

The test consisted of striking the specimen from an angle of exactly 45° and measuring the rebound to the nearest 0.1 degree. The procedure was repeated six times. Two specimens were tested and the results averaged. The percentage resilience was calculated as follows:

$$\% \text{ Resilience} = 100 \times \frac{1 - \text{Cos}\,\theta_2}{1 - \text{Cos}\,\theta_1} \qquad (2\text{-}4)$$

where θ_1 is the initial angle of displacement (45°) and

θ_2 is the angle of rebound.

2.6.4 Relaxed Modulus Apparatus (MR-100)

The term modulus is used to express the amount of pull per unit area required to stretch a vulcanisate to a given elongation. It expresses resistance to extension or stiffness in the vulcanisate. The modulus at 100% elongation (MR-100) represents a modulus at a relatively small extension and as such gives, for non-filled vulcanisates, a measurement that is related to the crosslink density.

The simplified diagram of the apparatus used is shown in Fig 2.8. A test piece (10 x 0.4 x 0.04 cm^3) was held by the two grips (A and B) which can be accurately extended by 100%. The force exerted by this extension was then measured by a beam balance (C) with sliding weights (D) giving a maximum load of 1 kg, accurate to 0.5 g. The balance is

Fig 2.8 The MR-100 Apparatus

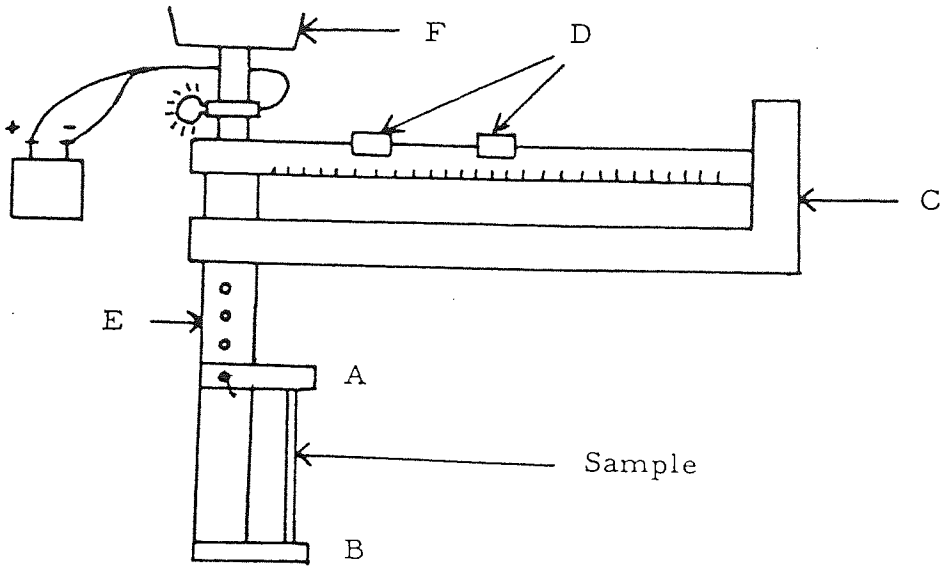

Fig 2.9 The Wallace-Shawbury Stress Relaxometer

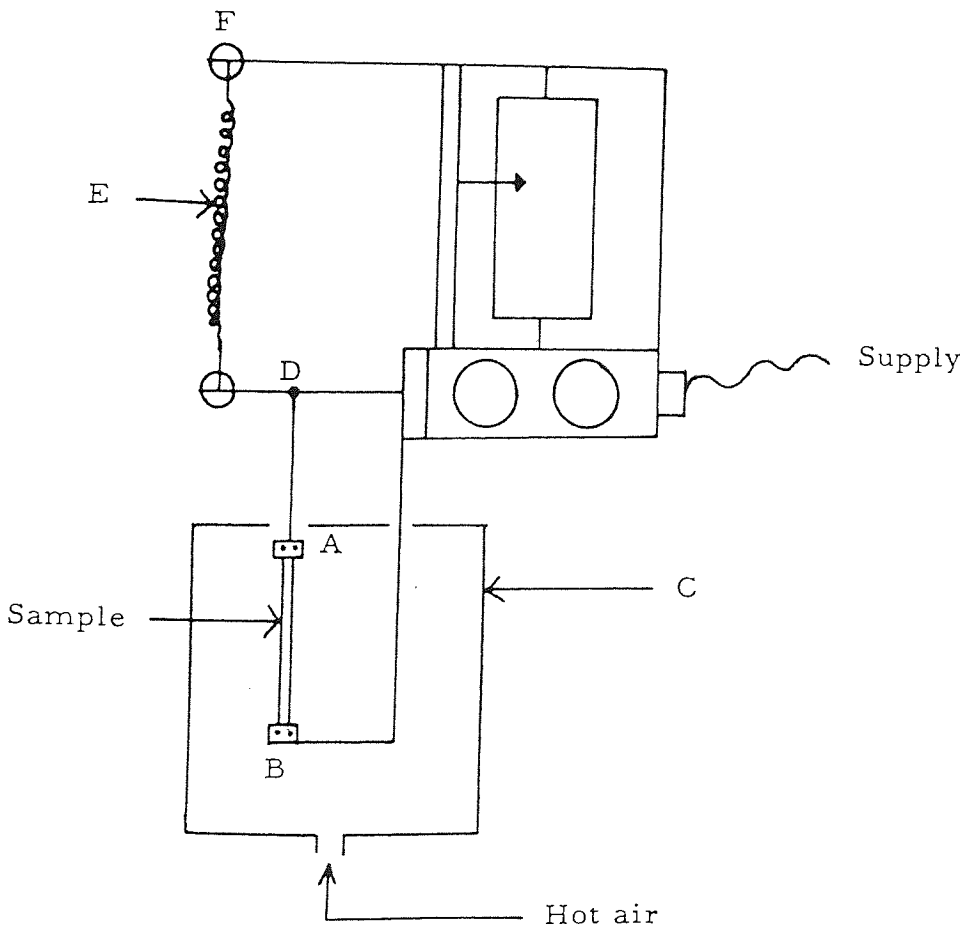

fitted with a device for counter-poising the weight of the sample holder assembly (E) attached to the balance pan (F) so that the change in extension of the test piece during the test period is within $\pm 1\%$.

2.6.5 The Wallace-Shawbury Stress Relaxometer

The stress-relaxation method is based upon the kinetic theory relationship between the tension (F) exerted by a stretched rubber sample and the number (N) per unit volume of stress-supporting network chains, i.e. chain segments between junction points in the network.

$$F = NkTA_o (\lambda - \lambda^{-2}) \qquad (2\text{-}5)$$

where all terms are as already defined for equation (1-6). If the extension ratio λ and the temperature are constant, the stress is proportional to the number of stress-supporting network chains (N), and if, during ageing, a number $(N_o - N)$ of the N_o chains originally present are broken, the ratio of the final tension F to the initial tension F_o is:

$$\frac{F}{F_o} = \frac{N}{N_o} \qquad (2\text{-}6)$$

Thus the decay in stress at constant extension during ageing is a direct measure of the degradation of the elastic network.

Fig 2.9 is a simplified diagram of the Wallace-Shawbury self-recording relaxometer (age tester) used in this work. The specimen (10 x 0.5 x 0.04 cm^3) was clamped between the two grips (A and B), totally enclosed in the constant temperature oven (C) set at the desired temperature and air flow. The upper specimen grip (A) is supported on a horizontal beam (D). The downward force exerted by the specimen is balanced by the upward force applied by the vertical helical stress spring (E). As the specimen relaxes during ageing, the beam (D) tilts very slightly. This movement energises a small electric motor which adjusts the position of the stress spring upper anchorage (F) to change the force applied by the spring until a condition of balance is restored to the beam. Attached to the spring anchorage mechanism is a pencil lead which is in contact with chart paper and change in the force applied by the spring is recorded in the form of a curve on the chart paper.

Although this equipment can measure intermittent relaxation, only continuous relaxation was measured in this work. When operating in this position, the specimen was held continuously at a fixed extension and the recorder gives a continuous trace of relaxation on the chart vertical axis. The specimen used was very thin so that the rate of relaxation was not diffusion controlled.

2.6.6 Oxygen Absorption Apparatus

Oxygen absorption provides very useful information on the oxidizability, or inhibition, during accelerated ageing of a vulcanisate in a closed system saturated with oxygen. The parameters which are investigated by this technique are:

(i) the rate at which a particular vulcanisate absorbs oxygen, and

(ii) the time needed to absorb a particular level of oxygen by the sample.

Data from oxygen absorption together with that from stress relaxation enables the amount of oxygen required to break a bond in the vulcanisate to be calculated. Because oxygen absorption is carried out in a closed system, loss of additives due to volatilization does not occur. The technique of stress relaxation is therefore more relevant to what happens in practice because the rubber is oxidised in a changing stream of air.

A simplified diagram of the oxygen absorption apparatus is shown in Fig 2.10. 0.3 g of the vulcanisate was weighed accurately and the thickness (0.008 inch) measured with a thickness guage. The sample was fixed in the holder such that oxygen could freely diffuse into the sample from both surfaces. The holder with the sample was then

Fig 2.10 Oxygen Absorption Pressure Transducer Method

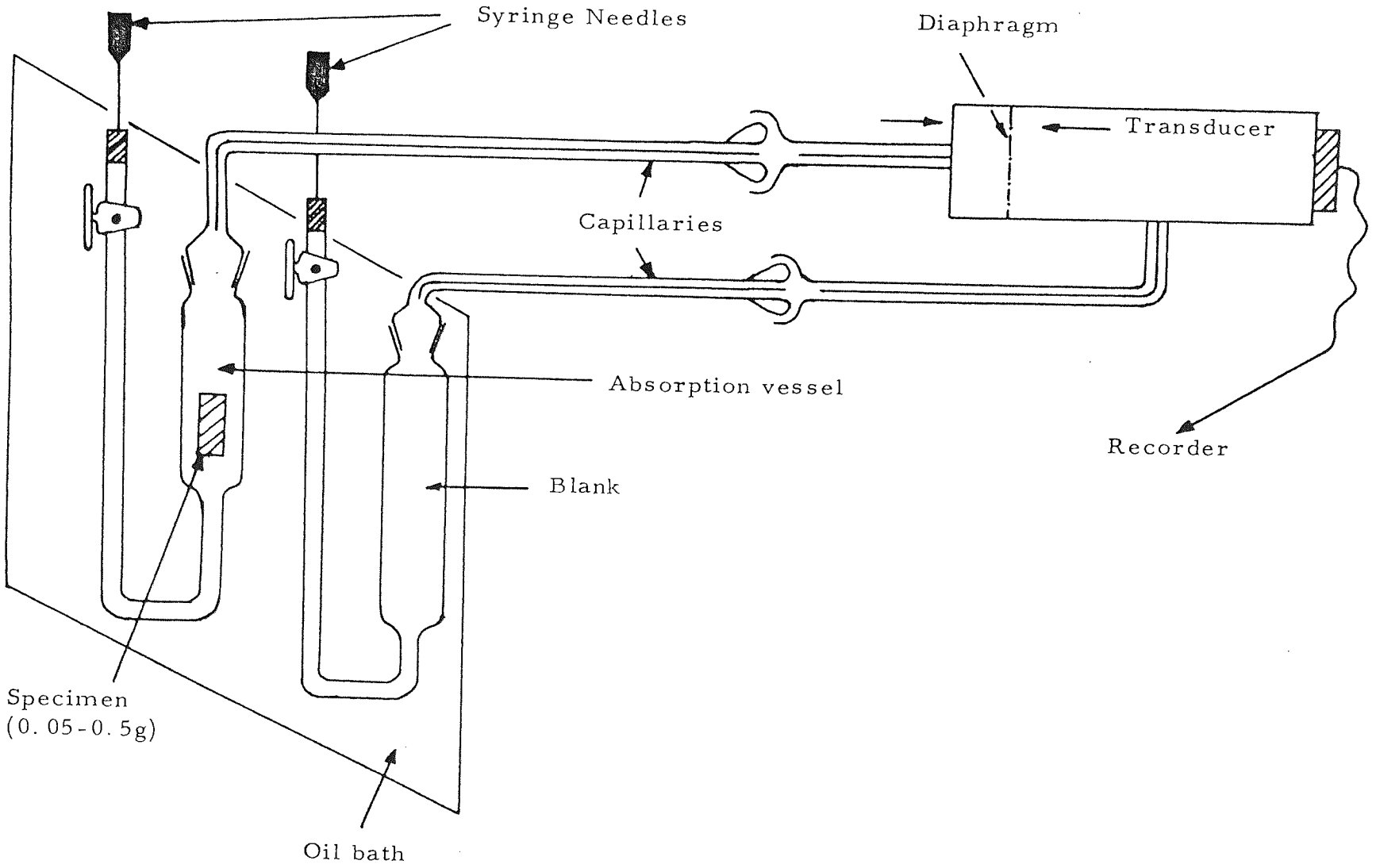

placed in the absorption vessel and the apparatus assembled. Silicone grease was applied to all joints to ensure that the system was air tight. The absorption vessel was then purged with oxygen and placed in a thermostated oil bath. Both the absorption vessel and the reference vessel incorporated to allow for any slight changes of temperature, were connected to the transducer. The apparatus was left for about 10 minutes so that the temperature in the vessels could be equilibrated. The vessels were vented to the atmosphere through the luer needle attachments. The sample was then left to absorb oxygen. The change in pressure was measured by the transducer and automatically recorded on a chart recorder (Leeds and Northrupp Speedomax 250). The maximum pressure change allowed was of the order of 5%. It was assumed that this change would not affect the kinetics of the oxidation process.

2.7 Infra Red (IR) Spectroscopy

The build up of carbonyl groups in the backbone of the rubber chains during thermal oxidation was estimated by absorption at 1735 cm^{-1} using a Perkin Elmer grating (Model 599) infra red spectrophotometer at normal scan speed. 1735 cm^{-1} is the characteristic absorption frequency of an ester carbonyl and the absorption at 1710 cm^{-1} is the normal frequency for a carboxylic acid carbonyl. The concentration of carbonyl modification was expressed as an index defined as the

ratio of the absorbance of the carbonyl group peak to that of a reference peak. The characteristic absorption peak at 2720 cm^{-1} due to a C-H stretching was used as reference.

The baseline technique shown in Fig 2.11 was used to determine the absorbance.

Fig 2.11 Carbonyl index measurement by baseline technique(224)

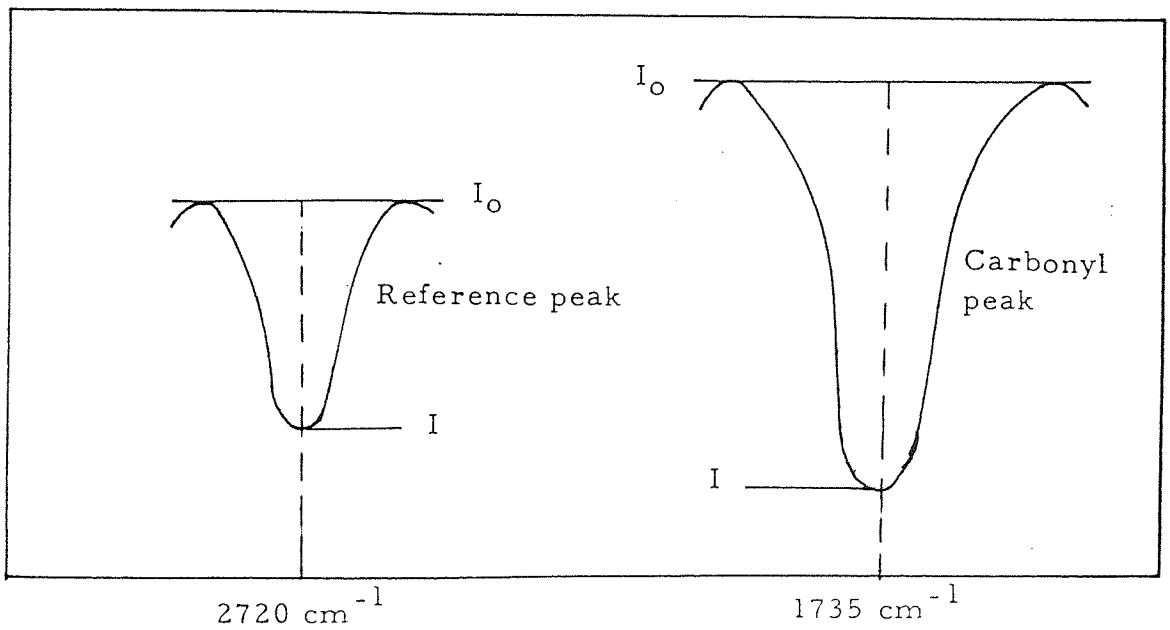

$$\text{Absorbance} = \log \frac{I_o}{I} \qquad (2\text{-}7)$$

$$\text{Carbonyl Index} = \frac{\text{Absorbance at 1735 } cm^{-1}}{\text{Absorbance at 2720 } cm^{-1}} \qquad (2\text{-}8)$$

2.7.1 Preparation of Films for I.R.Measurement

A film for I. R. measurements was cast from compounded NR latex on a glass plate. 10 ml of the latex was spread evenly on a glass plate over an area of 35 cm^2, and allowed to dry in a dessicator under nitrogen. The film when dry was carefully removed from the glass, cut to 2 cm x 3 cm with a sharp scalpel and then mounted on an infra-red 'specacard'. The film was vulcanised in a nitrogen atmosphere at 100°C for 30 minutes and the carbonyl index was determined during ageing as a function of time.

2.8 Scanning Electon Microscopy (SEM)

The dispersion of filler in filled vulcanisates was observed using a Stereoscan S600 (Cambridge Instruments Ltd) scanning electron microscope.

The function of a scanning electron microscope is similar in concept to that of a reflectance optical microscope. However, in place of the light source, an electron beam (or probe) is directed at the specimen. Probe electrons striking the sample do not penetrate very deeply and the majority of the secondary electron beam are from atoms on the surface of the sample. The secondary electron emissions and primary electrons(reflected from the surface of the specimen) are

then collected and used to modulate the brightness of a television display unit. In this way an accurate representation of the topography of the sample may be obtained. Since high energy electrons have a much shorter wavelength than light, far greater magnification (typically 100,000 X) is obtainable than for an optical microscope (typically 1000 X).

2.8.1 Procedure

Slices, 0.05 cm thick, were cut from the vulcanisate with a sharp scalpel. These samples were then mounted on small metal stubs with double sided celotape and electrical contact between the specimen and the stub was ensured by using a colloidal silver preparation (Acheson Colloids Ltd). The samples were gold-coated at 100 Å for 3 minutes in vacuo, to prevent the surface charging up under the electron beam, which can cause photographs of the SEM image to have very poor contrast.[228, 229]

The stub was then secured in the mounting pallet and positioned in the vacuum chamber of the equipment. The chamber was then evacuated to working vacuum (indicated by the Vacuum Ready Light) before obtaining photographs.

2.9 X-Ray Diffraction

The degree of crystallinity on a single extension of a conventionally cured rubber vulcanisate was assessed from X-ray diffraction intensity measurements obtained by using a Jeol Diffractometer (Model J. D. X-75). This equipment (see Fig 2.12) consists of the following:

(i) An X-ray source (A),

(ii) a collimator (B) for obtaining a beam of parallel X-rays,

(iii) a goniometer (C) for mounting the specimen,

(iv) a counter (D) for X-ray intensity measurement, and,

(v) an amplifier and recording system (E).

The specimen for X-ray diffraction measurement was made by extending a thin strip of the vulcanisate (0.5 mm thick) between the grips of an extensometer to the desired extension. While still extended, it was glued to an aluminium holder with a strong glue (Permabond 910) so that the hole (3 cm diameter) at the centre of the holder was completely covered. It was then left for some time to dry. When completely dry, the vulcanisate specimen remained glued to the sample holder in the stretched condition. The extensometer grips were then relaxed and the specimen removed. A wide range scan of the sample was then obtained with the diffractometer.

Fig 2.12 Schematic representation of an X-ray diffractometer

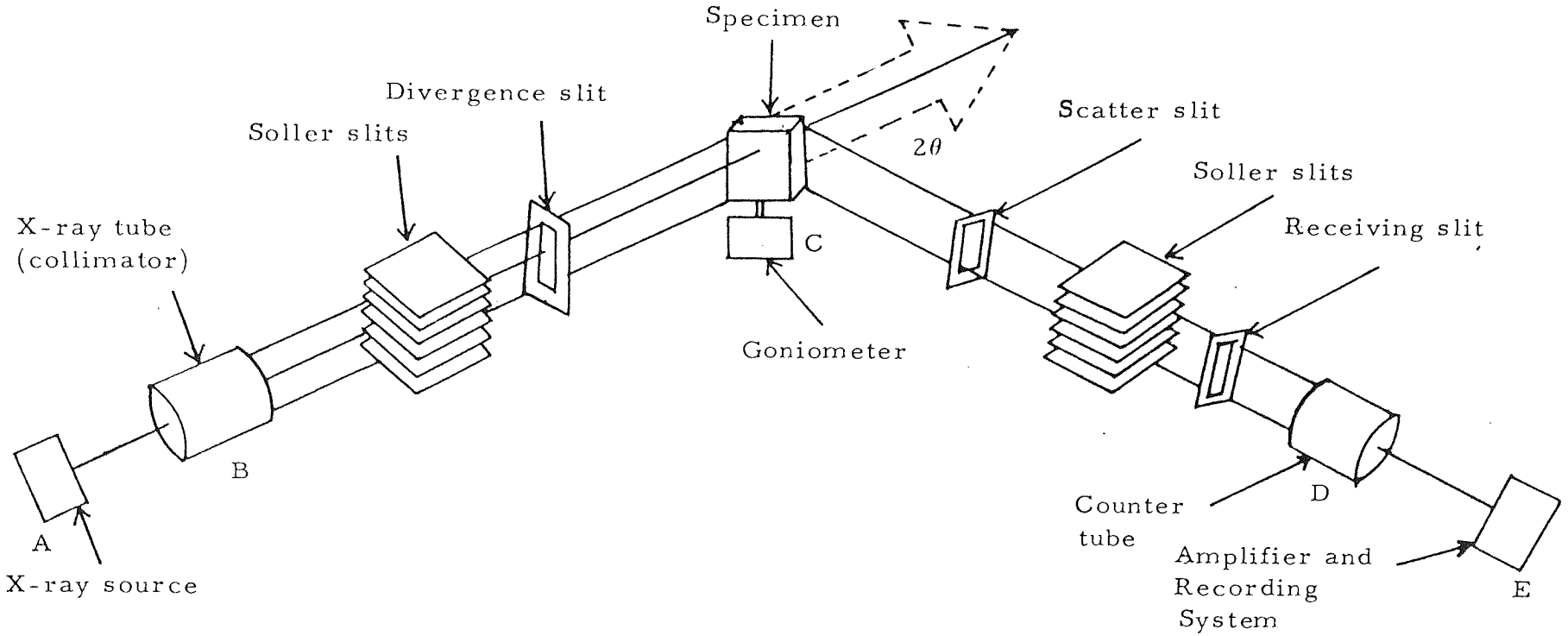

The instrument was set to detect low angles of diffraction initially and by selection of the correct gears on the goniometer a trace of peak intensity plotted against scattering angle (2θ) was obtained. The following operating conditions were used:

(i) Scan range, 4×10^3 c.p.s.

(ii) Scan speed, 2^o/min

(iii) Chart speed, 20 mm/min i.e. 20 minutes on the chart represents 2θ.

The degree of crystallinity was determined from the diffraction intensity using equation (2-9)[282]

$$1 - \chi_{cr} = \frac{(1/t')(I_{am}'/I_o')}{(1/t)(I_{am}/I_o)} \qquad (2\text{-}9)$$

where: χ_{cr} is the degree of crystallinity

I_{am} is the intensity of the amorphous region in an unextended sample.

I_{am}' is the intensity of the amorphous region in an extended sample.

I_o is the intensity of the incident X-rays on the unextended sample.

I_o' is the intensity of the incident X-rays on the extended sample, and

t and t' are their thicknesses respectively.

Since in the present work $I_o = I'$, Equation (2-9) becomes

$$(1 - \chi_{cr}) = \frac{I_{am}' \, t}{I_{am} \, t'} \qquad (2\text{-}10)$$

Equation (2-10) was used for calculating the degree of crystallinity from the intensity of the amorphous regions.

2.10 Measurement of Crosslink Density

2.10.1 Swollen Compression Measurement

The theory of the determination of C_1 from compression modulus of swollen vulcanisates has been discussed in Section 1.3.2.3. The Wallace-Smith Reticulometer was used in carrying out this measurement.

The equipment, developed by Smith[75], is produced by H·W·Wallace of Croydon and marketed under the name 'Wallace-Smith Reticulometer'. It is designed to measure rapidly and reproducibly the compression modulus of small specimens of rubber vulcanisates swollen to equilibrium. The apparatus consists of a standard Rubber Micro-Hardness Tester (see Fig 2.13) having a measuring ratio of 6:1, which has been modified as follows:

Fig 2.13 The Wallace Rubber Micro Hardness Tester

(Modified to form The Wallace-Smith Reticulometer)

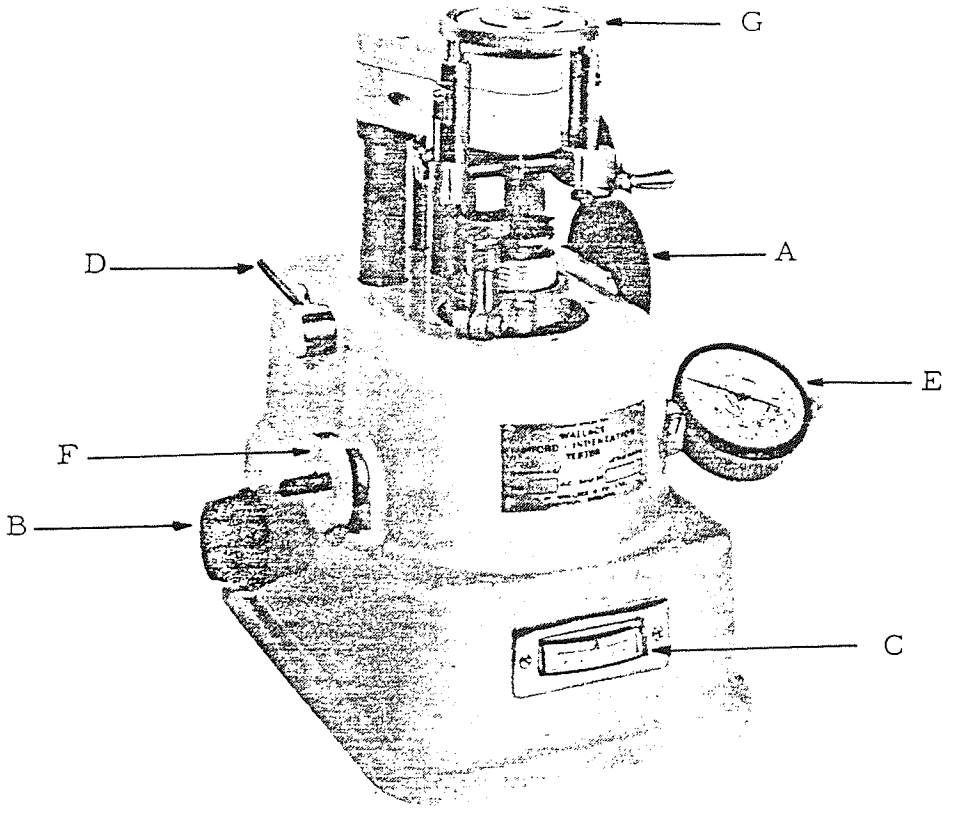

(i) The I. R. H. D dial guage is replaced by a dial micrometer graduated in 0. 01 mm divisions.

(ii) The hardness tester foot attachment is removed and replaced by the Reticulometer test cup. This consists of a circular flat base in a cup jacketed for the circulation of temperature-controlled water.

(iii) The I. R. H. D indentor is removed and replaced by a flat circular stainless steel disc 1. 9 cm in diameter

(iv) The small weight pan of the Micro-Hardness Tester is removed and replaced by a larger weight pan

Thermostated water at the test temperature was circulated through the reticulometer pot. The pot was filled with solvent before testing and allowed to equilibrate to the test temperature (25^{o}C); loss of solvent by evaporation was overcome by periodic addition of fresh solvent maintained at the test temperature.

2. 10. 1. 1 Preparation and Mensuration of Test Specimen

A sample was prepared by cutting a small square (0. 5 cm edge) from a vulcanisate sheet (0. 2 cm thick) using a sharp scalpel. The sample was weighed using an accurate balance and the linear dimensions determined accurately using a vernier microscope (accuray of 0. 001 cm). The area (A_o) of each specimen was computed from

the mensuration of all four sides and four 'height' measurements were averaged to give the unswollen height (h_o). At a later stage in this work, it was found more convenient to knock out samples from the sheet with a circular die (0.5 cm diameter).

2.10.1.2 Operation of the Reticulometer

Each test specimen was swollen to diffusion equilibrium as judged by the measurement of the swollen weight of the sample and was then placed in the reticulometer test cup which contained the same swelling agent maintained at a temperature of $25 \pm 0.5^{o}C$.

The reticulometer was switched on and the foot was lowered into the test cup by using the wheel (A) until it was well immersed in the solvent. The instrument was then zeroed using knob (B) and the foot was lowered onto the surface of the sample, a small pressure being applied by the wheel (A) until a positive reading was shown on the centre reading galvanometer (C). The pressure was then released until the reading just returned to zero. The column was locked by using the chrome lever (D). The dial guage (E) was set at 0/100 during this period by using the wheel (F). The compression (Δh) of the swollen sample was measured using the following procedure:

(a) 500 g (excess weight) was placed on the weight pan (G) for 20 seconds.

(b) The excess weight was removed and the sample was allowed to recover for 5 minutes.

(c) After relaxation, 25 g (dead load weight) was placed on the pan for 1 minute.

(d) The dead load weight was removed and the first experimental weight was added. The instrument was zeroed by using the wheel (F) and the dial guage reading (Δh) was noted.

(e) The first experimental weight was removed and the wheel (F) turned to return the dial guage to zero.

(f) After 20 seconds the dead load weight was placed on the pan for 60 seconds.

(g) Steps (d) to (f) were repeated for each experimental weight.

The following series of experimental loads were used in ascending order: 50, 100, 150, 200, 250, 300 g.

(h) The loading procedure was repeated in the reverse order with load being decreased in steps.

2.10.1.3 Analysis of Data

C_1 values were obtained from load and compression data by using Equation (1-13). $\overline{M}_{c\,(phys)}$ and hence the physical crosslink density

was obtained using equation (1-23) relating C_1 and $\overline{M}_{c\,(phys)}$. $\overline{M}_{c(\,chem)}$ and the chemical crosslink density were derived from C_1 values via the Moore Mullins and Watson equation (1-26). The treatment of equation (1-26) is shown in appendix (1-1) and the computer programs based on equations (1-13) and (1-26) are shown in appendices (1-3) and (1-4). These programs were used for the analysis of all swollen compression data.

2.10.2 Equilibrium Volume Swelling Measurements

Samples were cut, weighed accurately and placed in small weighing bottles. The appropriate swelling solvent was added, the bottles covered with polythene caps and placed in a thermostatically controlled water bath at 25°C. After the samples had swollen to equilibrium, they were removed and the excess solvent on the surface was removed by pressing lightly between two filter papers. The samples were then weighed immediately in closed weighing bottles before they were deswollen under vacuum at 45°C to constant weight. The difference in weight between the swollen samples and the deswollen samples gave the weight of the solvent absorbed.

2.10.2.1 Analysis of Data

The volume fraction of rubber network (V_r) in the swollen vulcanisates,

were calculated from the above measurements using the expression:

$$V_r = \frac{(W_2 - FW_1)\rho_r^{-1}}{(W_2 - FW_1)\rho_r^{-1} + W_3\rho_s^{-1}} \qquad (2\text{-}11)$$

where: W_1 = unswollen weight

W_2 = deswollen weight

W_3 = weight of the absorbed solvent

F = weight fraction of insoluble components

ρ_r and ρ_s = densities of rubber and solvent respectively

The constant C_1 was calculated by substituting in the modified Flory-Rhener equation (1-18). The C_1 value so obtained was converted to crosslink density values via the Moore, Mullins and Watson equation (1-26). The actual concentration of chemical and physical cross-links in filled vulcanisates was calculated by using equations (1-36) and (1-37) respectively.

All the data from swelling measurements were analysed using the computer programs shown in the appendices (1-5) and (1-6).

2.11 Chemical Probe Treatment

Changes in the network structure of vulcanisates during the application of a single extension and also during fatigue experiments were deter-

mined with the thiol/amine and triphenylphosphine probes, the theory of which has already been discussed in Section 1.3.4.

2.11.1 Treatment with Propan-2-thiol/Piperidine

The apparatus used initially for the treatment of samples with propan-2-thiol was that described by Saville and Watson[28]. At a later stage of this work, because of the difficulties encountered with recognising labelled samples after probe treatment, it was necessary to use a modified form of the apparatus (Fig 2.14). This had several compartments to separate each group of samples. Holes were made in the glass dividing walls of each compartment to ensure the free flow of the probe solution and nitrogen.

The probe solution was prepared by mixing 4.07 ml of propan-2-thiol, 4.27 ml of piperidine and 100 ml of AR grade n-heptane in a conical flask under nitrogen. The samples were placed in the separate compartments of the apparatus which was flushed out by passing nitrogen from (A) through (B). The probe operation was carried out under nitrogen to prevent oxidation of the probe itself and the swollen rubber. Enough probe solution was added to completely immerse the samples and the vessel was further purged with nitrogen for a few minutes before sealing it off by closing the taps. During the reaction, the tube was periodically shaken. At the end of the reaction

Fig 2.14 Apparatus for propan-2-thiol/piperidine probe treatment

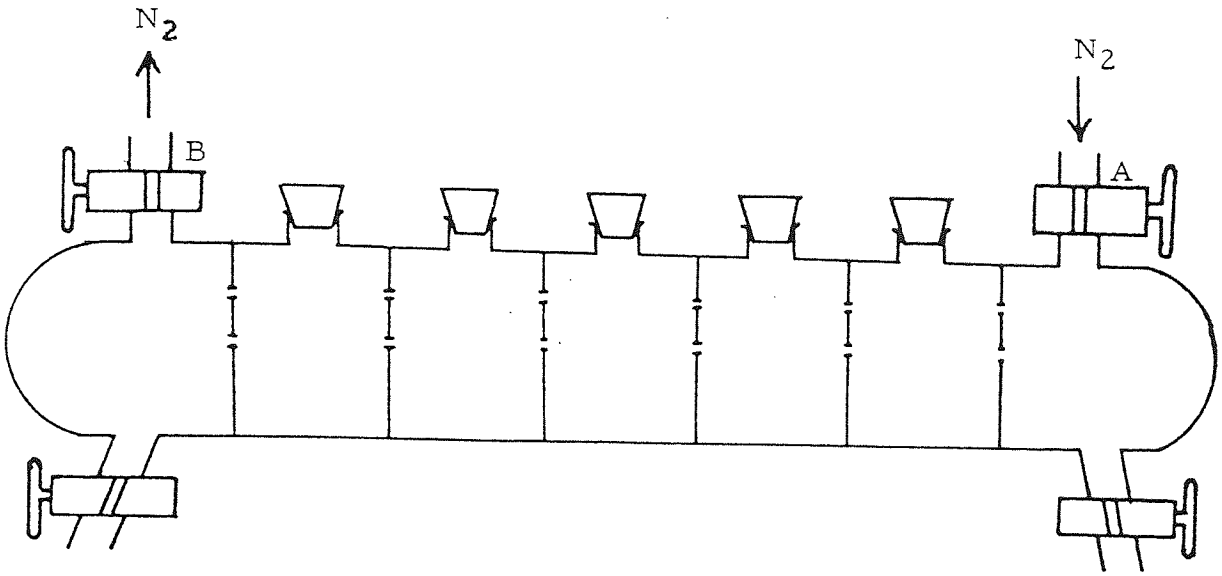

Fig 2.15 The H-tube apparatus for n-hexanethiol/piperidine probe treatment

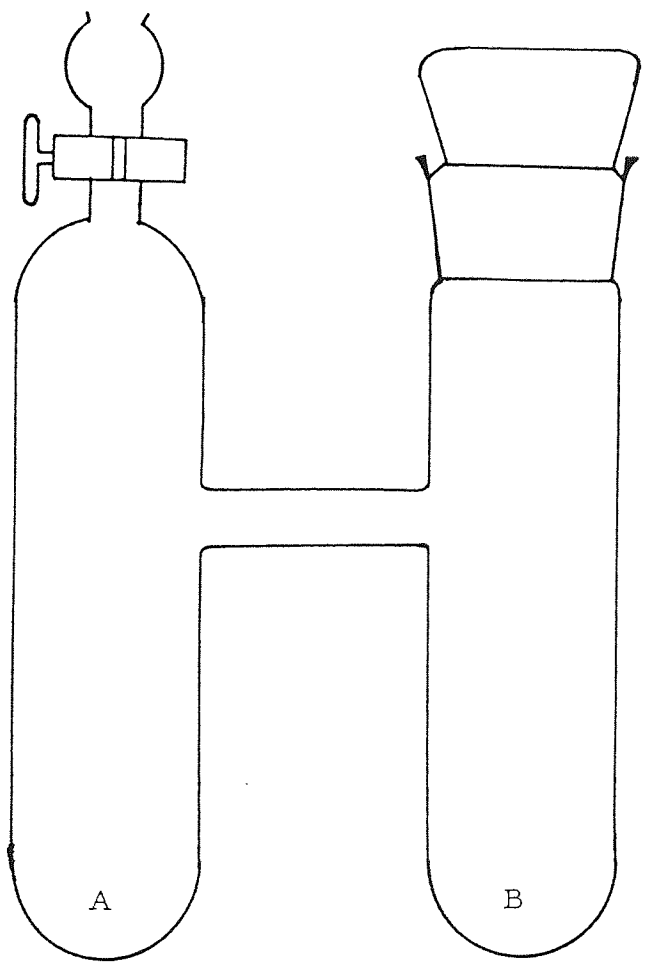

time (2 hours) the probe solution was run out from the vessel and destroyed in an excess of ammoniacal copper (II) sulphate. The samples were extracted four times (1 hour each) with petroleum ether (b. pt. 30-40) and then deswollen in a vacuum oven at 45°C to constant weight.

The chemical crosslink densities of the treated samples were determined as described in Section 2.10.

2.11.2 Treatment with n-hexane-thiol

The 'H' tube apparatus described by Saville and Watson (see Fig 2.15) was used for treatment of samples with n-hexane-thiol. The sample was placed in the arm (B) of the vessel and 10 ml of piperidine was added to it. 2.1 ml of n-hexane-thiol was then pipetted into arm (A). The vessel was stoppered and the liquids were degassed twice by the freeze-thaw technique using liquid nitrogen as coolant to prevent oxidation. The thiol was then allowed to run over into arm (B). The mixture was degassed for the final time before sealing off vessel under vacuum. The H-tube was then placed in a thermostatically controlled water bath at 25°C for 48 hours. After the reaction, the samples were extracted with petroleum ether (b. pt. 30-40) for 4 hours and deswollen for 48 hours under vacuum. Crosslink density values were determined for the treated samples.

2.11.3 Treatment with Triphenylphosphine

Strips of extracted vulcanisate were dried in the dark in a vacuum dessicator. A weighed sample (0.5g) was swollen for 24 hours in the dark in 20 ml of a 0.2 M solution of triphenylphosphine in toluene under dry nitrogen. The swollen rubber was deswollen under vacuum in the dark until a constant weight was obtained. The triphenylphosphine remained randomly distributed in the rubber matrix. The impregnated samples were then sealed in Carius tubes under vacuum (about 1 mm). The sealed tubes were immersed in an oil bath at 80°C for 96 hours. The tubes were then removed and opened carefully. The reaction products of probe treatment were then removed from the sample by cold sohxlet extraction in the dark for 24 hours using toluene. The extracted samples were dried to constant weight.

2.12 Determination of Total Sulphur Content

The oxygen flask method[225-227] was used for total sulphur determinations. The apparatus consisted of a 500 ml conical ground glass jointed oxygen combustion flask fitted with a B_{24} stopper containing fused-in platinum wire with platinum gauze leaves (Fig 2.16).

Fig 2.16 Apparatus for oxygen flask combustion: Conical flask with platinum gauze as sample holder.

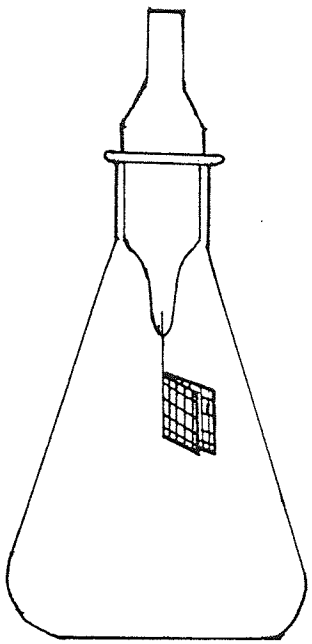

2.12.1 Reagents

1. Analar hydrogen peroxide (20 vol).
2. Reagent grade isopropyl alcohol.
3. Barium perchlorate solution (0.01M) adjusted to pH 2.5-4.0:

   3.363 g solid barium perchlorate (Analar) were dissolved in 200 ml distilled water and made up to 1000 ml with isopropyl alcohol. The pH was adjusted by the careful dropwise addition of perchloric acid, using bromophenol blue as an external indicator.

4. Thorin 2-(2-hydroxy-3, 6-disulpho-1-naphthylazo) phenylarsonic acid, sodium salt - 0.2% (w/v) aqueous solution.
5. Methyl blue - 0.0125% (w/v) aqueous solution.

   Equal volumes of thorin and methyl blue solutions were mixed freshly for each set of determinations.
6. Sulphuric acid - 0.01M standard solution.
7. Distilled water of very high purity.
8. Supply of oxygen.

2.12.2 Procedure

The sample was well homogenised on a laboratory mill and then sheeted out thinly. From this sheet a test portion (0.025 - 0.03 g) was cut out and weighed accurately. This test portion was then placed between the platinum gauze leaves attached to the combustion flask stopper (Fig 2-16). A small strip of ashless filter paper was inserted parallel to the wire support so that it projected about one inch to act as a taper. In some cases where the test portion was not completely coherent it was weighed onto a one inch filter paper square with a one inch taper and the carefully wrapped 'parcel' inserted between the platinum gauze leaves. It was essential to ensure that the test portion was totally enclosed by the gauze and the leaves were pressed together with forceps.

4 ml of distilled water and 20 drops of 20 vol hydrogen peroxide were placed in the clean combustion flask and oxygen was passed into the flask for one minute with the tube inserted. The tip of the taper was then lit, the oxygen tube removed from the flask and the test portion and stopper immediately inserted. With the stopper pressed firmly into place, the flask was tilted until the joint was covered by the hydrogen peroxide solution. The test portion burned at almost white heat for a few seconds. After combustion was complete the flask was shaken vigorously for about 2 minutes and then left to stand for a further 20 minutes with occasional shaking, until the cloudiness in the gas phase was cleared. The whole operation was conducted behind a transparent perspex shield as a precaution against the remote possibility of implosion.

The stopper and gauze were washed with isopropyl alcohol by placing 16 ml in the flared lip of the flask and then easing the stopper out gently so that the liquid was sucked in. This was repeated, the stopper withdrawn and the rest of the alcohol was used to wash through the gauze into the flask. 3-4 drops of thorin mixed indicator was added and the solution was titrated with standard barium perchlorate solution until the pale yellow-green colour of the indicator changed to pale pink with the formation of a barium complex. The titration was carried out with magnetic stirring. The end-point colour change is not distinct but with practice it was found to be reproducible.

In the combustion process, sulphur was converted partially to sulphur dioxide and partially to sulphur trioxide. The hydrogen peroxide ensured that sulphur dioxide was converted to the trioxide which could then be titrated as sulphate. The barium perchlorate solution was standardised by titrating with 5 ml of 0.01M sulphuric acid (known sulphur content) using thorin as indicator.

2.12.3 Expression of Results

$$\text{Total sulphur content (\%)} = \frac{A \times B}{C} \times 100 \qquad (2\text{-}12)$$

where: A = No of ml of barium perchlorate required for titration with test solution.

B = The weight of sulphur equivalent to 1 ml of 0.01M barium perchlorate.

C = Weight of test sample.

2.13 Determination of Sulphide Sulphur

The method used is essentially that contained in BS 903:Part 10. The assembly of the apparatus used is shown in Fig 2.17. In this method the metallic sulphides present in an extracted vulcanisate are decomposed by treating with hydrochloric acid. The hydrogen sulphide which is liberated is absorbed in cadmium acetate solution

to form cadmium sulphide which is then determined iodometrically.

2.13.1 Reagents

1. Cadmium acetate, buffered solution: 25 g cadmium acetate $(CH_3COO)_2Cd.2H_2O$, 25 g sodium acetate $CH_3COONa.3H_2O$ and 100 ml glacial acetic acid made up to 1000 ml with distilled water.
2. Sodium thiosulphate solution, 0.05M: 12.41g sodium thiosulphate ($Na_2S_2O_3.5H_2O$) was dissolved in fresh distilled water and made up to 1000 ml.
3. Hydrochloric acid, dilute: 1 vol. of concentrated acid (sp. grav. 1.18) to 1 vol. of water.
4. Iodine solution, 0.025M.
5. Starch solution, 1%(w/v).
6 Supply of nitrogen.

2.13.2 Procedure

The extracted rubber was homogenised on a laboratory micromill to a thin sheet. A 0.025 to 0.03 g test portion was cut from this sheet, weighed accurately and then placed in the boiling flask A (Fig 2.17). Cadmium acetate solution (100 ml) was placed in the absorbing vessel B and the Arnold bubblers C and D were half filled with the same

solution. The apparatus was then purged with nitrogen by passing nitrogen into D through to C for 10 minutes. The gas flow was adjusted to about one bubble per second in flask B.

50 ml of dilute hydrochloric acid was added slowly into the boiling flask and the nitrogen flow rate reduced to one or two bubbles per second in the absorbing vessel. The flask was gently heated to boiling for 45 minutes. Care was taken when boiling to prevent suck-back of cadmium acetate into the boiling flask.

The gas flow rate was increased near the completion of the reaction to sweep over the last traces of H_2S into the absorbing vessel.

The solution in Arnold bubbler C should remain clear at the end of the reaction. A yellow colouration is an indication that the flow rate was too fast. Whenever this occurred the analysis was repeated using a smaller sample weight or a reduced gas flow rate.

The absorption vessel and delivery tube were removed at the end of the reaction and the flask shaken to redisperse colloidal cadmium sulphide. Whilst held at an angle, V ml (about 20 ml) of 0.025M iodine solution was added to the flask, so that excess iodine was present. When all the precipitate had reacted with iodine, the vessel was removed and the excess iodine titrated with 0.05M sodium thio-

sulphate solution (Y ml) using starch as indicator. The concentration of iodine in terms of millilitres of standard thiosulphate solution was determined by titrating V ml of iodine solution with standard thiosulphate solution (X ml).

The iodine that has reacted with the cadmium sulphide is equivalent to the difference between the volume of thiosulphate used in standardisation and that used in the determination (X - Y).

2.13.3 Expression of Results

$$H_2S + (CH_3COO)_2Cd \longrightarrow CdS + 2CH_3COOH \qquad (2\text{-}13)$$

$$8CdS + 8I_2 \longrightarrow 8CdI_2 + S_8 \qquad (2\text{-}14)$$

$$I_2 + 2S_2O_3^{2-} \longrightarrow S_4O_6^{2-} + 2I^- \qquad (2\text{-}15)$$

1 mole of consumed iodine $\equiv$ 1g atom of sulphur

$$\text{No of moles of consumed iodine} = \frac{(X - Y)}{1000} . M \qquad (2\text{-}16)$$

$$\% \text{ weight of } S(S^-) = \frac{(X - Y)}{1000} . \frac{32M}{W} . 100\% \qquad (2\text{-}17)$$

$$= \frac{0.08(X - Y)}{W} \qquad (2\text{-}18)$$

where W is the weight of test portion in grammes.

2.14 Determination of Extractable Free Sulphur

2.14.1 Reagents

1. Cadmium acetate, buffered solution, was prepared as in previous section (2.12.1).
2. Hydrochloric acid, dilute: 1 vol concentrated acid with 1 vol water.
3. Sodium thiosulphate solution, 0.05M.
4. Nitric acid, dilute: 1 vol of concentrated acid (sp.grav. 1.42) with 1 vol of water.
5. Iodine solution, 0.025M.
6. Filter stick (Porosity No. 3).
7. Starch solution, 1% (w/v).
8. Copper gauze, 40-60 mesh per linear inch.
9. Supply of nitrogen.

2.14.2 Procedure

Copper spiral was made by cutting about 5 g of 40-60 mesh copper gauze to form a 1 cm wide strip. This was then loosely rolled to form a spiral approximately 2 cm in diameter and the turns were held in place by a loop of copper wire. The spiral was cleaned immediately before use by washing in hot concentrated hydrochloric acid and then immersing for a few seconds in dilute nitric acid. All traces of acid were removed by washing thoroughly with water and finally with acetone.

0.5 - 1 gm of the test portion of rubber together with the copper spiral were placed in a 150 ml extraction flask and extraction was carried out for 4 hours. A 1 cm square copper gauze was added and the extraction carried out for a further 1 hour. The sulphur obtained during this extraction reacted with copper to produce CuS. When extraction was complete the acetone in the flask was filtered off through a porosity No. 3 filter stick. The spiral was washed with three portions of about 20 ml of hot acetone, the washings being removed each time through the filter stick. The flask containing the copper spiral and filter stick were assembled into the apparatus (Fig 2.17) as flask A.

300 ml cadmium acetate solution was placed in the receiver B and the Arnold bubblers C and D were filled to a depth of about 1 cm with the same solution. A stream of pure nitrogen was then passed through the apparatus to sweep out the air and the flow rate was adjusted in flask B to one bubble per second. The remaining procedure was carried out as in the previous section (2.13.2) when determining sulphide sulphur.

2.14.3 Expression of Results

$$\% \text{ Extractable free sulphur} = \frac{0.08\,(X - Y)}{W} \qquad (2\text{-}19)$$

where W = weight of test portion in grammes.

Fig 2.17 Apparatus for the determination of sulphide sulphur

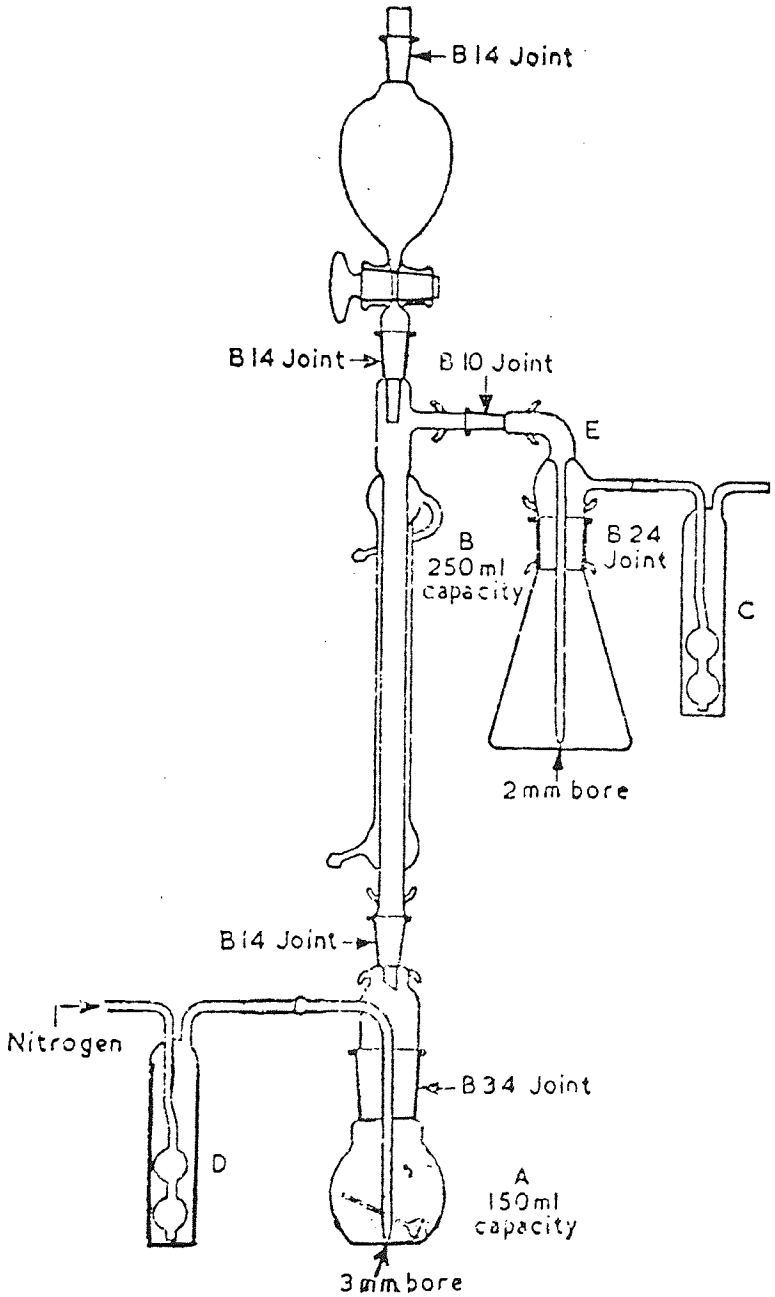

CHAPTER THREE

SINGLE EXTENSION STUDIES

3.1 Introduction

The aim of this study was to investigate the changes that occur in the crosslink composition and crosslink density as the result of a single extension of a natural rubber vulcanisate. If a vulcanised rubber is subjected to a single extension, crosslinks probably rupture and reform in the stressed state leading to a change in crosslink distribution and crosslink density. It is well known that permanent set is produced when a vulcanised rubber is held at a constant extension and subsequently released. According to the "two-network hypothesis", permanent set is the result of two interpenetrating but independent networks:

(i) the remains of the original network still with the original unstretched length will be in tension on release of the stress, and

(ii) a network formed during extension with the length attained on extension as the unstretched length and which will be in compression in the unstressed state.

The nature of the crosslinks in a vulcanisate probably affects the network changes that occur during a single extension, and the degree of crystallisation of the rubber on extension may also be an important factor. Three types of vulcanisates were examined in order to assist in the elucidation of the network changes:

(i) Filled and unfilled conventional vulcanisates, which possessed mainly polysulphidic, as well as mono and disulphidic cross-links.

(ii) a TMTD vulcanisate with principally monosulphidic crosslinks, and,

(iii) a peroxide vulcanisate that possessed only carbon-carbon crosslinks.

These investigations assessed:

(i) the change in polysulphidic crosslink content on single extension of conventionally vulcanised filled and unfilled rubber,

(ii) the change in the total crosslink density on single extension of conventional, TMTD and peroxide vulcanisates,

(iii) the relationship between the degree of extension and the permanent set produced,

(iv) the relationship between the degree of extension and the degree of crystallinity and,

(v) permanent set and equilibrium swelling changes upon a single extension were used to evaluate the number of crosslinks broken per unit volume and the recombination efficiency.

The permanent set resulting from extension of a sample is defined as:

$$\text{Permanent set (\%)} = \frac{l_1 - l_o}{l_o} \times 100 \qquad (3\text{-}1)$$

where: l_o is the unstretched length and l_1 is the final length after extension and recovery.

The set may change after subsequent treatment e.g. after swelling and deswelling in a solvent or after probe treatment, and the new set is given by:

$$\text{New set (\%)} = \frac{l_3 - (l_2 l_o / l_1)}{(l_2 l_o / l_1)} \times 100 \qquad (3\text{-}2)$$

where: l_2 is the length of the test piece before treatment and l_3 is that after treatment.

It is necessary to cut a sample of length (l_2) from the central portion of the dumb-bell for this test, which is equivalent to a length of $l_2 . \frac{l_o}{l_1}$ before set had taken place.

The expression[271] derived from Tobolsky's two network theory was used to calculate the number of crosslinks broken per unit volume and the recombination efficiency on a single extension:

$$\alpha = \frac{n_2}{(N - n_1)} = \frac{(\lambda_o^3 - 1)}{(\lambda' - \lambda_o^3 \lambda'^{-2})} \qquad (3\text{-}3)$$

where: α = $\dfrac{\text{No of crosslinks reformed per unit volume}}{\text{No of crosslinks unbroken per unit volume}}$

λ' = extension ratio

λ_o = 'set' ratio (l_1/l_o)

N = the number of crosslinks per unit volume in the unstretched state

n_1 = the number of crosslinks per unit volume which break on extension

n_2 = the number of crosslinks per unit volume which reform on extension

The number of crosslinks which break on a single extension is given by:

$$1 - \left[\frac{n_1}{N}\right] = \left[\frac{V_1}{V_2}\right]^{\frac{1}{3}} \left[\frac{\ln(1 - V_2) + V_2 + \chi V_2^2}{\ln(1 - V_1) + V_1 + \chi V_1^2}\right] \left[(1 + \alpha\lambda')\ 1 + \frac{\alpha}{\lambda'^2}\right]^{-\frac{1}{3}}$$

(3-4)

Table 3.1 Mix formulations

Ingredients	Parts by weight			
	A	B	C	D
NR	100	100	100	100
S	2.5	2.5		
ZnO	5	5	5	
SA	2	2	2	
CBS	0.6	0.6		
TMTD			3	
DICUP				1.5
HAF-black		40		

(ii) formulation B, filled conventional vulcanisate

(iii) formulation C, TMTD vulcanisate and

(iv) formulation D, peroxide vulcanisate

3.2.2 Compounding

The mixing of compounding ingredients for the gum stock was carried out on the open two-roll mill as described in Section 2.2.3.1. The black compound was prepared in the Banbury mixer using the typical mixing cycle described in Section 2.2.4.1. A measure of the compound viscosity during mixing was obtained by measuring the plasticity with the Wallace Rapid Plastimeter (Section 2.5.1), from which by reference to the calibration of $\overline{M}n$ and plasticity number shown in Fig 3.1, an appropriate value of $\overline{M}n$ of the rubber in the compound could be obtained. A more precise estimate of the number average molecular weight of the rubber in the compound was determined as soon as possible after compounding by measuring the intrinsic viscosity of the solution of the rubber (Section 2.5.2). The value of $\overline{M}n$ was required for crosslink density determination.

3.2.3 Vulcanisation

The curing characteristics of a compound were determined on the Monsanto Rheometer 100 (Section 2.3.1) before curing sheets of

Fig 3.1 The Calibration Curve of Wallace Plasticity Number Versus Number Average Molecular Weight ($\overline{Mn}$)

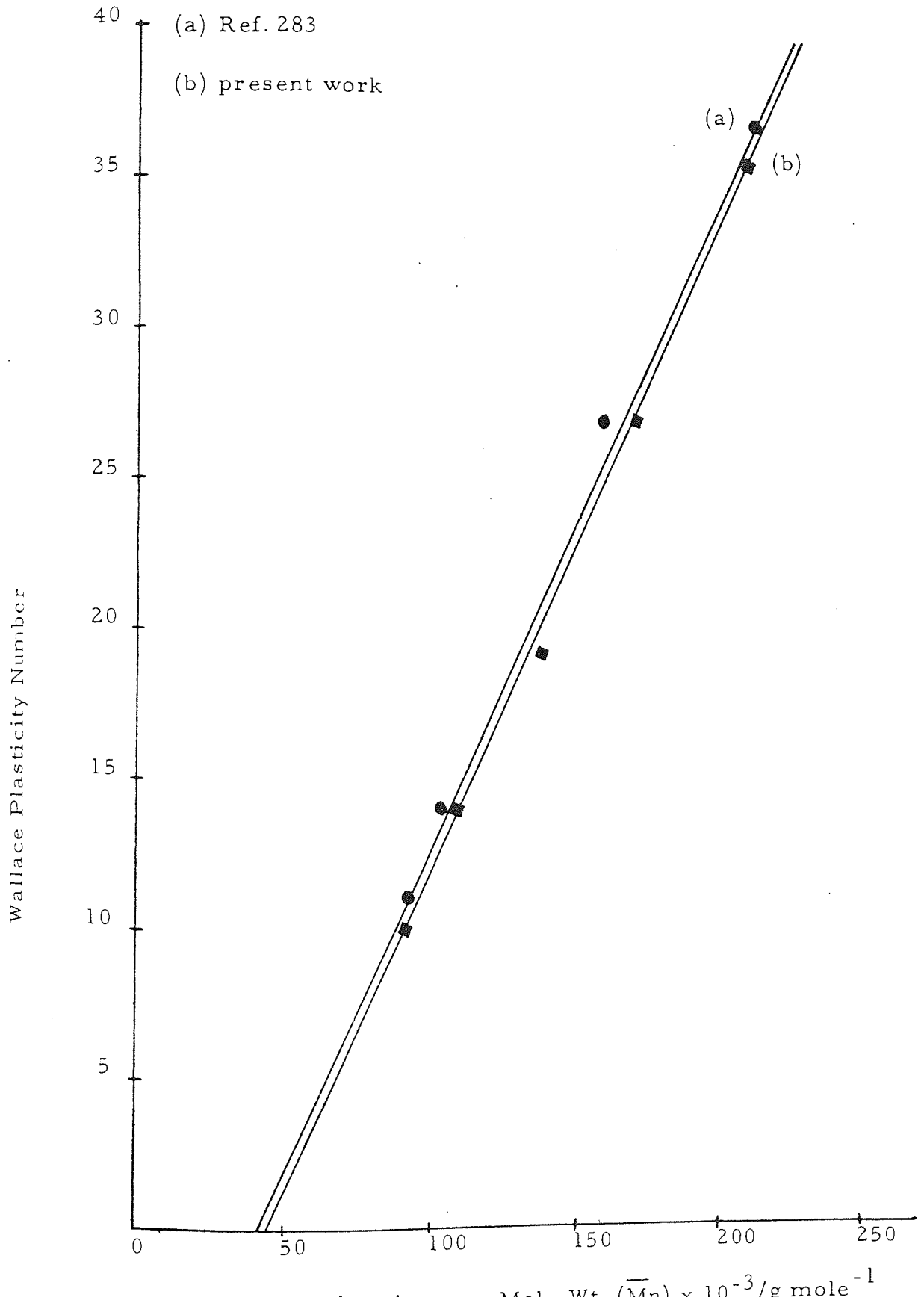

the rubber for testing. The Monsanto Rheometer was also used to establish that a uniform mixing of compounding ingredients had been attained by comparing rheographs of random samples of the compound. The curing characteristics of the four compounds under study are shown in Table 3.2. Vulcanisation of the compounds was carried out in a steam heated double daylight press as described in Section 2.3.2. 60 g of compound were used for moulding each sheet ($23 \times 7.6 \times 0.18$ cm^3) under the following conditions:

(i) Formulation A, cured at 140°C for 35 minutes,

(ii) formulation B, cured at 140°C for 18 minutes,

(iii) formulation C, cured at 140°C for 44 minutes, and

(iv) formulation D, cured at 160°C for 60 minutes.

The moulded sheets were cooled quickly in cold water at the end of the curing cycle.

The vulcanisation conditions were selected such that vulcanisates of comparable rheometer torques were obtained. Formulations A and D were therefore vulcanised to maximum torque while formulations B and C were vulcanised for an optimum cure time (t_{90}).

Table 3.2 Curing characteristics of NR compounds (composition of formulations in Table 3.1)

	Formulations			
	A	B	C	D
Rheometer temperature (°C)	140	140	140	160
Induction period, ti/(mins)	12	6	7	3
Overall first order curing rate constant (K)/min^{-1}	0.52	0.63	0.081	0.092
Optimum cure time, t_{90}/(mins)	21	18	44	35
Cure time for maximum torque/(mins)	35	30	70	60
Torque at 90% cure/(in-lb)	52	61	46	40
Maximum torque/(in-lb)	58	68	51	44

3.3 Single Extension Measurements

Vulcanisate samples were prepared and subjected to single extensions using the Hounsfield vertical tensometer as described in Section 2.6.2. The samples were subjected to various extensions ranging from 100 to 700% for one minute and when the stress had been removed, they were allowed to recover for 24 hours at room temperature. At the end of this recovery period the permanent set in the central region of the sample produced by the extension was determined using equation (3-1). The central region was then cut out and the equilibrium swelling ratio determined as described in Section 2.10.2. A control sample from an adjacent region of the rubber sheet (see Fig 3.2) was treated similarly.

Fig 3.2 Dumb-bell test piece

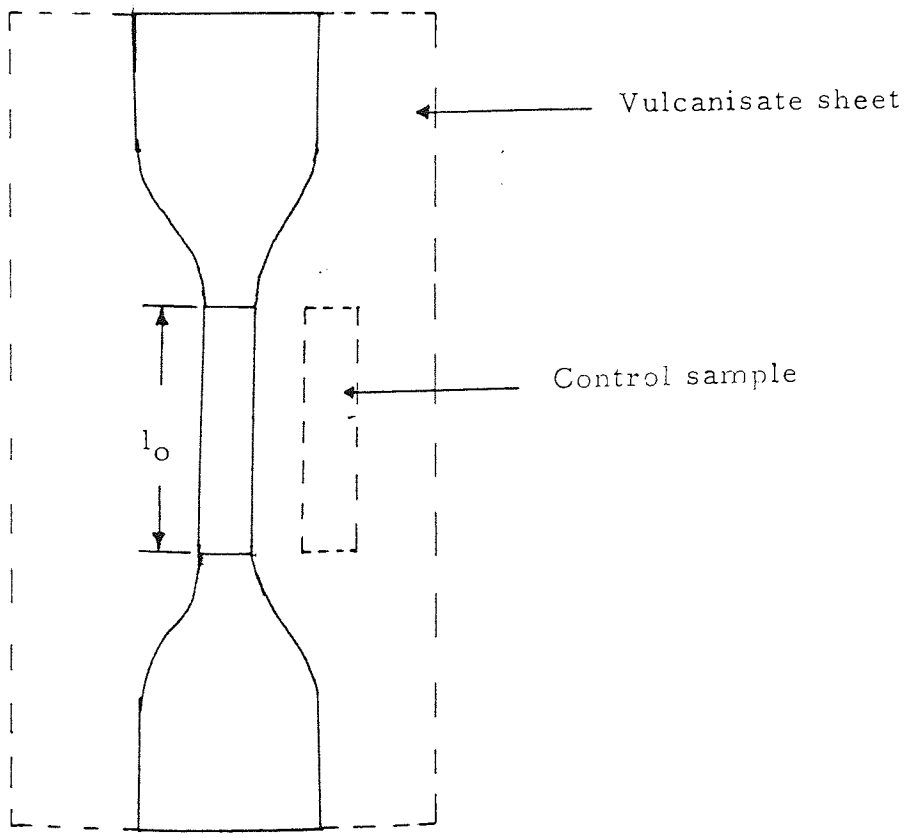

The permanent set remaining after this procedure was determined using equation (3-2). Both stretched and control samples were then treated with propan-2-thiol/piperidine probe, as described in Section 2.11.1 to destroy all polysulphide crosslinks. The linear dimensions of the samples were measured after probe treatment and the change in set resulting from probe treatment was determined (equation (3-2)). The density of polysulphide crosslinks in a sample was obtained by comparing the values of the chemical crosslink density before and after probe treatment; the polysulphide crosslink content in a sample was expressed as the percentage change in chemical crosslink density.

3.4 The Degree of Crystallinity

The relation between the extension ratio and the degree of strain-induced crystallinity (or molecular orientation) was established by two methods.

The onset of crystallisation/molecular orientation during extension could be estimated to be the extension at which there was a sudden rise in modulus of the sample. The modulus at any particular extension was obtained from the tangent to the stress-strain curve at that extension and the onset of crystallisation was determined from the plot of modulus against extension ratio. In the case of

black-filled vulcanisates, the application of the strain amplification factor (equation (1-29)) allows the local extension of the rubber matrix to be determined and the modulus was then derived from the plot of stress against local extension of the rubber matrix.

$$E = E_o (1 + 0.67fc + 1.62f^2c^2) \qquad (1\text{-}29)$$

where $f = 6.5$[99] and $c = 0.167$

An extension of 100% of the whole sample was found to be equivalent to 364% extension in the rubber matrix

The degree of crystallinity was assessed more accurately for gum vulcanisates by X-ray diffraction as described in Section 2.9.

3.5 Results and Discussions

3.5.1 Time to Equilibrium Volume Swelling

To ensure that samples were swollen to equilibrium during crosslink density determinations, the time to equilibrium volume swelling in the solvent was first estimated by monitoring swollen weights over a range of times. These values were then used to calculate the equilibrium volume fraction of rubber (Vr) for each rubber-solvent

system. Table 3.3 and Fig 3.3 show Vr as a function of time for NR vulcanisates in heptane and n-decane. The equilibrium swelling time was taken as the time to reach a constant value Vr. This was determined experimentally to be 14 hours in heptane and 18 hours in n-decane. However, to ensure that equilibrium swelling was achieved, a minimum swelling time of 24 hours was subsequently used for both equilibrium volume swelling and swollen compression modulus measurements.

3.5.2 The Rubber-Solvent Interaction Parameter (χ)

The rubber-solvent interaction parameter (χ) was calculated for swollen vulcanisates before and after probe treatment using swollen compression modulus (C_1) data and equilibrium volume swelling measurements (Vr), as described in Section 2.10.1 and 2.10.2 respectively. C_1 values were calculated from swollen compression measurements using equation (1-13):

$$C_1 = \frac{F}{\Delta h} \times \frac{h_o}{6A_o} \qquad (1\text{-}13)$$

The value obtained for C_1 was then substituted into equation (1-19) to obtain values of χ for a given vulcanisate/solvent system:

Table 3.3 Equilibrium volume swelling time for a conventional NR vulcanisate in heptane and n-decane

Swelling time/hr	Vr					
	Heptane			n-Decane		
	Sample Number			Sample Number		
	1	2	3	1	2	3
2	0.245	0.245	0.244	0.341	0.339	0.341
4	0.234	0.235	0.236	0.333	0.334	0.333
6	0.226	0.23	0.225	0.327	0.327	0.327
10	0.217	0.216	0.216	0.32	0.321	0.321
20	0.211	0.211	0.212	0.315	0.315	0.316
25	0.211	0.212	0.211	0.313	0.314	0.315

Fig 3.3 The Dependence of Volume Fraction of Rubber (Vr) on the Swelling Time

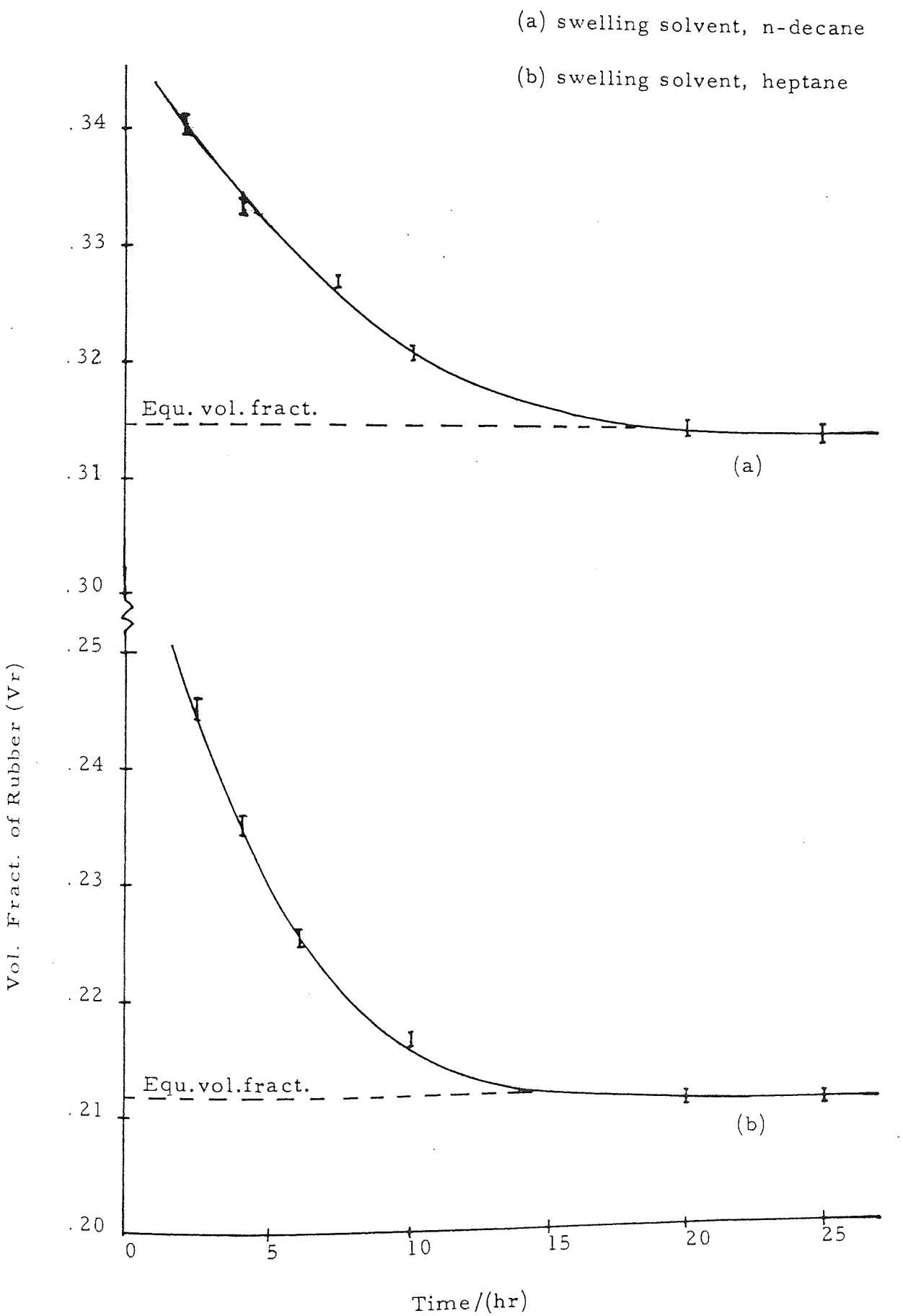

$$-\left[\ln(1 - Vr) + Vr + \chi Vr^2\right] = 2C_1V_o\frac{(Vr^{\frac{1}{3}} - Vr/2)}{RT} \qquad (1\text{-}19)$$

Typical χ values obtained for conventional, TMTD and peroxide vulcanisates are shown in Table 3.4.

Crosslink densities were subsequently determined from swelling data using these values of χ. The same value of χ was used for both gum and filled vulcanisates; χ was assumed to be unaffected by carbon black in filled vulcanisates. Although such an assumption is possibly not true, it is not expected to affect the changes in crosslink densities. Ideally χ should be determined for each sample but variations were small enough to allow for a universal value of χ to be used. χ values were found to be slightly different for conventional, TMTD and peroxide vulcanisates. A more significant change in χ value was obtained after treatment of the conventional vulcanisate with either propan-2-thiol or hexane thiol probes; the two χ values after probe treatment were not significantly different from each other. The change in values for different vulcanisates is attributable to their different network structure.

3.5.3 Effects of Single Extension on the Total and Polysulphide Crosslink Densities

Two different techniques were used to estimate the crosslink densities

Table 3.4 χ constant for NR vulcanisates (Average of three results quoted)

	$C_{1RN_2} \times 10^{-5}$ (Nm^{-2})	Vr	χ
Conventional vulc (original network)	1.779	0.316	0.446
TMTD vulc (original network)	1.692	0.307	0.442
Peroxide vulc (original network)	1.283	0.275	0.441
Conventional: After propane-2-thiol probe	0.904	0.231	0.429
Conventional: After hexane thiol probe	0.718	0.209	0.426

of stretched and unstretched specimens both before and after treatment with propan-2-thiol. The results obtained were then compared.

(i) Compression Modulus Technique

A vulcanisate sample was subjected to a single extension as described in Section 3.3 and then treated with propan-2-thiol as described in Section 2.11.1, to remove all polysulphidic crosslinks. The chemical crosslink densities before and after probe treatment were estimated from the C_1 values obtained using the compression modulus technique (Section 2.10.1) and the percentage polysulphidic crosslinks present in the sample were then estimated. Estimates of crosslink densities were carried out on an unstretched sample taken from an adjacent region of the vulcanisate sheet (see Fig 3.2). The changes in behaviour on a single extension were obtained by comparing the total and polysulphide crosslink densities of the stretched and unstretched samples.

Table 3.5, Fig 3.4 and Table 3.6, Fig 3.5 show the behaviour on single extensions ranging from 100 - 700%, of two conventional vulcanisates prepared from compounds having initial number average molecular weight ($\overline{Mn}$) values of rubber of 180,000 and 190,000 respectively. These results show that a small but reproducible reduction in polysulphide (S_x) crosslinks occurred during extension, which appears to be independent of the initial number average molecular weight of the rubber. The dependence of the change in polysulphide

Table 3.5 Effect of single extension on polysulphide crosslink content of a conventional NR vulcanisate ($\overline{M}n$ = 180, 000)

Sample number(a)	Unstretched			Stretched			Change in S_x crosslinks (%)
	Crosslink density(b)		% crosslink ($-S_x-$)	Crosslink density(b)		% crosslink ($-S_x-$)	
	Before probe	After probe		Before probe	After probe		
100	4.62	1.51	67.3	4.62	1.54	66.7	0.6
200	4.66	1.57	66.3	4.66	1.64	64.8	1.5
300	4.78	1.55	67.6	4.40	1.57	64.3	3.3
400	4.86	1.46	69.9	4.35	1.44	66.9	3.0
500	4.95	1.64	66.9	4.94	1.75	64.6	2.3
600	4.68	1.51	67.6	4.58	1.57	65.7	1.9
700	4.66	1.51	67.6	4.86	1.68	65.4	2.2

(a) represent % extension for stretched samples (b) Crosslink density = $\frac{1}{2}\overline{M}_{c(chem)} \times 10^2 / Kg\,mole\,Kg^{-1}\,RN$

Fig 3.4 The Dependence of Polysulphide Crosslinks Destroyed and Modulus on the Degree of Extension of a Gum Vulcanisate ($\overline{Mn}$ = 180, 000)

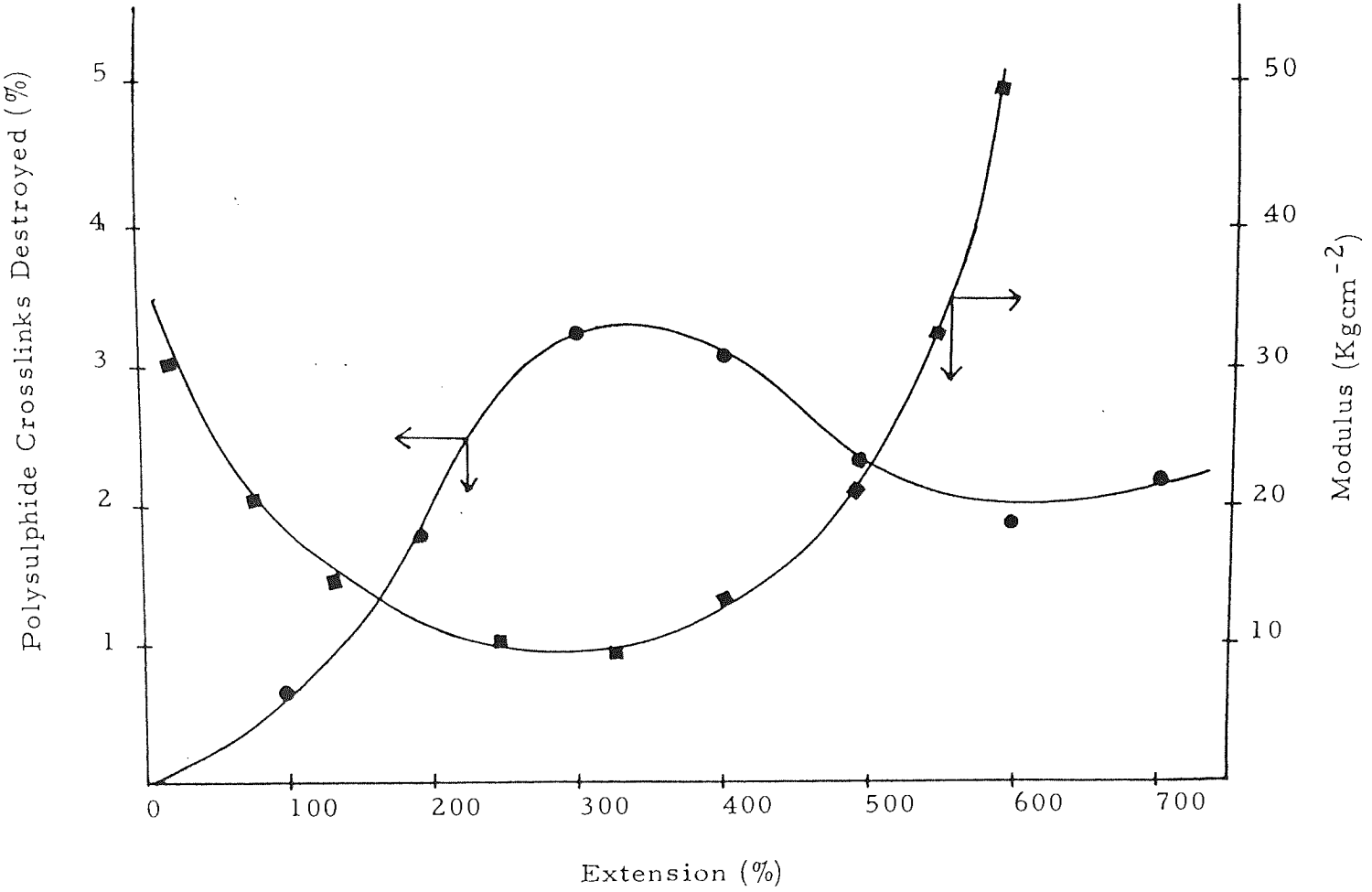

Table 3.6 Effect of single extension on polysulphide crosslink content of a conventional NR vulcanisate ($\overline{M}n$ = 190, 000)

Sample number(a)	Unstretched			Stretched			Change in S_x crosslinks (%)
	Crosslink density(b)		% crosslink ($-S_x-$)	Crosslink density(b)		% crosslink ($-S_x-$)	
	Before probe	After probe		Before probe	After probe		
100	5.62	2.17	61.4	5.62	2.19	61.0	0.4
200	5.67	2.20	61.2	5.67	2.28	59.8	1.4
300	5.71	2.19	61.7	5.42	2.24	58.7	3.0
400	5.83	2.12	63.6	5.79	2.27	60.8	2.8
500	5.83	2.12	63.6	5.81	2.20	62.1	1.5
600	5.54	2.11	61.9	5.58	2.22	60.2	1.7
700	5.67	2.15	62.1	5.38	2.15	60.0	2.1

(a) represent % extension for stretched samples (b) Crosslink density = $\frac{1}{2}\overline{M}_{c(chem)} \times 10^2 / Kg\,mole\,Kg^{-1}RN$

Fig 3.5 The Dependence of Polysulphide Crosslinks Destroyed and Modulus on the Degree of Extension of a Gum Vulcanisate ($\overline{Mn}$ = 190, 000)

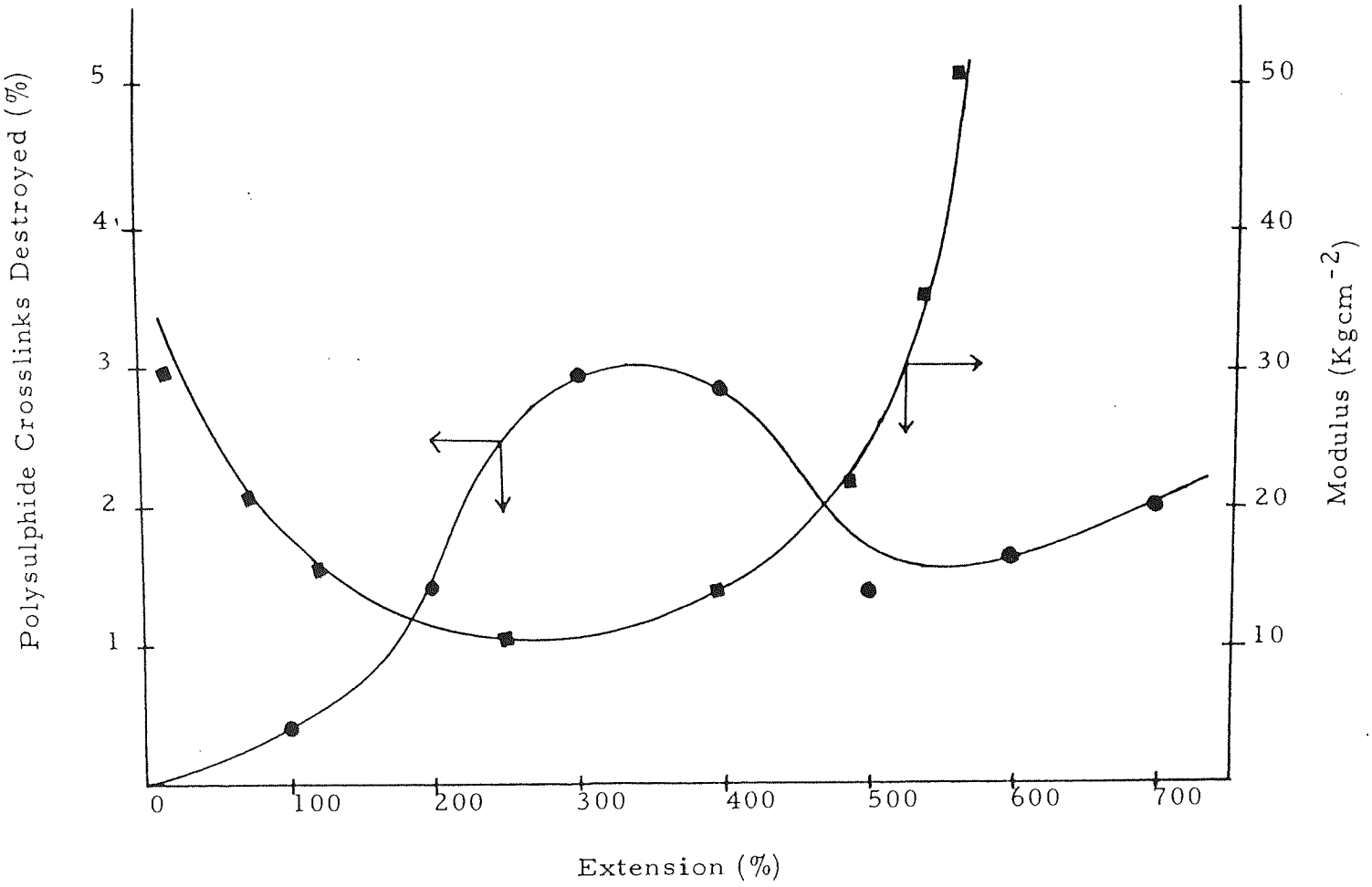

crosslink densities on the degree of extension (Fig 3.4 and 3.5), gave similar curves showing an increase in the extent of S_x breakdown on small extensions (i.e. up to about 300% extension) and then a decrease in the S_x breakdown on higher extensions which extensions coincide with the onset of strain induced crystallisation or molecular orientation. At the same time there is a sudden rise in modulus of the rubber at higher extensions. The onset of crystallisation, therefore, appears to reduce the rate of destruction of polysulphide crosslinks.

The observed trend of S_x breakdown on a single extension of an unfilled vulcanisate could be explained on the basis of the strength induced on stretching due to crystallisation or molecular orientation of the rubber, which is well known to occur in natural rubber vulcanisates at elongations above 200%. The result of the investigation carriedout in this work, of the relationship between the degree of extension and the degree of crystallisation by X-ray diffraction, shows that crystalline contents up to 44% could be obtained when a conventionally vulcanised natural rubber is stretched to 600% extension (see Fig 3.6). There is a strong possibility, as the evidence provided suggests, that at low extensions, the polysulphide crosslinks bear most of the stress applied on stretching and therefore break, but on further elongation when strain induced crystallisation or molecular orientation sets in, the polysulphide crosslinks begin to bear less stress and a decrease

Fig 3.6 Relation Between Degree of Extension and Degree of Crystallisation for a Conventionally Vulcanised NR

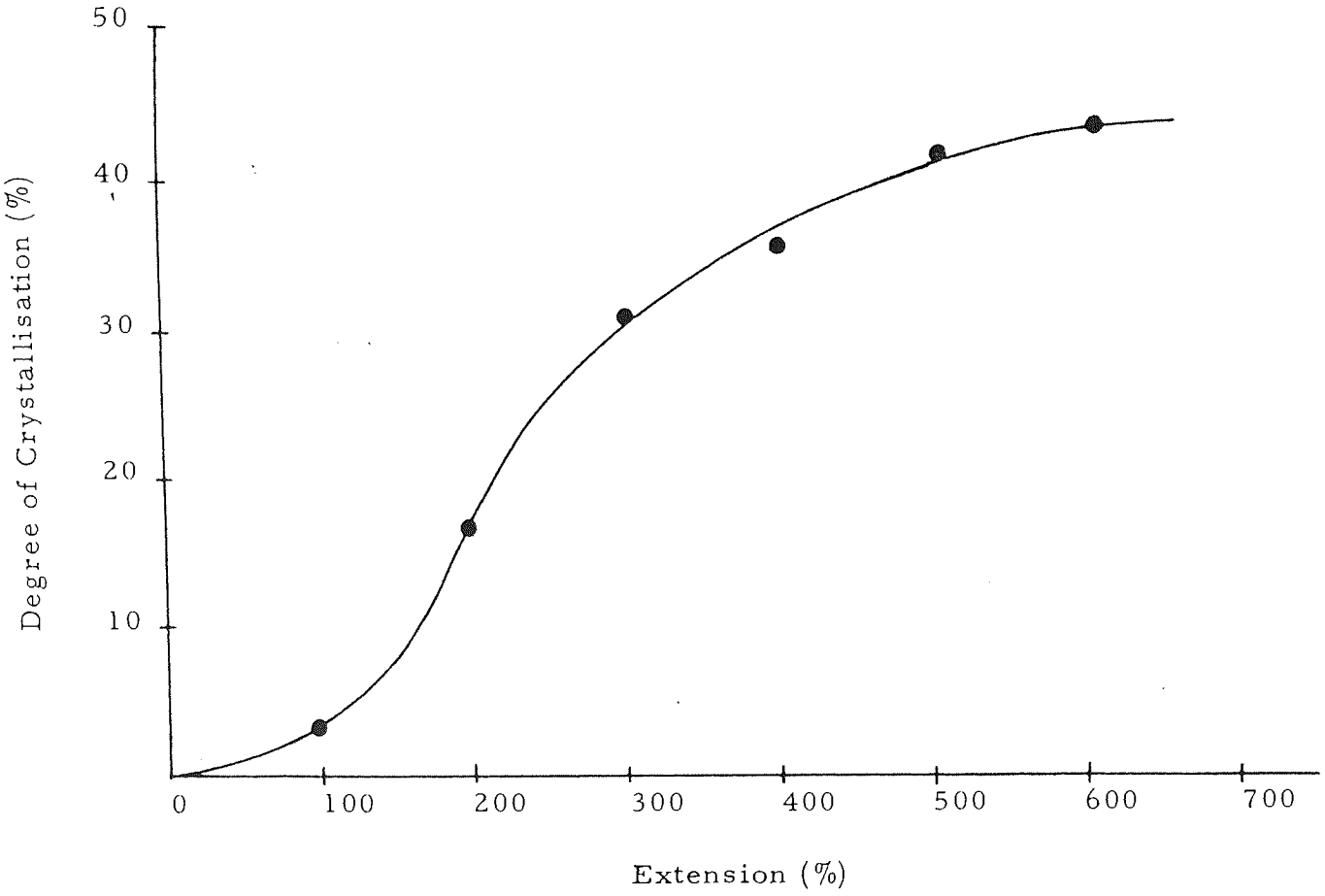

in S_x breakdown is observed. The breakdown of polysulphide crosslinks reported here seems to conform with the well known mechanism whereby local stress concentrations are relieved in conventional vulcanisate networks during repeated extensions. Polysulphide crosslinks are relatively weak and are thought to break during extension, thereby relieving the stress concentration by load redistribution; they are particularly characterised by their ability to participate in exchange reactions of breaking and reforming. Directly relevant investigations on stretched rubbers have been carried out by Thomas[271], who provided evidence indicating that breakage and reformation of crosslinks occur in the extended state. His investigation was not, however, extended to explore possible differences in the distribution of crosslinks in the rubbers.

The changes in the total chemical crosslink density on stretching are both positive and negative and do not appear to follow any particular trend. However, the slight variation in chemical crosslink density on stretching would not be expected to affect the observed trend in S_x crosslink destruction. It is not quite clear why there is a variation in the change in total crosslink density but it could be explained on the basis of the two network theory. The chemical crosslink density was estimated from C_1 values obtained from compression modulus. C_1 values may not absolutely reflect the crosslink density of the samples after extension presumably because of the contribution from

the second network formed in the stretched state since this will be in compression in the relaxed unstretched state. The variation in such a contribution may account for the variation in the crosslink density after stretching.

(ii) Equilibrium Volume Swelling

The equilibrium volume swelling technique was used to investigate the effect of a single extension on the crosslink density and polysulphidic crosslink distribution of a conventional vulcanisate with an $\overline{Mn}$ value of 214,000. The technique was also used to investigate the behaviour of a TMTD and a peroxide vulcanisate having $\overline{Mn}$ values of 194,000 and 195,000 respectively. The experiments were carried out as described in the preceding section and the chemical crosslink density of the stretched and unstretched specimens were estimated from their Vr values. In the case of the conventional vulcanisate, the chemical crosslink density before and after treatment with propan-2-thiol was also estimated from the values of Vr to obtain the change in polysulphide crosslinks on stretching.

Table 3.7 shows the effect of single extensions ranging from 100 to 700% on the crosslink density and polysulphide crosslink distribution of the conventional vulcanisate. The plot of the polysulphide crosslinks destroyed and the modulus versus the degree of extension is

Table 3.7 *Effect of a single extension on polysulphide crosslink content of a conventional NR vulcanisate* ($\overline{M}n$ = 214, 000)

Sample number[a]	Unstretched			Stretched			Change in S_x crosslinks (%)
	Crosslink density[b]		% crosslink (-S_x-)	Crosslink density[b]		% crosslink (-S_x-)	
	Before probe	After probe		Before probe	After probe		
100	5.35	1.85	65.4	5.33	1.90	64.4	1.0
200	5.28	1.82	65.5	5.29	1.92	63.7	1.8
300	5.27	1.98	62.4	5.31	2.18	58.9	3.5
400	5.32	1.86	65.0	5.37	2.06	61.6	3.4
500	5.37	1.86	65.4	5.46	2.05	62.5	3.0
600	5.47	1.87	65.8	5.57	2.05	63.2	2.6
700	5.52	1.85	66.5	5.65	1.99	64.8	1.7

(a) represent % extension for stretched samples (b) Crosslink density = $\frac{1}{2}\overline{M}_{c(chem)} \times 10^2$ / Kg mole Kg^{-1} RN

shown in Figure 3.7. The results are broadly comparable with those obtained using the compression modulus technique and similarly suggest that crystallisation or molecular orientation reduces the rate of destruction of S_x crosslinks on stretching. Although the reduction in S_x crosslinks on stretching is generally small (less than 4%), the reproducibility of the results using two different techniques suggests that the effect must be real.

Tables 3.8 and 3.9 show the effect of stretching on the crosslink density of the TMTD and the peroxide vulcanisates respectively. The curves relating the change in crosslink density to the percent extension are shown in Figure 3.8. It is evident from these results that a small increase in the crosslink density occurs on stretching, the larger the percent extension the larger the increase. At the highest extensions used, there were increases in crosslink density of about 2.4%, 1.2% and 1% for the conventional, TMTD and peroxide vulcanisates respectively. The slight increase in the density of crosslinks after extension could be due to the crosslink formation occurring in the stretched state. The highest value obtained for the conventional vulcanisate, perhaps reflects the weakness of the polysulphide crosslinks and their ability to undergo yielding and form new crosslinks. The observed breakdown of polysulphide crosslinks on stretching tends to support this view.

Fig 3.7 The Dependence of Polysulphide Crosslinks Destroyed and Modulus on the Degree of Crystallisation ($\overline{Mn}$ = 214,000)

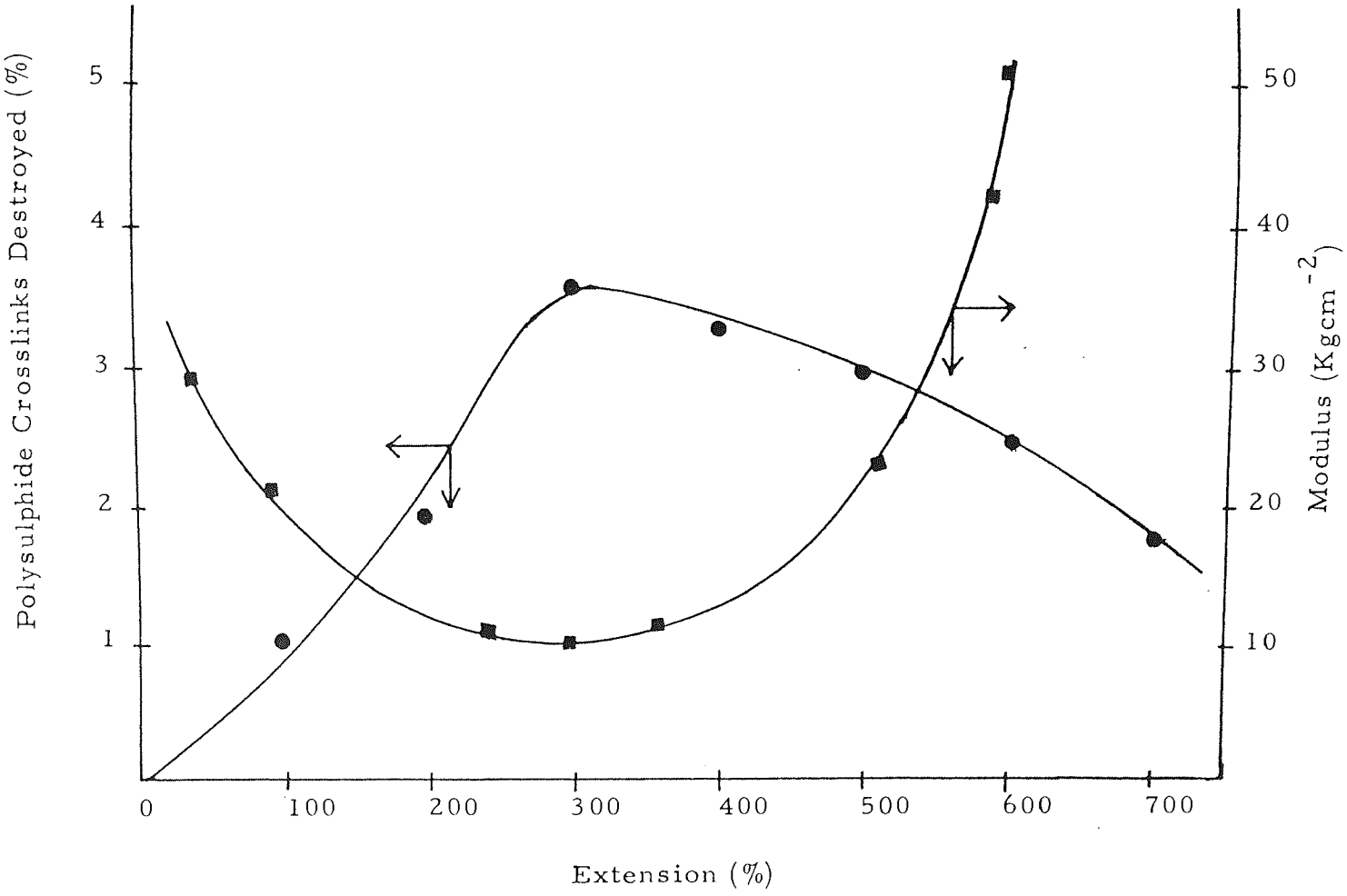

Table 3.8 Effect of single extension on the crosslink density of a TMTD vulcanisate ($\overline{Mn}$ = 195,000)

Sample	Unstretched			Stretched			Change in crosslink density x 10^2 Kg mol Kg^{-1} RN
	Vr	$C_1 x 10^{-5}$ (Nm^{-2})	crosslink density(a)	Vr	$C_1 x 10^{-5}$ (Nm^{-2})	crosslink density(a)	
100	0.3069	1.638	4.77	0.307	1.639	4.78	.01
200	0.306	1.625	4.73	0.3063	1.630	4.74	.01
300	0.3072	1.642	4.79	0.3077	1.649	4.82	.03
400	0.3067	1.635	4.77	0.3074	1.645	4.81	.04
500	0.3072	1.642	4.79	0.308	1.653	4.84	.05
600	0.3072	1.642	4.79	0.3082	1.656	4.85	.06

(a) Crosslink density = $\frac{1}{2}\overline{M}_{c(chem)} x 10^2$ / Kg mol Kg^{-1} RN

Table 3.9 Effect of single extension on the crosslink density of peroxide vulcanisate (original $\overline{Mn}$ = 195,000)

Sample	Unstretched			Stretched			Change in crosslink density$\times 10^2$ $Kgmol Kg^{-1} RN$
	Vr	$C_1 \times 10^{-5}$ (Nm^{-2})	crosslink density(a)	Vr	$C_1 \times 10^{-5}$ (Nm^{-2})	crosslink density(a)	
100	0.2746	1.229	3.19	0.2747	1.230	3.20	0.01
200	0.2749	1.233	3.21	0.2751	1.235	3.21	-
300	0.2758	1.243	3.25	0.2763	1.249	3.27	0.02
400	0.2768	1.254	3.29	0.2773	1.260	3.31	0.02
500	0.2750	1.337	3.21	0.2757	1.242	3.24	0.03
600	0.2763	1.249	3.26	0.2771	1.258	3.30	0.04

(a) Crosslink density = $\frac{1}{2}\overline{M}_{c(chem)} \times 10^2 / Kgmol Kg^{-1} RN$

Fig 3.8 Change in the Total Chemical Crosslink Density After a Single Extension

(a) Conventional

(b) TMTD

(c) Peroxide

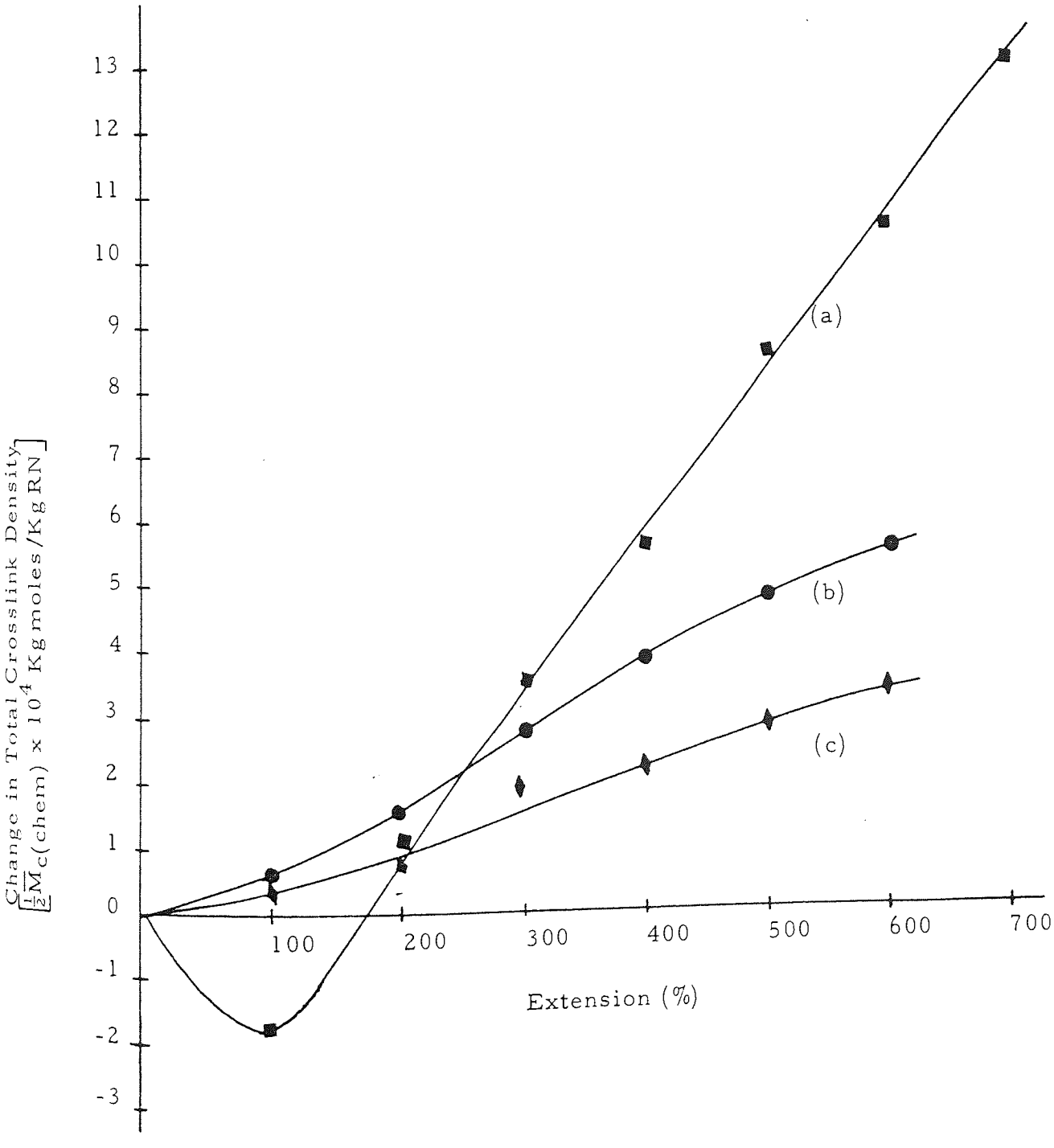

The crosslink density values obtained using both the compression modulus technique and the equilibrium swelling method agree within experimental error. However, a comparison of the change in crosslink density on stretching obtained by both methods reveals that while swelling gives a consistent increase in crosslink density with percent extension, the compression technique does not. This could be due to the fact that crosslink density values obtained with the compression technique are estimated from C_1 values which, as has already been explained, may not reflect the crosslink density in the stretched sample, presumably because of the contribution from the secondary network formed in the stretched state. It would appear, therefore, that although C_1 values may be more easily interpreted than equilibrium volume fraction (Vr) values, they may be less precise in estimating the density of crosslinks in a vulcanisate after stretching. In this light, a modification of the present methods of C_1 determination may seem desirable.

3.5.3.1 The Effect of Filler (HAF-black)

The effect of single extension on the crosslink density and polysulphide crosslink distribution of a filled conventional vulcanisate ($\overline{Mn}$ =189, 000) was investigated by using the equilibrium volume swelling technique to estimate the density of crosslinks in the stretched and unstretched vulcanisate samples before and after treatment with propan-2-thiol.

The swollen compression modulus technique was not used because the magnitude of the effect of filler on stress-strain measurements was unknown (see Section 1.3.3).

Table 3.10 shows the change in crosslink densities and polysulphide crosslink content after single extensions ranging from 100-500%. The dependence of the polysulphide crosslink destruction on the degree of extension is shown in Figure 3.9. It can be seen to follow a similar pattern as that obtained for an unfilled vulcanisate. However, the S_x breakdown at a particular extension is slightly higher than the corresponding value obtained for the unfilled vulcanisate. As with the gum vulcanisate, the decrease in the extent of S_x breakdown on higher extensions coincides with molecular orienation deduced by the sudden rise in modulus. The modulus at any extension was estimated from the stress-strain curve of a sample after application of a strain amplification factor, to account for the distortion of the stress pattern in the rubber matrix due to the presence of the filler.

The slightly higher values of S_x breakdown observed for a filled vulcanisate compared with the corresponding values for a gum vulcanisate may be due to the fact that the actual strain occurring locally in the rubber matrix of the vulcanisate is much higher than that observed for the vulcanisate as a whole. In fact, it was found by calculation (see Section 3.4) that an extension of a sample by

Table 3.10 Effect of single extension on polysulphide crosslink content of a carbon-black filled conventional NR vulcanisate ($\overline{Mn}$ = 189,000)

Sample number[a]	Unstretched			Stretched			Change in S_x crosslinks (%)
	Crosslink density[b]		% crosslink ($-S_x-$)	Crosslink density[b]		% crosslink ($-S_x-$)	
	Before probe	After probe		Before probe	After probe		
100	5.87	2.62	55.4	5.89	2.83	52.0	3.4
200	5.92	2.66	55.1	5.94	2.94	50.5	4.6
300	6.03	2.75	54.4	6.07	3.04	49.9	4.5
400	5.95	2.65	55.5	5.99	2.85	52.4	3.1
500	6.18	2.84	54.0	6.24	3.02	51.6	2.4

(a) represent % extension for stretched samples (b) Crosslink density = $\frac{1}{2}\overline{M}_{c(chem)} \times 10^2 / Kg\,mole\,Kg^{-1}\,RN$

Fig 3.9 Change in Polysulphide Crosslinks on Single Extension of Carbon Black Filled Vulcanisate

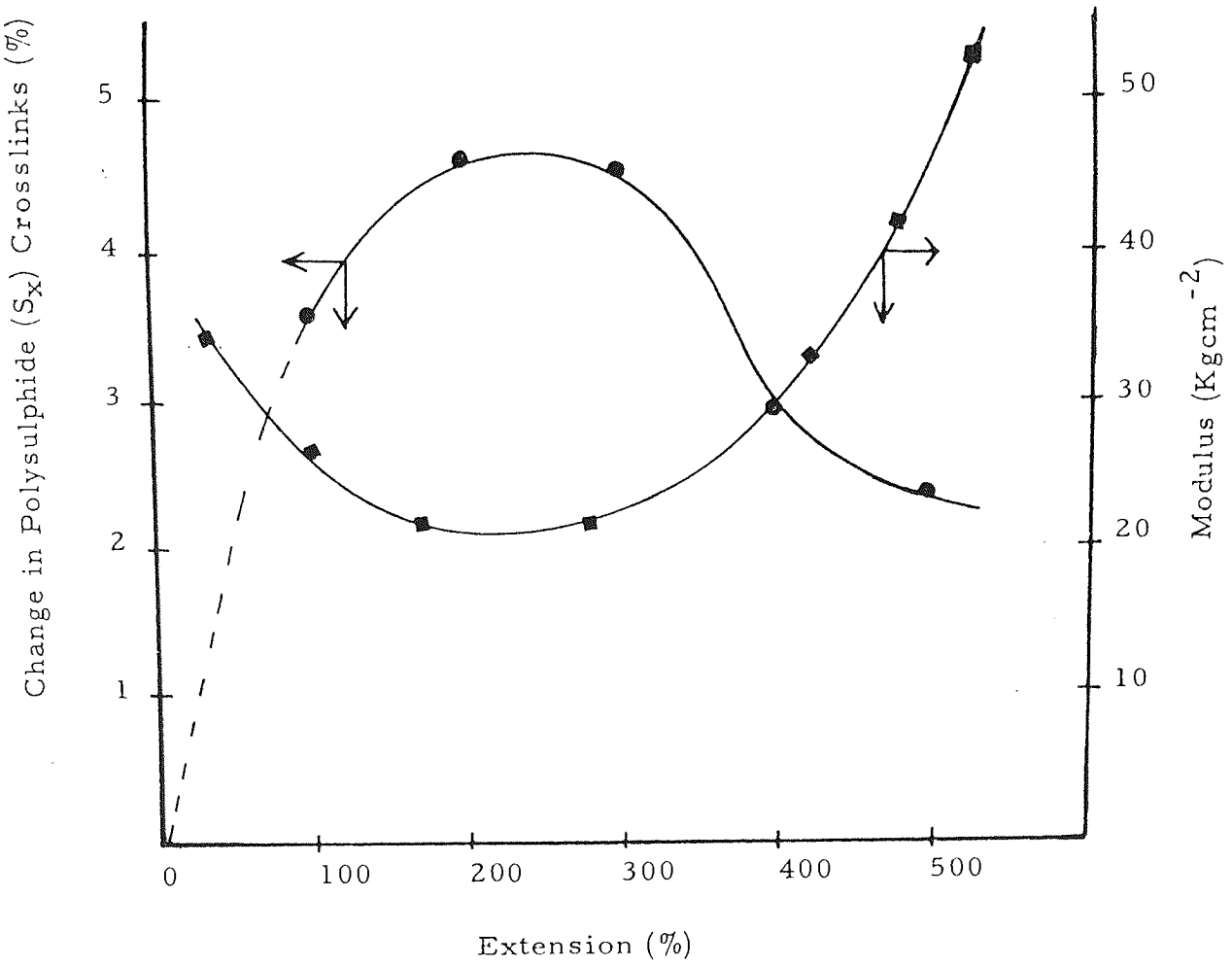

100% was equivalent to 364% extension in the rubber matrix.

3.5.4 The Relationship Between the Degree of Extension and the Permanent Set Produced

A vulcanisate sample was subjected to single extensions ranging from 100-700% for one minute and the permanent set produced after 24 hours recovery period was estimated using equation (3-1). The new set after swelling and deswelling in a solvent or after probe treatment was then estimated by using equation (3-2). The permanent sets which occurred after stretching of the conventional, TMTD and peroxide vulcanisates are shown in Tables 3.11, 3.12 and 3.13 respectively.

The dependence of the permanent set (%) on the degree of extension is shown in Figure 3.10. The larger the extension, the greater the permanent set produced. The conventional vulcanisate containing mainly polysulphidic, as well as mono and disulphidic crosslinks, produced the largest set at the highest extension used. The comparable set in the peroxide vulcanisate possessing only carbon-carbon crosslinks was very small, about 24% of that of the conventional vulcanisate. The TMTD vulcanisate with principally monosulphide crosslinks showed intermediate behaviour, about 36% of that produced by the polysulphidic network. The permanent set remaining after swelling and deswelling of conventional samples in n-decane was only

Table 3.11 Changes in set and crosslink recombination efficiency on single extension of a conventionally vulcanised NR (Formulation A, Table 2.1)

Extension (%)	Set after 24 hrs recovery period (%)	Set after swelling & deswelling (%)	Set after treatment with Propan-2-thiol (%)	Crosslinks reformed / Crosslink unbroken by stress (%)	Crosslinks broken on extension (%)	Recombination efficiency (%)
100	1.4	1.0	-	1.7	2.6	64.2
200	2.9	2.1	-	2.2	4.1	51.6
300	4.2	3.3	0.05	2.6	6.0	41.0
400	5.5	4.5	0.89	2.8	7.8	33.5
500	6.9	5.8	1.15	3.1	9.7	28.8
600	7.9	6.7	1.67	3.1	11.0	25.0
700	8.7	7.4	2.05	3.0	11.8	22.3

Table 3.12 Changes in set and crosslink recombination efficiency on single extension of a TMTD vulcanised NR (Formulation E, Table 2.1)

Extension (%)	Set after 24 hrs recovery period (%)	Set after swelling & deswelling (%)	Crosslink reformed / Crosslink unbroken by stress (%)	Total crosslinks broken by extension (%)	Recombination efficiency (%)
100	0.61	0.6	1.0	1.4	75.2
200	1.4	1.1	1.2	2.0	55.6
300	2.6	1.9	1.2	2.8	43.2
400	3.2	2.3	1.2	3.2	35.9
500	3.6	2.6	1.2	3.8	29.7
600	3.8	2.7	1.1	4.2	26.1

Table 3.13 Changes in set and crosslink recombination efficiency on single extension of a peroxide vulcanised NR (Formulation D, Table 2.1)

Extension (%)	Set after 24 hrs recovery period (%)	Set after swelling & deswelling (%)	Crosslink reformed / Crosslink unbroken by stress (%)	Total crosslinks broken on extension (%)	Recombination efficiency (%)
100	0.15	0.15	0.3	0.3	94.8
200	0.50	0.50	0.5	0.9	59.7
300	0.82	0.81	0.6	1.2	52.2
400	1.23	1.20	0.7	1.9	37.2
500	1.59	1.50	0.8	2.3	32.2
600	1.91	1.80	0.8	2.8	27.3

Fig 3.10 The Dependence of Permanent Set on the Degree of Extension

(a) Conventional cure

(b) TMTD cure

(c) Peroxide cure

(d) Conventional cure after treatment with propan-2-thiol

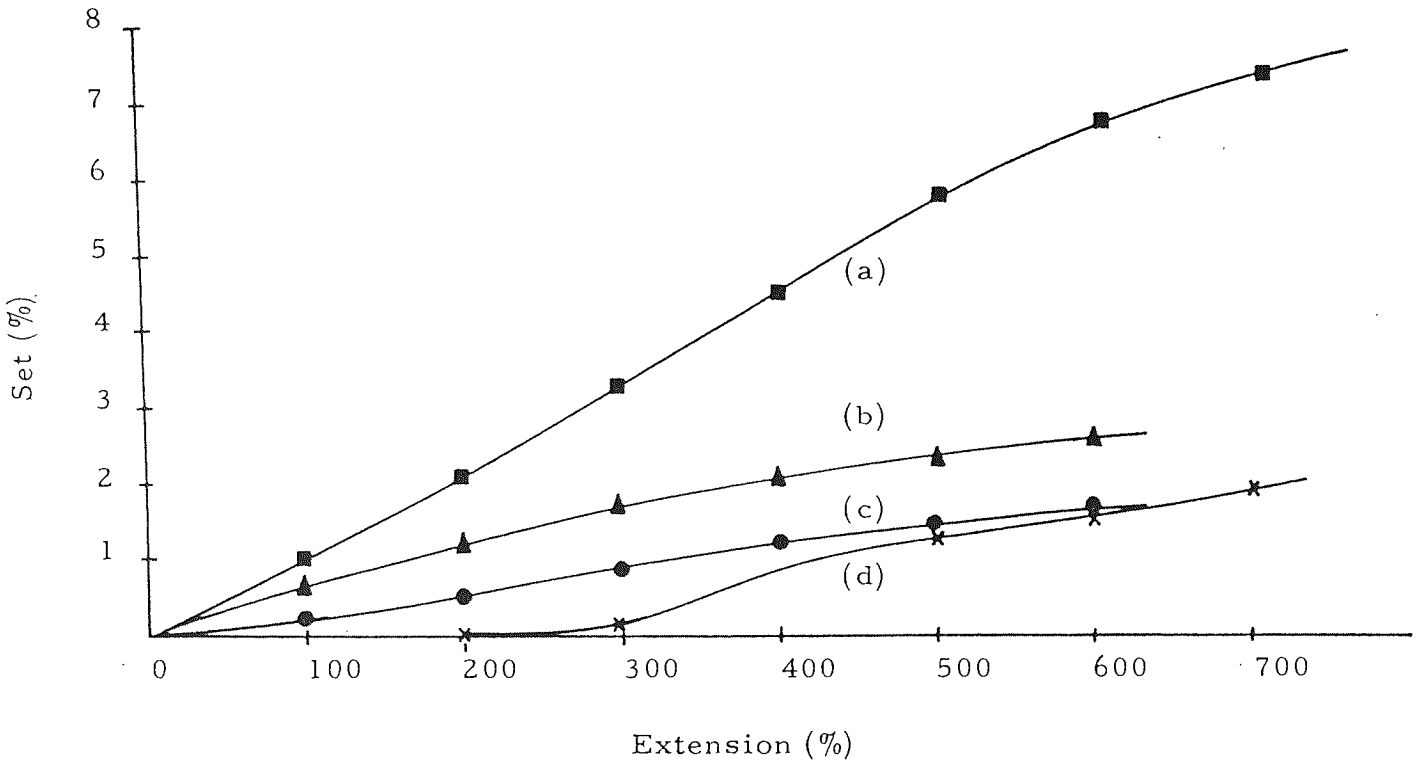

about 1% less than that after 24 hours recovery and the reductions in set after swelling and deswelling of TMTD and peroxide vulcanisates were even lower. The slight reduction in permanent set after swelling and deswelling of samples in decane is perhaps an indication that pure viscoelastic recovery of the stretched samples was incomplete after 24 hours.

The permanent set produced on extension of the conventional vulcanisate was found to reduce substantially after treatment of the samples with propan-2-thiol. In fact, permanent set was removed completely from samples subjected to low extensions.

Permanent set in a stretched vulcanisate has been shown [268, 271] to reflect the crosslinks formed in the stretched state presumably from recombination of broken ends of crosslinks. In the present investigations, the comparatively large permanent set produced on extension of the conventional vulcanisate suggests that a large number of crosslinks break and reform during extension. The small permanent set produced in the peroxide vulcanisate with 'strong' carbon-carbon crosslinks, indicated little cleavage of crosslinks. The substantial reduction in set on treatment of the conventional vulcanisates with propan-2-thiol is clear evidence for changes in the polysulphidic crosslinks during stretching and possibly indicates that the second network formed during stretching is made up mainly of polysulphidic

crosslinks. The fact that the set did not disappear completely in samples subjected to high extensions would imply that some mono and disulphidic crosslinks are also formed or that mono and disulphide crosslinks may cleave but at a significantly slower rate than polysulphides. The formation of mono and disulphidic crosslinks is more likely since there is a slight increase in crosslink density in these systems although the polysulphide crosslink density decreases. The slightly higher permanent set produced in the TMTD vulcanisate compared with the peroxide suggests that monosulphide crosslinks may be more readily cleaved and reformed than carbon-carbon crosslinks.

3.5.4.1 The Effect of Filler (HAF-black)

The effect of filler on the relationship between the degree of extension and the set produced was investigated using the filled conventional vulcanisate containing 40 parts by weight of HAF-black. The dependence of permanent set on the degree of extension is shown in Figure 3.11. The permanent set produced at the highest extension and after 24 hours recovery period was found to be almost twice as large as that produced by the comparable gum vulcanisate. The subsequent reduction in set after swelling and deswelling in n-decane was also larger. The larger set produced by the filled vulcanisate could be accounted for on the basis of the fact that a much larger strain than

Fig 3.11 The Dependence of Permanent Set on the Degree of Extension for Filled Vulcanisate

(a) Set after 24 hrs recovery from applied stress

(b) Set after equilibrium swelling in n-Decane followed by deswelling

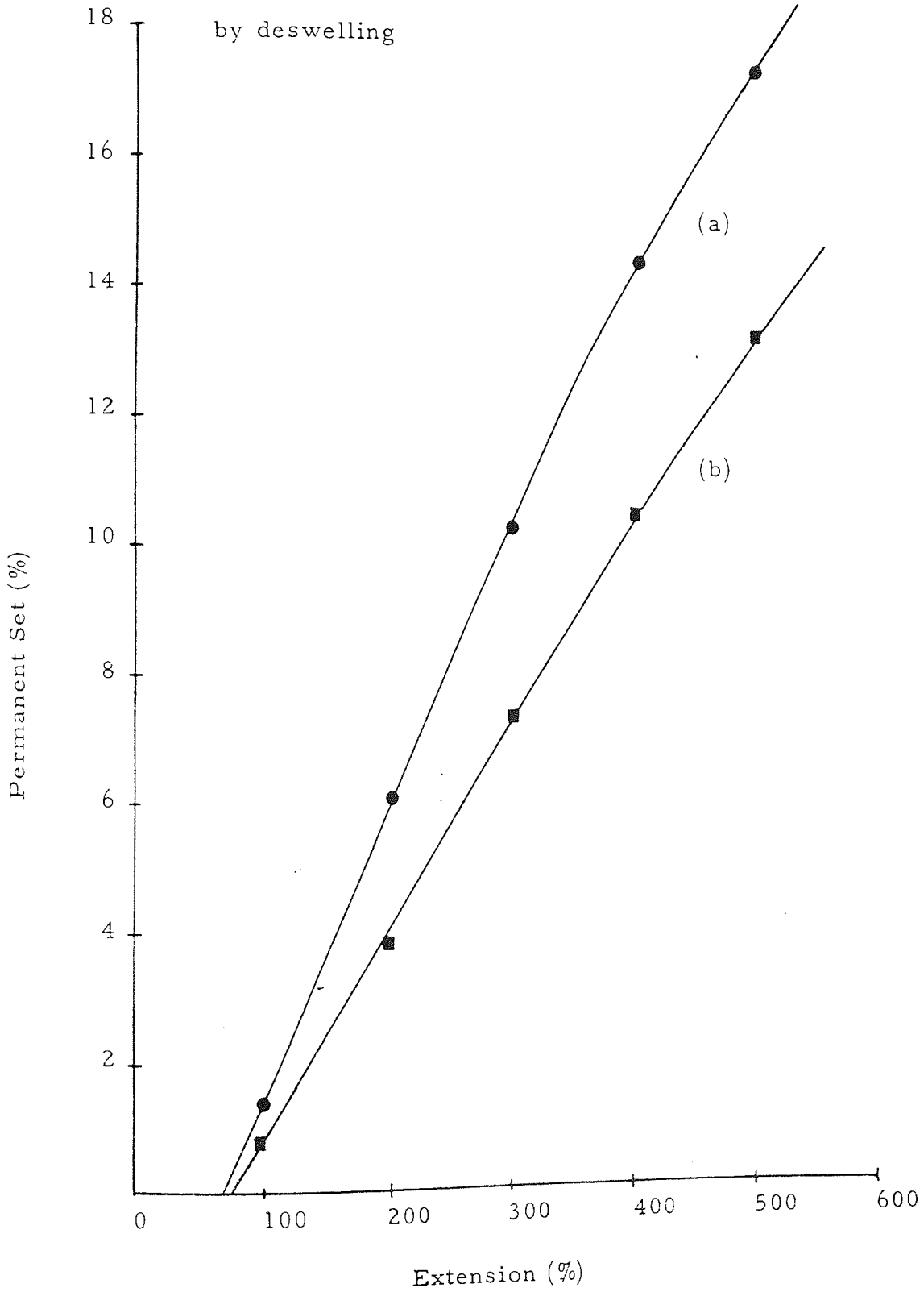

that observed for the whole sample is actually imposed locally on the rubber matrix. Moreover, the physical presence of filler in the vulcanisate may prevent the complete visco-elastic recovery of the rubber matrix after extension. Part of the permanent set observed, may even be the result of the physical separation of the filler particles which would not be expected to relax.

3.5.5 The Effect of Single Extension on the Number of Crosslinks Broken per Unit Volume and the Recombination Efficiency

The number of crosslinks broken per unit volume and the efficiency of recombination of a vulcanisate were calculated from set and equilibrium volume swelling data using equations (3-4) and (3-5). Tables 3.11, 3.12 and 3.13 show these results for conventional, TMTD and peroxide vulcanisates respectively. The dependence of the number of crosslinks broken per unit volume on the degree of extension is shown in Figure 3.12 while Figure 3.13 shows the dependence of the crosslink recombination efficiency on the degree of extension. The plots of α (number of crosslinks reformed per unit volume/number of crosslinks unbroken during extension per unit volume) versus extension (%) are shown in Figure 3.14.

The results obtained show that there is always a net cleavage of crosslinks after a single extension; the greater the extension (%)

Fig 3.12 The Dependence of the Total Crosslinks Broken per Unit Volume on the Degree of Extension

(a) Conventional cure

(b) TMTD cure

(c) Peroxide cure

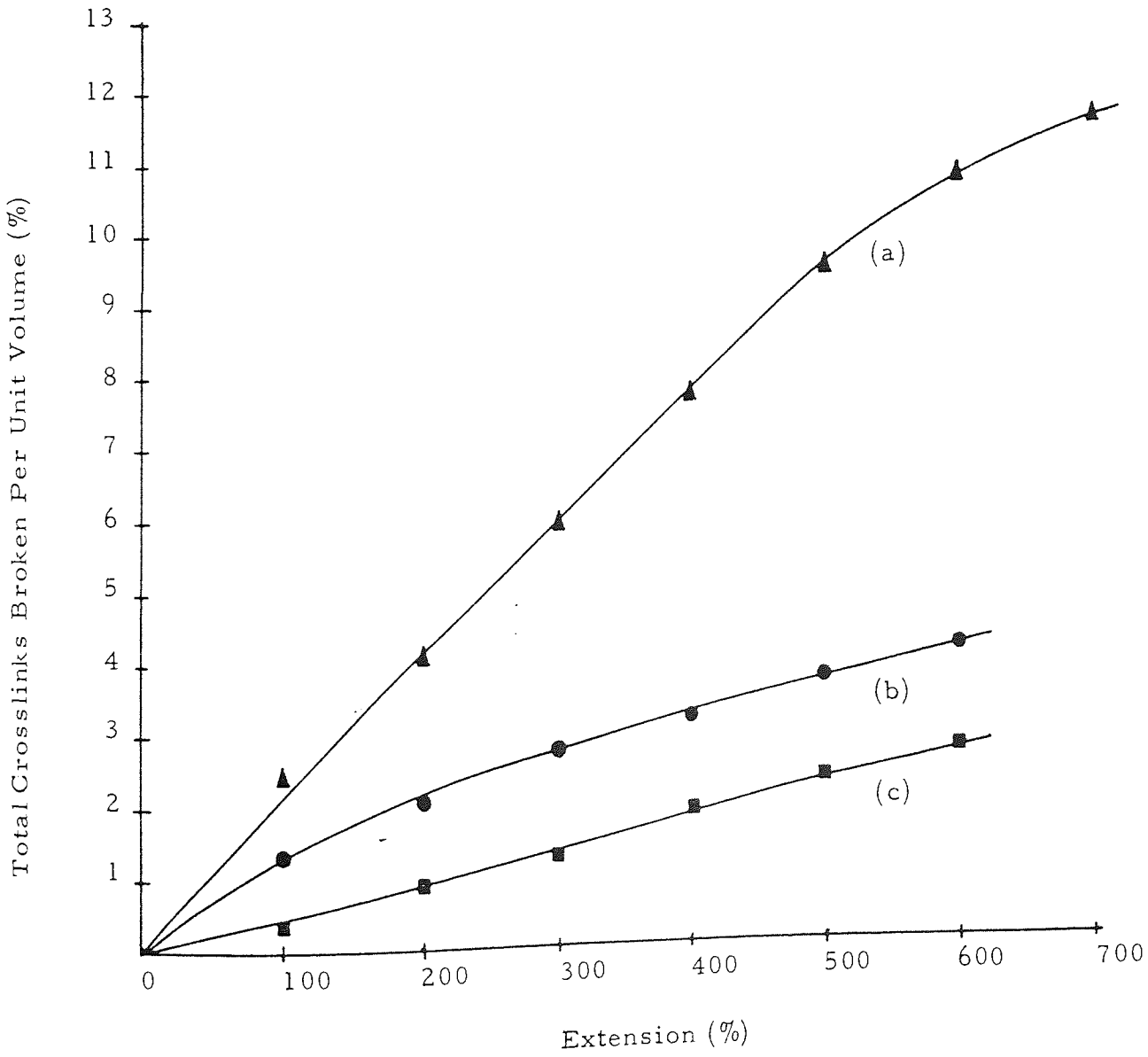

Fig 3.13 The Dependence of Recombination Efficiency on the Degree of Extension

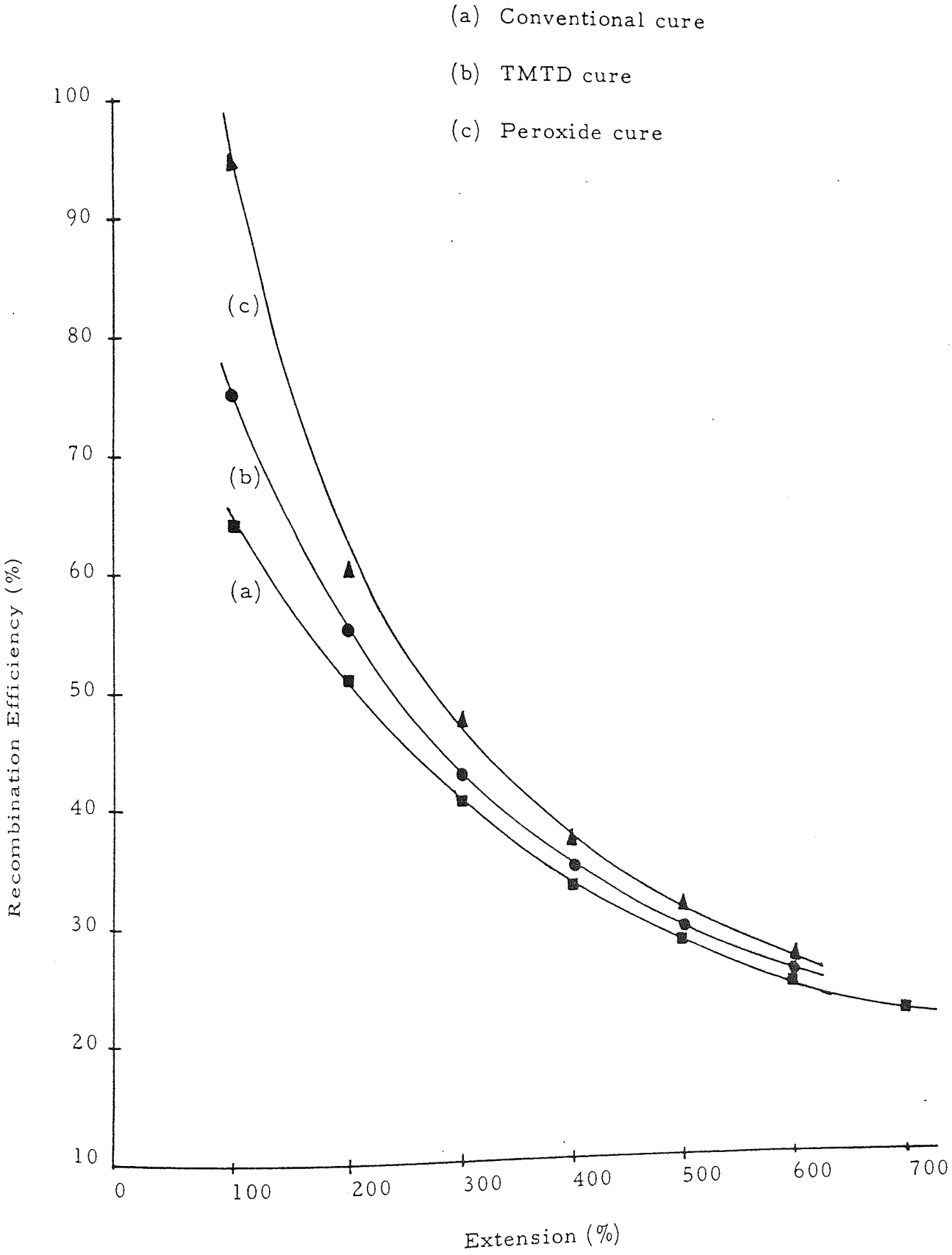

Fig 3.14 The Dependence of α on the Degree of Extension

(a) Conventional cure

(b) TMTD cure

(c) Peroxide cure

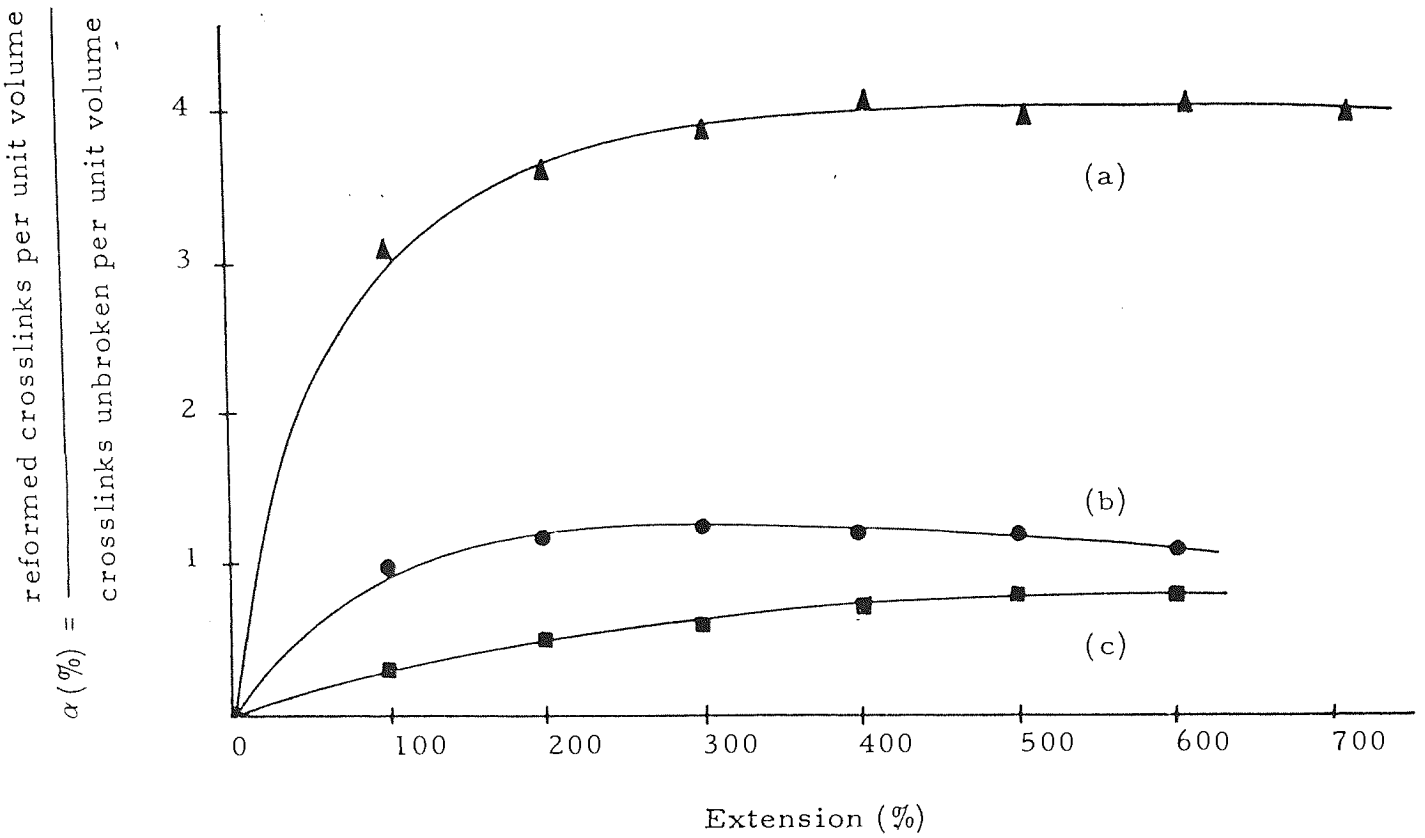

the greater the number of crosslinks broken per unit volume. As with the permanent set produced after stretching, the conventional vulcanisate had the highest number of crosslinks broken per unit volume (ca 12%), followed by the TMTD vulcanisate (ca 4%) and then the peroxide vulcanisate (less than 3%). These values, again reflect the comparative strengths of the different crosslinks; the polysulphidic crosslinks are thought to be mechanically weakest followed by the monosulphide and carbon-carbon crosslinks in ascending order. However, the strength of the vulcanisates varies in the inverse order, a peroxide vulcanisate having about half the tensile strength of a conventional vulcanisate containing mainly polysulphidic crosslinks capable of undergoing yielding. The number of crosslinks broken per unit volume on stretching a conventional vulcanisate did not decrease at higher extensions whereas the number of polysulphide crosslinks broken per unit volume was found to decrease from a maximum at higher extensions (see Section 3.5.3). The total number of crosslinks broken on extension continued to increase at higher extensions. There is convincing evidence from these findings to suggest that even though fewer polysulphide crosslinks are destroyed at higher extensions, more mono and disulphide crosslinks are broken at the same time, the total number of crosslinks broken per unit volume therefore being greater with increased percent extension.

The dependence of the recombination efficiency of broken crosslinks on the degree of extension is shown in Fig 3.13 and it can be observed that recombination efficiency was higher at low extensions than at higher extensions. These results would also seem to suggest that the peroxide vulcanisates had a higher recombination efficiency than the TMTD and conventional vulcanisates. This may be explained in terms of the competitive reactions involving crosslink formation and main chain modification. The polysulphenyl radicals ($-S_x^{\cdot}$) resulting from cleavage of polysulphide crosslinks are more likely to modify the main chain than combine with themselves to form new polysulphidic crosslinks. At higher elongations, the frequency of collisions of radicals would be less and so the rate of reformation would be less.

CHAPTER FOUR

CHANGES IN VULCANISATE NETWORKS DURING VULCANISATION AND IN FATIGUE

4.1 Introduction

The chemistry of the formation and maturation of sulphur crosslinks has been studied previously by other workers[26, 27] and it has been shown that polysulphide crosslinks, formed initially during accelerated sulphur vulcanisation of natural rubber, can undergo a number of subsequent competing reactions, the relative rates of which are temperature dependent. These reactions include:

(i) the decrease in length of the polysulphide crosslinks which may occur repetitively until the crosslinks are reduced to monosulphides, releasing in the process sulphur which is available for further crosslinking; this process is catalyzed by accelerator complexes in the vulcanisate,

(ii) the initial polysulphide crosslinks may undergo elimination by thermal scission at the carbon-sulphur bond, leading to main chain modification in the form of cyclic sulphides,

(iii) interchange between polysulphide crosslinks at their points of attachment to the network chain may take place, which occurs more readily in a stressed system and leads to stress relaxation with no overall change in the crosslink composition of the network, and

(iv) some polysulphide crosslinks may be completely destroyed.

The four reactions indicated above constitute the crosslink maturing process which controls the structure of the network during vulcanisation and seem likely to contribute to its behaviour in service, both under stress and at elevated temperatures.

Vulcanisates are subjected to a variety of deformations during service which may lead to a rise in temperature inside the rubber. It is very likely, therefore, that a rubber vulcanisate will undergo structural changes during use owing to mechanical and thermal effects. A detailed review of the literature on the effects of fatigue on rubber networks was presented in Section 1.7 from which it was apparent that there is considerable disagreement on the mechanism of fatigue. In the present study, the changes in the network structure of both gum and carbon black filled vulcanisates were examined during vulcanisation and also during fatigue. The effects of a phenolic antioxidant, 4,4' butylidene bis(2-t-butyl-5-methyl phenol) and an amine antioxidant,

N-isopropyl-N'-phenyl-p-phenylenediamine, on possible changes in network structure were also examined. It is hoped that a knowledge of such structural changes will help in predicting the behaviour of rubber vulcanisates during prolonged use. The conventional vulcanisation system, which is more generally used in practice, was chosen for the preparation of vulcanisate test sheets.

4.2 Preparation of vulcanisates

4.2.1 Formulations

The following six formulations, the composition of which is shown in Table 4.1, were used for the preparation of conventional vulcanisates.

(1) Formulation A, a gum vulcanisate with no antioxidant (control).

(2) Formulation B, a gum vulcanisate containing N-isopropyl-N'-phenyl-p-phenylene diamine (IPPD).

(3) Formulation C, a gum vulcanisate containing 4,4'-butylidene, bis(2-t-butyl, 5-methyl phenol) (SWP).

(4) Formulation D, HAF-black filled vulcanisate with no antioxidant.

(5) Formulation E, HAF-black filled vulcanisate containing IPPD, and

(6) Formulation F, HAF-black filled vulcanisate containing SWP.

Table 4.1 Compound formulations

Ingredient	Parts by weight					
	A	B	C	D	E	F
Natural rubber	100	100	100	100	100	100
Sulphur	2.5	2.5	2.5	2.5	2.5	2.5
Zinc oxide	5	5	5	5	5	5
Stearic acid	2	2	2	2	2	2
CBS	0.6	0.6	0.6	0.6	0.6	0.6
IPPD		2			2	
SWP			2			2
HAF-black				40	40	40

4.2.2 Compounding

The compounding of gum formulations was carried out on a two-roll mill using the mixing cycle described in Section 2.2.3.1. The black formulations were mixed in the Banbury mixer using the typical mixing cycle described in Section 2.2.4.1. The initial number average molecular weight ($\overline{Mn}$) of the rubber before vulcanisation was estimated from intrinsic viscosity measurements (Section 2.5.2) and this value was used for the estimation of chemical crosslink density.

4.2.3 Vulcanisation

The Monsanto rheometer was used to determine the curing characteristics of all compounds as well as to establish uniformity of mixing of the compounding ingredients. The curing characteristics of the six compounds under investigation are shown in Table 4.2. The vulcanisation of all compounds was carried out in a hot press as described in Section 2.3.2. All the vulcanisate sheets for fatigue tests were cured in the fatigue mould at 140°C for an optimum cure time (see Table 4.2). The moulded sheets were then cooled in cold water to quench any further crosslinking reactions.

The curing characteristics of the compounds indicate that IPPD (formulation B) slightly increases the cure rate constant (K) while

Table 4.2 Curing characteristics of NR compounds (compositions are shown in Table 4.1)

	Formulations					
	A	B	C	D	E	F
Rheometer temperature (^{o}C)	140	140	140	140	140	140
Induction period, ti/(mins)	11.5	10	13	7	6	9
Cure rate constant (K)/min^{-1}	0.52	0.53	0.51	0.62	0.63	0.6
Optimum cure time, t_{90}/(mins)	22	18	22	20	16	18
Cure time for maximum torque /(mins)	33	32	35	30	29	31
Torque at 90% cure/(in lb)	50.4	51.3	49.5	63	63.5	62.1
Maximum torque/(in lb)	56	57	55	70	70.5	69

SWP (formulation C) appears to decrease it. The induction period (ti) for the vulcanisation of the compound containing IPPD is shorter than that containing no added antioxidant (formulation A), while the compound containing SWP has a longer induction period. A similar effect is shown by both IPPD and SWP in filled vulcanisates. The presence of HAF-black in filled compounds increases the curing rate constant. The results of the curing characteristics also show that in filled and unfilled compounds, IPPD seems to increase slightly the maximum rheometer torque attained while SWP slightly decreases it.

4.3 Results and Discussion

4.3.1 Changes in Vulcanisate Networks During Vulcanisation

The overall concentrations of crosslinks present as mono, di and polysulphides in a natural rubber gum vulcanisate were estimated from the results of volume swelling measurements after treatment with thiol/amine probes as described in Sections 2.11.1. and 2.11.2. The appropriate χ value (Table 3.4) was used for the estimation of chemical crosslink densities before and after treatment with a chemical probe. The crosslinking efficiency of sulphur, E, defined as the number of sulphur atoms combined in the network per chemical crosslink present, was calculated from the measured concentration of crosslinks in the extracted vulcanisate and the amount of sulphur

chemically combined, $[Sc]$. The amount of combined sulphur was estimated by using equation (1-41):

$$Sc = \frac{S_T - [S^{=}]}{3200} \quad \text{gram atoms} \qquad (1\text{-}41)$$

The total sulphur content (S_T) and the amount of sulphide sulphur ($S^{=}$) were determined as described in Sections 2.12 and 2.13 respectively. The F-value, defined as the number of gram ions of sulphide per gram mole of chemical crosslink present per gram of rubber was estimated by using equation (1-42):

$$F = \frac{[S^{=}]}{\frac{1}{2}\overline{M}_{c(chem)}} \qquad (1\text{-}42)$$

The percentage concentrations of mono, di and polysulphide crosslinks in gum vulcanisates cured for various cure times ranging from 11-60 minutes are reported in Table 4.3. The dependence of the degree of chemical crosslinking on the vulcanisation time is shown in Fig 4.1. Table 4.4 summarizes the results of the other chemical characterisation of the vulcanisates. The vulcanisates were prepared using formulation A (Table 4.1) and contained no added antioxidant. The rubber was milled to an initial number average molecular weight ($\overline{Mn}$) value of 196,000. The results in Table 4.3 show that in the early stages of crosslinking the crosslinks are predominantly polysulphidic (ca 80%) with much smaller amounts of mono and disulphide

Table 4.3 The distribution of crosslinks in vulcanisate networks containing no antioxidant

(Formulation A, Table 4.1) $\overline{Mn}$ = 196,000

Cure time (mins)	Crosslink density[a]			% crosslinks[b]		
	(1) Vulcanised network	(2) After P-2-T probe treatment of (1)	(3) After H-T probe treatment of (2)	$-S_x-$	$-S_2-$	$-S_1-$
11	3.57	0.707	-[c]	80	-[c]	-[c]
15	5.25	0.934	-[c]	82	-[c]	-[c]
25	5.93	1.84	0.433	69	24	7
35	5.61	2.27	0.887	59	25	16
45	5.25	2.91	1.59	45	25	30
60	5.06	3.09	1.68	39	28	33

(a) Crosslink density = $\frac{1}{2}\overline{M}_{c(chem)} \times 10^2$ / Kg mole Kg^{-1} RN (b) Average of three determinations quoted

(c) Samples were too highly swollen after probe treatment to be manageable

Table 4.4 Chemical characterisation of vulcanisate networks containing no antioxidant

(Formulation A, Table 4.1)

Cure time (mins)	Chemical crosslink density $(x10^5)$ (a)	Combined Sulphur $[S_c]$		Sulphide Sulphur $[S^=]$		E (d)	F (e)
		wt(%)	$[S_c]$ (b) $x10^5$	wt(%)	$[S^=]$ (c) $x10^5$		
15	3.57	1.2	37.5	0.16	5.0	10.5	1.4
25	5.93	2.18	68.1	0.304	9.5	11.5	1.6
35	5.61	2.12	66.3	0.358	11.2	11.8	2.0
45	5.25	2.09	65.3	0.397	12.4	12.4	2.4
60	5.06	2.06	64.4	0.397	13.0	12.7	2.5

(a) Gram-mole chemical crosslinks per gram rubber network (b) Gram-atom of sulphur per gram rubber network
(c) Gram-ion of sulphide per gram rubber network
(d) Number of sulphur atoms combined in the network per chemical crosslink present
(e) Number of sulphide ions formed per chemical crosslink in the network

crosslinks. In fact, no mono and disulphide crosslinks could be detected in vulcanisates cured for 11 and 15 minutes because the vulcanisate samples were too highly swollen after treatment with hexanethiol to be manageable. In contrast, substantial monosulphide concentrations were observed in vulcanisates cured for 45 and 60 minutes, the vulcanisate cured for 60 minutes having about 33% monosulphidic crosslinks. The concentration of disulphides observed for vulcanisates cured for 35, 45 and 60 minutes changed only slightly with increasing cure time, remaining fairly constant at about 25% of the total crosslinks. The curves showing the dependence of mono and disulphidic, the polysulphidic and the overall crosslink density on the cure time (Fig 4.1), illustrates clearly the fact that when cure time is extended beyond the optimum, crosslink reversion becomes pronounced. This is attributable to the thermal destruction of polysulphide crosslinks, which can be seen to fall sharply in density. Increasing the cure time well beyond optimum causes only slight changes in the densities of mono and disulphide crosslinks.

The increasing complexity of the vulcanisate network with cure time is reflected in the changes in efficiency parameter E (the number of sulphur atoms combined in the vulcanisate network per chemical crosslink formed), which affords a measure of the overall complexity of the network (see Table 4.4). It is shown that the formation of one crosslink requires the combination of 11 sulphur atoms initially at

Fig 4.1 Relation between degree of chemical crosslinking and vulcanisation time for a NR gum vulcanisate without antioxidant (Formulation A, Table 4.1)

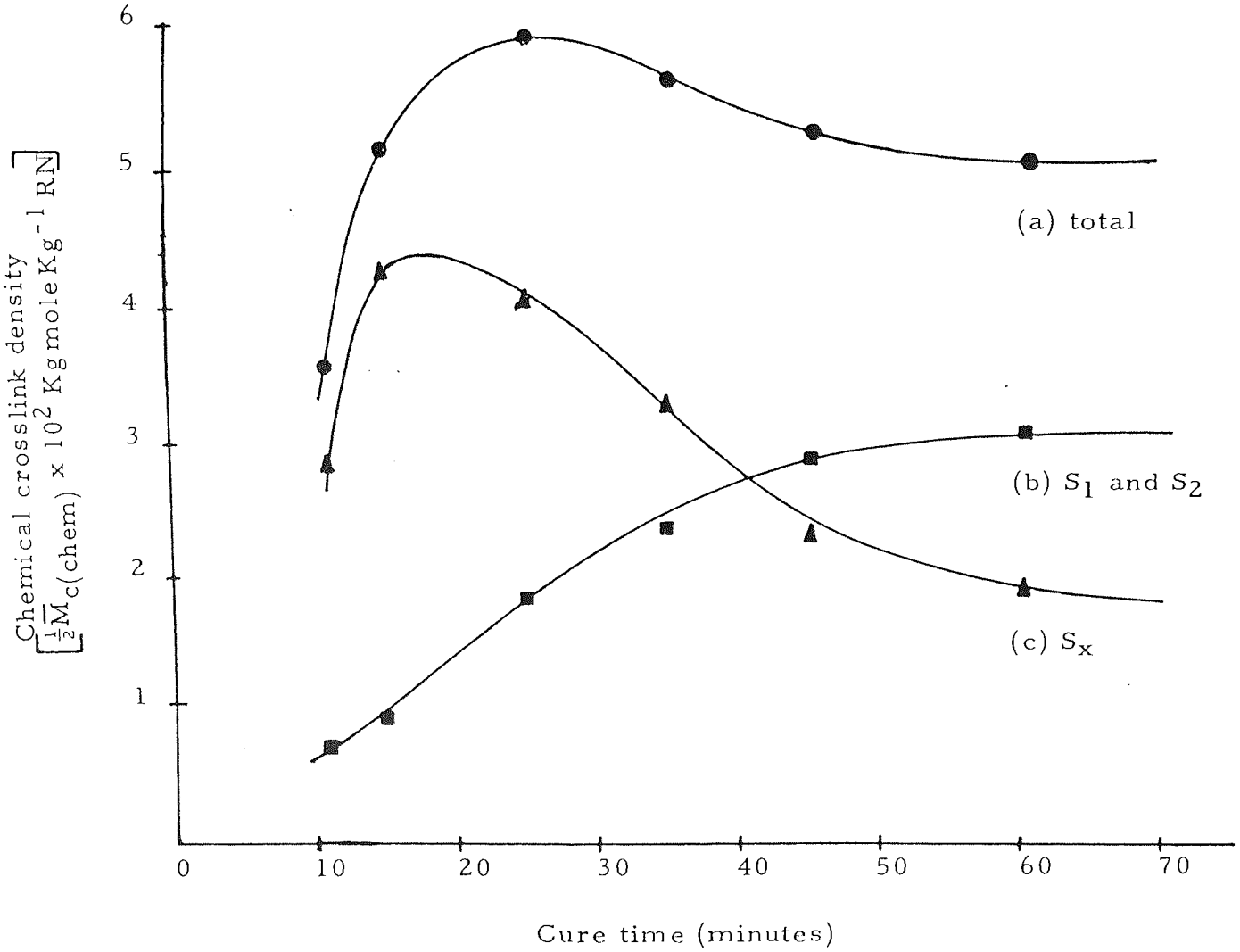

15 minutes cure time but this increased to 13 as cure proceeded to 60 minutes. The increase in F values from 1.4 after 15 minutes cure to 2.5 after 60 minutes cure time also shows the increasing inefficiency in the crosslinking with increasing cure time. On extended cure beyond the optimum cure time, crosslink reversion leads to mainchain modification mainly by cyclic monosulphide formation. Other workers[284] have attributed this to the low accelerator concentration present at such cure times in a conventional vulcanisate; the desulphuration proceeds slowly, and polysulphide crosslinks undergo thermal destruction, giving rise to zinc sulphide and probably also to cyclic monosulphides. The increase in sulphide ion concentration with cure time shown in Table 4.4 and the predominance of polysulphide crosslinks at all stages of cure (see Table 4.3) suggests that such reactions may actually be taking place.

4.3.1.1 The Effect of Filler (HAF-black)

The effect of HAF-black on vulcanisate network structure during vulcanisation was investigated using a conventional system (formulation D) containing 40 parts by weight of HAF-black. The initial number average molecular weight ($\overline{Mn}$) of rubber after compounding was 190,000. The percentage concentration of mono, di and polysulphidic crosslinks observed for vulcanisates cured for a range of times are presented in Table 4.5 while Fig 4.2 shows the dependence of the

Table 4.5 The distribution of crosslinks in HAF-black filled vulcanisate networks without antioxidant

(Formulation D, Table 4.1) $\overline{M}n = 190,000$

Cure time (mins)	Crosslink density[a]			% crosslinks[b]		
	(1) Vulcanised network	(2) After P-2-T probe treatment of (1)	(3) After H-T probe treatment of (2)	$-S_x-$	$-S_2-$	$-S_1-$
9	4.02	0.923	-[c]	77	-[c]	-[c]
15	5.25	0.989	-[c]	81	-[c]	-[c]
25	6.18	2.52	1.13	59	23	18
35	5.97	3.08	1.71	48	23	29
45	5.46	3.47	1.95	36	28	36
60	5.26	3.82	2.17	27	32	41

(a) Crosslink density = $\frac{1}{2}\overline{M}_{c(chem)} \times 10^2$ / Kg mole Kg^{-1} RN (b) Average of three determinations quoted

(c) Samples were too highly swollen after probe treatment to be manageable

Fig 4.2 Relation between degree of chemical crosslinking and vulcanisation time for a carbon black filled NR vulcanisate without antioxidant (Formulation D, Table 4.1)

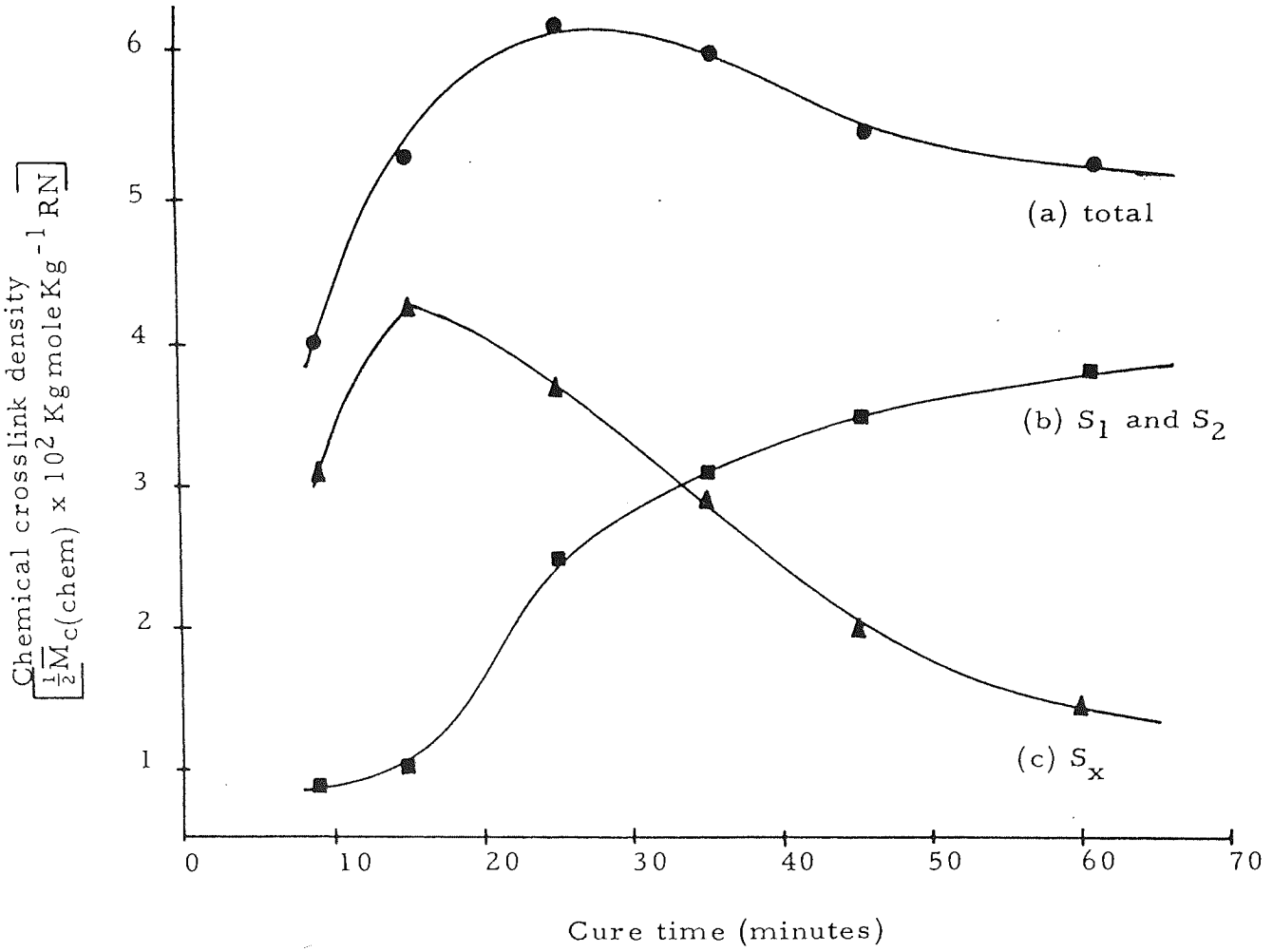

densities of mono, di and polysulphide crosslinks as well as the total crosslink density on the cure time.

The major effect of carbon black on the distribution of crosslinks in the vulcanisates, was observed to be the reduction in the percentage of polysulphidic crosslinks present at the optimum cure time. As with the corresponding gum vulcanisate, the overall density of crosslinks increased to a maximum at the optimum cure and then decreased slowly on extended cure. However, the total crosslink densities were higher in the presence of carbon black even though the crosslink densities were corrected for the restrictions in swelling due to rubber-filler attachment, by using equation (1-36) (see Section 1.3.3.3). The inability to differentiate effectively between crosslinks introduced by the curing agent and those involving rubber-filler interaction, is perhaps one of the major obstacles to the quantitative structural elucidation of filled vulcanisates.

The reduction of the polysulphidic nature of a filled vulcanisate when compared to a gum vulcanisate could be due either to the initial insertion of shorter sulphidic crosslinks during vulcanisation or to the more rapid transformation of longer crosslinks to shorter ones in the presence of carbon black. It is possible, however, that both events may be occurring simultaneously. The presence of carbon black was observed to reduce the scorch time and to increase the

rate of cure during vulcanisation (see Table 4.2). The increased rate of cure in the presence of carbon black would appear to suggest that the rapid'maturation' of polysulphidic crosslinks to shorter ones may be mainly responsible for reduction in the polysulphidic crosslinks observed. In fact, the curve showing the dependence of polysulphide crosslink density on cure time (Fig 4.2) indicates that the decrease in the density of polysulphide crosslinks from a maximum at optimum cure time is very rapid indeed. The increase in the rate of cure caused by HAF-black can be attributed to its alkalinity which is well known to facilitate vulcanisation, presumably either by accelerating the formation of the active sulphurating agent, or by increasing its solubility in rubber. The efficiency of crosslinking in the presence of carbon black could not be investigated because of the difficulty experienced in the determination of the sulphur content of filled vulcanisates.

4.3.1.2 The Effect of Antioxidants on Gum Vulcanisate Structure

The effects of an amine antioxidant, N-isopropyl-N'-phenyl-p-phenylene diamine (IPPD), and a phenolic antioxidant, 4,4' butylidene bis(2-t-butyl-5-methyl phenol) (SWP) on the network structure of gum vulcanisates were investigated using vulcanisates prepared with formulations B and C. The initial $\overline{Mn}$ values of the rubber before vulcanisation were 195,000 and 196,000 respectively.

Table 4.6 shows the distribution of mono, di and polysulphidic crosslinks in vulcanisates containing IPPD which were cured for various times ranging from 10-65 minutes. Figure 4.3 illustrates the relationship between the densities of the different crosslinks with vulcanisation time. The overall crosslink density also increases with cure time and passes through a maximum. The crosslink density at any particular cure time was slightly higher than that of the corresponding vulcanisate containing no added antioxidant. The percentage concentration of polysulphidic crosslinks was generally less than that of the vulcanisate without antioxidant and decreased from about 74% at 10 minutes cure time to 30% after 65 minutes cure. The percent concentrations of mono and disulphide crosslinks were very low in the vulcanisate cured for 10 minutes and could not be detected because the samples were too highly swollen after probe treatment. The concentration of these crosslinks then increased steadily with further cure time.

Table 4.7 summarizes the results of the other chemical characterisation of the vulcanisates cured for various times. The E value increased from about 11 after 15 minutes cure time to 14 after 65 minutes curing. The F value also increased with cure time from about 1 to 3.

Table 4.6 The distribution of crosslinks in vulcanisate networks containing IPPD

(Formulation B, Table 4.1) $\overline{M}n$ = 195,000

Cure time (mins)	Crosslink density[a]			% crosslinks[b]		
	(1) Vulcanised network	(2) After P-2-T probe treatment of (1)	(3) After H-T probe treatment of (2)	$-S_x-$	$-S_2-$	$-S_1-$
10	3.74	0.961	-[c]	74	-[c]	-[c]
15	5.35	1.68	0.59	69	20	11
25	6.02	2.09	0.85	65	21	14
35	5.85	2.46	1.29	58	20	22
45	5.52	3.01	1.38	45	30	25
65	4.75	3.32	1.76	30	33	37

(a) Crosslink density = $\frac{1}{2}\overline{M}_{c(chem)} \times 10^2$ /Kg mole Kg^{-1} RN (b) Average of three determinations quoted

(c) Samples were too highly swollen after probe treatment to be manageable

Fig 4.3 Relation between degree of chemical crosslinking and vulcanisation time for a conventional NR vulcanisate containing IPPD (Formulation B, Table 4.1)

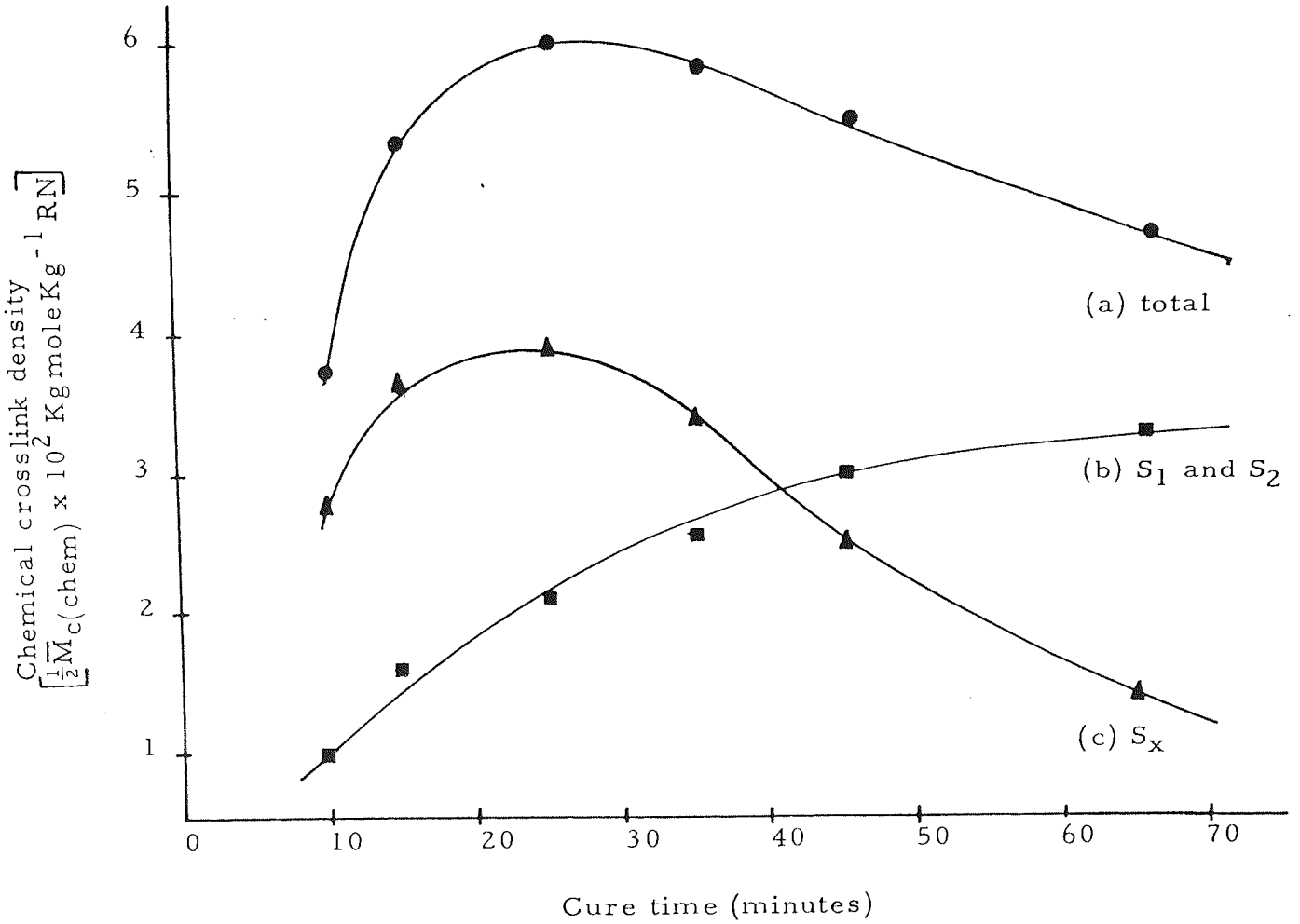

Table 4.7 Chemical characterisation of vulcanisate networks containing IPPD

(Formulation B, Table 4.1)

Cure time (mins)	Chemical crosslink density ($x10^5$)(a)	Combined Sulphur $[S_c]$		Sulphide Sulphur $[S^=]$		E(d)	F(e)
		wt(%)	$[S_c]$ (b) $x10^5$	wt(%)	$[S^=]$ (c) $x10^5$		
15	5.35	1.87	58.3	0.20	6.3	10.9	1.2
25	6.02	2.23	69.8	0.244	7.6	11.6	1.3
35	5.85	2.19	68.4	0.28	8.6	11.7	1.5
45	5.52	2.13	66.6	0.352	11.0	12.1	2.0
65	4.75	1.99	62.2	0.442	13.8	13.1	2.9

(a) Gram-mole chemical crosslinks per gram rubber network
(b) Gram-atom of sulphur per gram rubber network
(c) Gram-ion of sulphide per gram rubber network
(d) Number of sulphur atoms combined in the network per chemical crosslink present
(e) Number of sulphide ions formed per chemical crosslink in the network

The overall effect of IPPD on the network structure of gum vulcanisate networks during vulcanisation appears to be very small. The slight increase in the chemical crosslink density in a vulcanisate containing IPPD (Table 4.6) when compared to that without antioxidant (Table 4.3), may be explained on the basis of the slightly higher rate of cure observed in vulcanisates containing IPPD which is basic in nature and may therefore be expected to increase the rate of vulcanisation. The increased rate of cure may also be responsible for the slightly lower percentage polysulphide crosslinks observed in vulcanisates containing IPPD, the polysulphide crosslinks are more readily transformed by 'maturation' processes to crosslinks containing mono and disulphides and to sulphides in main chain modifications. The slightly higher E and F values observed in these vulcanisates, perhaps reflects the increased complexity of the networks.

Table 4.8 shows the distribution of mono, di and polysulphide crosslinks in vulcanisates containing SWP which were cured for cure times ranging from 13 to 65 minutes. The curves showing the dependence of the densities of the different types of crosslink on the vulcanisation time is given in Figure 4.4. while Table 4.9 shows the variation of E and F values with vulcanisation time. The total crosslink density increases with vulcanisation time and passes through a maximum at about 25 minutes. These values were generally slightly lower than those for the corresponding vulcanisates without antioxidants.

Table 4.8 The distribution of crosslinks in vulcanisate networks containing SWP

(Formulation C, Table 4.1) $\overline{Mn}$ = 196,000

Cure time (mins)	Crosslink density[a]			% crosslinks[b]		
	(1) Vulcanised network	(2) After P-2-T probe treatment of (1)	(3) After H-T probe treatment of (2)	$-S_x-$	$-S_2-$	$-S_1-$
13	5.03	1.08	-[c]	79	-[c]	-[c]
18	5.48	1.42	-[c]	74	-[c]	-[c]
25	5.51	1.80	0.915	67	16	17
35	5.13	2.29	1.05	55	24	20
45	4.86	2.71	1.54	44	24	32
65	4.58	3.07	1.84	33	27	40

(a) Crosslink density = $\frac{1}{2}\overline{M}_{c(chem)} \times 10^2$ / Kg mole Kg^{-1} RN (b) Average of three determinations quoted

(c) Samples were too highly swollen after probe treatment to be manageable

Fig 4.4 Relation between degree of chemical crosslinking and vulcanisation time for a conventional NR vulcanisate containing SWP (Formulation C, Table 4.1)

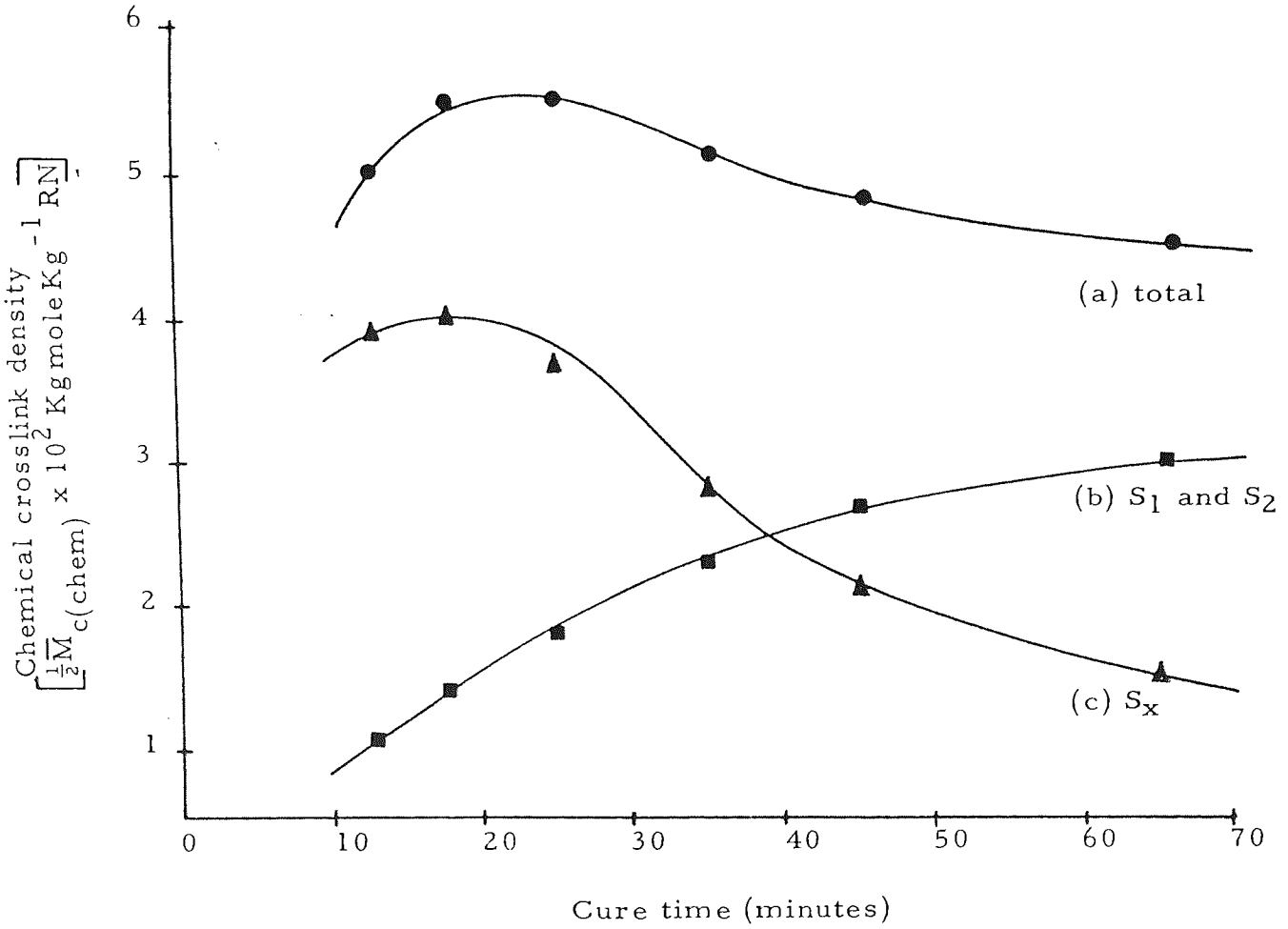

Table 4.9 Chemical characterisation of vulcanisate networks containing SWP

(Formulation C, Table 4.1)

Cure time (mins)	Chemical crosslink density ($\times 10^5$)[a]	Combined Sulphur $[S_c]$		Sulphide Sulphur $[S^=]$		E[d]	F[e]
		wt(%)	$[S_c]^{(b)} \times 10^5$	wt(%)	$[S^=]^{(c)} \times 10^5$		
18	5.48	1.93	60.3	0.262	8.2	11	1.5
25	5.51	2.17	67.8	0.305	9.5	12.3	1.8
35	5.13	2.10	65.7	0.375	11.7	12.8	2.3
45	4.86	2.0	63.1	0.403	12.6	13	2.6
65	4.58	1.98	61.9	0.454	14.2	13.5	3.1

(a) Gram-mole chemical crosslinks per gram rubber network
(b) Gram-atom of sulphur per gram rubber network
(c) Gram-ion of sulphide per gram rubber network
(d) Number of sulphur atoms combined in the network per chemical crosslink present
(e) Number of sulphide ions formed per chemical crosslink in the network

However, the polysulphide crosslink contents were similar to those observed for vulcanisates without anitoxidants. As would be expected, the percentage of polysulphide crosslinks decreased with vulcanisation time from about 79% at 13 minutes to 33% after 65 minutes cure time. The percentage concentration of mono and disulphide crosslinks consequently increased from very low values in the early stages of vulcanisation. The mono and disulphide crosslink concentrations again could not be determined in vulcanisates cured for 13 and 18 minutes. The concentration of disulphidic crosslinks remained fairly constant on extended cure. The observed E and F values increased with cure time; the E value increased from 11 after 18 minutes cure time to 14 after 65 minutes cure time while F values increased from 1.5 to 3 within the same period. The increases in both E and F values with cure time reflect the increasing complexity of the networks as vulcanisation proceeded. The slightly higher values of E and F, when compared to those observed for the control vulcanisate, suggests that SWP like IPPD increases slightly the network complexity or the inefficiency of vulcanisation.

The most remarkable effect of SWP appears to be the reduction in the total crosslink density in the vulcanisate. The most obvious explanation of this effect is that it is due to the retardation of the rate of vulcanisation observed in vulcanisates containing SWP. SWP also increases the induction time during vulcanisation and the maximum

rheometer torque attained is slightly lower than that for a control vulcanisate without antioxidant. The retardation of the rate of cure caused by SWP, a phenol, may be attributed to its acidic nature. An acidic environment is known to reduce the rate of vulcanisation in conventional systems.

Figures 4.5, 4.6 and 4.7 summarise the relative effects of the antioxidants IPPD and SWP on the dependence respectively of the total crosslinks, the polysulphidic crosslink and the mono and disulphidic crosslink densities on the vulcanisation time. Although the overall effects are apparently not significant, it is remarkable that IPPD does tend to increase slightly the total crosslink density at optimum cure while SWP decreases it. The greater reduction of polysulphide crosslink density by IPPD on prolonged cure is equally remarkable. The behaviours of IPPD and SWP are attributable to their basic and acidic nature which respectively accelerate and retard the rate of vulcanisation.

In conclusion, it can be seen that the vulcanisate structure changes with cure time. The presence of HAF-black and antioxidants influences the maturing process and, thereby the relative structures of the final vulcanisates. Other factors which have not been investigated in the present project must be anticipated to play important roles, including:

Fig 4.5 The dependence of total chemical crosslink density on vulcanisation time

(a) control

(b) SWP

(c) IPPD

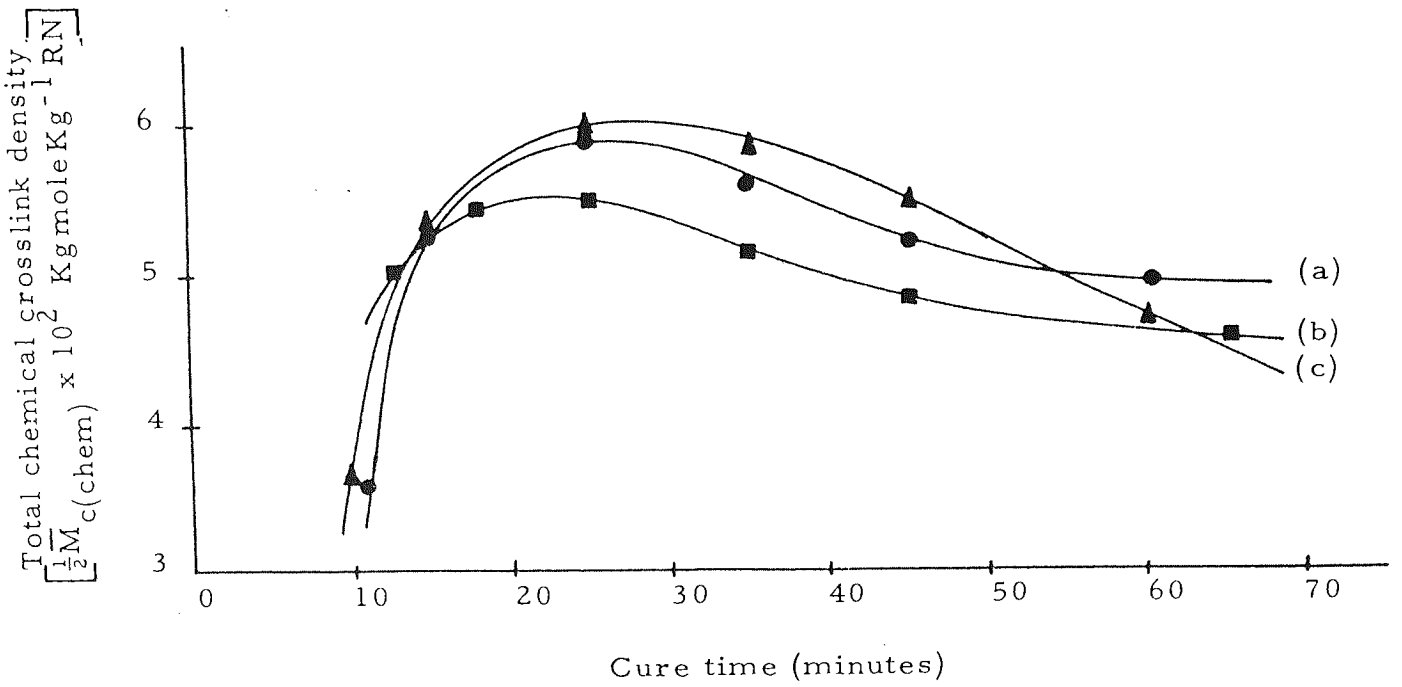

Fig 4.6 The dependence of polysulphide crosslink density on vulcanisation time

(a) control

(b) SWP

(c) IPPD

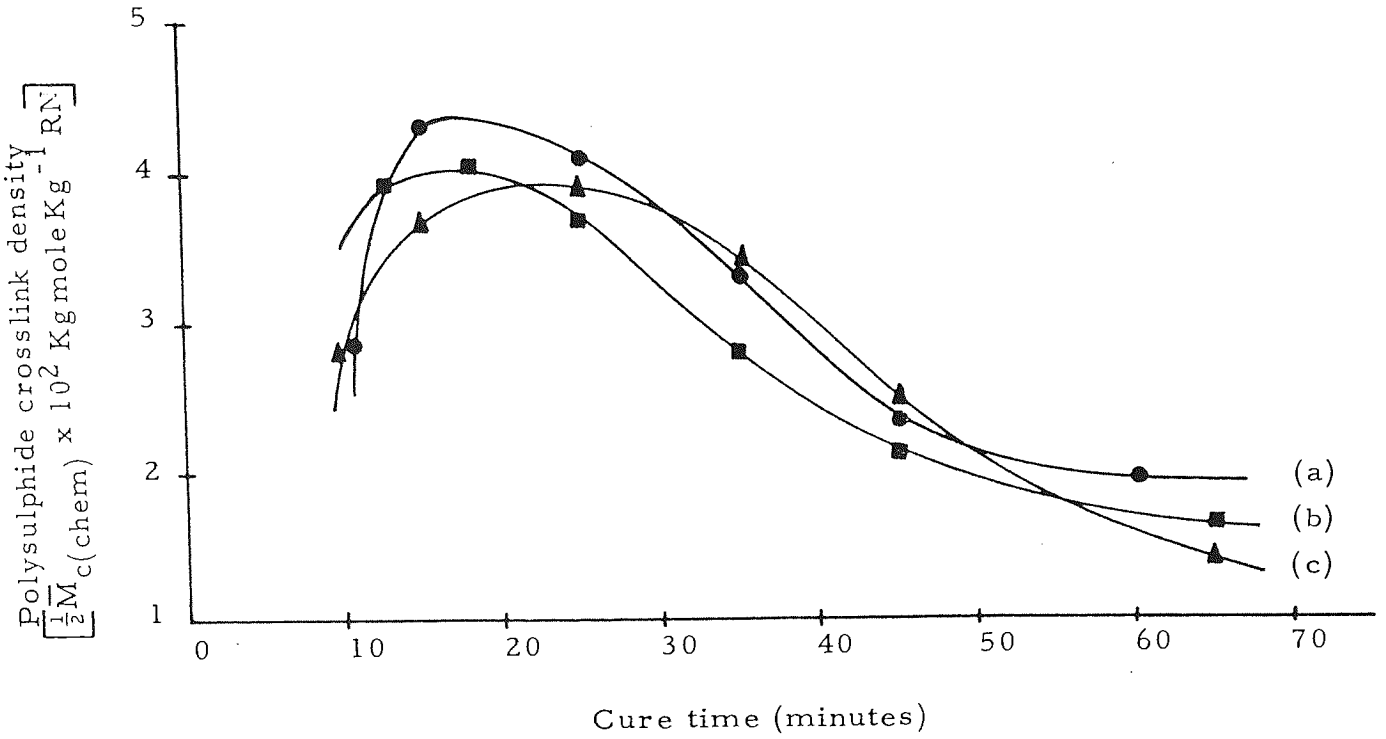

Fig 4.7 The dependence of mono and disulphidic crosslink density on vulcanisation time

(a) IPPD

(b) SWP

(c) control

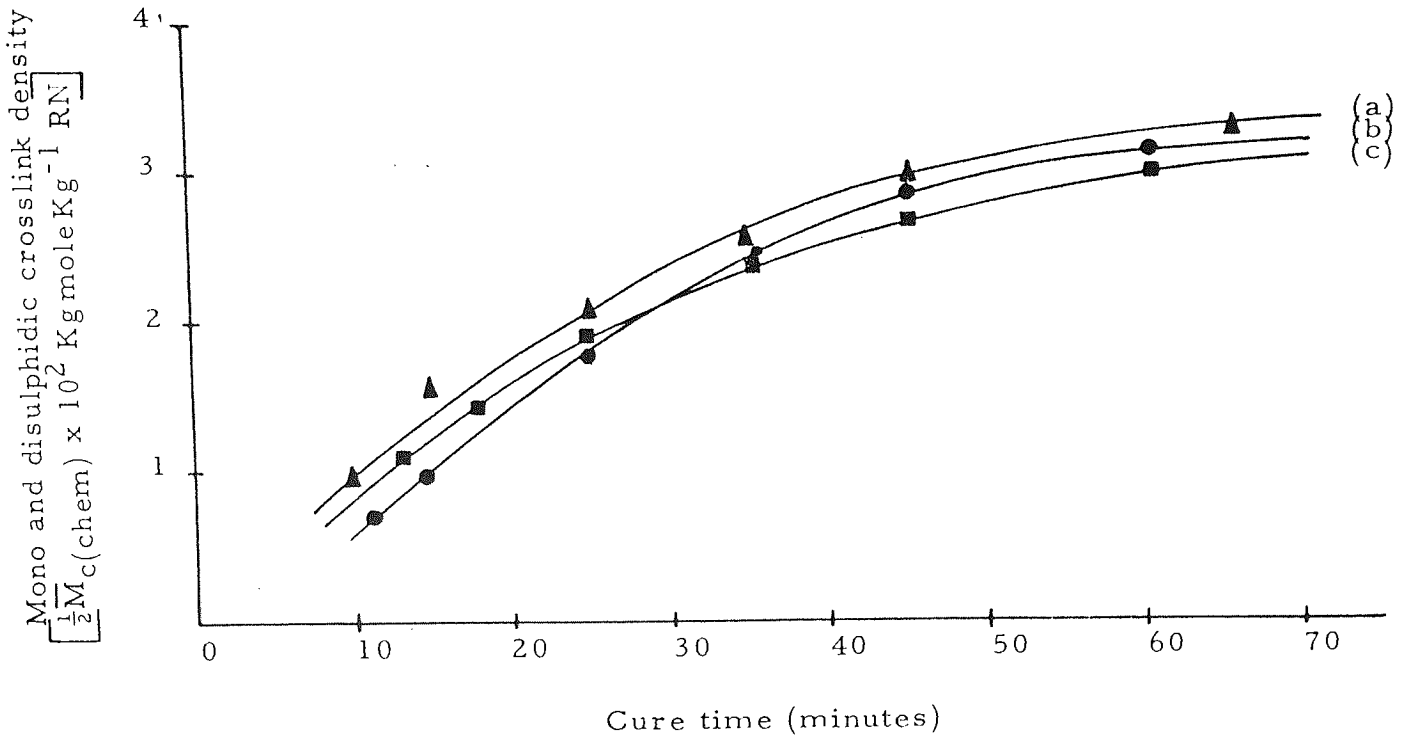

(i) the structure and concentration, and thus reactivity, of the accelerator-activator complexes which are responsible for both the conversion of elemental sulphur into the active sulphurating agent and the desulphuration of the polysulphide crosslinks,

(ii) the length of the sulphur chain in the active sulphurating agent, which will be determined by the ratio of sulphur to accelerator in the compound and will in turn determine the sulphur chain length of the initially formed sulphidic crosslinks, and

(iii) the temperature of vulcanisation which is bound to influence the relative rates and extents of the competitive reactions constituting the maturing process.

4.3.2 Changes in Vulcanisate Networks During Fatigue

Vulcanisate sheets for fatigue tests were prepared from compounds using formulations A, B, C, D and F, and curing at 140°C for optimum cure times (see Table 4.2). The effect of the antioxidants IPPD and SWP, and of HAF-black on the changes in networks during fatigue was investigated. A number of samples were cut from a vulcanised sheet together with samples from adjacent regions of the sheet for comparison. For a given vulcanisation these samples were then subjected to fatigue at 100% elongation for a range of fatigue cycles, up to

failure. Analyses were then carried out to assess the effects of the number of fatigue cycles on the vulcanisate network structure, which was compared with the unfatigued control samples taken from vulcanisate sheet.

Table 4.10 shows the chemical crosslink densities of fatigued and unfatigued samples before and after treatment with propan-2-thiol to remove all polysulphide crosslinks. Formulation A was used in the preparation of the vulcanisate which contained no added antioxidant, and the initial number average molecular weight ($\overline{Mn}$) of the rubber before vulcanisation was 184,000. The results obtained show that a reduction in the fraction of crosslinks that are polysulphide crosslinks occurred during fatigue but there was an overall increase in crosslink density. The reduction increased from 3% after 5 kilocycles to 16% after 80 kilocycles and the increase in crosslink density is presumably due to the formation of mono and disulphide crosslinks during fatigue.

Table 4.11 shows the change in polysulphide crosslinks during fatigue of a vulcanisate of a rubber ($\overline{Mn}$ = 185,000) containing IPPD. The samples were fatigued for a range of cycles during which time the percentage of crosslinks that are polysulphidic decreased by 2% after 5 kilocycles and as much as 10% after 90 kilocycles of fatigue with approximately the same overall increase in crosslink density.

Table 4.10 The change in polysulphidic crosslinks during fatigue of a conventional gum vulcanisate containing no antioxidant (Formulation A, Table 4.1) $\overline{Mn}$ = 184,000

Fatigue cycles x 10^2	Unfatigued sample adjacent to test piece			Fatigued test piece			% change in $-S_x-$ crosslinks
	Crosslink density[a] x 10^2		%crosslinks[b] ($-S_x-$)	Crosslink density[a] x 10^2		%crosslinks[b] ($-S_x-$)	
	Before probe	After probe		Before probe	After probe		
50	5.44	1.73	68	5.53	1.90	66	2
100	5.44	1.70	69	5.56	1.98	64	5
300	5.44	1.67	69	5.56	2.24	60	9
600	5.45	1.68	69	5.59	2.54	55	14
800	5.45	1.63	70	5.58	2.55	54	16

(a) Kg-mole chemical crosslinks per Kg rubber network (b) Average of three determinations quoted

Table 4.11 The change in polysulphidic crosslinks during fatigue of a conventional gum vulcanisate containing IPPD (Formulation B, Table 4.1) $\overline{Mn}$ = 185,000

Fatigue cycles x 10^{-2}	Unfatigued sample adjacent to test piece			Fatigued test piece			% change in $-S_x-$ crosslinks
	Crosslink density[a] x 10^2		%crosslinks[b] $(-S_x-)$	Crosslink density[a] x 10^2		%crosslinks[b] $(-S_x-)$	
	Before probe	After probe		Before probe	After probe		
50	5.54	1.95	65	5.66	2.10	63	2
100	5.54	1.95	65	5.65	2.15	62	3
300	5.55	1.88	66	5.69	2.32	59	7
600	5.54	1.89	66	5.69	2.43	57	8
900	5.54	1.85	67	5.71	2.47	57	10
1200	5.55	1.86	67	5.72	2.43	58	9

(a) Kg-mole chemical crosslinks per Kg rubber network (b) Average of three determinations quoted

Similar experiment on the change in percentage of crosslinks that are polysulphidic during fatigue are reported in Table 4.12 for SWP antioxidant. The initial $\overline{Mn}$ value of rubber used for the tests was 184,000. There is also evidence in this case to show that polysulphide crosslinks are destroyed during fatigue; an increase in the number of fatigue cycles leading to an increase in the percentage of polysulphide crosslinks destroyed. The percentage of polysulphide crosslinks destroyed increased from approximately 2% after 5 kilocycles to 13% after 90 kilocycles of fatigue. The overall dependence of the percentage polysulphide crosslinks destroyed on the number of fatigue cycles during fatigue of the three vulcanisates is shown in Figure 4.8. Although a greater number of polysulphide crosslinks are destroyed at higher fatigue cycles, the rate of further polysulphide crosslink destruction decreases with increasing fatigue cycle time. This is possibly due to the change in network distribution which presumably leads to a reduction in the net stress at higher fatigue time. The effect of the addition of antioxidants is to reduce the initial rate of polysulphide crosslinks destruction, IPPD being more effective than SWP in this respect, to increase the fatigue life as shown in Table 4.13.

The results of the distribution of mono, di and polysulphide crosslinks in the three vulcanisates before and after fatiguing to failure is also presented in Table 4.13. It is shown that while there is a reduction in the percentage concentration of polysulphide crosslinks after fatig-

Table 4.12 The change in polysulphidic crosslinks during fatigue of a conventional gum vulcanisate containing SWP (Formation C, Table 4.1) $\overline{Mn}$ = 184,000

Fatigue cycles x 10^2	Unfatigued sample adjacent to test piece			Fatigued test piece			% change in $-S_x-$ crosslinks
	Crosslink density[a] x 10^2		%crosslinks[b] $(-S_x-)$	Crosslink density[a] x 10^2		%crosslinks[b] $(-S_x-)$	
	Before probe	After probe		Before probe	After probe		
50	5.38	1.59	70	5.49	1.75	68	2
100	5.38	1.68	69	5.50	1.89	66	3
300	5.38	1.66	69	5.52	2.14	61	8
600	5.36	1.61	70	5.52	2.34	58	12
900	5.39	1.56	71	5.54	2.30	59	12
1200	5.39	1.55	71	5.57	2.31	59	12

(a) Kg-mole chemical crosslinks per Kg rubber network (b) Average of three determinations quoted

Fig 4.8 The relation between % reduction of polysulphidic crosslinks and the number of fatigue cycles during fatigue of unfilled NR vulcanisate containing different antioxidants

(a) control (no antioxidant)

(b) SWP

(c) IPPD

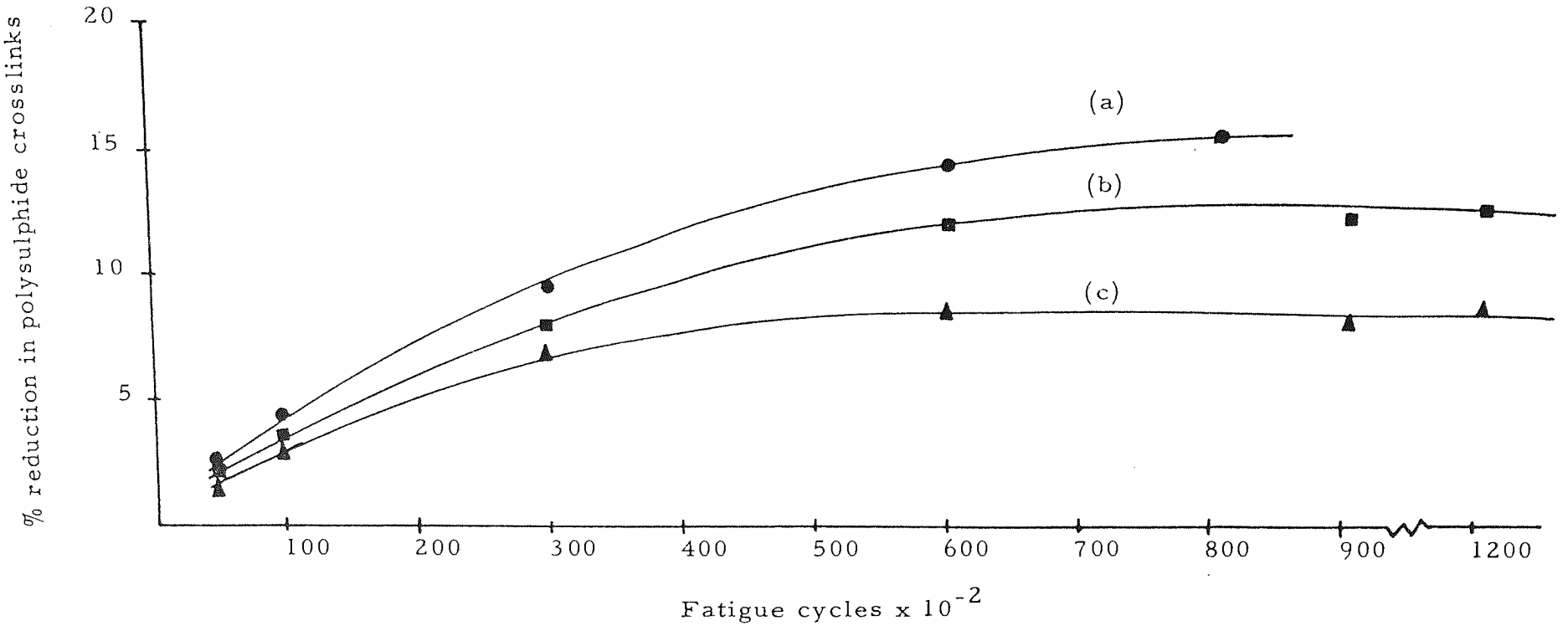

Table 4.13 The distribution of crosslinks in gum vulcanisate networks before and after fatiguing to failure (Formulations A, B and C, Table 4.1)

Formulation		Crosslink density[a]			% Crosslinks		
		original network	After P-2-T probe	After H-T probe	$-S_x-$	$-S_2-$	$-S_1-$
A	unfatigued	5.56	1.72	0.53	69	21	10
	fatigued[1]	5.72	2.65	0.73	54	33	13
B	unfatigued	5.64	1.93	0.61	66	23	11
	fatigued[2]	5.82	2.63	0.81	55	31	14
C	unfatigued	5.39	1.62	0.70	70	17	13
	fatigued[3]	5.55	2.41	0.97	57	26	17

(a) Crosslink density = $\frac{1}{2}\overline{M}_{c(chem)} \times 10^2$ Kg mole Kg^{-1} RN

(1) Fatigue life = 83,000 cycles
(2) Fatigue life = 150,000 "
(3) Fatibue life = 130,000 "

uing to failure, the net change in polysulphide crosslink densities are of the same order. The concentration of mono and disulphide crosslinks increased during fatigue of all samples, there being more new disulphide crosslinks formed than monosulphides. IPPD again showed evidence that there is a smaller increase in disulphide crosslink content of a vulcanisate containing it, than SWP vulcanisates or control. The results clearly suggest that during fatigue of a gum vulcanisate, polysulphide crosslinks are cleaved and are converted to disulphides and monosulphides quite probably via a free radical mechanism. During fatigue, polysulphidic crosslink cleavage occurs as a result of mechanical and thermal effects, leading to the formation of monosulphenyl, $RS^{\cdot}$, disulphenyl $RSS^{\cdot}$, and polysulphenyl, $RS_x^{\cdot}$, radicals. These radicals may form new mono, di and polysulphide crosslinks on further fatiguing, by attachment to the rubber main chain or they may react disproportionately with other polysulphide crosslinks to form new free radicals. It can be suggested that the relative rates of formation of mono, di and polysulphide crosslinks during fatigue will depend upon the stabilities of the radicals formed. The higher rate of disulphide crosslink formation observed in the present investigations may be the result of the much greater stability of the RSS· radical when compared with the RS·, because of the gain in energy due to the delocalisation of the unpaired electron over the unoccupied d orbitals of the adjacent sulphur atom in RSS· (R-S⋍S).

The results of other chemical characterisation of fatigued and unfatigued vulcanisates are presented in Table 4.14. These results show a slight decrease in E values after fatigue. The efficiency parameter after treatment with triphenyl phosphine (E') increased and subsequently, E'-1, which gives a measure of main chain modifications, increased slightly. Although the increases in E'-1 values suggest that main chain modifications occur during fatigue, the changes observed are too small to be of any significance. The slight decrease in the amount of combined sulphur, $[Sc]$, observed in the three vulcanisates after fatiguing, and the almost constant value of the amount of sulphur present as zinc sulphide, would suggest that some sulphur from the crosslinks appears as free sulphur. However, no significant changes were observed in the amount of extractable free sulphur. The copper spiral method used in the determination of extractable free sulphur may have been insensitive to the slight variation, if any, in the concentration of free sulphur which occurred during fatigue.

4.3.2.1 The Effect of Filler (HAF-black)

The effect of HAF-black on the change in percentage concentration of polysulphide crosslinks during fatigue of a filled vulcanisate without antioxidant is shown in Table 4.15. As with the gum vulcanisate, the decrease in percentage of polysulphide crosslinks increased with

Table 4.14 Chemical characterisation of vulcanisate networks before and after fatiguing to failure (Formulations A, B and C, Table 4.1)

Formulation		Crosslink density[a] ($\times 10^5$)	$[S_c]$[b] ($\times 10^5$)	$[S^=]$[c] ($\times 10^5$)	Extractable free sulphur[b] ($\times 10^5$)	E[d]	E'[e]	E'-1
A	unfatigued	5.56	65.1	10.2	2.53	11.7	8.3	7.3
	fatigued	5.72	62.3	10.2	2.56	10.9	9.0	8.0
B	unfatigued	5.64	63.7	11.5	2.47	11.3	7.9	6.9
	fatigued	5.82	60.5	11.1	2.5	10.4	8.2	7.2
C	unfatigued	5.39	64.7	11.08	2.56	12.0	8.0	7.0
	fatigued	5.55	62.7	11.2	2.56	11.3	8.9	7.9

(a) Gram-mole chemical crosslinks per gram rubber network
(b) Gram-atom of sulphur per gram rubber network
(c) Gram-ion of sulphide per gram rubber network
(d) Number of sulphur atoms combined in the network per chemical crosslink present
(e) Number of sulphur atoms combined in the network per chemical crosslink after treatment with triphenyl phosphine.

Table 4.15 The change in polysulphidic crosslinks during fatigue of an HAF-black filled conventional vulcanisate without antioxidant (Formulation D, Table 4.1) $\overline{Mn}$ = 179,000

Fatigue cycles x 10^2	Unfatigued sample adjacent to test piece			Fatigued test piece			% change in $-S_x-$ crosslinks
	Crosslink density[a] x 10^2		%crosslinks[b] ($-S_x-$)	Crosslink density[a] x 10^2		%crosslinks[b] ($-S_x-$)	
	Before probe	After probe		Before probe	After probe		
50	5.75	2.48	57	5.87	2.71	54	3
100	5.71	2.53	56	5.83	2.88	51	5
200	5.72	2.56	55	5.85	3.04	48	7
400	5.80	2.62	55	5.95	3.44	42	13
600	5.90	2.57	56	6.06	3.62	40	16

(a) Kg-mole chemical crosslinks per Kg rubber network (b) Average of three determinations quoted

the number of fatigue cycles experienced, increasing from 3% after 5 kilocycles to 16% after 60 kilocycles. Tables 4.16 and 4.17 show the results obtained for vulcanisates containing IPPD and SWP respectively. There is evidence for a reduction in the rate of polysulphide crosslink destruction in the vulcanisates containing antioxidants, IPPD being more effective than SWP. This effect is seen more clearly in Figure 4.9 which shows the dependence of the rate of polysulphidic crosslink reduction on the number of fatigue cycles experienced. They show similar trends to those obtained for the corresponding gum vulcanisates. However, the magnitude of the change observed is slightly higher in the filled vulcanisates. This is apparently attributable to the higher strain energy input per fatigue cycle in the filled vulcanisates, resulting in the generation of more thermal energy within the vulcanisate.

The results of the distribution of mono and disulphidic crosslinks before and after fatiguing samples to failure are presented in Table 4.18. These results, show that many more new disulphide crosslinks than monosulphide are formed during fatigue. It can be suggested that during fatigue polysulphide crosslinks are cleaved and eventually lead to the formation of new mono and disulphide crosslinks. The formation of more disulphide crosslinks than monosulphide may be attributed to the higher stability of the disulphenyl radicals when compared to the monosulphenyl radicals, because of their ability to delocalise their free electron over the d orbital of the second sulphur atom.

Table 4.16 The change in polysulphidic crosslinks during fatigue of an HAF-black filled conventional vulcanisate containing IPPD (Formulation E, Table 4.1) $\overline{Mn}$ = 179,000

Fatigue cycles x 10^{-2}	Unfatigued sample adjacent to test piece			Fatigued test piece			% change in $-S_x-$ crosslinks
	Crosslink density[a] x 10^2		%crosslinks[b] $(-S_x-)$	Crosslink density[a] x 10^2		%crosslinks[b] $(-S_x-)$	
	Before probe	After probe		Before probe	After probe		
50	6.00	2.84	53	6.09	3.06	50	3
200	5.97	2.79	53	6.05	3.13	48	5
400	6.07	2.75	55	6.19	3.34	46	9
600	6.04	2.77	54	6.17	3.50	43	11
800	6.11	2.83	54	6.24	3.64	42	12

(a) Kg-mole chemical crosslinks per Kg rubber network (b) Average of three determinations quoted

Table 4.17 The change in polysulphidic crosslinks during fatigue of an HAF-black filled conventional vulcanisate containing SWP (Formulation F, Table 4.1) $\overline{Mn}$ = 178,000

Fatigue cycles x 10^{-2}	Unfatigued sample adjacent to test piece			Fatigued test piece			% change in $-S_x-$ crosslinks
	Crosslink density[a] x 10^2		%crosslinks[b] $(-S_x-)$	Crosslink density[a] x 10^2		%crosslinks[b] $(-S_x-)$	
	Before probe	After probe		Before probe	After probe		
50	5.81	2.43	58	5.93	2.61	56	2
200	5.84	2.41	59	5.98	2.83	53	6
400	5.97	2.53	58	6.09	3.19	48	10
600	5.92	2.44	59	6.05	3.28	46	13
800	5.86	2.39	59	6.00	3.26	46	13

(a) Kg-mole chemical crosslinks per Kg rubber network (b) Average of three determinations quoted

Fig 4.9 The relation between % reduction of polysulphide crosslinks and fatigue cycles during fatigue of carbon black filled NR vulcanisates containing different antioxidants.

(a) control (no antioxidant)

(b) SWP

(c) IPPD

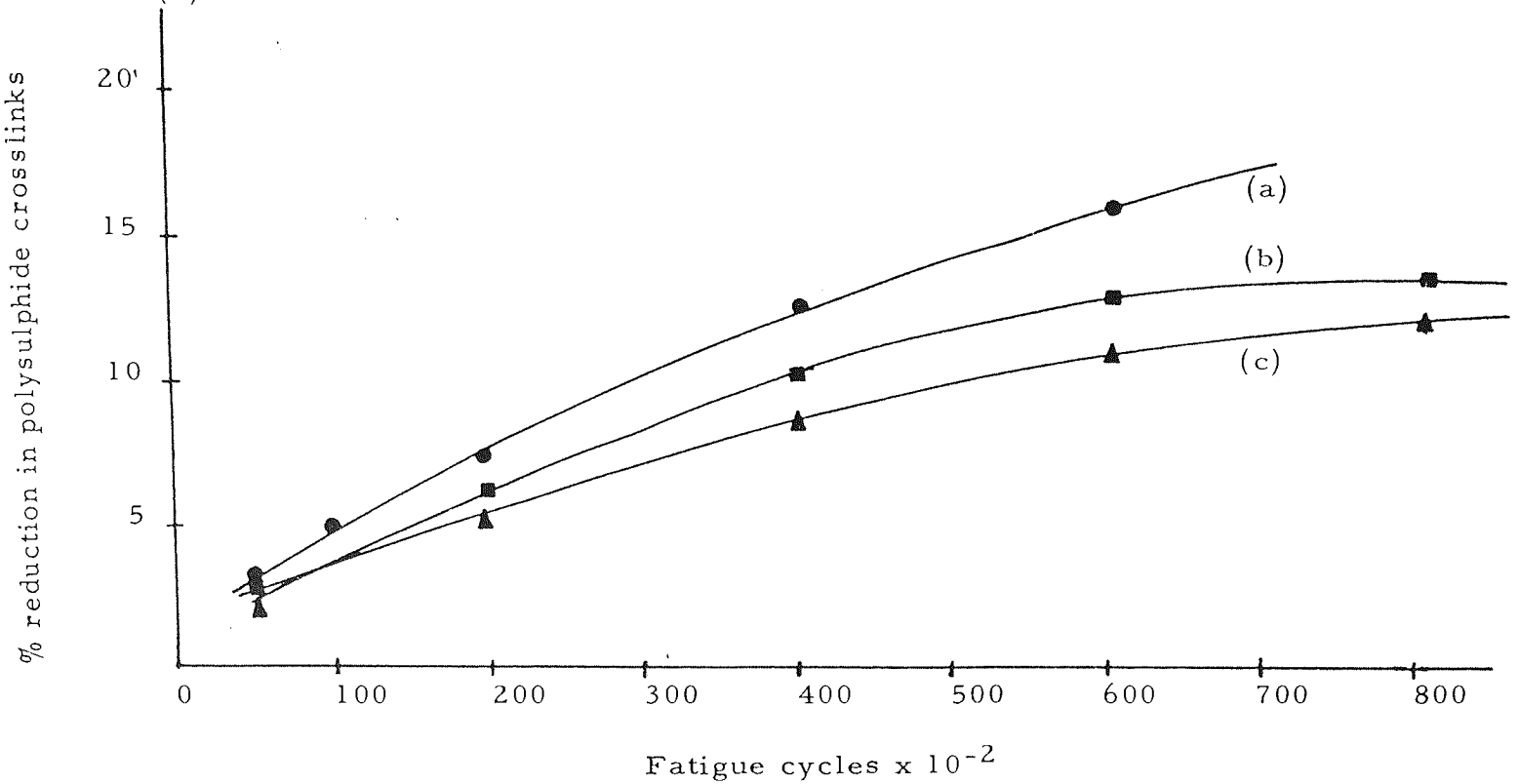

Table 4.18 The distribution of crosslinks in HAF-black filled vulcanisate networks before and after fatiguing to failure (Formulations D, E and F, Table 4.1)

Formulation		Crosslink density[a]			% Crosslinks		
		original network	After P-2-T probe	After H-T probe	$-S_x-$	$-S_2-$	$-S_1-$
D	unfatigued	5.81	2.52	0.99	57	26	17
	fatigued[1]	5.96	3.59	1.24	40	39	21
E	unfatigued	5.95	2.68	0.84	55	31	14
	fatigued[2]	6.09	3.53	1.01	42	41	17
F	unfatigued	5.69	2.36	0.96	58	25	17
	fatigued[3]	5.86	3.27	1.24	44	35	21

(a) Crosslink density = $\frac{1}{2}\overline{M}_{c(chem)} \times 10^2$ Kg mole Kg^{-1} RN

(1) Fatigue life = 63,000 cycles
(2) Fatigue life = 90,000 "
(3) Fatigue life = 760,000 "

CHAPTER FIVE

STUDIES ON CHAIN ENDS

5.1 Introduction

A detailed review of the literature on the effect of chain ends on rubber properties was presented in Section 1.8 from which it was apparent that chain ends are elastically ineffective and do not contribute to the overall strength of the rubber network. Free chain ends in rubber vulcanisates may act as points of weakness during a fatigue process and their presence may affect the fatigue life of vulcanisates. It is possible that the presence of intentional flaws, for example cut initiated fatigue or the presence of fillers, may mask this effect.

The number of free chain ends in a vulcanisate may be controlled by:

(i) the initial molecular weight of a rubber prior to crosslinking.

(ii) Oxidative scission during ageing. An aged vulcanisate network could be envisaged to differ from that of an unaged counterpart mainly in terms of differences in concentration of chain ends,

reflecting the extent to which oxidative scission of the rubber chains has occurred.

(iii) The use of a vulcanisable free radical acceptor that can combine with the free radicals of rubber produced during mastication and then become incorporated into the main chain during crosslinking, reducing the number of free chain ends in the network. A previous study[285] has shown that bis(diisopropyl) thiophosphoryl disulphide (DIPDIS) (see Equation 2-1) is able to play such a role and a quantitative assessment of the reduction of free chain ends based on changes in the C_1 constant of the Mooney Rivlin equation was described. However, this study was not extended to explore the possible effect that a reduction in chain ends would have on fatigue.

In each of the above cases, the change in the concentration of free chain ends was expected to affect the physical properties of the rubber.

The effects of chain end concentration on fatigue and other physical properties was the subject of an investigation in this project, involving the following approach:

(i) A preliminary investigation to assess the fatigue resistance, as well as other physical properties, of a series of conventional vulcanisates prepared from NR masticated to different initial molecular weights, and therefore having varying concentrations of free chain ends. The effect of filler on fatigue resistance of these vulcanisates was also investigated.

(ii) Whereas in (i) chain ends were produced by milling, chain ends can also be produced by oxidative ageing. A series of NR vulcanisates were prepared from NR latex, which possessed a high initial $\overline{Mn}$ and hence low chain end concentration. These vulcanisates were then oxidatively aged for various times and the effects of ageing on fatigue resistance were assessed.

(iii) To determine the fatigue resistance of a series of vulcanisates prepared from NR latex which had previously been oxidised to different extents by treating with oxygen at an elevated temperature for various times. In this case chain ends were produced before vulcanisation.

(iv) To study the effect of the reduction in concentration of chain ends on fatigue resistance. The number of free chain ends in a vulcanisate network was reduced by masticating NR with a vulcanisable free radical acceptor such as DIPDIS under a nitrogen

atmosphere. The effects on fatigue were assessed.

The percentage of free chain ends combined in the vulcanisate after modification by mastication could be assessed from changes in the C_1 constant. When NR is masticated to a molecular weight of $\overline{M}n$ and then crosslinked, the elastic constant C_1 of the Mooney-Rivlin equation (1-7) is related to $\overline{M}_{c(chem)}$ by the Moore, Mullins and Watson equation (1-26):

$$C_1 = \left[\frac{\rho RT}{2\overline{M}_{c(chem)}} + 0.78 \times 10^5\right]\left[1 - 2.3\overline{M}_{c(chem)}\overline{M}n^{-1}\right] Nm^{-2} \quad (1\text{-}26)$$

When NR is masticated to the same $\overline{M}n$ value but in the presence of a radical acceptor that will produce terminal groups which can subsequently combine with the network during vulcanisation, then the value of C_1 obtained, C_1', is different even though the value of $\overline{M}_{c(chem)}$ is kept constant by using the same formulation, and the vulcanisates are mixed and vulcanised under identical conditions. If $\overline{M}_{c(chem)}$ is constant, this change in C_1 must be due to a change in the only remaining variable ($\overline{M}n$) which changes to an apparent value $\overline{M}n'$ when the reactive end of the molecule combines with the network. If the chain end modification is 100% effective, then the value of $\overline{M}n'$ becomes very large and the number of free chain ends very small. The value of $\overline{M}n'$ may be obtained, using the expression: (285)

$$\overline{Mn}' = \frac{2.3\ \overline{Mn}\ C_1\ \overline{M}_{c(chem)}}{\overline{Mn}(C_1 - C_1') + 2.3C_1'\ \overline{M}_{c(chem)}} \qquad (5\text{-}1)$$

The percentage chain ends combined (%C. E. C) is given by the relation:

$$\%\ C.E.C = \left(1 - \frac{\overline{Mn}}{\overline{Mn}'}\right) x\ 100 \qquad (5\text{-}2)$$

A combination of (5-1) and (5-2) gives the expression:

$$\%\ C.E.C = \frac{(2.3\overline{M}_{c(chem)} - \overline{Mn})(C_1 - C_1')}{2.3\ C_1\ \overline{M}_{c(chem)}} \qquad (5\text{-}3)$$

The percentage chain ends combined after mastication with DIPDIS was estimated using equation (5-3). Because many determinations were involved in the investigation, a computer program, based on equations (5-1) and (5-2), was written for all calculations. This program is shown in appendix 1-9.

5.2 Preparation of Vulcanisates

5.2.1 Formulations

The assessment of the effect of initial number average molecular weight of rubber ($\overline{Mn}$) on the fatigue resistance, as well as other physical properties, was carried out using gum and carbon black

filled vulcanisates prepared according to formulations A and B respectively, the compositions of which are shown in Table 5.1. The investigations on the reduction of free chain ends by mastication with DIPDIS was carried out by using formulations C and D (Table 5.1). The formulations used for the preparation of vulcanisates from latex are shown in Tables 2.3 and 3.4.

Table 5.1 Compound formulations

Ingredients	Formulations: Parts by weight			
	A	B	C	D
Natural rubber	100	100	100	100
Sulphur	2.5	2.5	0.5	0.5
Zinc oxide	5	5	5	5
Stearic acid	2	2	2	2
CBS	0.6	0.6		
DMDS			1.63	1.63
DIPDIS			3	
HAF-black		40		

5.2.2 Compounding of Dry Rubber

5.2.2.1 $\overline{Mn}$ Variation in Gum Stock

The compounding of the conventional gum formulation (A) was carried out on the open mill as described in Section 2.2.3.1. The initial molecular weight of the rubber was varied by masticating portions of a single batch of compounded rubber to various extents on the mill.

5.2.2.2 $\overline{Mn}$ Variation in Black Stock

The mixing of carbon-black formulation (B) was carried out in the Banbury mixer described in Section 2.2.4.1. Two types of compounds having various initial molecular weights were prepared by using two mixing cycles. The first (fixed mixing cycle) was designed to study the effect of initial molecular weight on fatigue while minimising the effect of filler dispersion. The second (variable mixing cycle) was intended for the study of the effects of filler dispersion. In the fixed mixing cycle, portions of a single sample of rubber were first masticated to various plasticities, and compounds were prepared from them according to a fixed mixing cycle. This procedure ensured that compounds of different initial molecular weights but with similar dispersion were obtained. In

the variable mixing cycle, a single large mixing was first prepared from the same original sample of rubber according to the fixed mixing cycle, and portions of this were then milled for various extents on the open mill. Such a procedure ensured that compounds were produced which had different initial molecular weights but with filler dispersion varying in a systematic manner with the initial molecular weights. Details of the two mixing cycles are shown below:

(a) Fixed mixing cycle

0 minutes : added rubber of known plasticity

2 minutes : added all ingredients except sulphur and carbon black

3 minutes : added one half of black

4 minutes : added remainder of black

6 minutes : dumped compound

Sulphur was added on the open mill for 2 minutes

(b) Variable mixing cycle

This was the same as above except that the milling time on the open mill was varied such that compounds were produced which had different initial molecular weights with filler dispersion varying systematically with initial molecular weights.

5.2.2.3 Mastication with DIPDIS

All the rubber for mastication with DIPDIS was first purified by extracting with acetone as described in Section 2.2.2, to prevent the competition by indigenous radical acceptors which may be present in the rubber. The rubber was first sheeted on a water cooled laboratory two-roll mill so it could be extracted efficiently but this was kept to a minimum so that very little reduction in molecular weight occurred. The mastication of extracted NR under an atmosphere of nitrogen was carried out both in the vertical masticator (unirotor mixer) and in the RAPRA torque rheometer described in Sections 2.2.3.2 and 2.2.3.3 respectively.

5.2.3 Preparation of Vulcanisates From Latex

The preparation of aqueous dispersions of compounding ingredients suitable for NR latex was carried out as described in Section 2.4.2 and the mixing of the ingredients with latex was carried out as in Section 2.4.3. The mix was allowed to mature before casting and curing, as described in Section 2.4.4.

5.2.4 Preparation of Vulcanisates from Dry Rubber Compounds

The Monsanto rheometer (Section 2.3.1) was first used to determine

the curing characteristics at 140°C of the rubber compound, and to establish that there was good dispersion of compounding ingredients during mixing. The curing characteristics of the different formulations are shown in Table 5.2. Vulcanisation of a compound was

Table 5.2 Curing characteristics of dry rubber compounds (composition of formulations shown in Table 5.1)

	Formulations			
	A	B	C	D
Rheometer temperature /(°C)	140	140	140	140
Induction period, t_i, /(min)	12	7.5	15	10
Cure rate constant (K) /min^{-1}	0.51	0.61	0.50	0.51
Optimum cure time (t_{90}) /mins	21	19	35	29
Cure time for maximum torque /mins	33	30	50	40
Torque at 90% cure/(in lb)	50	62	49	48
Maximum torque /(in lb)	55	69	54	53

carried out in the appropriate mould placed between the platens of a heated press (Section 2.3.2). Curing was carried out at 140°C for the optimum cure time and vulcanisate test pieces were prepared for the following tests:

(a) Fatigue

(b) Tensile strength

(c) Resilience

(d) Tension stress at 100% extension (MR100)

(e) Stress relaxation

(f) Oxygen absorption

5.2.5 Preparation of Cut Initiated Fatigue Test Specimens

Cut initiated test samples for fatigue tests were prepared as follows: a dumb-bell sample was loaded into a groove in a suitable template such that the central region was aligned between parallel engraved marks. A needle of 0.3 mm diameter was then placed in a perpendicular hole located in the centre of the engraved marks and pushed through the rubber sample. In this way a central cut of given dimension was initiated in the test piece.

5.3 Effect of Initial Number Average Molecular Weight of Rubber ($\overline{Mn}$) on Fatigue and Other Physical Properties

A number of vulcanisate mixes were prepared, as described previously, in which the initial number average molecular weight varied according to the rubber open-milling time and in order to ensure that the degree of chemical crosslinking was identical in each vulcanisate, these mixes were vulcanised simultaneously in a single press. Test pieces were prepared for a given set of conditions with and without cut initiation.

5.3.1 Fatigue

Fig 5.1 shows the dependence of fatigue life of a gum vulcanisate on the initial molecular weight of rubber. There is evidence to show that the fatigue life increased with the initial molecular weight of rubber, from 69 kilocycles for a vulcanisate with an $\overline{Mn}$ value of 118,000 to 78 kilocycles for one with an $\overline{Mn}$ value of 301,000. It is shown that the effect of cut initiation is to reduce drastically the fatigue life of a vulcanisate. However, a vulcanisate with a higher initial molecular weight gave only a slightly better fatigue life than that with a lower $\overline{Mn}$ value.

5.3.1.1 Effect of Filler

Fig 5.2 shows the dependence of fatigue life on the initial molecular weight of rubber in an HAF-black filled vulcanisate, which may be compared with the behaviour of an unfilled system shown in Fig 5.1. The results were obtained testing vulcanisates prepared by using the fixed mixing cycle described in Section 5.2.2.2. This was designed to minimise the effect of filler dispersion while studying the effect of initial molecular weight on fatigue. As with the unfilled vulcanisate, the fatigue increased with increasing initial molecular weight. However, the fatigue lives observed were generally lower than those of unfilled vulcanisates and the dependence of fatigue life on initial molecular weight was also less. It must, however be borne in mind that the mixing cycle did not necessarily ensure identical filler dispersions in these vulcanisates so that the behaviour shown in figure 5.2 may have to take account of this problem. The S.E.M micrographs of the vulcanisates prepared using the fixed mixing cycle are presented in appendix 2.1. They show that filler dispersions were not exactly identical in all vulcanisates. In the study of the effect of cut initiation on the fatigue of filled vulcanisates with varying initial molecular weight, the problem may be greater since the effect of dispersion perhaps masks the effect of cut initiation completely as fillers may also act as flaws in the sample.

The effect of dispersion on fatigue is shown more clearly in tests carried out with vulcanisates prepared by using the variable mixing cycle (Section 5.2.2.2) which was designed specifically to study the effect of dispersion. Fig 5.3 shows the dependence of fatigue life on the milling time. Although the initial molecular weight of rubber would be expected to decrease with increased time of milling and reduce fatigue life, the effect of an improved dispersion with increased milling time results in a vulcanisate with better fatigue life. The S.E.M micrographs shown in appendix 2.2 illustrates beyond doubt the effect of milling time on filler dispersion.

5.3.2 Other Physical Properties

The results of the effect of initial molecular weight on other physical properties of rubber such as tensile strength, resilience, modulus at 100% extension, and stress relaxation, are shown in figures 5.4, 5.5, 5.6 and 5.7 respectively. The dependence of these properties on the initial average molecular weight of rubber are similar to those of fatigue, the higher the initial molecular weight of rubber before vulcanisation the better the particular physical property of the vulcanisate. It should, however, be taken into account that main chain scission may occur during vulcanisation and this will be equivalent to a reduction in $\overline{Mn}$. If this is the case, the value of $\overline{Mn}$ quoted may not be an exact measure of the $\overline{Mn}$ or chain end concentration in the vulcanisate.

Fig 5.1 The dependence of fatigue life of gum vulcanisates on the initial molecular weight of rubber ($\overline{Mn}$)

(a) Uncut samples

(b) Cut initiated samples

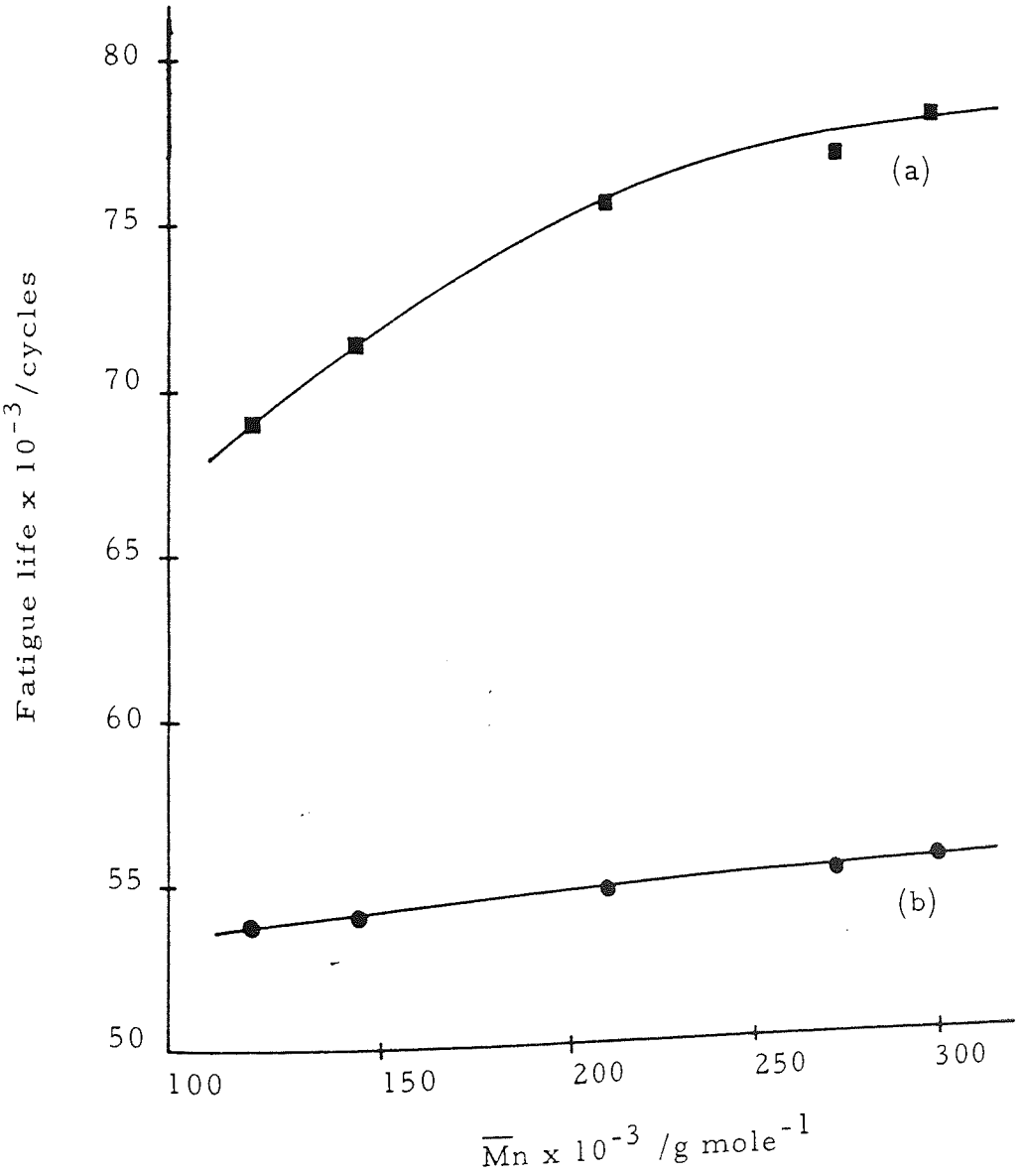

Fig 5.2 The dependence of fatigue life of filled vulcanisates on initial molecular weight of rubber ($\overline{Mn}$)

(fixed mixing cycle)

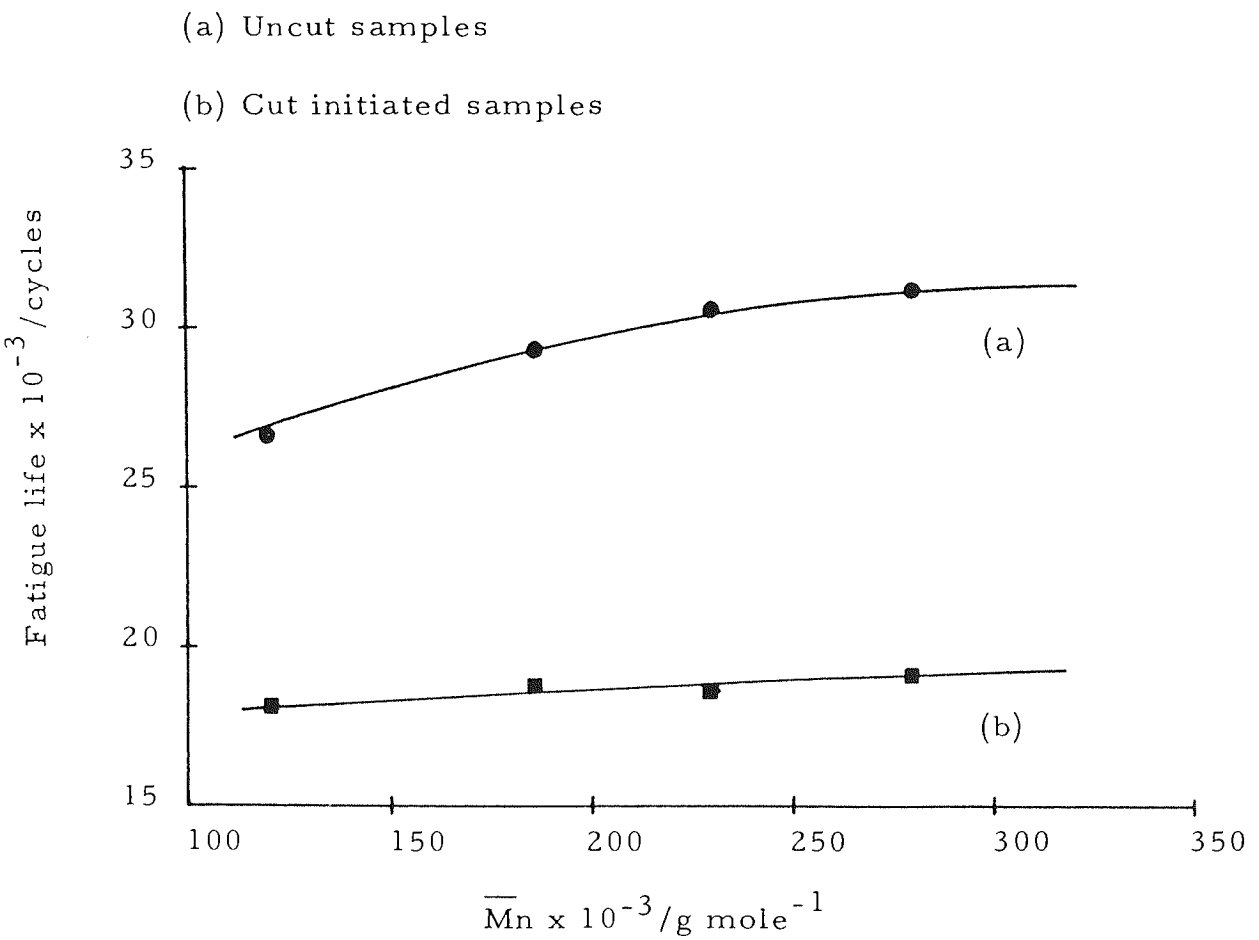

Fig 5.3 The dependence of fatigue life of filled vulcanisates on milling time (variable mixing cycle)

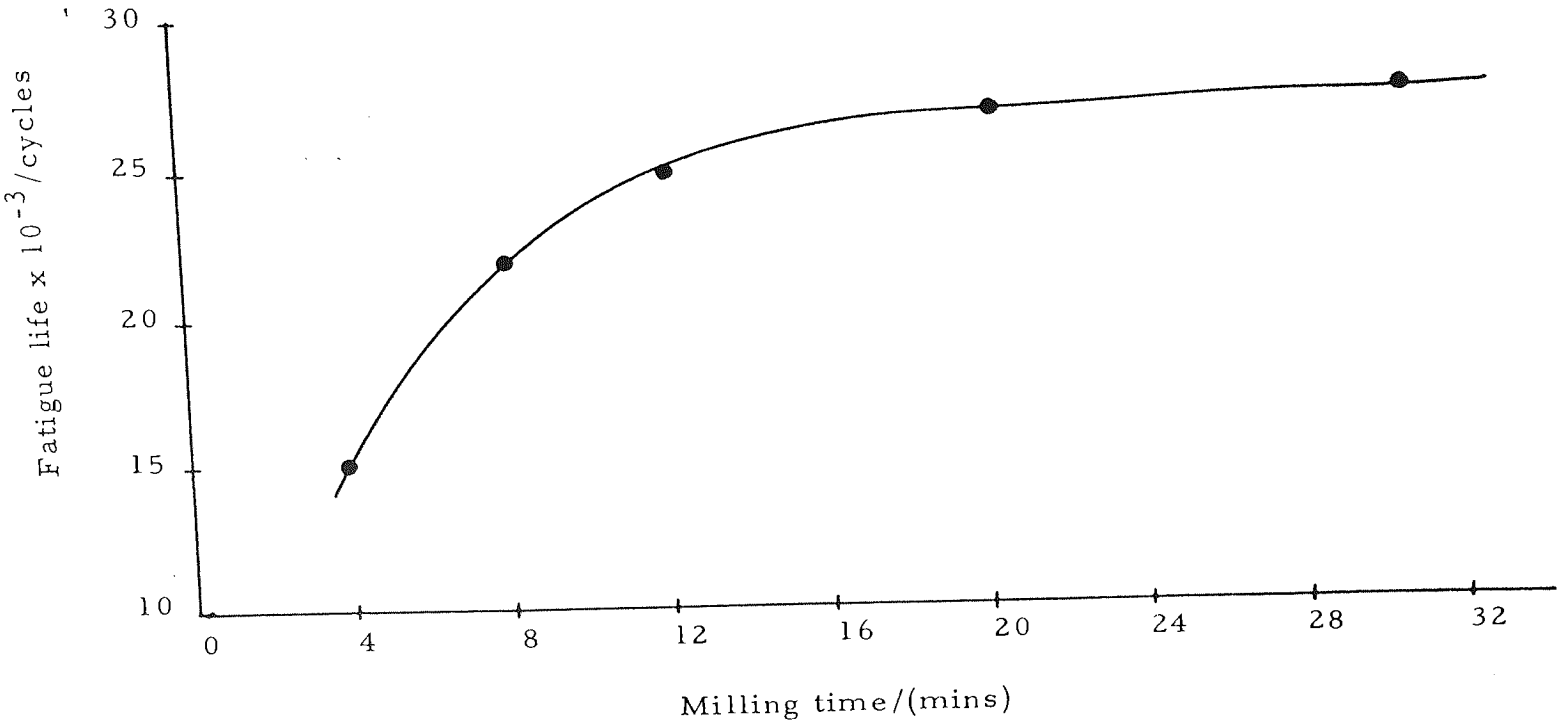

Fig 5.4 The variation of tensile strength of gum vulcanisates with initial molecular weight of rubber ($\overline{Mn}$)

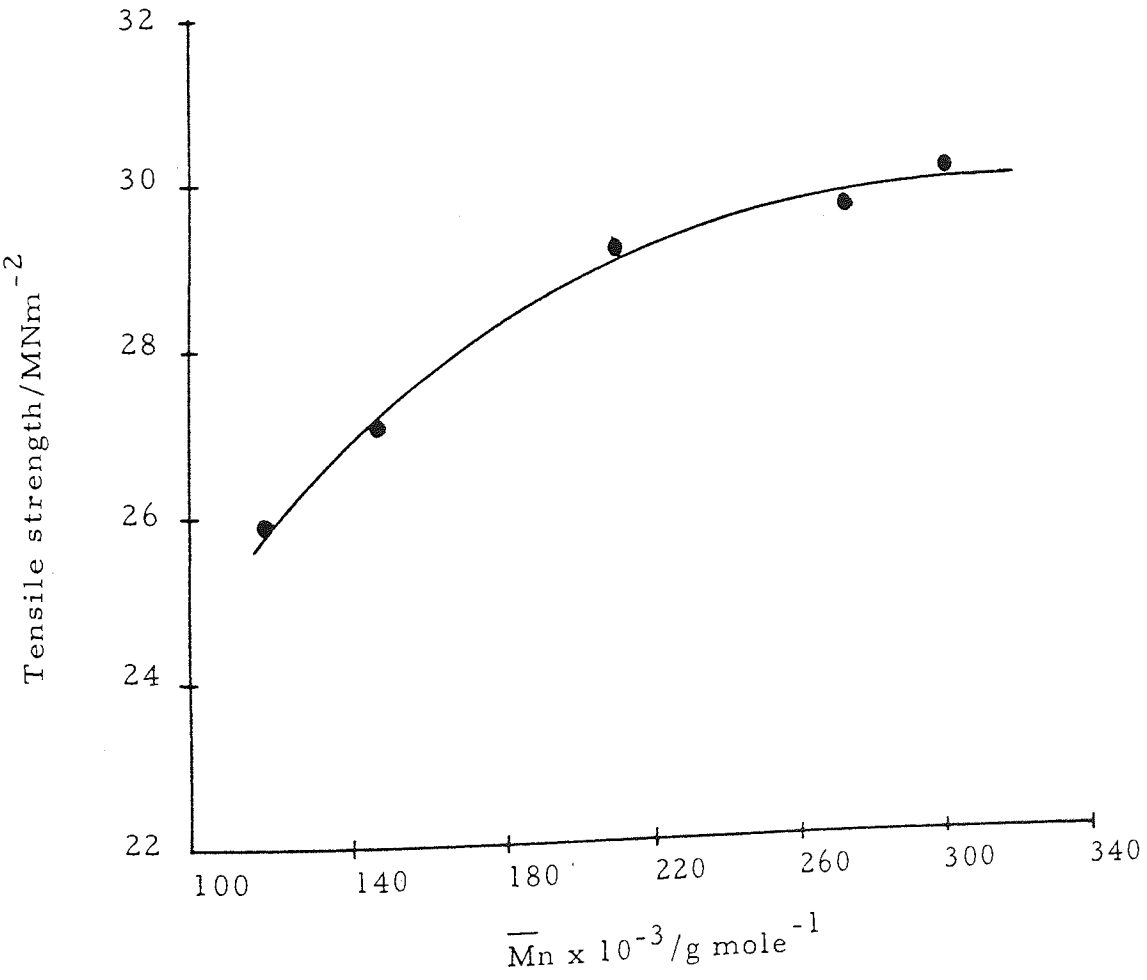

Fig 5.5 The variation of resilience (%) with initial molecular weight of rubber ($\overline{Mn}$) (gum vulcanisate)

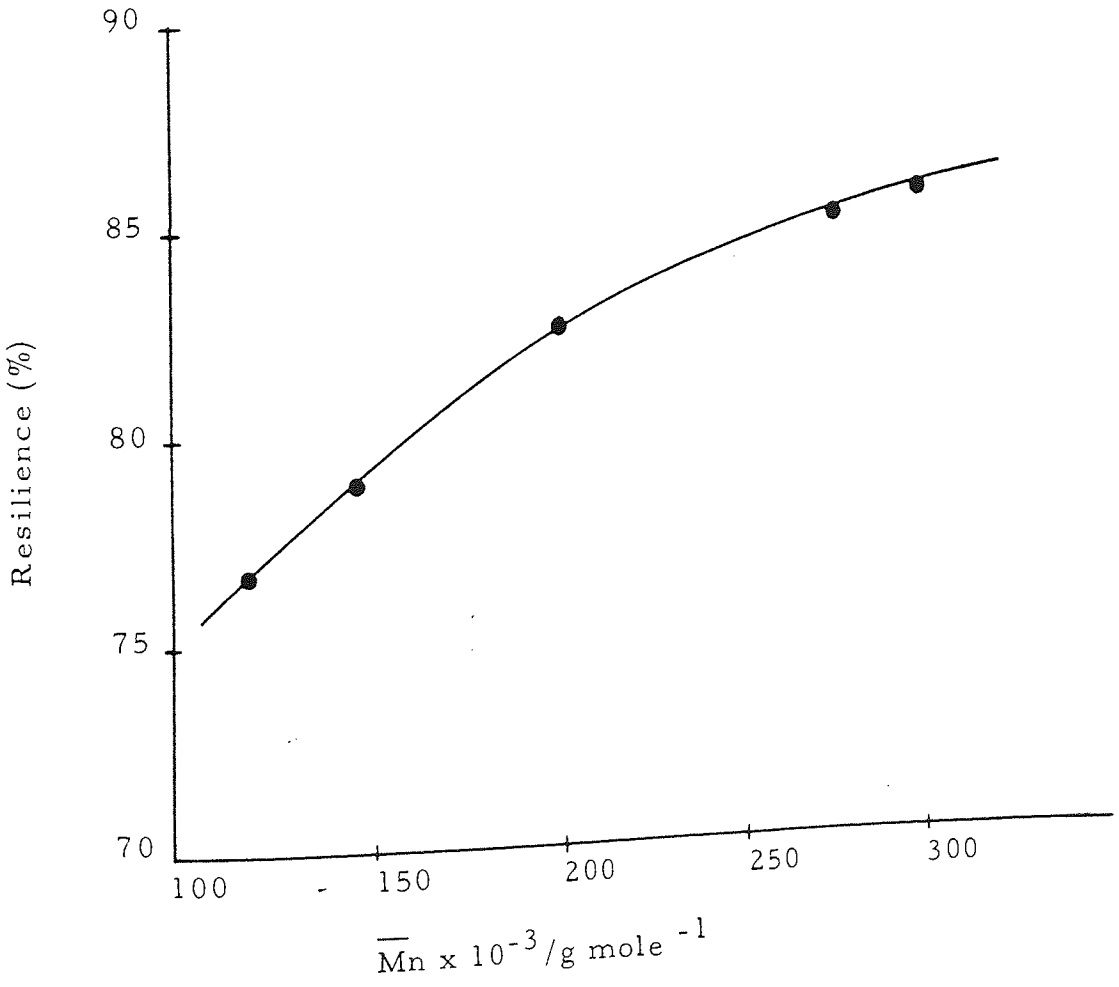

Fig 5.6 The dependence of the modulus at 100% extension on initial molecular weight of rubber ($\overline{Mn}$)

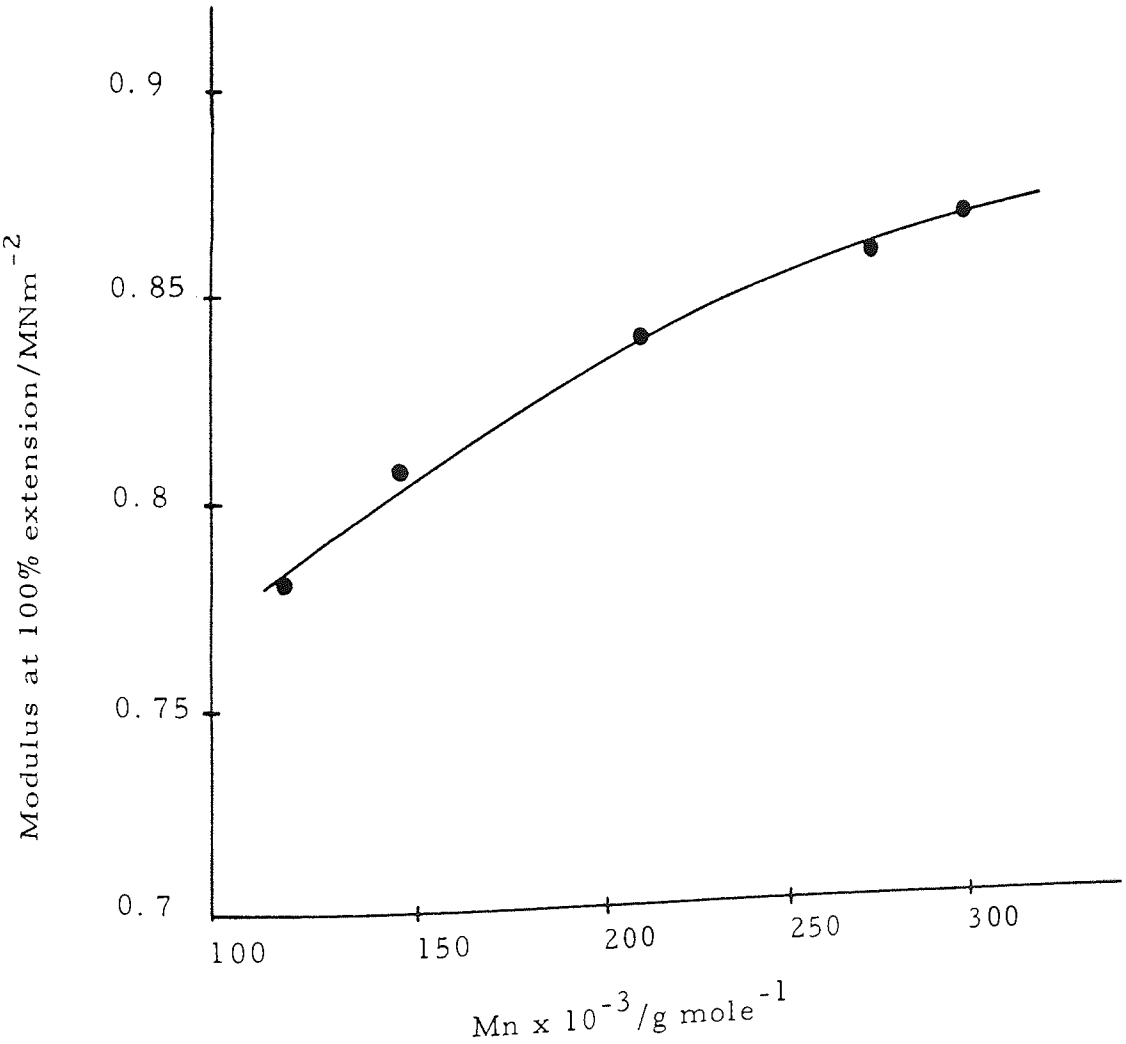

5.3.3 Discussion

The effect of initial molecular weight of rubber on fatigue resistance and other physical properties may be explained on the basis of the final vulcanisate structure. At a very low $\overline{Mn}$ value when the rubber chains are so short (high concentration of chain ends) that a coherent network is difficult to form, the physical properties such as fatigue resistance and tensile strength will be low; increasing $\overline{Mn}$ causes the level of physical properties to rise steadily at first and then more slowly until further increases in $\overline{Mn}$ are almost without effect. The effect of $\overline{Mn}$ on fatigue resistance may also be attributed to the slight variation in the internal viscosity of the rubber as a result of milling to various extents. It can be suggested that the ability to generate a flaw during fatigue depends upon the ability of the broken rubber chain ends to separate, which will be a function of the internal viscosity of the rubber. Curve (b), Fig 5.1, shows that cut propogation is almost independent of $\overline{Mn}$ while curve (a) shows that the generation and then propogation of a flaw is highly dependent on initial molecular weight of rubber. It can be suggested, therefore, that a vulcanisate with a high initial $\overline{Mn}$ value of rubber will be more resistant to cut initiation than one with a low $\overline{Mn}$ value of rubber.

The effect of $\overline{Mn}$ on fatigue life of rubber may also be associated with the heat build-up which occurs during stress. It has already been observed that resilience, which is a measure of the energy dissipated as heat during recovery from a deformation, decreases with a fall in the initial molecular weight of rubber. Heat build-up is associated with resilience, increasing as resilience decreases.

Another factor which may be important in explaining the observed effect of initial average molecular weight on fatigue, is the rate of oxygen absorption by the vulcanisates. Fig 5.8 shows the rate of oxygen absorption, by four vulcanisates having varying initial molecular weights, during an accelerated ageing test at 60°C. The rate of oxygen absorption increased steadily with ageing time after an initially slow rate. The initial slow rate of oxidation is presumably due to the presence of indigenous antioxidants. The rate of oxygen absorption decreased as the initial molecular weight of rubber increased, the vulcanisate prepared from latex (very high $\overline{Mn}$) showing a much slower rate of oxygen absorption. It should, however, be taken into account that the rate at which the different vulcanisates absorbed oxygen is also dependent on the amount of natural antioxidant present in the vulcanisates. The vulcanisate (d) prepared from latex is more likely to contain a higher amount of indigenous antioxidants than the other vulcanisates (a, b, c) prepared from masticated rubber since some antioxidants present in solid rubber

Fig 5.7 The variation of continuous stress relaxation at 80°C with initial molecular weight of rubber

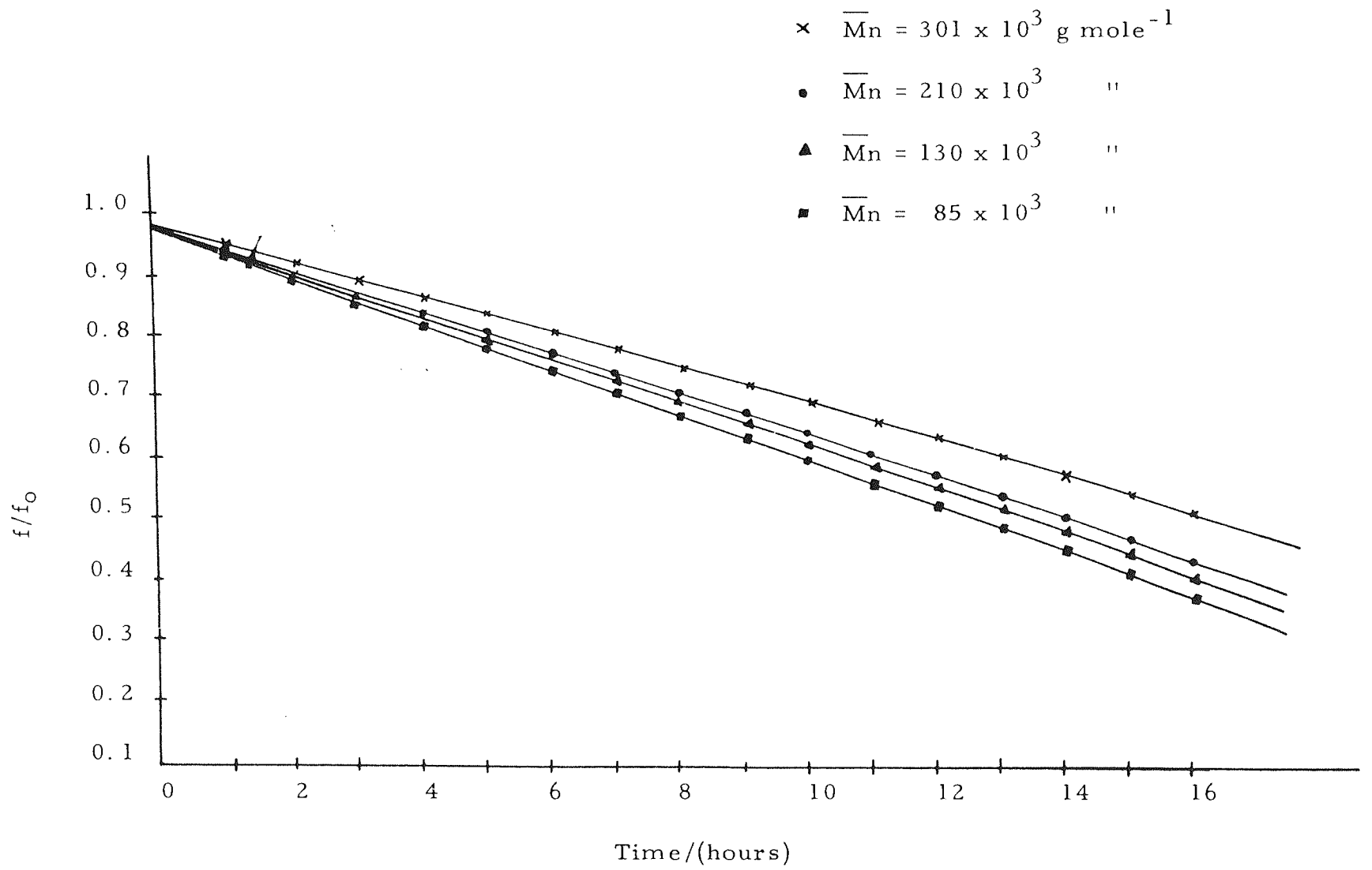

Fig 5.8 Oxygen absorbed as a function of ageing time at 60°C

(a) $\overline{Mn}$ = 94 x 10^3 g mole $^{-1}$

(b) $\overline{Mn}$ = 147 x 10^3 "

(c) $\overline{Mn}$ = 292 x 10^3 "

(d) $\overline{Mn}$ = 515 x 10^3 (latex rubber) "

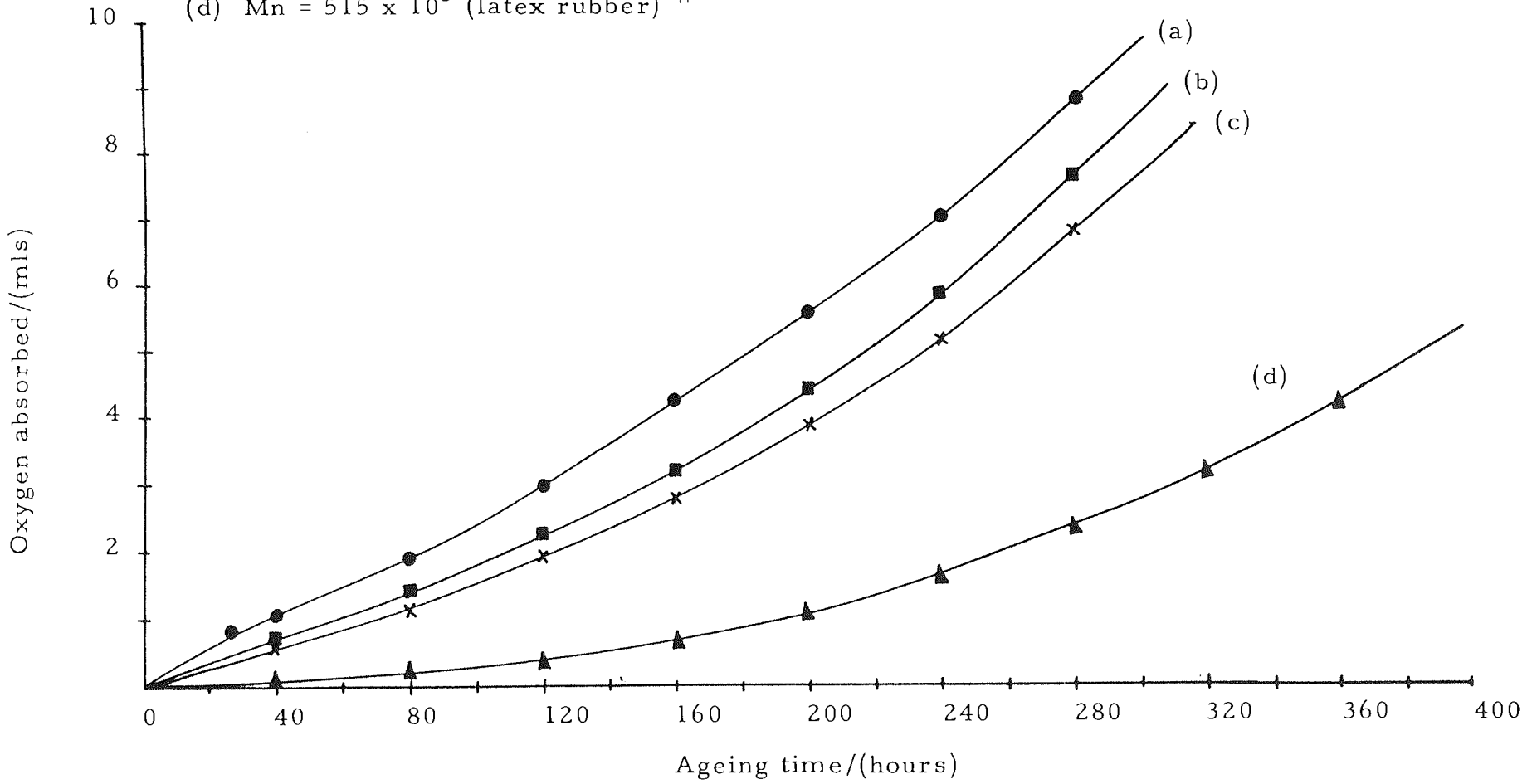

may have been used up as a result of the oxidation which occurs during milling.

5.4 Effect of Initial $\overline{Mn}$ of Latex Rubber on Fatigue

5.4.1 Oxidised Latex

The fatigue resistance of a series of vulcanisates prepared from latex rubber of varying initial molecular weights was also investigated. The initial molecular weight of latex rubber was varied by bubbling oxygen through latex at 60°C for various times. The value of $\overline{Mn}$ was estimated from intrinsic viscosity measurements.

Figure 5.9 shows the variation of the initial average molecular weight of latex rubber with time of oxidation of the latex. The initial molecular weight of rubber decreased slowly at first and then more rapidly as oxidation proceeded, until further oxidation resulted in no measurable reduction in the initial average molecular weight. The initial slow decrease at the start of oxidation could be attributed to the presence of naturally occurring antioxidants in the rubber, and there was a rapid decrease in number average molecular weight, when these had been consumed. The dependence of fatigue life of latex vulcanisates on the initial molecular weight of the latex rubber before vulcanisation is shown in figure 5.10. It can be seen that,

Fig 5.9 The dependence of $\overline{Mn}$ of NR on the time of thermal oxidation of latex at 60°C

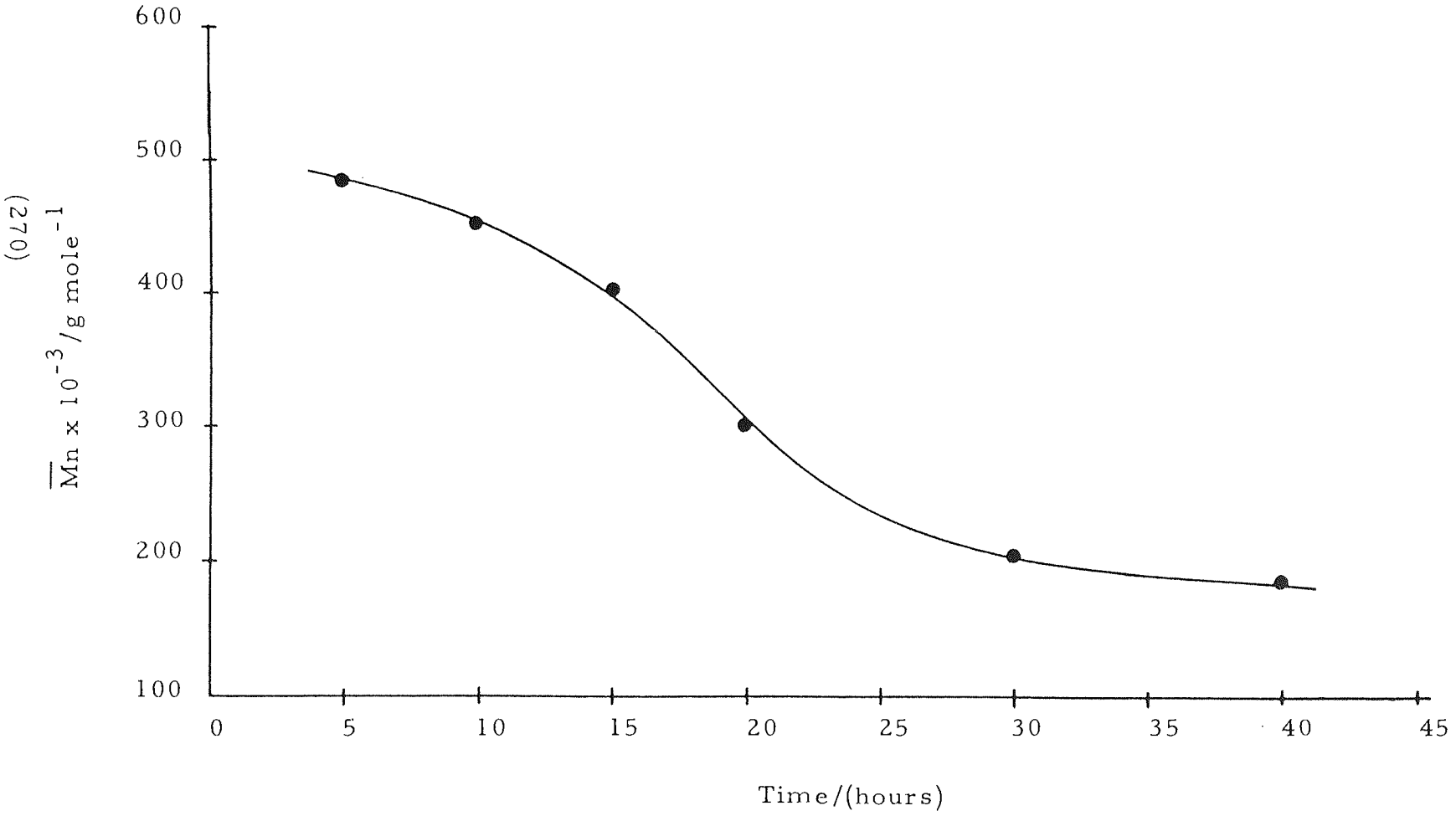

Fig 5.10 The dependence of fatigue life of latex vulcanisate on the initial molecular weight ($\overline{Mn}$) of latex rubber

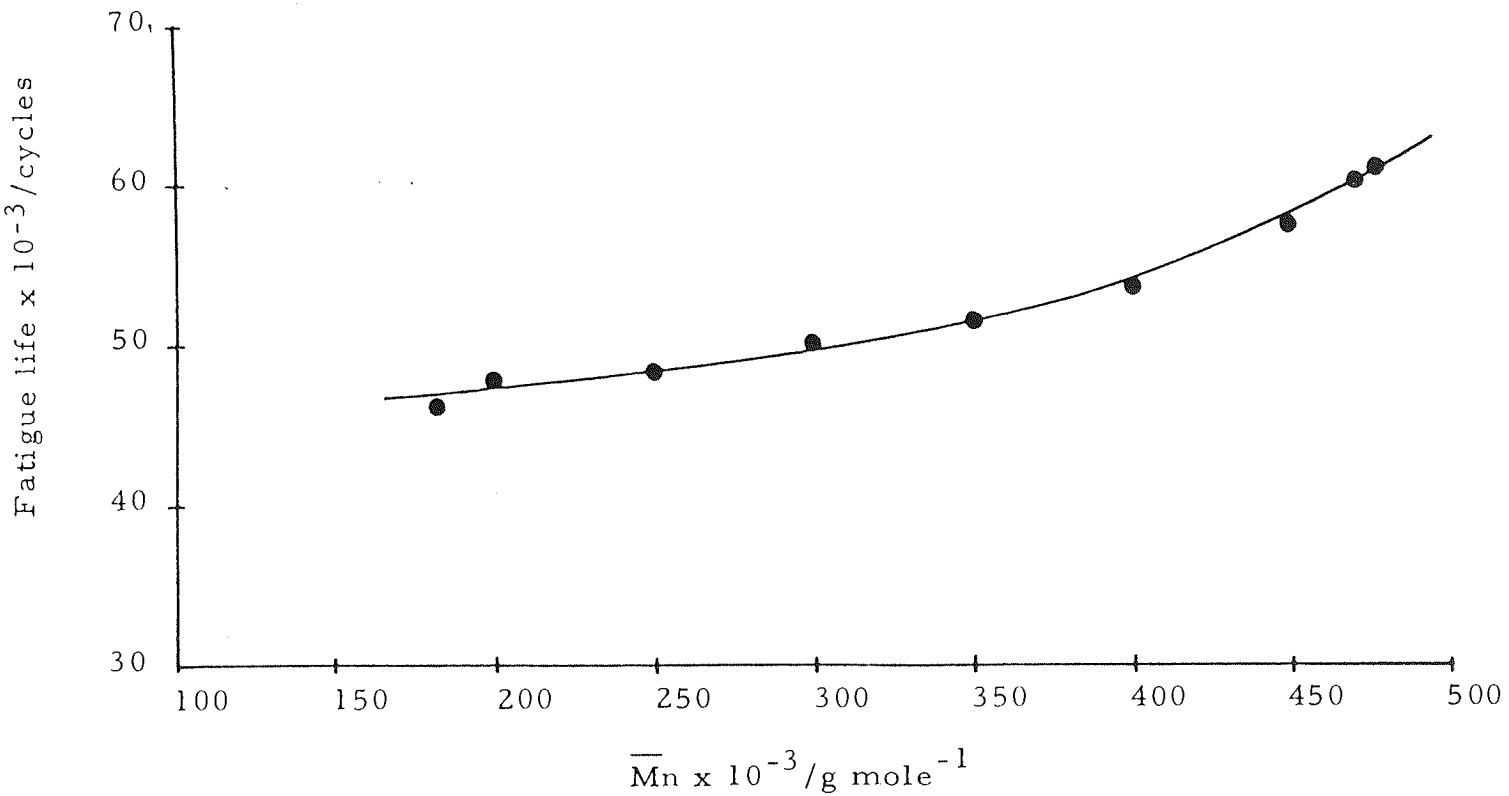

like dry rubber, the fatigue life increased with increasing initial molecular weight of the latex rubber. The effect may be explained on the same basis, discussed previously in 5.3.3.

5.4.2 Oxidative Ageing of Latex Vulcanisates

Apart from milling, chain ends were also produced by oxidative ageing. A series of NR vulcanisates were produced from NR latex, which possessed a high initial $\overline{Mn}$ and therefore low concentration of chain ends. These were then oxidatively aged at 80°C for various times and the effects of ageing on fatigue resistance were assessed. The oxidation of the natural rubber main chain is accompanied by secondary reactions of the initially formed peroxides, leading to the formation of various functional groups of which the carbonyl group predominates.(223) A generalised oxidation scheme for the natural rubber main chain is shown in scheme 5.11, while scheme 5.12 illustrates reactions of oxidised sulphur crosslinks in a natural rubber vulcanisate. The carbonyl index may then be used as a measure of free chain end concentration.

Fig 5.13 shows the dependence of carbonyl index and fatigue life of a latex vulcanisate on the time of oven ageing at 80°C. The carbonyl index was estimated as described in Section 2.7, and increased with ageing time, increasing slowly at first and then rapidly on further

Scheme 5.11 Oxidation of NR main chain[208]

Initiation: Production of R· or ROO·

Propogation:

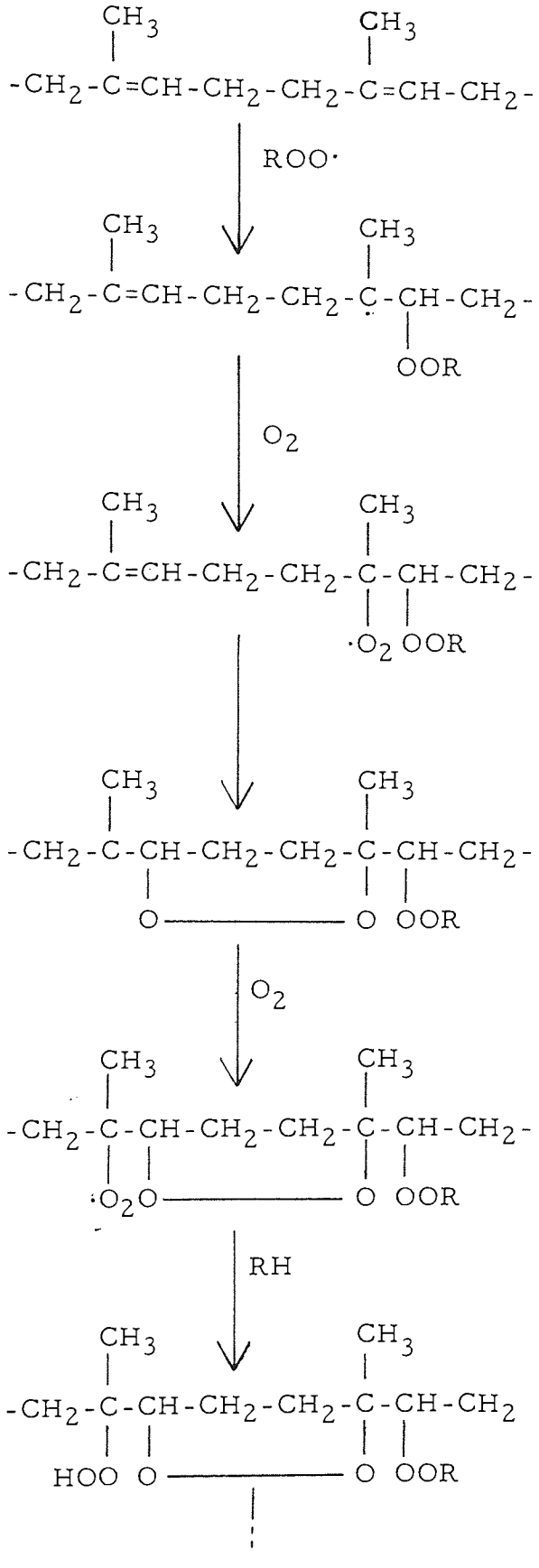

Scheme 5.11 continued

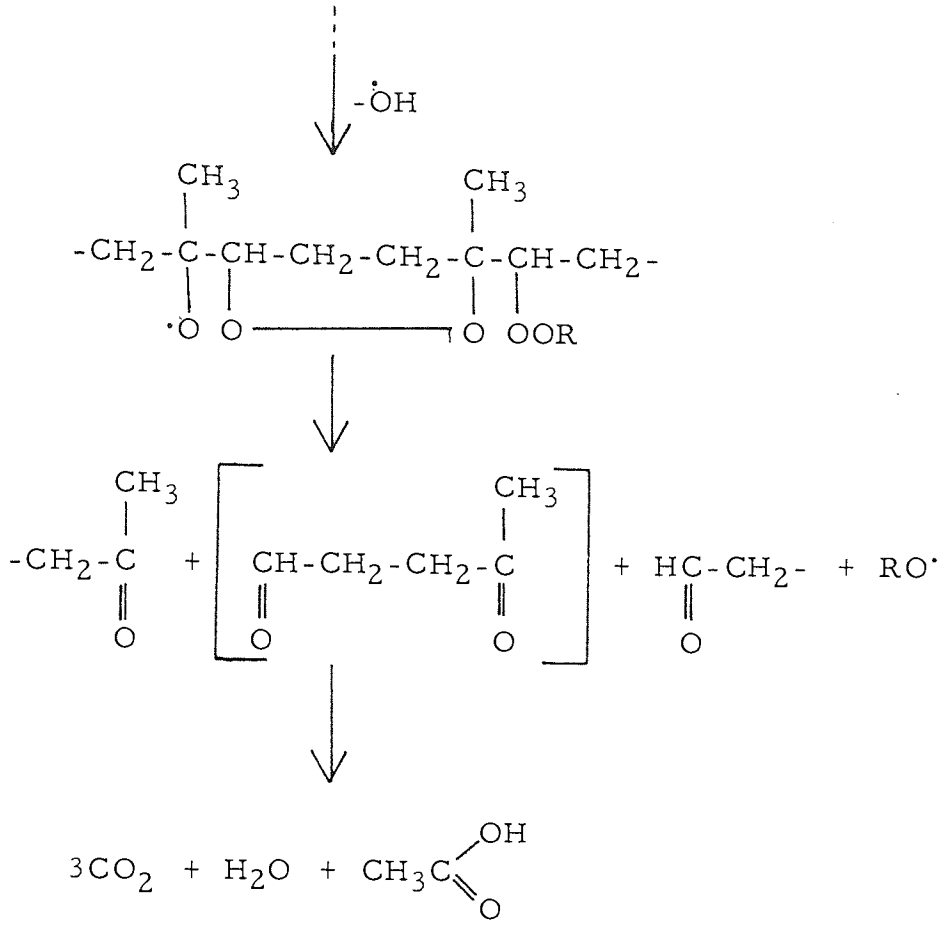

Scheme 5.12 Reactions of oxidised sulphur crosslinks[220]

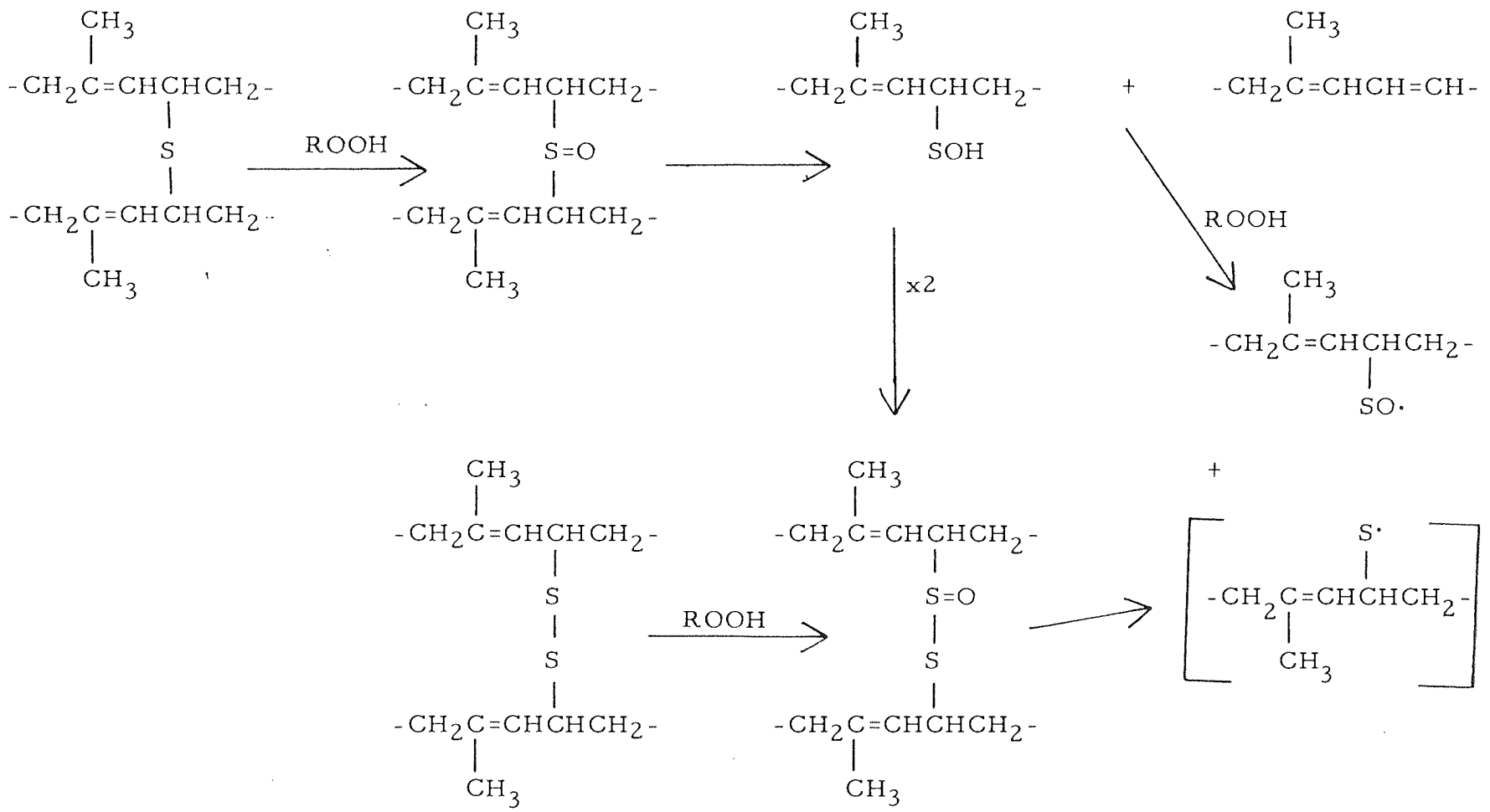

(275)

Fig 5.13 The variation of carbonyl index and fatigue life of latex vulcanisate with time of oven ageing at 80°C

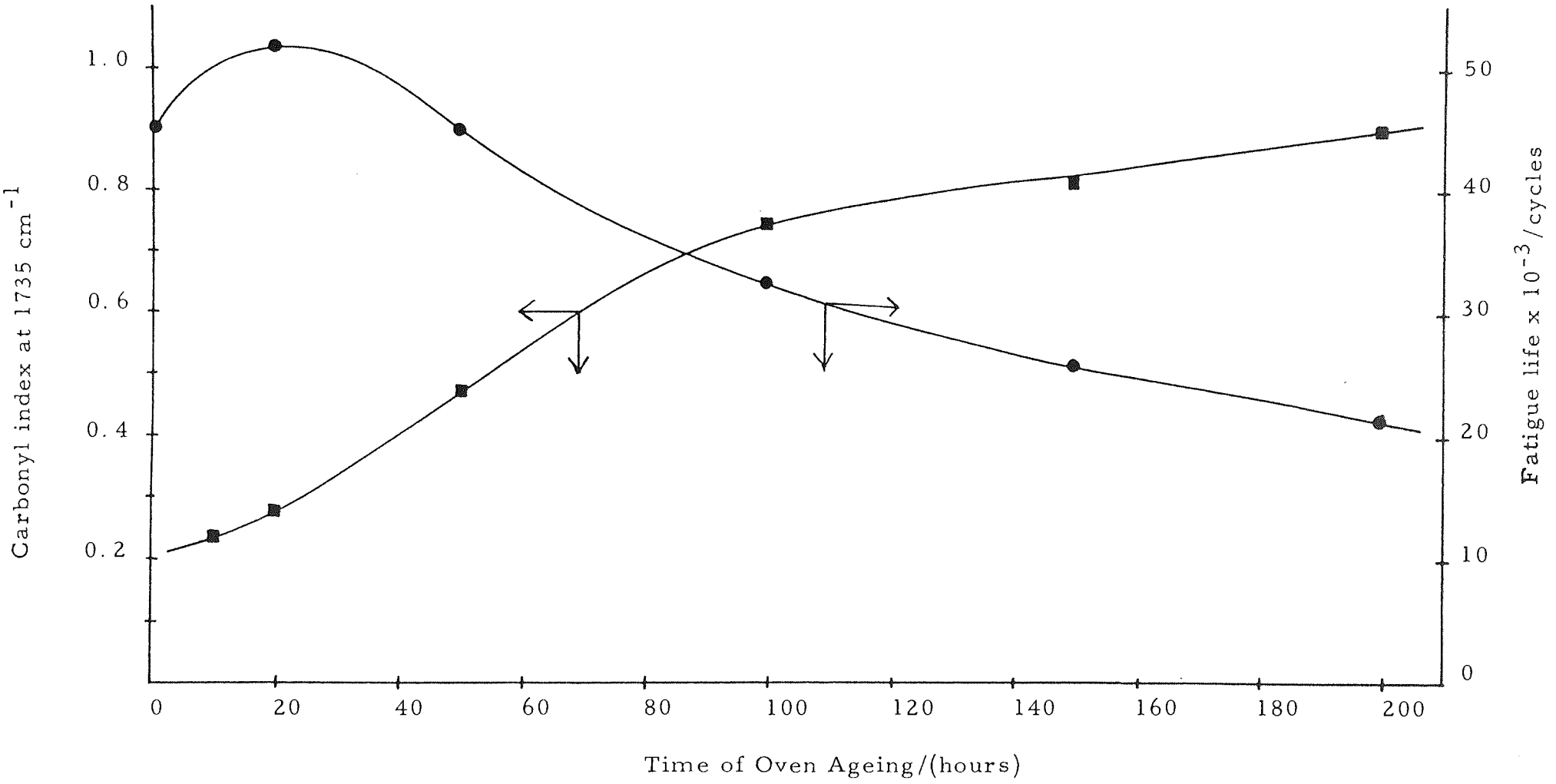

ageing. The increase in carbonyl index suggests that chain end concentrations increased during ageing. Although carbonyl terminated chain ends were most certainly produced during oxidative ageing (see scheme 5.11), it was not possible to estimate quantitatively the exact concentration of free chain ends produced because other carbonyl groups, which do not terminate chain ends can also be formed. The initial slow formation of carbonyl groups may be attributed to the prevention of oxidation by the natural occurring antioxidants in the vulcanisate. The fatigue life of the vulcanisate increased with ageing time during the initial 20 hours and then decreased steadily with further ageing. The initial increase in fatigue life may be explained on the basis of the crosslink maturation process which occurred resulting in the formation of more crosslinks. The increase in crosslink density presumably masked the effect of the chain ends produced during this period. The further decrease in fatigue life with ageing was presumably due to the increase in chain end concentration. It is not certain to what extent chain end concentration contributes to the fatigue failure during ageing, since other factors such as scission of sulphur crosslinks and main chain modification may also contribute.

5.5 The Effect of Reduction of Molecular Chain Ends on Fatigue

The effect of the reduction of the number of molecular chain ends in a NR vulcanisate on the fatigue resistance was investigated by masticating acetone extracted NR with bis(diisopropyl)thiophosphoryl disulphide (DIPDIS) under a nitrogen atmosphere. Advantage was taken of the mechanochemical degradation which occurs during mastication, to combine the free radicals produced from DIPDIS with some of the polymeric free radicals produced by the rupture of the rubber molecules to form active end groups according to the following scheme:

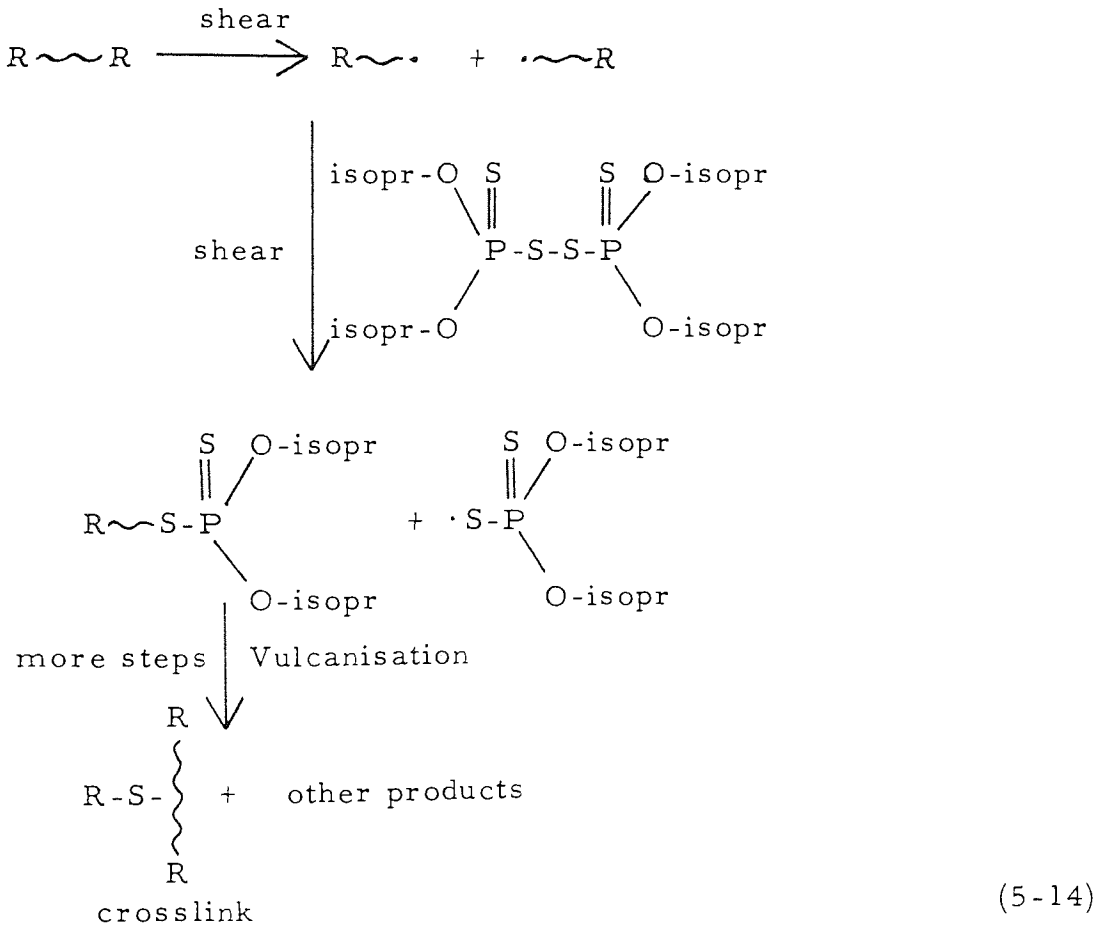

(5-14)

It has been shown by model compound studies that groups of similar structure, derived from tetramethyl thiuram disulphide and 2-mercaptobenzthiazole, are the precursors to crosslinks[26, 27] and it was hoped that the end groups produced during mastication with DIPDIS would react during the subsequent vulcanisation reaction in a similar manner and effectively tie the loose chain ends into the network.

The radical acceptor efficiency of DIPDIS during mastication was assessed by determining its effectiveness in reducing the molecular weight of rubber as a function of time. Changes in molecular weight and molecular weight distribution of rubber were determined from both intrinsic viscosity measurements (Section 2.5.2) and gel permeation chromatography (Section 2.5.3). The percentage of chain ends combined (%CEC) after vulcanisation was estimated by using equation (5-3).

Fig 5.15 and 5.16 show the variation of initial molecular weight of rubber ($\overline{Mn}$) as a function of time during mastication with DIPDIS in the RAPRA torque rheometer and the vertical masticator respectively. The number average molecular weight ($\overline{Mn}$), assessed by intrinsic viscosity measurement, decreased with time of mastication, decreasing more sharply in the first few minutes of mastication. Both figures show that the resulting molecular

Fig 5.15 The dependence of $\overline{Mn}$ on the mixing time in the RAPRA torque rheometer ($\overline{Mn}$ estimated from intrinsic viscosity)

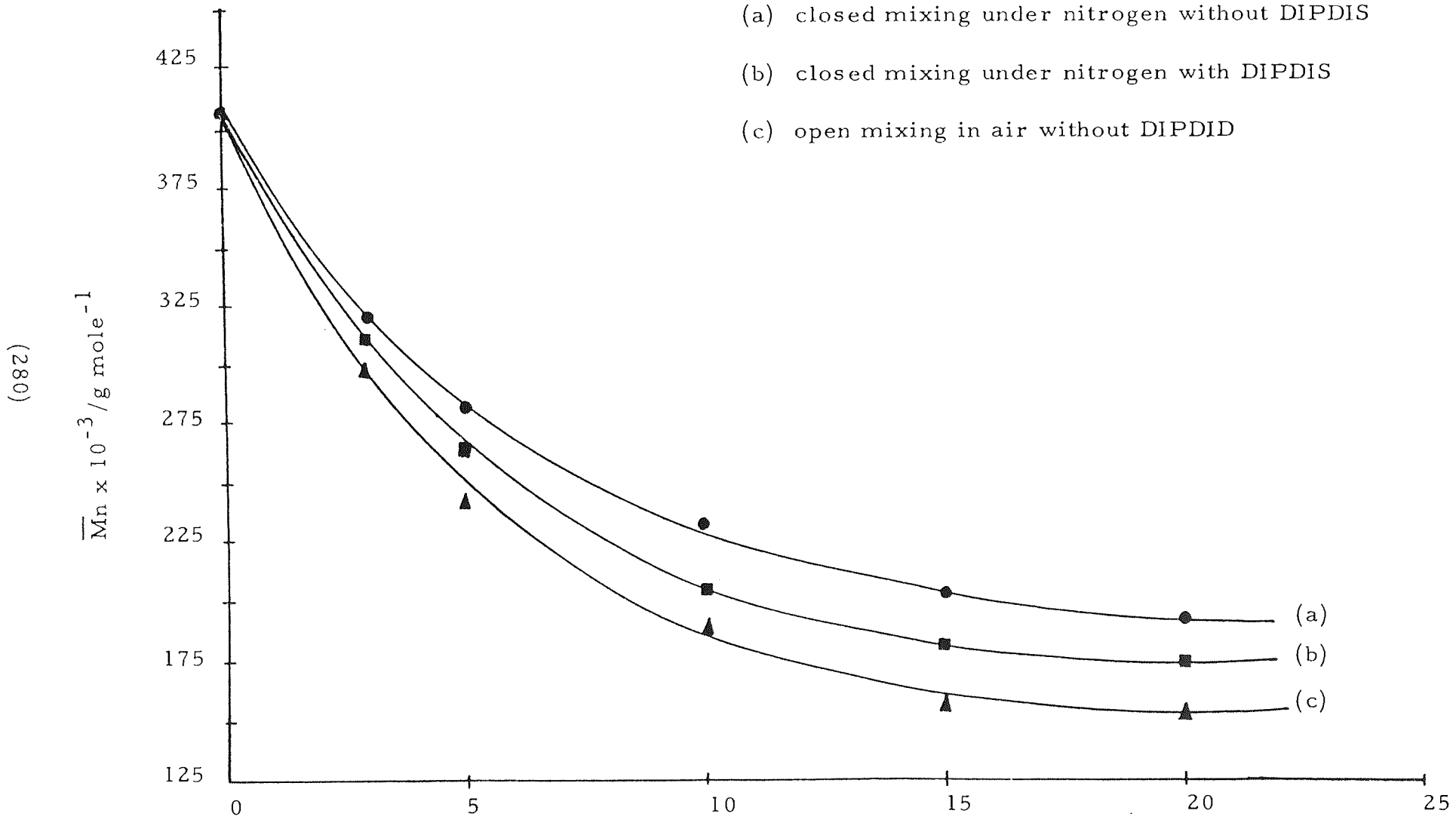

Fig 5.16 The dependence of $\overline{Mn}$ on the time of mastication in the vertical masticator ($\overline{Mn}$ estimated from intrinsic viscosity)

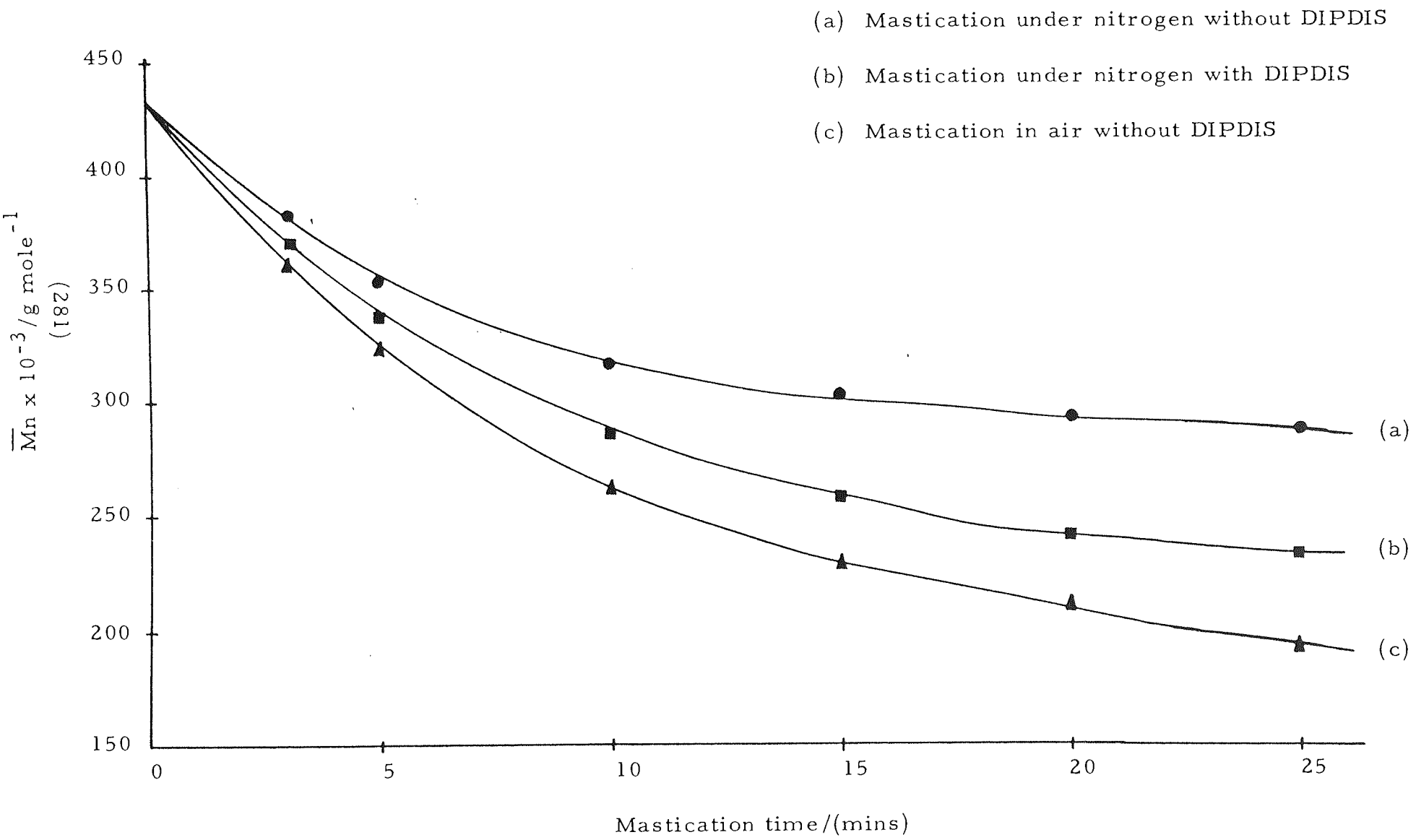

weight decreases during mastication with DIPDIS under nitrogen, are greater than those obtained when the rubber is masticated on its own in nitrogen but less than that obtained when masticated alone in air. The greater reduction in molecular weight of rubber during mastication under nitrogen in the presence of DIPDIS is presumably due to the radical acceptor activity of DIPDIS, resulting in the formation of active groups. The much greater reduction in $\overline{Mn}$ during mastication of rubber alone in an atmosphere of oxygen is obviously the result of the much greater radical acceptor activity of oxygen. Although the RAPRA torque rheometer reduces rubber to a lower molecular weight than the vertical masticator, due to the higher shear mixing possible, the radical acceptor efficiency of DIPDIS is higher in the vertical masticator than in the torque rheometer. This can be seen in the larger molecular weight decrease during mastication of rubber in the vertical masticator under nitrogen with DIPDIS, than when the rubber is masticated on its own under nitrogen. The greater activity of DIPDIS in the vertical masticator may be due to the total exclusion of oxygen made possible during mastication in this machine. Oxygen presumably competes with DIPDIS for available free rubber radicals in the torque rheometer, in which the total exclusion of oxygen is not possible.

Fig 5.17 shows the variation of $\overline{Mn}$ (estimated by GPC) with mastication time in the vertical masticator. The results are similar to

Fig 5. 17 The dependence of $\overline{Mn}$, estimated by GPC, on the time of mastication in the vertical masticator

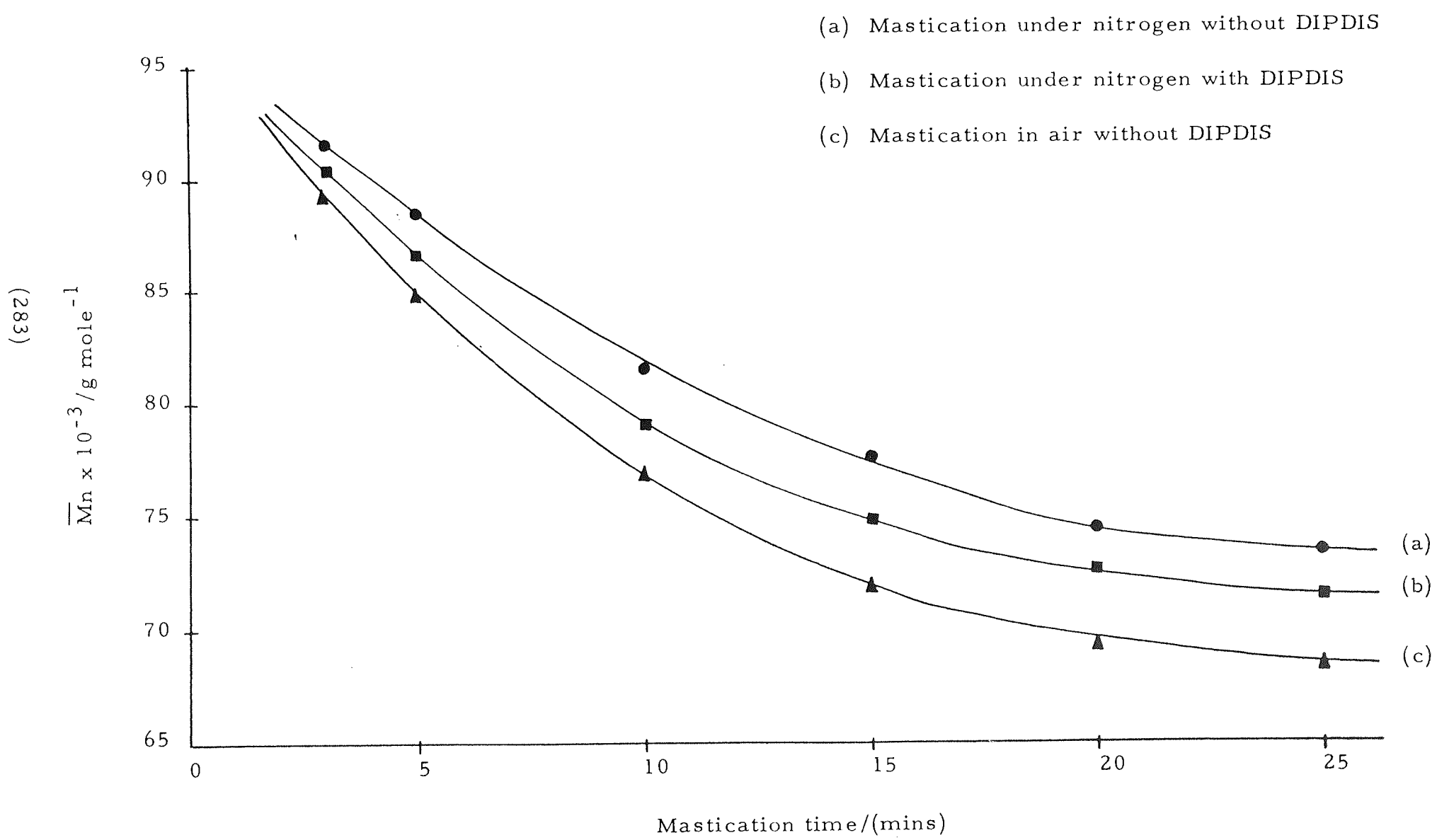

those obtained from intrinsic viscosity measurements, with $\overline{Mn}$ also decreasing as a function of time. However, the $\overline{Mn}$ values obtained were much lower than those obtained from intrinsic viscosity measurements. The use of viscosity to measure $\overline{Mn}$ is empirical and hence may show considerable errors which may depend on the molecular weight distribution. Fig 5.18 and 5.19 show the molecular weight distribution estimated by GPC during mastication of rubber under nitrogen with and without DIPDIS respectively. There is evidence of a shift to lower molecular weight in the presence of DIPDIS, and of the molecular weight distribution becoming narrower with increasing mastication time.

The observed radical acceptor activity of DIPDIS during mastication under nitrogen, resulting in the reduction of molecular weight of rubber, suggests that the rubber is modified by the formation of end groups. Table 5.3 illustrates the ability of these end groups to react with the rubber main chains to form crosslinks during vulcanisation resulting in an increase in the percentage of chain ends combined in the network. Vulcanisates prepared from the modified rubber are seen to have a higher C_1 value due to a reduced number of chain ends than those prepared from rubber masticated to the same molecular weight in air and vulcanised under identical conditions. The continued reaction of the end groups as vulcanisation

Fig 5.18 Molecular weight distribution (estimated by GPC) during mastication of NR with DIPDIS under nitrogen, in the vertical masticator

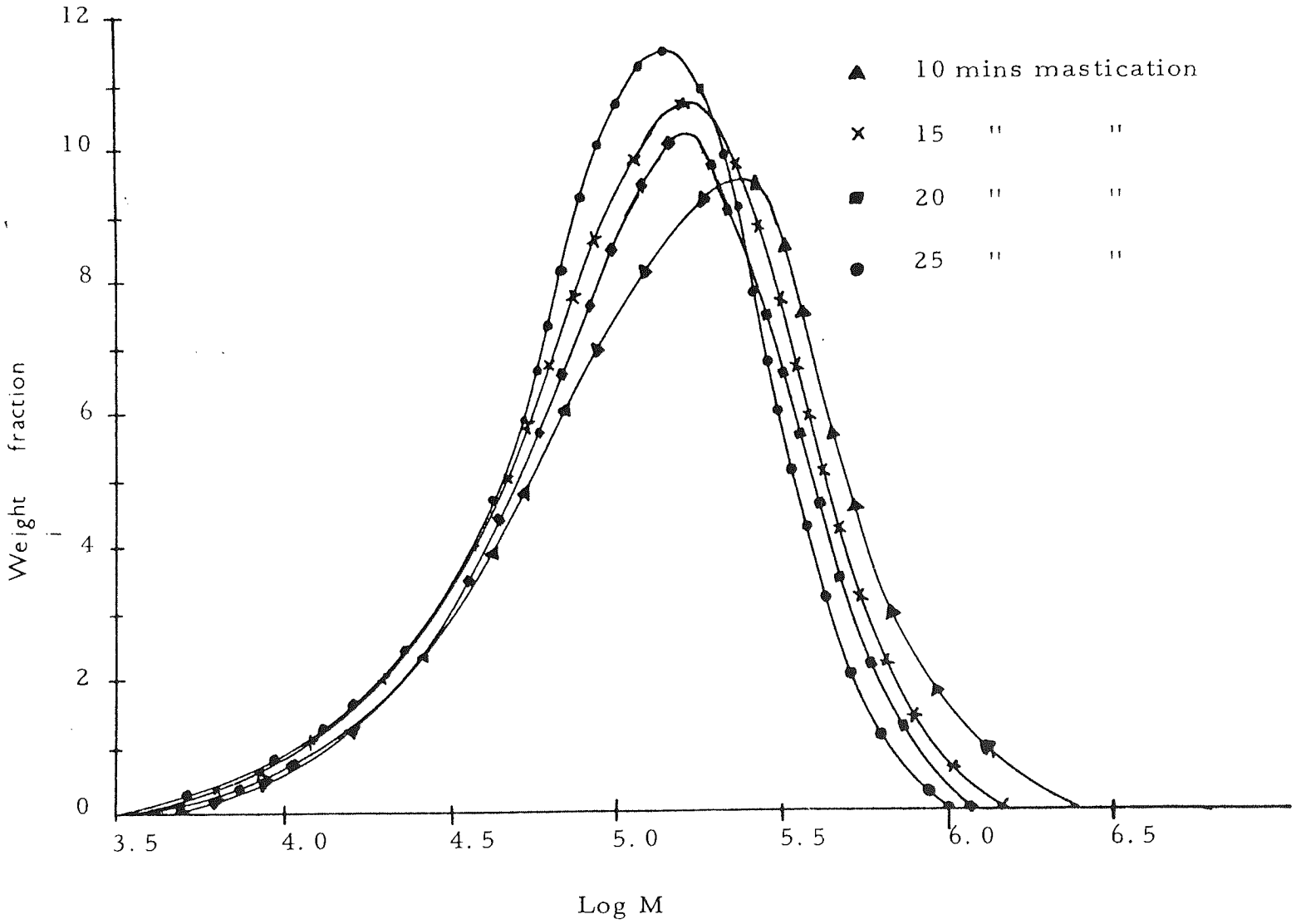

Fig 5.19 Molecular weight distribution (estimated by GPC) during mastication of NR alone under nitrogen, in the vertical masticator

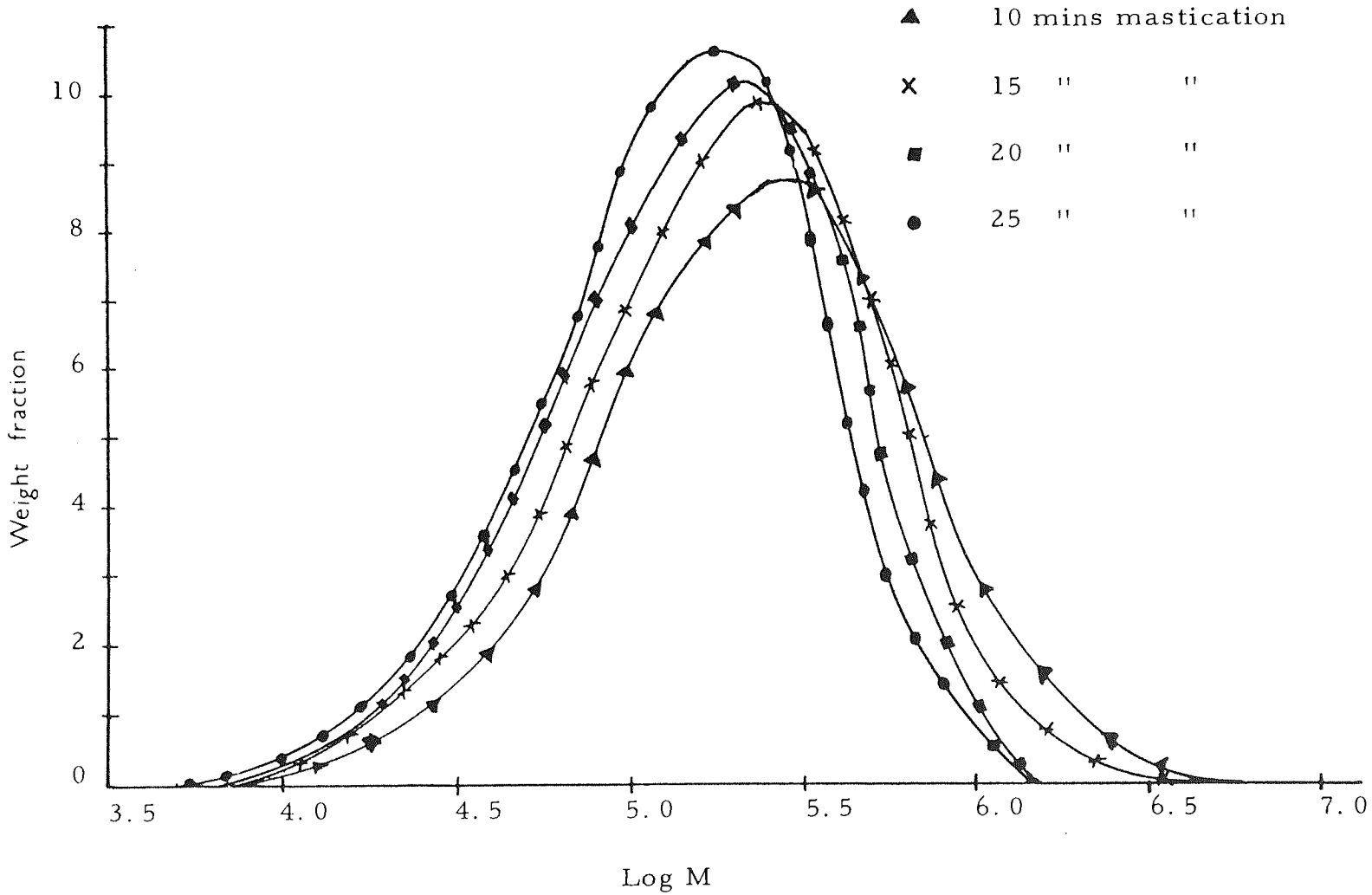

Table 5.3 Percentage of chain ends combined (%CEC) for rubber masticated with DIPDIS under nitrogen to an $\overline{Mn}$ = 166 Kg mole^{-1} and vulcanised at 140°C for different cure times.

	Cure time (mins)	$C_1 \times 10^{-5}$ Nm^{-2}	$\overline{M}_{c(phys)}$ Kg mole^{-1}	$\overline{M}_{c(chem)}$ Kg mole^{-1}	$\overline{Mn}'$ Kg mole^{-1}	%CEC
A(1)	10	0.9	12.7	22.1	221	25
N(2)	10	1.0				
A	20	1.25	9.1	14.5	243	31
N	20	1.35				
A	30	1.34	8.5	13.2	249	33
N	30	1.44				
A	40	1.32	8.6	13.5	260	36
N	40	1.43				
A	50	1.19	9.6	15.5	276	39
N	50	1.32				
A	60	1.16	9.8	16.0	288	42
N	60	1.30				

(1) mastication without DIPDIS in air

(2) mastication with DIPDIS in nitrogen

proceeded can be seen from the increase in the percentage of chain ends combined from 25 to 42 when the cure time was increased from 10 to 60 minutes.

The reduction in the concentration of free chain ends by mastication with DIPDIS resulted in a 9% improvement in the fatigue resistance of a vulcanisate cured for optimum cure time. The fatigue life of the vulcanisate with DIPDIS was 54.6 kilocycles and that without DIPDIS was 50.1 kilocycles. This improvement is less than would be expected for the calculated 57% increase in the value of initial molecular weight ($\overline{Mn}$) as a result of modification by DIPDIS to an apparent value of $\overline{Mn}'$. It should, however,be borne in mind, the chain scission which occurs during vulcanisation and which would effectively result in a lower value of $\overline{Mn}'$. The quantitative estimation of the percentage of chain ends combined was based on the assumption that two end groups are produced per rubber molecule during mastication. While this might be true for mastication in oxygen, mastication under nitrogen may lead to a branched structure. resulting in many end groups per molecule. If this is the case, the percentage of chain ends combined, quoted in Table 5.3, may not therefore be absolute.

CHAPTER SIX

CONCLUSIONS AND SUGGESTIONS FOR FURTHER WORK

6.1 Conclusions

It has been shown in this project that changes in vulcanisate networks occur when vulcanisates experience fatigue, either during a single extension or during continuous stressing. These changes include the following:

(i) a slight increase in the crosslink density,

(ii) a reduction in the concentration of polysulphide crosslinks,

(iii) an increase in the concentration of mono and disulphide crosslinks, with more new disulphide crosslinks than monosulphides being formed, and

(iv) main chain modifications may also be taking place.

It was suggested that these changes are due to mechanical and thermal effects associated with the applied stress.

The magnitude of the changes in vulcanisate networks is evidently greater during continuous fatigue than during application of a single extension. It was shown that a small but reproducible reduction in

polysulphide crosslinks occurred during a single extension, which appeared to be independent of the initial number average molecular weight of the rubber. The extent of the reduction in polysulphide crosslinks depended on the degree of extension, increasing with the degree of extension up to about 300% and then decreasing at higher extensions. It was shown that the decrease in the breakdown of polysulphide crosslinks occurred at the same extension at which there was a sudden rise in modulus. It was therefore suggested that the onset of crystallisation presumably reduced the rate of destruction of polysulphide crosslinks by redistribution of the stress. Clear evidence for changes in polysulphide crosslinks during stretching was also shown by the substantial reduction in set after probe treatment of conventional vulcanisates and it was suggested that the second network formed during stretching presumably comprised of polysulphide crosslinks.

While a reduction in polysulphide crosslink concentration of less than 4% was observed after a single extension of a conventionally cured vulcanisate, a reduction of about 16% in the concentration of polysulphide crosslinks was observed after fatiguing to failure. The magnitude of the change in vulcanisate networks during fatigue was clearly shown to be dependent on the number of fatigue cycles experienced. It was shown that although an increase in the number of fatigue cycles led to an increase in the percentage of polysulphide

crosslinks destroyed, the rate of polysulphide crosslink destruction decreased with increasing cycle time. It can be suggested that this was possibly due to the change in network distribution which led to a reduction in the net stress at higher fatigue time. It was also evident that while there was a reduction in the percentage concentration of polysulphide crosslinks after fatiguing, the concentration of mono and disulphide crosslinks increased, there being more new disulphide crosslinks formed than monosulphides. It was suggested that this was presumably due to the change of polysulphide crosslinks to form new mono, di and polysulphide crosslinks. The relative rates of formation of the different crosslinks during fatigue was considered to be dependent upon the stabilities of the sulphenyl free radicals formed. The higher rate of disulphide crosslink formation was considered to be the result of the much greater stability of the disulphenyl (RSS·) radical compared to the monosulphenyl (RS·) radical; this greater stability was due to the reduction in the energy of the radical due to the delocalisation of the unpaired electron over the unoccupied d orbitals of the adjacent sulphur atom in (RSS·). A slight decrease in the efficiency parameter, E, was observed after fatigue of a conventionally cured vulcanisate. Although a small increase in the value of E'-1, which gives a measure of main chain modification, suggests that main chain modification occurred during fatigue, the change observed was too small to be considered of any significance.

The presence of HAF black and antioxidants (IPPD and SWP) have been shown to influence the maturing process during vulcanisation and hence the nature of the final vulcanisate. The influence on the maturing process is attributable to the acidic or basic nature of these additives which affects the cure characteristics. An acidic additive such as SWP was shown to slightly retard vulcanisation rate while IPPD, which is basic in nature, slightly decreases the rate of vulcanisation. There was evidence to suggest that a reduction in the rate of polysulphide crosslink destruction occurred during fatigue of vulcanisates containing antioxidants, IPPD being more effective than SWP. The greater magnitude of the change observed in filled vulcanisate networks during continuous fatigue and on application of a single extension was the result of the higher strain energy input per cycle in the filled vulcanisate.

The investigations carried out in this project have shown that the initial molecular weight of rubber affected other physical properties such as tensile strength and resilience as well as fatigue; increasing the initial molecular weight of rubber caused the level of physical properties to rise. This has been explained on the basis of the final vulcanisate structure, which decreases in free chain end concentration and becomes more coherent with increasing initial molecular weight. The effect of initial molecular weight is also attributable to the internal viscosity of the rubber. It can be suggested that the

ability of a cut to propogate depends upon the ability of the broken rubber chain ends to separate, which will be a function of the internal viscosity of the rubber. The increase in fatigue life of a vulcanisate with increasing $\overline{Mn}$ may also be associated with the heat build-up which occurred during stressing, increasing as resilience decreased. It was evident that resilience increased with increase in $\overline{Mn}$. The rate of oxygen absorption during accelerated ageing of vulcanisates was shown to increase as the initial molecular weight of rubber decreased suggesting that the susceptibility of a vulcanisate with a low value of $\overline{Mn}$ to oxidation during fatigue, may be a factor contributing to its lower fatigue life.

It has been confirmed in this project that it is possible to terminate free rubber radicals produced during mastication of rubber under nitrogen with DIPDIS. The product is capable of further reaction during vulcanisation effectively tieing the loose chain ends into the network. It was shown that such a reduction in the concentration of free chain ends resulted in a 9% improvement in the fatigue resistance of the vulcanisate. Unfortunately, however, such a method of reduction in concentration of free chain ends is of limited practical application because the modification process involves mastication under anaerobic conditions, which precludes the use of open two roll mills and large internal mixers.

6.2 Suggestions for Further Work

(1) Studies could be carried out on the effect of more extensions, other than a single extension, on the changes in crosslink distribution of NR vulcanisates. It is possible that the redistribution of crosslinks after a single extension may affect the changes in network structure on subsequent extensions.

(2) Development of a method to assess the 'critical strain' required for the onset of crystallisation. Such a method could then be used to study the effect of chain irregularity (cis/trans content of NR) on critical strain for crystallisation and on fatigue resistance.

(3) Studies of the changes in vulcanisate networks of a non-crystallising rubber such as SBR or other synthetic rubbers. A comparison may then be made with the observed changes in NR vulcanisates during a single extension and in fatigue.

(4) Use may be made of an extruder as an anaerobic mixer to carry out radical acceptor reactions.

(5) Assessment of the improvements in properties of filled vulcanisates using DIPDIS and attempt to determine free chain end

concentrations. The filler itself may reduce free chain ends concentration because of the carbon gel effect.

(6) Investigate the possibility of producing vulcanisates with reduced entanglement contribution. This may lead to the production of more elastic vulcanisate networks.

APPENDIX ONE

COMPUTER PROGRAMS

Appendix 1-1 Treatment of the Moore, Mullins and Watson Equation to Derive $\overline{M}_{c(chem)}$

The equation is given by:

$$C_1 = \left[\frac{\rho RT}{2\overline{M}_{c(chem)}} + 0.78 \times 10^5\right]\left[1 - 2.3\frac{\overline{M}_{c(chem)}}{\overline{M}n}\right] Nm^{-2} \qquad (1)$$

where all terms are as described previously. $\overline{M}_{c(chem)}$ was derived by solving the above equation as follows:

Let $\overline{M}_{c(chem)} = X$, $\frac{\rho RT}{2} = A$, $0.78 \times 10^5 = B$ and $\frac{\overline{M}n}{2.3} = D$

Substituting in (1),

$$C_1 = \left(\frac{A}{X} + B\right)\left(1 - \frac{X}{D}\right) \qquad (2)$$

$$C_1 = \frac{A}{X} - \frac{AX}{DX} + B - \frac{BX}{D} \qquad (3)$$

$$C_1X = A - \frac{AX}{D} + BX - \frac{BX^2}{D} \qquad (4)$$

$$\frac{BX^2}{D} + C_1X + \frac{AX}{D} - BX - A = 0 \qquad (5)$$

$$\frac{BX^2}{D} + X\left(C_1 + \frac{A}{D} - B\right) - A = 0 \qquad (6)$$

(6) is a quadratic equation of the form

$$aX^2 + bX - c = 0 \qquad (7)$$

$$X = \frac{-b \pm \sqrt{b^2 - 4ac}}{2a} \qquad (8)$$

where $a = \frac{B}{D}$, $b = (C_1 + \frac{A}{D} - B)$ and $c = -A$

X or $M_{c(chem)}$ was obtained from C_1 by writing a computer program based on (8). The negative root was rejected as C_1 is always positive.

Appendix 1-2 Program for the evaluation of initial number average molecular weight ($\overline{Mn}$) of rubber from intrinsic viscosity data.

```
LIST

1  HOME
2  INPUT "SAMPLE NUMBER ";SN
10  HOME
20  INPUT "                        TO = ";O
30  INPUT "                         K = ";K
40  INPUT "                     ALPHA = ";A
50  INPUT " NUMBER OF SETS OF DATA = ";Z
55  PRINT : PRINT
57  PR# 2
58  PRINT "SAMPLE NUMBER ";SN
59  PRINT : PRINT
60  PRINT "               VISCOSITIES"
65  PRINT "RELATIVE        SPECIFIC        REDUCED"
70  READ D:T = D
80  READ D:C = D
90 RV = T / O:RV =  INT (RV * 1000 + .5) / 1000
100 SV = RV - 1:SV =  INT (SV * 1000 + .5) / 1000
110 Y = (RV - 1) / C:Y =  INT (Y * 1000 + .5) / 1000
120  PRINT RV,SV,Y
130 B = B + Y
140 U = U + Y ↑ 2
150 E = E + C
160 F = F + C ↑ 2
170 G = G + Y * C
180 H = B * E
190 J = B ↑ 2
200 L = F ↑ 2
210 N = N + 1
220  IF Z > N GOTO 70
230 SX =  SQR ((F - L / Z) / (Z - 1))
240 SY =  SQR ((U - J / Z) / (Z - 1))
250 M = (G - H / Z) / (F - L / Z)
260 I = (B - M * E) / Z:I =  INT (I * 1000 + .5) / 1000
270 R = M * SX / SY
280 MO = (I / K) ↑ (1 / A)
290 MO =  INT (MO * 1000 + .5) / 1000
300  PRINT : PRINT
320  PRINT "      INTRINSIC VISCOSITY = "I
330  PRINT "VISCOSITY AVERAGE MOL.WT. = "MO
340  PRINT "  CORRELATION COEFFICIENT = ";R
350  RESTORE
360  PRINT : PRINT
370  PRINT "VALUES OF T     VALUES OF C"
380 N = 0
390  READ D:P = D
392  READ D:Q = D
394  PRINT P,Q
396 N = N + 1
398  IF Z > N GOTO 390
399  END
400  DATA  87.2,.32,75.5,.21,70.4,.16,67.2,.13,64,.09
500  PR# 0
```

Appendix 1-3 Program for the evaluation of C_1, $\overline{M}_{c(phys)}$, $\overline{M}_{c(chem)}$ and crosslink densities from swollen compression data

```
LIST

10  HOME
20  INPUT "SAMPLE NUMBER ";SN
30  PR# 2
40  PRINT "80N";
50  PRINT "SAMPLE NUMBER = ";SN
60  PR# 0
70  HOME
80  PRINT : PRINT : PRINT : PRINT
90  INPUT "ORIGINAL X-SECT AREA(CM↑2)=";AO
100  PRINT
110  INPUT "ORIGINAL HEIGHT(CM)=";HO
120  PRINT
130 N = 12
140  INPUT "  AT 50 GRAMMES,LOADING STRAIN = ";X
150 Y = 50
160  GOSUB 1040
170  INPUT "           AND UNLOADING STRAIN = ";X
180  GOSUB 1040
190  PRINT
200  INPUT " AT 100 GRAMMES,LOADING STRAIN = ";X
210 Y = 100
220  GOSUB 1040
230  INPUT "           AND UNLOADING STRAIN = ";X
240  GOSUB 1040
250  PRINT
260  INPUT " AT 150 GRAMMES,LOADING STRAIN = ";X
270 Y = 150
280  GOSUB 1040
290  INPUT "           AND UNLOADING STRAIN = ";X
300  GOSUB 1040
310  PRINT
320  INPUT " AT 200 GRAMMES,LOADING STRAIN = ";X
330 Y = 200
340  GOSUB 1040
350  INPUT "           AND UNLOADING STRAIN = ";X
360  GOSUB 1040
370  PRINT
380  INPUT " AT 250 GRAMMES,LOADING STRAIN = ";X
390 Y = 250
400  GOSUB 1040
410  INPUT "           AND UNLOADING STRAIN = ";X
420  GOSUB 1040
430  PRINT
440  INPUT " AT 300 GRAMMES,LOADING STRAIN = ";X
450 Y = 300
460  GOSUB 1040
470  INPUT "           AND UNLOADING STRAIN = ";X
480  GOSUB 1040
481  INPUT "ARE YOUR VALUES CORRECT? Y/N  ";D$
482  IF D$ = "Y" GOTO 490
483  GOSUB 2000
484  GOTO 70
490 G = R * C
500 J = C ↑ 2
```

```
510 K = B ↑ 2
520 SY =  SQR ((H - K / N) / (N - 1))
530 SX =  SQR ((E - J / N) / (N - 1))
540 M = (D - G / N) / (E - J / N)
550 P = M * SX / SY:P =  INT (P * 1000 + .5) / 1000
560 C1 = M * HO / 6 / AO * 98.0556 / 1.67E - 4:C1 =  INT (C1 / 100 + .5) *
    100
570  PR# 2
580  PRINT : PRINT
590  PRINT "       C1 = ";C1;"  NEWTONS/M↑2"
600  PRINT "    CORRELATION COEFF.=";P
610  PR# 0
620  PRINT : PRINT
630  INPUT "           DENSITY(G./CM↑-3) =";DE
640 R = 8.31434
645  PRINT : PRINT : PRINT
650  INPUT " TEMPERATURE (DEGREES C) = ";T
655  PRINT : PRINT : PRINT
660  INPUT "INITIAL MOLECULAR WEIGHT(KG/MOL)<NORMAL M.WT/1000>=";MN
670 T = T + 273
680 MC = DE * R * T / 2 / C1 * 1000:MT =  INT (MC * 1000 + .5) / 1000
690  PRINT : PRINT
700  PR# 2
710  PRINT "      MC(PHYS)=";MT;"  KG/MOL"
720 CL = 1 / 2 / MC:CD =  INT (CL * 1000 + .5) / 1000
730  PRINT "  CLD(PHYS)=";CD;" MOL/KG"
740 B = DE * R * T * 10 ↑ 3 / 2 / MN * 2.3 - .78E5 + C1
750 A = .78E5 / MN * 2.3
760 C =  - DE * R * T * 10 ↑ 3 / 2
770 D = ( - B +  SQR (B ↑ 2 - 4 * A * C)) / 2 / A
780 E = ( - B -  SQR (B ↑ 2 - 4 * A * C)) / 2 / A
790 F =  INT (D * 1000 + .5) / 1000
800 G =  INT (E * 1000 + .5) / 1000
810  IF F < 0 THEN  GOTO 830
820  PRINT "    MC(CHEM)=";F;"KG./MOL"
830  IF G < 0 THEN  GOTO 850
840  PRINT "   MC(CHEM)= ";G;"KG/MOL"
850 CL = 1 / 2 / D:CD =  INT (CL * 1000 + .5) / 1000
860  IF CL < 0 THEN  GOTO 880
870  PRINT "   CLD(CHEM)= ";CD;"MOL/KG"
880 CL = 1 / 2 / E:CD =  INT (CL * 1000 + .5) / 1000
890  IF CL < 0 THEN  GOTO 910
900  PRINT "   CLD(CHEM)= ";CD;"MOL/KG"
910  PRINT : PRINT : PR# 0
911  INPUT "DO YOU WISH TO CALCULATE CHI? Y/N"A$
912  IF A$ = "Y" GOTO 920
913  INPUT "DO YOU WISH TO CALC C1 FOR ANOTHER SAMPLE? Y/N";B$
914  IF B$ = "N" GOTO 1030
915  GOSUB 2000
916  GOTO 10
920  INPUT "SOLVENT MOLAR VOL(M↑3/G.MOL)=";VO
```

```
930  INPUT "         DESWOLLEN WEIGHT = ";WR
940  INPUT "           SOLVENT WEIGHT = ";WS
950  INPUT "          SOLVENT DENSITY = ";DS
960 V = WR / DE / (WR / DE + WS / DS)
970 X =  - ( LOG (1 - V) + V + 2 * C1 * VO / R / T *(V ↑ (1 / 3)) / V ↑
     2
980 Y =  INT (X * 1000 + .5) / 1000
990  PRINT : PRINT
1000  PR# 2
1010  PRINT "                        CHI = ";Y
1020  PR# 0
1021  INPUT "DO YOU WISH TO CALC C1 ETC. FOR ANOTHER S
     AMPLE? Y/N";C$
1022  GOSUB 2000
1025  IF C$ = "Y" GOTO 10
1030  END
1040 W = Y ↑ 2
1050 V = X ↑ 2
1060 B = B + Y
1070 C = C + X
1080 D = D + Y * X
1090 E = E + V
1100 H = H + W
1110  RETURN
2000 W = 0
2010 V = 0
2020 B = 0
2030 C = 0
2040 D = 0
2050 E = 0
2060 H = 0
2070  RETURN
```

Appendix 1-4 Program to evaluate $\overline{M}_{c(phys)}$, $\overline{M}_{c(chem)}$ and crosslink densities directly from C_1 data

```
]LIST

 50  TEXT
 60  HOME
 70  GOSUB 2000
 80  PRINT "PROGRAM TO EVALUATE MC,CHEM FROM C1 DATA "
 90  GOSUB 3000
100  HOME
105  GOSUB 2000
110  INPUT "TEMPER                TURE OF DETERMINATION=";T
120 T = T + 273
125  GOSUB 2000
130  INPUT "DENSITY OF RUBBER=";DE
140 RH = DE * 1000
145  GOSUB 2000
150  INPUT "NO AVERAGE M. WT.OF RUBBER=";M
152  PRINT "SAMPLE NO.="
153  INPUT L
154  PR# 2
156  GOSUB 2000
156  PRINT "SAMPLE NO.=";L
158  PR# 0
160  INPUT "VALUE OF C1(N.M↑-2) =";C
162  PR# 2
164  PRINT "C1=";C
165  PR# 0
166  PR# 0
170 R = 8.314
180 A = RH * R * T / 2
190 B = .78 * 10 ↑ 5
200 D = M / 2.3
210 E = A - (D * (B - C))
220 F = A * B * D
230 X1 = ( - E + (E ↑ 2 + (4 * F)) ↑ .5) / (2 * B)
240 X2 = ( - E - (E ↑ 2 + (4 * F)) ↑ .5) / (2 * B)
250 D1 = 1 / (2 * X1)
255 D1 =  INT ((D1 * 10 ↑ 5) + .5) / 100000
260 D2 = 1 / (2 * X2)
265 D2 =  INT ((D2 * 10 ↑ 5) + .5) / 100000
270  IF X1 < 0 GOTO 330
280  PR# 2
290  PRINT "MC.-CHEM.(KG./MOLE)="; INT (X1 * 1000) / 1000
```

```
310  PRINT "CLD.-CHEM.(MOLE/KG.)=";D1
320  PR# 0
322 J = RH * R * T / (2 * C)
323 K = 1 / (2 * J)
324  PR# 2
325  PRINT "MC.-PHYS.(KG./MOLE)="; INT (J * 1000 + .5) / 1000
326  PRINT "CLD.-PHYS.(MOLE/KG.)="; INT (K * 100000 + .5) / 100000
327  PR# 0
330  IF X2 < 0 GOTO 390
340  PR# 2
350  PRINT "MC.-CHEM.(KG./MOLE)="; INT (X2 * 1000) / 1000
370  PRINT "CLD.-CHEM.(MOLE/KG.)=";D2
380  PR# 0
382 J = RH * R * T / (2 * C)
383 K = 1 / (2 * J)
384  PR# 2
385  PRINT "MC.-PHYS.(KG./MOLE)="; INT (J * 1000 + .5) / 1000
386  PRINT "CLD.-PHYS.(MOLE/KG.)="; INT (K * 100000 + .5)100000
387  PR# 0
390  PRINT "DO YOU HAVE ANY MORE CALCULATIONS TO MAKE? Y/N"
400  INPUT A$
410  IF A$ = "Y" GOTO 152
420  END
2000  FOR Z = 1 TO 5
2010  PRINT
2020  NEXT Z
2030  RETURN
3000  FOR Y = 1 TO 5000
3010  NEXT Y
3020  RETURN
```

Appendix 1-5 Program for the evaluation of V_r, $\overline{M}_{c(phys)}$, $\overline{M}_{c(chem)}$ and crosslink densities from equilibrium volume swelling data

```
]LIST

1  HOME
3  INPUT "DENSITY OF RUBBER = ";DE
5  INPUT "DENSITY OF SOLVENT = ";DS
7  INPUT "CHI = ";K
9  INPUT "MOLAR VOLUME = ";VO
11  INPUT "VOLUME FRACTION OF RUBBER NETWORK        (VRN) = ";V
13  INPUT "VOLUME FRACTION OF RUBBER HYDROCARBON    (VRH) = ";H
15  INPUT "VOLUME FRACTION OF NON-REINFORCING      FILLER = ";F
17  INPUT "TEMPERATURE (DEG C) = ";T
18 T = T + 273
19  INPUT "NUMBER AVERAGE MOL.WT.= ";MN
21  INPUT "VOLUME FRACTION OF HAF-BLACK = ";U
22  INPUT "VOLUME FRACTION CORRECTION FACTOR = ";W
23  INPUT "SAMPLE NUMBER ";SN
25  PRINT "40N";
27  PR# 2
29  HOME
31  PRINT "SAMPLE NUMBER = ";SN
33  PR# 0
35  INPUT "WEIGHT OF DESWOLLEN RUBBER = ";WR
37  INPUT "WEIGHT OF SOLVENT = ";WS
70 VA = WR / DE / (WR / DE + WS / DS) * W
80 V1 =  INT (VA * 10000 + .5) / 10000
85  PR# 2
90  PRINT "VR = ";V1
91  PR# 0
102 R = 8.3143
104 A =  LOG (1 - VA) + VA + K * VA ↑ 2
110 B = V ↑ (1 / 3) * (1 - F) ↑ (2 / 3) * R * T
120 C = 2 * VO * H * VA ↑ (1 / 3)
130 D =  - A * B / C
140 E =  INT (D)
145  PR# 2
150  PRINT "C1-RH(N/M↑2) =";E
155  PR# 0
165 X = 10 ↑ 3 * DE * R * T / 2
170 Y = .78E5
180 Z = MN / 2.3
190 A = Y / Z
200 B = D + X / Z - Y
210 C =  - X
220 Q1 = ( - B +  SQR (B ↑ 2 - 4 * A * C)) / 2 / A
230 Q2 = ( - B -  SQR (B ↑ 2 - 4 * A * C)) / 2 / A
235 Q3 =  INT (Q1 * 10000 + .5) / 10000:Q4 =  INT (Q2 * 10000 + .5) / 1000
    0
```

```
237  PR# 2
240  PRINT "MC.CHEM-RH(KG/MOLE)=";Q3
245  IF Q4 < 0 GOTO 260
250  PRINT "MC CHEM-RH = ";Q4
260 C2 = 1 / 2 / Q3:C3 =  INT (C2 * 100000 + .5) / 100000
270  PRINT "CLD CHEM-RH(MOLE/KG)=";C3
275  PR# 0
290 U1 = C2 / (1 + 3.63 * U):U2 =  INT (U1 * 100000 + .5) / 100000
295  PR# 2
300  PRINT "CLD CHEM(ACTUAL) = ";U2
310 MC = 10 ↑ 3 * DE * R * T / 2 / E
320 CL = 1 / 2 / MC
330 CA = CL / (1 + 2.6 * U)
340 M =  INT (MC * 10000 + .5) / 10000
350 L =  INT (CL * 100000 + .5) / 100000
360 A =  INT (CA * 100000 + .5) / 100000
370  PRINT "MC PHYS(KG/MOLE)=";M
380  PRINT "CLD PHYS(MOLE/KG)=";L
390  PRINT "CLD PHYS (ACTUAL) = ";A
392  PRINT : PRINT
400  GOTO 23
```

Appendix 1-6 Program for the evaluation of $\overline{M}_{c(phys)}$, $\overline{M}_{c(chem)}$ and crosslink densities directly from V_r data

```
]LIST

10  HOME
20  REM  TO CALCULATE MC-CHEM FROM VR VALUES
30  INPUT " CHI =";K
40  INPUT " TEMPERATURE(DEG.C)=";T
50 T = T + 273
60  INPUT "MOLAR VOLUME OF SOLVENT(M↑3)=";V0
70  INPUT "NUMBER AVERAGE MOL.WT.(KG/MOLE)=";MN
80  INPUT "DENSITY OF RUBBER(G/CC)=";DE
90  INPUT "VOLUME FRACTION OF RUBBER NETWORK(VRN)=";V
100  INPUT "VOLUME FRACTION OF RUBBER HYDROCARBON(VRH)=";H
120  INPUT "VOLUME FRACTION OF CARBON-BLACK=";U
130  INPUT "VOLUME FRACTION OF NON-REINFORCING FILLER=";F
140  INPUT "VOLUME FRACTION CORRECTION FACTOR=";W
150  INPUT "SAMPLE NUMBER=";SN
160  PRINT "40N";
170  PR# 2
180  HOME
190  PRINT "SAMPLE NUMBER=";SN
200  PR# 0
210  INPUT "VOLUME FRACTION OF RUBBER VULCANIZATE(VR)=";VA
220 VA = VA * W
230  PR# 2
240  PRINT "VR =";VA
250  PR# 0
260 R = 8.3143
270 A =  LOG (1 - VA) + VA + (K * VA ↑ 2)
280 B = V ↑ (1 / 3) * (1 - F) ↑ (2 / 3) * R * T
290 C = 2 * V0 * H * VA ↑ (1 / 3)
300 D =  - A * B / C
310 E =  INT (D)
320  PR# 2
330  PRINT "C1(N/M↑2) =";D
340  PR# 0
350 X = 10 ↑ 3 * DE * R * T / 2
360 Y = .78E5
370 Z = MN / 2.3
380 A = Y / Z
390 B = D + X / Z - Y
400 C =  - X
410 Q1 = ( - B +  SQR (B ↑ 2 - 4 * A * C)) / 2 / A
420 Q2 = ( - B -  SQR (B ↑ 2 - 4 * A * C)) / 2 / A
```

```
430 Q3 =  INT (Q1 * 10000 + .5) / 10000:Q4 =  INT (Q2 * 10000 + .5) / 1000
    0
440  PR# 2
450  PRINT "MC.-CHEM.(KG/MOLE)=";Q3
460  IF Q4 < 0 GOTO 480
470  PRINT "MC.-CHEM.(KG/MOLE)=";Q4
480 C2 = 1 / 2 / Q3:C3 =  INT (C2 * 100000 + .5) / 100000
490  PRINT "CLD.-CHEM(MOLE/KG)=";C3
500  PR# 0
510 U1 = C2 / (1 + 3.63 * U):U2 =  INT (U1 * 100000 + .5) / 100000
520  PR# 2
530  PRINT "CLD.-CHEM.(ACTUAL)=";U2
540 MC = 10 ↑ 3 * DE * R * T / 2 / E
550 CL = 1 / 2 / MC
560 CA = CL / (1 + 2.6 * U)
570 M =  INT (MC * 10000 + .5) / 10000
580 L =  INT (CL * 100000 + .5) / 100000
590 A =  INT (CA * 100000 + .5) / 100000
600  PRINT "MC.-PHYS.(MOLE/KG)=";M
610  PRINT "CLD.-PHYS(MOLE/KG)=";L
620  PRINT "CLD.-PHYS.(ACTUAL)=";A
630  PRINT : PRINT
640  GOTO 150
```

Appendix 1-7 Program for the evaluation of the number of crosslinks broken per unit volume and the recombination efficiency, from equilibrium volume swelling and set data

```
]LIST

2  INPUT "SAMPLE NUMBER ";SN
3  PR# 2
4  PRINT "80N";
5  HOME
6  PRINT "SAMPLE NUMBER = ";SN
8  PR# 0
10  INPUT "WEIGHT OF DESWOLLEN RUBBER 1 = ";WR
20  INPUT "DENSITY OF RUBBER = ";DE
30  INPUT "WEIGHT OF SOLVENT 1 = ";WS
40  INPUT "DENSITY OF SOLVENT = ";DS
50  INPUT "CHI = ";K
60  INPUT "MOLAR VOLUME = ";VO
70 VA = WR / DE / (WR / DE + WS / DS)
80 V1 =  INT (VA * 1000 + .5) / 1000
85  PR# 2
90  PRINT "VR 1 = ";V1
100 M = DE * 1E3 * VO * (VA ↑ (1 / 3) - VA / 2) / (K * VA ↑ 2 +  LOG (1 -
     VA) + VA)
105 M =  - M
110 MC =  INT (M * 1000 + .5) / 1000
120  PRINT "1MC(PHYS) = ";MC
130 C = 1 / 2 / M
140 CL =  INT (C * 1000 + .5) / 1000
145  PRINT "1CLD = ";CL
147  PR# 0
150  INPUT "WEIGHT OF DESWOLLEN RUBBER 2 = ";WR
160  INPUT "WEIGHT OFSOLVENT 2 = ";WS
180 VB = WR / DE / (WR / DE + WS / DS)
190 V2 =  INT (VB * 1000 + .5) / 1000
195  PR# 2
200  PRINT "2VR = ";V2
210 M = DE * 1E3 * VO * (VB ↑ (1 / 3) - VB / 2) / (K * VB ↑ 2 +  LOG (1 -
     VB) + VB)
220 M =  - M
230 MC =  INT (M * 1000 + .5) / 1000
240  PRINT "2MC(PHYS) = ";MC
250 C = 1 / 2 / M
260 CL =  INT (C * 1000 + .5) / 1000
270  PRINT "2CLD = ";CL
275  PR# 0
305  INPUT "LAMBDA NOUGHT = ";B
310  INPUT "LAMBDA DASHED = ";C
330  PRINT
335 A = (B ↑ 3 - 1) / (C - B ↑ 3 / C ↑ 2):A1 =  INT (A * 1000 + .5) / 1000
```

```
337  PR# 2
340  PRINT "UNBROKEN CROSS-LINKS REFORMED = ";A1
345  PRINT
350 G = (VA / VB) ↑ (1 / 3)
355 H = ( LOG (1 - VB) + VB + k * VB ↑ 2) / ( LOG (1 - VA) + VA + k * VA ↑
    2)
360 I = 1 / ((1 + A * C) ↑ 2 * (1 + A / C ↑ 2)) ↑ (1 / 3)
365 X = G * H * I:X1 =  INT (X * 1000 + .5) / 1000
370  PRINT "          UNBROKEN CROSS-LINKS = ";X1
375  PRINT
380 Y = 1 - X:Y1 =  INT (Y * 1000 + .5) / 1000
385  PRINT "            BROKEN CROSS-LINKS = ";Y1
390  PRINT
395 Z = A * (1 - Y) / Y:Z1 =  INT (Z * 1000 + .5) / 1000
400  PRINT "       RECOMBINATION FRACTION = ";Z1
405  PRINT
410 Z = Z * 100:Z2 =  INT (Z * 1000 + .5) / 1000
415  PRINT "     RECOMBINATION EFFICIENCY = ";Z2
420  PR# 0
```

Appendix 1-8 Program to calculate broken and unbroken crosslinks directly from V_r and set data

```
]LIST

10  REM  TO CALCULATE BROKEN AND UNBROKEN CROSSLINKS FROM SET DATA
20  INPUT "SAMPLE NUMBER=";SN
25  PRINT : PRINT : PRINT
30  PR# 2
35  PRINT "SAMPLE NUMBER=";SN
40  PR# 0
50  INPUT "LAMBDA NOUGHT=";B
60  INPUT "LAMBD DASHED=";C
70  INPUT "VOLUME FRACTION OF SWOLLEN UNSTRETCHED RUBBER=";V1
80  INPUT "VOLUME FRACTION OF SWOLLEN STRETCHED RUBBER=";V2
90  INPUT "CHI=";K
100  PR# 2
110  PRINT "LAMBDA NOUGHT=";B
120  PRINT "LAMBDA DASHED="C
130  PRINT "V1=";V1
140  PRINT "V2=";V2
150  PR# 0
160 AL = (B ↑ 3 - 1) / (C - (B ↑ 3 * C ↑  - 2))
170 D = (V1 / V2) ↑ (1 / 3)
180 E = ( LOG (1 - V2) + V2 + (K * V2 ↑ 2)) / ( LOG (1 - V1) + V1 + (K * V
    1 ↑ 2))
190 F = ((1 + (AL * C)) ↑ 2 * (1 + (AL / (C ↑ 2)))) ↑  - (1 / 3)
200 G = D * E * F
210  REM  G = 1-N1/N (FRACTION OF UNBROKEN CROSS-LINKS)
220 H = 1 - G
230  REM  H = N1/N (FRACTION OF CROSS-LINKS BROKEN)
240  REM  ALPHA = (NO. OF CROSS-LINKS REFORMED/NO. UNBROKEN BY STRESS)
250  REM  ALPHA = N2/(N-N1)
260 J = AL * G / H
270  REM  J = N2/N1 (RECOMBINATION FRACTION)
280 L =  INT (J * 100000 + 0.5) / 1000
290  REM  L = %RECOMBINATION FRACTION
300  PR# 2
310  PRINT "ALPHA="; INT (AL * 1000 + .5) / 1000
320  PRINT "FRACTION OF CROSS-LINKS UNBROKEN="; INT (G * 1000 + 0.5) / 100
    0
330  PRINT "FRACTION OF CROSS-LINKS BROKEN="; INT (H * 1000 + 0.5) / 1000
340  PRINT "FRACTION OF BROKEN CROSS-LINKS REFORMING NEW X-LINKS="; INT (J
     * 1000 + 0.5) / 1000
350  PRINT "RECOMBINATION EFFICIENCY=";L
355  PRINT : PRINT : PRINT
360  PR# 0
380  PRINT "DO YOU WISH TO CONTINUE? Y/N
390  INPUT A$
400  IF A$ = "Y" GOTO 20
410  END
```

Appendix 1-9 Program to evaluate modified $\overline{M}n$ ($\overline{M}n'$) and the percentage of free chain ends combined, from change in C_1 data

```
LIST

10  REM  TO CALCULATE COMBINED FR
     EE CHAINENDS FROM C1 DATA
20  INPUT "SAMPLE NUMBER=";SN
30  PR# 2
40  PRINT "SAMPLE NUMBER=";SN
50  PR# 0
60  INPUT "ORIGINAL C1=";B
70  IPUT "MODIFIED C1=";C
80  INPUT "ORIGINAL NO. AVERAGE M
     OL.WT.=";D
90  INPUT "MC.-CHEM=";E
100  PR# 2
110  PRINT "ORIGINAL C1=";B
120  PRINT "MODIFIED C1=";C
130  PRINT "ORIGINAL MN=";D
140  PRINT "MC.-CHEM.  =";E
150  PRINT
160  PR# 0
170 F = (2.3 * E * R * D) / (B *
     (B - C) + (2.3 * E * C)
180 G = (1 - (D / F)) * 100
190  REM  F=MODIFIED NO. AVERAGE
     MOL.WT.
200  REM  G=COMBINED CHAIN ENDS(%
     )
210  PR# 2
220  PRINT "MODIFIED MN
      =";INT (F)
230  PRINT "COMBINED CHAIN ENDS(%
     )=";INT (G * 100 + .5) / 10
     0
235  PRINT : PRINT
240  PR# 0
250  PRIN "DO YOU WISH TO CONTIN
     UE?Y/N"
260  INPUT A$
270  IF A$ = "Y" GOTO 20
280  END
```

APPENDIX TWO

SCANNING ELECTRON MICROSCOPE (SEM) MICROGRAPHS

Appendix 2-1 SEM micrographs of HAF-black filled vulcanisates prepared using the fixed mixing cycle (designed for similar filler dispersion)

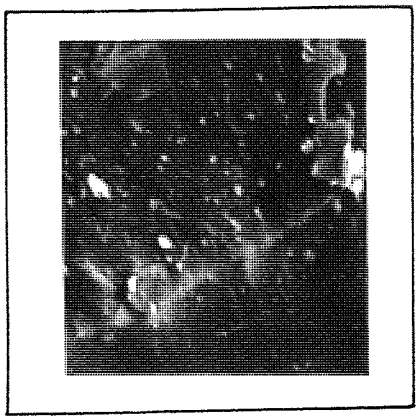

(a)

a, b, c and d were milled for the same time (2 minutes) on the mill after the mixing cycle in the Banbury.

(b)

(c)

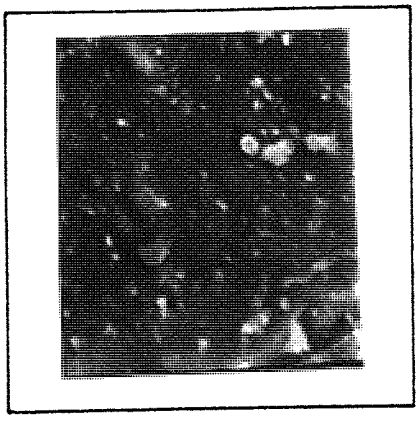

(d)

Appendix 2-2 SEM micrographs of HAF-black filled vulcanisates prepared using the variable mixing cycle (designed for varying filler dispersion)

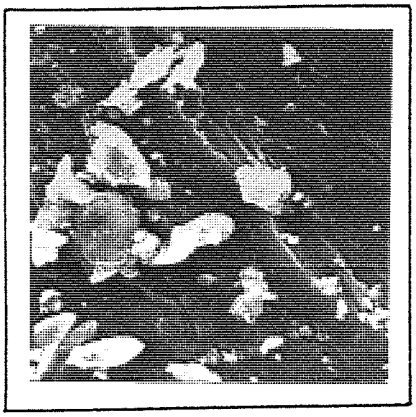

(a) 4 minutes milling

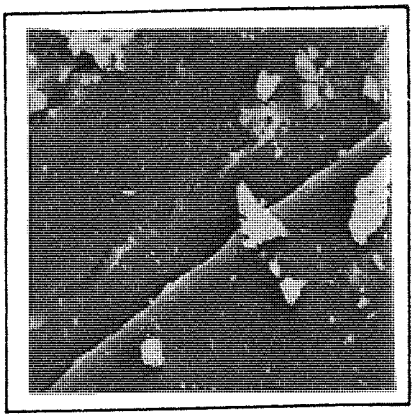

(b) 8 minutes milling

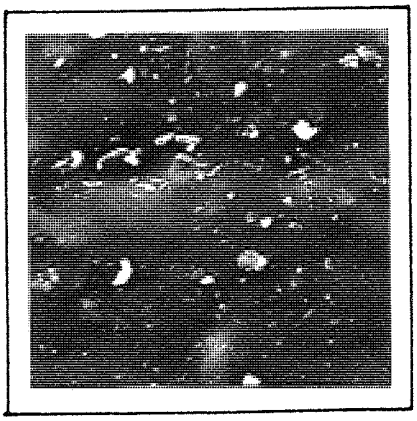

(c) 12 minutes milling

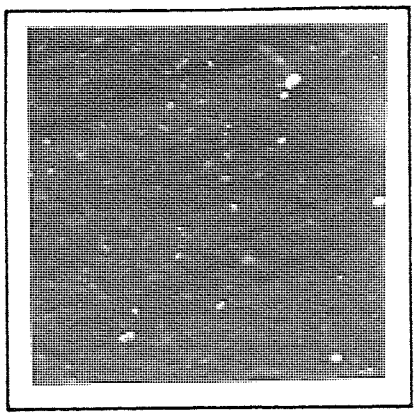

(d) 30 minutes milling

REFERENCES

1. S T Semegen, Chapt in 'Rubber Technology' (Ed M Morton) Van Nostrand Reinhold, New York (1973) P 152
2. C D Harries, 'Untersuchungen uber die naturlichen und Kunstlichen Kankschukarten', Springer, Berlin, 51, (1919)
3. J R Katz, Naturwiss, 13, 411, (1925)
4. R Pummerer, G Ebermeyer and K Gerlach, Ber., 64, 809, (1931)
5. T Hancock, 'Origin and Progress of India Rubber Manufacture', 13, (1857)
6. H Staudinger, Kautschuk, 5, 128, (1929); Rubb. Chem. Technol , 3, 586, (1930)
7. M Pike and W F Watson, J. Polym. Sci., 9, 229, (1952)
8. W F Busse, Ind. Eng. Chem , 24, 140, (1932)
9. F H Cotton, Trans. IRI, 5, 153, (1932)
10. W Kauzman and H Eyring, J Am. Chem Soc, 62, 3113, (1940)
11. G Ayrey, C G Moore and W F Watson, J Polym Sci, 19, 1, (1956)
12. D J Angier and W F Watson, J Polym Sci, 20, 235, (1955); Trans IRI, 33, 22, (1956)
13. D J Angier and W F Watson, J Polym Sci, 18, 129, (1955)
14. D J Angier and W F Watson, Trans IRI, 33, 22, (1957)

15. G L Slonminskii and E V Retsova, Rubb Chem Technol, 33, 457, (1960)

16. E H Andrews and P E Reed, 'Molecular Fracture', Chapt in Developments in Polymer Fracture - 1, (Ed E H Andrews) Appl Sci Publ, London, (1979) P 17

17. B Ranby and J F Rabek, ESR Spectroscopy in Polymer Research, Springer, Heidelberg

18. J Sohma and M Sakaguchi, Adv Polym Sci, 20, 109, (1976)

19. C Goodyear, 'Gum Elastic and its Varieties', New Haven, (1855)

20. T Hancock, 'Personal narrative of the origin and progress of Casutchoui in England', J L Hancock Ltd, (1920)

21. J F Smith, Rubber in Engineering Conf, Kuala Lumpur, (1974); M. P. R. A. reprint No 764

22. F Bueche, J Polym Sci, 24, 189, (1957)

23. F Bueche, J Polym Sci, 33, 259, (1958)

24. W L Cox and C R Parks, Rubb Chem Technol, 39, 785, (1966)

25. M L Studebaker, Rubb Chem Technol, 39, 1359, (1966)

26. M Porter, 'The chemistry of sulphur vulcanisation of natural rubber', Chapt in The Chemistry of Sulphides, (Ed A V Tobolsky) Interscience, New York, (1968) P 165

27. L Bateman, C G Moore, M Porter and B Saville, 'Chemistry of Sulphides', Chapt in The Chemistry and Physics of Rubber-like Substances, (Ed L Bateman) Maclaren, London, (1963) P449

28. B Saville and A A Watson, Rubb Chem Technol, 40, 100, (1967)

29. W Scheele,Rubb Chem Technol, 34, 1306, (1961)

30. C G Moore, J Polym Sci, 32, 503, (1958)

31. L Bateman, R W Glazebrook and C G Moore, J Appl Polym Sci, 1, 257, (1959)

32. E R Rodger, 'Vulcanisation Systems', Chapt in Developments in Rubber Technology-1, (Ed A Whelan and K S Lee) Appl Sci Publ, London, (1979) P 105

33. M A Wheelans, 2nd Ann Nat Conf IRI, Blackpool, May, (1974)

34. D A H Hammersley, D G L Lloyd,A J Neale and E R Rodger, Intern Rubb Conf, Moscow, (1969)

35. W Scheele, O Lorenz and D Dummer Rubb Chem Technol, 29, 1, (1956)

36. C G Moore, Chapt in Proceedings NRPRA Jubilee Conf, Cambridge (Ed L Mullins) Maclaren, London, (1965)

37. I I Ostrosmislenskii , J Russian Phys Chem Soc, 47, 1885, (1915)

38. M Braden, W P Fletcher and G P McSweeney, Trans IRI, 30, 44, (1954)

39. M Braden and W P Fletcher, Trans IRI, 31, 155, (1955)

40. Y L Chow and G T Knight, Proc Int Rubb Conf, Brighton,(1977)

41. D S Pearson and G G A Bohn, Rubb Chem Technol, 45, 193, (1972)

42. C S L Baker, D Barnard and M Porter, Ka t und Gummi Kunst, 26, 540, (1973)

43. C S L Baker, 'Vulcanisation with Urethane Reagents' NR Tech Bulletin, M. R. P. R. A., Hertford, (1978)

44. C S L Baker and R Newell, NR Technol, 8 (Pt 2), 33, (1977)

45. A Whelan and K S Lee (Ed), 'Developments in Rubber Technology-2, Synthetic Rubbers,' Appl Sci Publ, London, (1981)

46. H Staudinger, Helv Chim Acta, 8, 41, (1925)

47. K H Meyer, Von Susich and Evalko, Kolloidzeitschrift, 59, 208, (1932)

48. E Guth and T James, J Chem Phys, 11, 455, (1943)

49. F T Wall, J Chem Phys, 10, 485, (1942)

50. P J Flory and J Rehner, J Chem Phys, 11, 512, (1943)

51. P J Flory and J Rehner, J Chem Phys, 11, 521, (1943)

52. R S Rivlin and D W Saunders, Phil Trans Roy Soc, A243, 251, (1951)

53. M Mooney, J Appl Phys, 11, 582, (1940)

54. L G R Treloar, 'Physics of Rubber Elasticity', Oxford, (1975), P 59

55. P J Flory, 'Principles of Polymer Chemistry', Cornell Univ Press, Ithaca, New York, (1953), P 432

56. A Ciférri, J Poly Sci, 54, 149, (1961)

57. E Guth, H M James and H Mark, 'Advances in Colloid Science', Interscience Publ, New York, (1946)

58. G M Bartenev, J Tech Phys, USSR, 20, 461, (1950)

59. M Morton, V R Allen and R D Gates, US Dept Com Office Tech Serv PB Rept, 150491 (1959); Chem Abst, 56, 10345, (1962)

60. A V Tobalsky, D W Carlson and N Indictor , J Polym Sci, 54, 175, (1961)

61. A N Gent and A G Thomas, J Polym Sci, 28, 625, (1958)

62. L Mullins, J Appl Polym Sci, 2, 1, (1959)

63. L Mullins, S Gumbrell and R Rivlin, Trans Farad Soc, 49, 1495, (1953)

64. P J Flory, Ind Eng Chem, 38, 417, (1946)

65. L A Wood, J Wash Acad Soc, 47, 281, (1957)

66. L R G Treloar, Trans Farad Soc, 50, 881, (1954)

67. W Kuhn, Kolloidzschr, 68, 2, (1934)

68. W Kuhn and F Grun, Kolloidzeitschrift, 101, 248, (1942)

69. W Kuhn and H Kuhn, Helv Chim Acta, 29, 1095, (1946)

70. A Isihara, N Hashitsume and M Tatibana, J Chem Phys, 18, 108, (1951)

71. M C Wang and E Guth, J Chem Phys, 20, 1144, (1952)

72. R F Boyer and R L Miller, Rubb Chem Technol, 50, 798, (1977)

73. G Gent, Trans Farad Soc, 42, 585, (1946)

74. E F Cluff, E K Gladding and R Pariser, J Polym Sci, 45, 341, (1960)

75. D A Smith, J Polym Sci, 16(c), 525, (1967)

76. L D Loan, Monograph 17, Soc Chem Ind, London, (1963) P 24

77. E Kay, E B Moore and D K Thomas, Polymer, 10, 55, (1969)

78. A H Khan-Khadin and D A Smith, Polymer, 10, 711, (1969)

79. R E Melley and J E Stuckey, J Appl Polym Sci, 14, 2327, (1970)

80. P J Flory, J Chem Phys, 18, 108, (1950)

81. L Mullins, J Polym Sci, 19, 225, (1956)

82. L D Loan, J Appl Polym Sci, 7, 2259, (1963)

83. G M Bristow and W F Watson, Trans Farad Soc, 54, 1567, (1958)

84. G Crespi and M Bruzzone, Chem Ind (Milan), 41, 741, (1959)

85. W J Bobear, Ind Eng Chem Prod Res Dev, 3, 277, (1964)

86. C G Moore and B R Trego, J Appl Polym Sci, 8, 1957, (1964)

87. B Butenuth, Rubber Age, 94(5), 737, (1964); Rubb Chem Technol, 37, 326, (1964)

88. M Porter, J Appl Polym Sci, 11, 2255, (1967)

89. G M Bristow and M Porter, J Appl Polym Sci, 11, 2215, (1967)

90. E Guth and O Gold, Phys Rev, 53, 322, (1938)

91. L Mullins, J Rubb Res, 16, 275, (1947)

92. L Mullins, Phys Colloid Chem, 54, 239, (1950)

93. C G Moore and W F Watson, J Polym Sci, 19, 237, (1956)

94. R Simha, J Phys Chem, 44, 25, (1940)

95. J Rehner, J Appl Phys, 14, 638, (1943)

96. H M Smallwood, J Appl Phys, 15, 758, (1944)

97. E Guth, J Appl Phys, 16, 20, (1945)

98. E Guth, Proc Rubb Technol Conf (2nd), London, (1948) P 353

99. L Mullins and N R Tobin, J Appl Polym Sci, 9, 2993, (1965)

100. A M Bueche, J Polym Sci, 15, 105, (1955)

101. G Kraus, Rubber World, 135, 67; 254, (1956)

102. M Porter, Rubb Chem Technol, 40, 866, (1967)

103. M L Studebaker and L G Nabors, Proc Intern Rubb Conf, Washington, (1959) P 237

104. J W Seller, M P Wagner, B J Dewitt, C C Stueber and J H Bachmann, J Appl Polym Sci, 5, 397, (1961)

105. O Lorenz and C R Parks, J Polym Sci, 50, 299, (1961)

106. G Kraus, J Appl Polym Sci, 7, 861, (1963)

107. B B Boonstra and G L Taylor, Rubb Chem Technol, 38, 943, (1965)

108. R M Russell, British Polym J, 1, 53, (1969)

109. C G Moore, B Saville and B R Trego, unpublished paper

110. B R Trego, Ph. D. Theses, 1965

111. M B Evans and B Saville, Proc Chem Soc, (1962) P 18

112. D S Campbell and B Saville, Proc Intern Rubb Conf, Brighton (1967) P 1

113. D S Campbell, J Appl Polym Sci, 13, 1201, (1969)

114. G Gorin, G Doughty and R Gideon, J Chem Soc, B, 729, (1967)

115. C G Moore and B R Trego, J Appl Polym Sci, 5, 299, (1961)

116. C G Moore and B R Trego, Tetrahedron, 18, 205, (1962)

117. C G Moore and B R Trego, Tetrahedron, 19, 1251, (1963)

118. C G Moore and M Porter, Revue Gen Caoutch, 39, 1768, (1962)

119. L Bateman, R W Glazebrook and C G Moore, J Appl Polym Sci, 1, 257, (1959)

120. R E Humphrey and J L Porter, Analyt Chem, 36, 1812, (1964)

121. R E Humphrey and J M Hawkins, Analyt Chem, 36, 1957, (1964)

122. C G Moore and B R Trego, J Appl Polym Sci, 8, 1957, (1964)

123. C G Moore and M Porter, J Appl Polym Sci, 11, 2227, (1967)

124. W N Hess and K A Burgess, Rubb Chem Technol, 36, 754, (1963)

125. R W Smith and A L Black, Rubb Chem Technol, 37, 338, (1964)

126. A Angioletti, Rubb Chem Technol, 29, 753, (1956)

127. A N Gent, P B Lindley and A G Thomas, J Appl Polym Sci, 8, 455, (1964)

128. G J Lake and P B Lindley, J Appl Polym Sci, 8, 707, (1964)

129. R S Rivlin and A G Thomas, J Polym Sci, 10, 291, (1953)

130. A G Thomas, J Appl Polym Sci, 3, 168, (1960)

131. G J Lake, P B Lindley and A G Thomas, Proc 2nd Intern Conf on Fracture, Brighton, (1969) P 493

132. H W Greensmith, J Appl Polym Sci, 7, 993, (1963)

133. H W Greensmith, J Appl Polym Sci, 3, 175, (1960)

134. A G Thomas, J Polym Sci, 18, 177, (1955)

135. G J Lake and P B Lindley, Rubb J, 146(10), 24, (1964)

136. G J Lake and P B Lindley, Rubb J, 146(11), 30, (1964)

137. G J Lake and P B Lindley, J Appl Polym Sci, 10, 343, (1966)

138. G J Lake and P B Lindley, Rubb Chem Technol, 39, 348, (1966)

139. G J Lake and P B Lindley, J Appl Polym Sci, 9, 1233, (1965)

140. G J Lake and A G Thomas, Proc Roy Soc, A300, 208, (1967)

141. W F Busse, Ind Eng Chem, 26, 1194, (1934)

142. S M Cadwell, R A Merrill, C M Sloman and F L Yost, Ind Eng Chem (Anal Ed), 12, 10, (1940)

143. J H Dillon, 'Advances in Colloid Science', vol 3, Int Sci Publ, New York, (1950) P 219

144. C J Derham, G J Lake and A G Thomas, J Rubb Res Inst Malaya, 22(2), 191, (1969)

145. G J Lake and P B Lindley, 'Physical Basis of Yield and Fracture', Conf Proc, Oxford, (1966) P 176

146. G J Lake, Rubb Chem Technol, 45, 309, (1972)

147. E H Andrew, J Mech Phys Solids, 11, 231, (1963)

148. A G Thomas, J Polym Sci, 31, 467, (1958)

149. A N Gent, J Appl Polym Sci, 6, 497, (1962)

150. J H Fielding, Ind Eng Chem, 35, 1259, (1943)

151. J A.C Harwood and A R Payne, J Appl Polym Sci, 12, 889, (1968)

152. J C Halpin, Rubb Chem Technol, 38, 1007, (1965)

153. K W Scott, Polym Eng Sci, 7, 158, (1967)

154. J R Beatty, Rubb Chem Technol, 37, 1341, (1964)

155. H W Greensmith, L Mullins and A G Thomas, 'Strength of Rubbers', Chapt in The Chemistry and Physics of Rubber-like Substances, (Ed L Bateman), Maclaren, London, (1963) P 249

156. A M Neal and A J Northam, Ind Eng Chem (Anal Ed), 23, 1449, (1931)

157. H Winn and J R Shelton, Ind Eng Chem , 37, 67, (1945)

158. J M Buist and G E Williams, India Rubb World, 124, 320; 447;567, (1951)

159. G Scott, 'Atmospheric Oxidation and Antioxidants', Elsevier, Amsterdam, (1965)

160. T Kemperman, Rev Gen Caout, 40, 406, (1963)

161. W E Mochel, J Polym Sci, 8, 583, (1952)

162. A L Klebamskii, J Polym Sci, 30, 763, (1958)

163. W E Mochel, J R Nichols, C J Mighton, J Am Chem Soc, 70, 2185, (1948)

164. G L Slonimskii, V A Kargin, G N Buiko, E V Reztsova and M L'yuis-Riera, Starenie i Utomlenie, U.N.I.T.O. Rezinshchikov Konf, (1953) P 100

165. G J Lake, Rubber Age, 104(9), 39, (1972)

166. M K Khromov and K N Lazareva, Kauch i Rezina, 5, 32, (1979)

167. N K Khromov, K N Lazareva and M M Resnikovskii, Sov Rubb Technol, 23(9), 12, (1963)

168. C L M Bell, J Appl Polym Sci, 9, 3101, (1965)

169. P B Lindley and A G Thomas, Proc 4th Rubb Technol Conf, London, (1962) P 428 (IRI)

170. F J Bueche, J Appl Polym Sci, 7, 1165, (1963)

171. D Bernard, L Bateman, J E Cunneen and J F Smith, 'Oxidation of Sulphides', Chapt in The Chem and Phys of Rubberlike Substances, (Ed L Bateman), Maclaren, London, (1963) P 593

172. J I Cunneen,Rubb Chem Technol, 41, 182, (1968)

173. J R Shelton, Rubb Chem Technol, 30, 1251, (1957)

174. J C Ambelang, R H Kline, O M Lorenz, C R Parks and C Wadelin, Rubb Chem Technol, 36, 1497, (1963)

175. E V Reztsova, B G Lipkena and G L Slonimskii, Zh Fiz Khim, 33, 656, (1959)

176. S F B Morse, reported in Royle Forum, John Royle and Sons, 44, 5, (1948)

177. W J Thomson, Soc Chem Ind, 4, 710, (1885)

178. A Von Rossem and H W Talen, Rubb Chem Technol, 4, 490, (1931)

179. E P W Kearsley, Rubber Age, 27, 649, (1930)

180. F J Norton, Rubber Age, 47, 87, (1940)

181. S Eccher, Rubb Chem Technol, 13, 566, (1940)

182. R G Newton, Rubb Chem Technol, 18, 504, (1945)

183. B S Biggs, Rubb Chem Technol, 31, 1015, (1958)

184. A.S.T.M. Special Techn Publ No 229 (1958)

185. L D Loan, R W Murray and P R Story, J IRI, 2, 73, (1968)

186. G J Lake, Rubber Age, 104(8), 30, (1972)

187. R G Newton, India Rubb J, 121, 257, (1951)

188. E H Andrew, D Barnard, M Braden and A N Gent, 'Ozone Attack on Rubbers' Chapt in The Chem and Phys of Rubber-like Substances (Ed L Bateman) Maclaren, London, (1963) P 329

189. M Braden and A N Gent, J Appl Polym Sci, 3, 90; 100, (1960)

190. A N Gent and J E McGrath, J Polym Sci, A3, 1473, (1960)

191. A N Gent and H J Hirakawa, J Polym Sci, 15(Pt A2), 157 (1967)

192. D J Buckley and S B Robison, J Polym Sci, 19, 145, (1956)

193. T Matsuda and M Tanaka, J Soc Rubb Ind Japan, 26, 407 (1953); Rubb Abst, 33, 2986, (1955)

194. G J Lake and P B Lindley, J Appl Polym Sci, 9, 2031, (1965)

195. D C Edwards and E B Storey, Trans IRI, 31, 45, (1955)

196. A S Kuzminsky, 'The Mechanisms of Fatigue Resistance and Antifatigue Agents in Elastomers', Chapt in Developments in Polymer Stabilisation-4 (Ed G Scott), Appl Sci Publ, London, (1981)

197. L M Begunovskaya, V G Zhakova, B K Karmin and V G Epshtein, Stareine i Utomlenie, 31, (1953)

198. G Scott, 'Mechanisms of antioxidant action', Chapt in Developments in Polymer Stabilisation-4, (Ed G Scott) Appl Sci Publ, London, (1981)

199. S D Razumosky, G E Zaikov, Ozone and its reactions with organic compounds, Nanka, Moscow, (1974)

200. R M Murray, Rubber Age, 85, 623, (1959)

201. A P C Cumming and M R Horton, IRI Conf, Manchester, April (1969)

202. R F Shaw, Z T Ossefort and W T Tonley, Rubber World, 130, 636. (1954)

203. W F Tuley, Ind Eng Chem, 31, 714, (1939)

204. R Criegee, Paper presented at 120th meeting, Am Chem Soc, September, (1951)

205. R W Murray; in 'Polymer Stabilisation', (Ed W L Hawkins) Interscience, New York, (1972)

206. J C Andries, D B Ross and H E Diem, Rubb Chem Technol, 48, 41, (1975)

207. S W Ferris, S S Kurtz and J S Sweely, Symp on Effect of Ozone on Rubber, ASTM spec publ 229, 72, (1958)

208. J I Cunneen, Oxidative Ageing of Vulcanised NR, Chapt in proc of NAPRA Jubilee conf, (Ed L Mullins), Maclaren (1964) P 196

209. A Dibbo, Trans IRI, 40, 202, (1964)

210. P B Lindley, Rubber Developments, 19(4), 168, (1966)

211. D G Lloyd and J Payne, Rubb News, June (1967) P 26

212. Monsanto Technical Bulletin, 0/RC-5

213. S B Miller, Rubber Age, 98(5), 60, (1966)

214. B E Clapson and R A Dove, Rubb J, 154(12), 41, (1972)

215. J E Stuckey, 'High temperature stability in rubber vulcanisates' Chapt in Developments in Polymer Stabilisation-1, (Ed G Scott) Appl Sci Publ, London, (1979) P 101.

216. V A Shershnev, N I Lebedeva, S M Kavun, Kauchuk i Rezina, 1, 13, (1975)

217. L Mullins, 'Effect of fillers in rubber', Chapt in The Chem and Phys of Rubber-like Substances, (Ed L Bateman) Maclaren, London, (1963) P 301

218. A N Gent, P B Lindley and A G Thomas, J Appl Polym Sci, 8, 465, (1964)

219. G J Lake and P B Lindley, Rubb J, 146(11), 30, (1964)

220. M S S Coker, G Scott and A A Sweis, Polym Degradation and Stability, 4, 333, (1982)

221. K T Paul, RAPRA Bulletin, 26, 29, (1972)

222. K T Paul, RAPRA Members J, November (1963) P 273

223. J L Bolland, Quart Rev, 3, 1, (1954)

224. E Wing, Instrumental Methods of Chemical Analysis, McGraw-Hill, (1960) P 82

225. S Schoniger, Mikrochim Acta, (1955) P 123

226. Ibid, Mikrochim Acta, (1955) P 869

227. A Macdonald, in 'Advances in Analytical Chemistry and Instrumentation,' Vol 4, Interscience-Wiley, (1965)

228. W D Basom, Rubb Chem Technol, 50, 875, (1977)

229. R J Seward, Rubb Chem Technol, 43, 1, (1970)

230. E S Dizon and A E Hicks, Rubb Chem Technol, 47, 231, (1974)

231. B A Dogadkin and Z N Tarasova, Rubb Chem Technol, 27, 883, (1954)

232. J C Ambelang in 'Vulcanisation of Elastomers" (Ed G Alliger and I J Sjothum), Reinhold Publ Corp (1964) P 126

233. B A Dogadkin, Z N Tarasova and I I Goldberg, Proc 4th Rubb Technol Conf, London, (1962) P 65

234. A Dibbo and D G Lloyd, Proc 4th Int Rubb Conf, Brighton, (1967) P 83

235. A J Kuzminskii and L T Lyabchanskaya, Rubb Chem Technol, 29, 770, (1956)

236. L Bateman, J I Cunneen, C G Moore, L Mullins and A G Thomas in 'The Chem and Phys of Rubber-like Substances', (Ed L Bateman) Maclaren, London, (1963) P 715

237. W Cooper, Chem Ind, 52, 1341, (1955)

238. W Cooper, J Polym Sci, 28, 195, (1958)

239. E B McCall, J Rubb Res Inst Malaya, 22, 354, (1969)

240. G M Bristow and R F Tiller, Kautschuk Gummi, 23, 55, (1970)

241. J Lal, Rubb Chem Technol, 43, 664, (1970)

242. E Southern in 'Elastomers: Criteria for Engineering Design', (Ed C Hepburn and R J W Reynolds), Appl Sci Publ, London, (1979) P 273

243. D G Lloyd, 'Fatigue and its reduction in NR', Monsanto Techn Bulletin, March (1966) LA24/1

244. J I Cunneen and R M Russell, J Rubb Res Inst, Malaya, 22, 300, (1969)

245. A Gregory, M.Sc. Thesis, University of Aston, (1971)

246. A J Rigby, M.Sc. Thesis, University of Aston, (1969)

247. J E Stuckey, Rubber Technol Conf, Kharagpur, India, (1981)

248. W S Howard and C R Wilder, Paper presented at the meeting of the Division of Rubber Chem, Am Chem Soc, Philadelphia, October, (1974)

249. M M Podkolzina, S B Petrova and T V Federova, Kausch Rezine 2, 16, (1978); Intern Polym Sci Technol, 5(2), (1978)

250. S Ohto, M Ueda and S Murakami, Nippon Gormu Kyokaishi, 48(12), 775, (1975); Intern Polym Sci Technol, 2(12), (1975)

251. G B Nando and S K De, Polymer,21, 10, (1980)

252. P J Flory, Chem Revs, 35, 51, (1944)

253. P J Flory, 'Principles of Polymer Chemistry', Cornell University Press, (1953), P 461

254. L Mullins and A G Thomas, J Appl Polym Sci, 43, 13, (1960)

255. E Helfand and A E Tonelli, Macromol, 7, 832, (1974)

256. A E Oberth, Rubb Chem Technol, 44, 152, (1971)

257. G Kraus and G A Moczvgenba, J Polym Sci, A2,. 277, (1964)

258. J Scanlan, J Polym Sci, 43, 501, (1960)

259. L C Case, J Polym Sci, 45, 397, (1960)

260. D C Edwards, Rubb Chem Technol, 48, 202, (1975)

261. R F Hoffman and R H Gobran, Rubb Chem Technol, 46, 139, (1973)

262. J F Fellers and M Rahbar-Semanani, J Polym Sci, 12, 2035, (1974)

263. H C Baker and H W Greensmith, Trans and Proc IRI, 42, 194, (1966)

264. A V Tobolsky, I B Prettyman and J H Dillon, J Appl Phys, 15, 380, (1944)

265. J P Berry and W F Watson, J Polym Sci, 18, 201, (1955)

266. A V Tobolsky and R D Andrews, Rubb Chem Technol, 18, 731, (1945)

267. M D Stern and A V Tobolsky, J Chem Phys, 14, 93, (1946); Rubb Chem Technol, 19, 1178, (1946)

268. R D Andrews, A V Tobolsky and E E Hanson, J Appl Phys, 17, 352, 1946

269. J P Berry, J Scanlan and W F Watson, Trans Farad Soc, 52, 1137, (1956)

270. K W Scott and R S Stein, J Chem Phys, 21, 1281, (1953)

271. A G Thomas, J Polym Sci Symp, 48, 145, (1974)

272. J Scanlan and W F Watson, Trans Farad Soc, 52, 740, (1956)

273. L A Mikeska, U.S. Pat 2, 471, 115 (Sept 19, 1946)

274. J G Pimblott, G Scott and J E Stuckey, J Appl Polym Sci, 19, 865, (1975)

275. W F Watson and D Wilson, J Sci Ind, 31, 98, (1954)

276. G E Decker, R W Wise and D Guerry, Rubb Chem Technol, 36, 451, (1963)

277. A Y Coran, Rubb Chem Technol, 37, 668, 689, (1964)

278. Ibid, Rubb Chem Technol, 38, 1, (1965)

279. G M Bristow and B Westall, J Appl Polym Sci, 9, 494, (1965)

280. D G Lloyd, 'Fatigue Failure and its reduction in NR', Monsanto Techn Bulletin, LA24/1

281. The Monsanto Fatigue to Failure Tester Handbook

282. M Kakudo and N Kasai, 'X-ray Diffraction by Polymers' Elsevier Publ Comp, (1972) P 362

283. L Mullins and W F Watson, J Appl Polym Sci, 1, 245, (1959)

284. M Porter, T D Skinner and M A Wheelans, J Appl Polym Sci, 11, 2271, (1967)

285. G Reza, Ph. D Thesis, University of Aston, (1979)